Modelado Estocástico e Integración de Recursos Energéticos Distribuidos en la Red Eléctrica Inteligente

---

Stochastic Modelling and Integration of Distributed Energy Resources in the Smart Grid

Ph.D. Dissertation
by
Emilio José Palacios-García

Supervisor
Antonio Moreno-Muñoz
Co-supervisor
José María Flores-Arias

Programa de Doctorado en Computación Avanzada, Energía y Plasmas
Departamento de Ingeniería Electrónica y de Computadores
Universidad de Córdoba

Córdoba, Spain
January 2018

TITULO: *MODELADO ESTOCÁSTICO E INTEGRACIÓN DE RECURSOS ENERGÉTICOS DISTRIBUIDOS EN LA RED ELÉCTRICA INTELIGENTE*

AUTOR: *Emilio José Palacios García*

Campus de Rabanales
Ctra. Nacional IV, Km. 396 A
14071 Córdoba

https://www.uco.es/ucopress/index.php/es/
ucopress@uco.es

TÍTULO DE LA TESIS: Modelado Estocástico e Integración de Recursos Energéticos Distribuidos en la Red Eléctrica Inteligente

DOCTORANDO: Emilio José Palacios García

INFORME RAZONADO DE LOS DIRECTORES DE LA TESIS

(se hará mención a la evolución y desarrollo de la tesis, así como a trabajos y publicaciones derivados de la misma)

El doctorando Emilio José Palacios García ha realizado satisfactoriamente y en los plazos previstos el trabajo de investigación presentado en esta memoria de tesis habiendo alcanzado todos los objetivos planteados en la memoria inicial.

El trabajo ha abordado un análisis de las técnicas de modelado de la demanda para el sector residencial y el uso de dichos modelos en la mejora de la integración de recursos distribuidos dentro de la idea de *Smart Grid* o red inteligente. En base a esto el doctorando ha desarrollado un modelo de demanda para el sector residencial basado en técnicas estocásticas y con una filosofía *bottom-up*. Dicho modelo está compuesto a su vez de tres bloques diferenciados que poseen características y factores de influencia específicos que deben ser tratados de forma separada.

Del mismo modo ha realizado una amplia labor en el uso práctico del modelo tanto para la evaluación de diferentes escenarios, como para la integración de recursos renovables distribuidos, pasando por el desarrollo de algoritmos para mejorar la estabilidad de la red o respuesta a la demanda.

Así mismo, ha realizado dos estancias de investigación de 3 meses cada una en la Universidad de Aalborg (Dinamarca) de cara a la obtención del título de doctor con mención internacional. En dicha entidad ha trabajado extensivamente en la integración de los contadores inteligentes en la gestión de la red eléctrica junto con los modelos de predicción desarrollados, de cara a mejorar la gestión de la misma.

Esto ha dado fruto a una línea de colaboración conjunta con dicha universidad en el cual el doctorando ha participado activamente durante todo el periodo de la tesis y se prevé continúe haciendo en un futuro. El doctorando ha sido también beneficiario de una beca FPU del ministerio de educación desde el segundo año de doctorado. Así mismo, se ha integrado en el equipo de trabajo de un proyecto nacional.

En el ámbito formativo, tal y como se puede comprobar en la relación de actividades desarrolladas, el doctorando no solo ha completado los ítem propios del programa sino que realizado numerosos cursos, ha participado en contratos con empresas e incluso desde su incorporación como FPU ha asistido al curso de formación del profesorado novel impartido por dicha universidad para mejorar así su formación no solo como investigador sino también como docente.

Todos los desarrollos anteriores y la calidad del trabajo se plasman en los resultados generados por dicha tesis, los cuales han sido publicados en revistas con un alto factor de impacto dentro del campo y que han seguido un hilo argumental preciso que ha permitido presentar este trabajo como un compendio de publicaciones.

En total el doctorando ha realizado 3 publicaciones en revistas Q1 y Q2 como primer autor y un capítulo de libro en una editorial de reconocido prestigio dentro del campo de estudio. A esto hay que añadirle numerosas colaboraciones en otras publicaciones de alto impacto, así como más de una decena de publicaciones en congresos con revisión por pares, algunos de ellos clave en el área.

Por todo ello, a nuestro juicio cumpliendo con los requisitos necesarios para optar al grado de doctor, se autoriza la presentación de la tesis doctoral.

Córdoba, 15 enero 2018
Firma de los directores

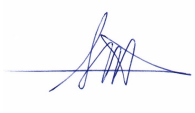

Fdo.: Antonio Moreno Muñoz

Fdo.: José María Flores Arias

Mención de Doctorado Internacional

Esta tesis doctoral cumple con los requisitos establecidos por la Universidad de Córdoba para la obtención del Título de Doctor con Mención Internacional:

- Estancias internacionales predoctorales de investigación:

  Microgrids research group. Department of Energy Technology. Aalborg University. Aalborg, Dinamarca. Supervisor: **Josep M. Guerrero**. *Full Professor*. Leader of the research programme in Microgrids.

  - 3 meses (21/03/2015 – 26/06/2015)
  - 3 meses (01/08/2016 – 31/10/2016)

- Cuenta con el informe previo de dos doctores expertos con experiencia acreditada pertenecientes a instituciones de educación superior europeas:

  - **Dr. Pierluigi Siano**. *Full Professor*. Department of Industrial Engineering, University of Salerno. Salerno, Italia.
  - **Dr. Alexander Huhn**. *Associate Professor*. Hochschule für Technik und Wirtschaft (University of Applied Sciences). Berlin, Alemania.

- Una doctora perteneciente a una institución de educación superior no española forma parte del tribunal de la tesis:

  - **Dr. Sarah Rönnberg**. *Associate Professor*. Department of Engineering Sciences and Mathematics. Luleå University of Technology. Skellefteå, Suecia.

- La tesis doctoral se ha redactado y se defenderá **íntegramente en inglés**.

Córdoba, 15 enero 2018
El doctorando

Fdo. Emilio José Palacios García

Tesis como compendio de artículos

Esta tesis doctoral cumple con los requisitos establecidos por la Universidad de Córdoba para la presentación como compendio de artículos. Incluye **3 artículos** publicados en revistas incluidas en los dos primeros cuartiles de la última relación publicada por el Journal Citations Report (JCR), así como **1 capitulo de libro** publicado por una editorial de reconocido prestigio en el campo de la investigación como es *The Insitution of Engineering and Technology (IET)* el cual pasó un riguroso proceso de revisión por pares. En todas esta publicaciones el doctorando aparece como primer firmante del trabajo habiendo aceptado los coautores su presentación en esta tesis doctoral.

- **Palacios-Garcia E. J.**, Chen A., Santiago I., Bellido-Outeiriño F. J., Flores-Arias J. M., Moreno-Munoz A., Stochastic model for lighting's electricity consumption in the residential sector. Impact of energy saving actions. *Energy & Buildings* 2015;89:245–259.
  JCR: 2.935 (2015). 6/61(Q1) - Construction & Building Technology; 31/88(Q2) - Energy & Fuels; 6/126 (Q1) - Engineering, Civil. doi: 10.1016/j.enbuild.2014.12.028.

- **Palacios-Garcia E. J.**, Moreno-Muñoz A., Santiago I., Moreno-Garcia I. M., Milanés-Montero M. I., PV Hosting Capacity Analysis and Enhancement Using High Resolution Stochastic Modeling. *Energies* 2017;10:1488.
  JCR: 2.626 (2016). 45/92(Q2) - Energy & Fuels. doi: 10.3390/en10101488.

- **Palacios-Garcia E. J.**, Moreno-Munoz A., Santiago I., Flores-Arias J. M., Bellido-Outeirino F. J., Moreno-Garcia I. M., A stochastic modelling and simulation approach to heating and cooling electricity consumption in the residential sector. *Energy* 2017;144:1080–1091.
  JCR: 4.520 (2016). 3/58(Q1) - Thermodynamics; 17/92(Q1) - Energy & Fuels. doi: 10.1016/j.energy.2017.12.082.

- **Palacios-Garcia E. J.**, Moreno-Munoz A., Santiago I., Flores-Arias J. M., Bellido-Outeirino F. J., Distributed energy resources integration and demand response: the role of stochastic demand modelling. In: Moreno-Munoz A, editor. *Large Scale Grid Integration of Renewable Energy Sources*, London: Institution of Engineering and Technology; 2017, p. 245–278. doi:10.1049/PBPO098E_ch8.

Córdoba, 15 enero 2018
El doctorando

Fdo. Emilio José Palacios García

Tesis Doctoral subvencionada por el Programa de Formación del Profesorado Universitario (FPU) del Ministerio de Educación, Cultura y Deporte.
Referencia: **FPU14/02508**

Así mismo ha sido parcialmente subvencionada por el Proyecto de I+D del Programa Estatal de Investigación Científica y Técnica de Excelencia 2013 (MINECO). *Sistema de Gestión Energética de una Comunidad Inteligente (SCEMS)*.
Referencia: **TEC2013–47316–C3–1–P**.
Y el Proyecto de I+D+I del Programa Estatal de Investigación, Desarrollo e Innovación Orientada a los Retos de la Sociedad 2016 (MINECO). *Control y Gestión de Nanorredes Aislables (COMING)*.
Referencia: **TEC2016–77632–C3–2–R**.

'If you want something you can have it,
but only if you want everything that goes with it,
including all the hard work and the despair,
and only if you're willing to risk failure'.

Philip Pullman
Clockwork

Agradecimientos / Acknowledgements

Tras todo el desarrollo detrás de este trabajo y los años trascurridos hasta la culminación del mismo es imposible encontrar las palabras adecuadas para expresar mi más sincera gratitud a todos aquellos que han hecho posible que llegara este día.

Me gustaría dar las gracias en primer lugar a Antonio Moreno, director de esta tesis, quien no solo ha conseguido con su magnífica orientación y guía que esto sea una realidad, sino que ha servido como fuente de inspiración y apoyo durante el largo camino recorrido. Del mismo modo, debo expresar mi gratitud al co-director José María Flores quien allá por el año 2013 y con la colaboración de Kiko Bellido consiguió implantar en mi la curiosidad y pasión necesarias para entrar en el 'mundillo' de la investigación. Tampoco puedo olvidar mencionar a la profesora Isabel Santiago pionera en el departamento en el estudio de las técnicas de modelado y cuya ayuda ha sido imprescindible en todo momento. Sin su colaboración probablemente este trabajo nunca se hubiera finalizado. Si alguien tiene la culpa de que esté hoy aquí sois vosotros por vuestras magnificas enseñanzas.

También debo agradecer su apoyo a mis compañeros de laboratorio. Han sido 5 años trabajando en un ambiente inmejorable. Gracias a Chen, Francisco Navarro, Javier Beamuz que, pese a no formar parte de la universidad a día de hoy, seguís siendo grandísimos amigos. Y por supuesto a Isabel Moreno, quien ha sido partícipe de la evolución de esta tesis, tanto para las alegrías como para los agobios. Aunque eso sí, el café y tostada de media mañana que no falte. Siguiendo en la universidad es imposible no mencionar a los miembros del departamento, a los que una vez llamé profesores y que a día de hoy puedo llamar compañeros. Con especial agradecimiento a Víctor Pallarés, siempre con nuevos desarrollos e ideas que compartir, a Juan Luna por los ratos de 'cacharreo' con las PCBs que tan bien vienen para desconectar y a Aurora Gil con sus lámparas, que ha dejado más de una vez a oscuras mi salón para conseguir nuevas medidas.

I would also like to thank all the people I met at Aalborg University. First of all, to Prof. Josep Guerrero, for giving me the opportunity of working as part of the Microgrids research group. Thanks to Dr. Mehdi Savaghebi, Dr. Juan C. Vásquez (Juancho), Dr. Amjad Anvari-Moghaddam, and Dr. Yajuan Guan for all the knowledge that we shared. To my friends Mohammed and Saher for all the great moments we spend together. And of course, to Enrique Rodriguez for the great work we carried out together and the future developments that are to come. Sin moverme de Aalborg tengo que mencionar a Hector Pandiella y Jesús Serrano, hoy dos grandes amigos que no hubiera conocido de no haber sido por mis estancias.

También debo agradecer a mis amigos todo el apoyo que me han prestado durante todo este tiempo. Tanto a los que mantenemos el contacto desde la distancia Luis, Celia, Carlos, Javi, Xarly como a los que veo a menudo y que siempre consiguen que salga para 'despejarme', Antonio, Paco, Fin, Monte, Alberto... seguro que me he dejado alguien, pero necesitaría un capítulo solo para agradeceros vuestro apoyo. *And of course, thanks to Angela Byrne not only for proofreading parts of this dissertation and helping me with any language related doubt, but also for her support during the last year. I think there is no way to repay for that and no words for expressing my gratefulness to you.*

Y por último y no por ello menos importante a mi familia sin los cuales no sería nadie hoy. A ellos quiero dedicar las últimas palabras de esta sección. A mi hermana Aurora, esa gran personita que por mucho que nos chinchemos siempre será la mejor para mí. A mi madre Rosa María por enseñarme que la curiosidad y el afán por aprender deben ser una filosofía de vida. Y a mi padre Emilio que me ha inculcado que solo el trabajo y el esfuerzo sirven para lograr nuestras metas. Por vosotros hoy estoy aquí y seguiré adelante.

Gracias.

Abstract

The residential sector accounts for approximately 30% of the energy consumed in developed countries. This demand is currently covered not only by fossil fuels but also renewable energy sources that ensure a reduction in polluting emissions but which are generally distributed, generate intermittently and are difficult to manage. This requires the development of energy policies that reduce global consumption, as well as control and management systems that target the final consumer.

In order to deal with this issue a detailed knowledge of the consumers' behaviour is needed, both at an aggregate level for the management of the system and at an individual level for the development of measures to adapt their consumption. Furthermore, in this novel context, the feasibility of the different available strategies must be studied in addition to the benefits that can be obtained from their implementation and the control measures that can be developed.

This PhD Thesis addresses the development of an energy modelling system for the residential sector as a way of predicting the electricity demand in households and establishing demand response strategies, energy policies and control actions that ease the integration process of distributed energy resources accordingly.

The selected modelling technique follows the so-called bottom-up methodology, which enables the consumption in the residential sector as the sum of the individual contributions of each device installed in each household to be obtained. In addition, the simulation of these profiles is carried out using stochastic techniques that allow the heterogeneous and unpredictable behaviour of residents to be reproduced with a high temporal resolution.

The modelling system has been divided into three main components which include the consumption due to lighting systems, the heating and air conditioning devices demand and the general appliances consumption. This has facilitated a detailed study of different energy saving policies and the assessment of potential demand response strategies, as well as the development of novel energy management techniques.

All of these measures together with the modelling system have been implemented in a simulation tool which was also provided with renewable production data, collected in actual installations. Therefore, not only has the consumption been studied on its own, but also the integration of various resources has been assessed. Some of the studied measures are: replacing devices with more efficient technologies in the case of lighting systems, implementing low-level demand response strategies for household appliances, studying the impact on the low-voltage grid of increasing installation rates of certain technologies such as air conditioning systems and developing novel control techniques in the context of a smart community that can improve the hosting capacity of renewable solar production.

Finally, the models and strategies studied in this work have been combined with an advanced metering infrastructure under the umbrella of a smart building. In this context, they provided an additional source of information towards the digitalisation of the electrical system where the extensive use of data allows for the implementation of even more advanced control strategies and will undoubtedly lead to future developments under the paradigm of Smart Grids.

Resumen

El sector residencial representa aproximadamente el 30% de la energía consumida en los países desarrollados. Esta demanda está actualmente cubierta no solo por combustibles fósiles sino también por fuentes renovables que aseguran una reducción en las emisiones contaminantes, pero que generalmente se encuentran distribuidas, producen intermitentemente y son difíciles de gestionar. Esto exige el desarrollo de políticas energéticas que reduzcan el consumo global y sistemas de control y gestión que tengan como objetivo el consumidor final.

Solucionar estos retos pasa por conocer el comportamiento los consumidores, tanto a nivel agregado para la gestión del sistema, como a nivel individual para el desarrollo de medidas de adaptación de su propio consumo. Además, en este contexto novedoso es necesario estudiar la viabilidad de las distintas estrategias, los beneficios que se pueden obtener y las medidas de control adicionales que pueden ser desarrolladas.

La siguiente Tesis doctoral plantea el desarrollo de un sistema de modelado del consumo en el sector residencial como medio para predecir las necesidades de demanda eléctrica dentro de la red inteligente y establecer a partir de ellas medidas de respuesta a la demanda, políticas energéticas y acciones de control que ayuden a la integración de los recursos energéticos distribuidos.

La técnica de modelado escogida sigue una metodología bottom-up (de abajo a arriba) que permite obtener el consumo en el sector residencial como la suma de las contribuciones de cada dispositivo instalado en cada vivienda. Además, la simulación de dichas curvas se ha realizado mediante técnicas estocásticas que permiten reproducir el comportamiento heterogéneo y poco predecible de los residentes con altas resoluciones temporales.

El sistema de modelado se ha dividido en tres componentes principales que son el consumo en iluminación, el consumo en calefacción y aire acondicionado y el consumo en electrodomésticos de uso generales. Esto ha permitido un estudio detallado de las distintas medidas de ahorro energético y potenciales estrategias de respuesta a la demanda así como el desarrollo de novedosas técnicas de gestión energética.

Todas estas medidas junto con el sistema de modelado han sido implementadas en una herramienta de simulación en la cual se han incluido también datos de producción renovable recogidos en instalaciones reales. De este modo, no solo se ha estudiado el consumo de forma independiente, sino que diversas medidas energéticas han sido también evaluadas. Algunas de ellas han sido: la sustitución de dispositivos por tecnologías más eficientes en el caso de sistemas de iluminación, la implementación de estrategias de respuesta a la demanda a bajo nivel para los electrodomésticos disponibles en los hogares, el estudio del impacto en la red de baja tensión del aumento de determinadas tecnologías como los sistemas de aire acondicionado y el desarrollo de técnicas de control en el contexto de una comunidad inteligente que mejoren la capacidad de acogida de producción fotovoltaica.

Finalmente, los modelos y estrategias estudiadas han sido integradas junto con un sistema de contadores inteligentes bajo el paraguas de un edificio gestionable. En este contexto, han aportado una fuente adicional de información hacia la digitalización del sistema eléctrico donde el uso masivo de datos permite implementar estrategias de control aun más avanzadas y que dará pie sin lugar a dudas a futuros desarrollos.

Thesis Details

Thesis Title:	Stochastic Modelling and Integration of Distributed Energy Resources in the Smart Grid
Título de la Tesis:	Modelado Estocástico e Integración de Recursos Energéticos Distribuidos en la Red Eléctrica Inteligente
Author:	Emilio José Palacios-García
Supervisor:	Prof. Dr. Antonio Moreno-Muñoz
Co-supervisor:	Prof. Dr. José María Flore-Arias

Publications related with the PhD Thesis

1^{st} authored journal papers

[J1] **Palacios-Garcia E. J.**, Chen A., Santiago I., Bellido-Outeiriño F. J., Flores-Arias J. M., Moreno-Munoz A., Stochastic model for lighting's electricity consumption in the residential sector. Impact of energy saving actions. *Energy & Buildings* 2015;89:245–59. doi: 10.1016/j.enbuild.2014.12.028.

[J2] **Palacios-Garcia E. J.**, Moreno-Muñoz A., Santiago I., Moreno-Garcia I. M., Milanés-Montero M. I., PV Hosting Capacity Analysis and Enhancement Using High Resolution Stochastic Modeling. *Energies* 2017;10:1488. doi: 10.3390/en10101488.

[J3] **Palacios-Garcia E. J.**, Moreno-Munoz A., Santiago I., Flores-Arias J. M., Bellido-Outeirino F. J., Moreno-Garcia I. M., A stochastic modelling and simulation approach to heating and cooling electricity consumption in the residential sector. *Energy* 2017;144:1080–91. doi: 10.1016/j.energy.2017.12.082.

1^{st} authored book chapter

[B1] **Palacios-Garcia E. J.**, Moreno-Munoz A., Santiago I., Flores-Arias J. M., Bellido-Outeirino F. J., Distributed energy resources integration and demand response: the role of stochastic demand modelling. In: Moreno-Munoz A, editor. *Large Scale Grid Integration of Renewable Energy Sources*, London: Institution of Engineering and Technology; 2017, p. 245–78. doi:10.1049/PBPO098E_ch8.

Co-authored journal papers

[J4] Bellido-Outeirino F. J., Flores-Arias J. M., Linan-Reyes M., **Palacios-Garcia E. J.**, Luna-Rodriguez J. J.. Wireless sensor network and stochastic models for household power management. *IEEE Trans Consum Electron* 2013;59:483–91. doi:10.1109/TCE.2013.6626228.

[J5] Moreno-Garcia I. M., **Palacios-Garcia E. J.**, Pallares-Lopez V., Santiago I., Gonzalez-Redondo M. J., Varo-Martinez M., et al. Real-Time Monitoring System for a Utility-Scale Photovoltaic Power Plant. *Sensors* 2016;16:770. doi:10.3390/s16060770.

[J6] Santiago I., Trillo-Montero D., Luna-Rodríguez J. J., Moreno-Garcia I. M., **Palacios-Garcia E. J.**. Graphical Diagnosis of Performances in Photovoltaic Systems: A Case Study in Southern Spain. *Energies* 2017;10:1964. doi:10.3390/en10121964.

1^{st} authored publications in proceedings with peer review

[C1] **Palacios-García E. J.**, Flores-Arias J. M., Chen A., Quiles-Latorre F. J., Bellido-Outeiriño F. J.. Home energy management system based on daily demand prediction and ZigBee network. *2015 IEEE Int. Conf. Consum. Electron. ICCE 2015, IEEE*; 2015, p. 315–6. doi:10.1109/ICCE.2015.7066428.

[C2] **Palacios-García E. J.**, Guan Y., Savaghebi M., Vásquez J. C., Guerrero J. M., Moreno-Munoz A., et al. Smart metering system for microgrids. *IECON 2015 - 41st Annu. Conf. IEEE Ind. Electron. Soc., IEEE*; 2015, p. 3289–94. doi:10.1109/IECON.2015.7392607.

[C3] **Palacios-Garcia E. J.**, Moreno-Munoz A., Santiago I., Moreno-Garcia I. M., Milanes-Montero M. I.. Smart community load matching using stochastic demand modeling and historical production data. *EEEIC 2016 - Int. Conf. Environ. Electr. Eng., IEEE*; 2016, p. 1–6. doi:10.1109/EEEIC.2016.7555885.

[C4] **Palacios-Garcia E. J.**, Rodriguez-Diaz E., Anvari-Moghaddam A., Savaghebi M., Vasquez J. C., Guerrero J. M., et al. Using smart meters data for energy management operations and power quality monitoring in a microgrid. *2017 IEEE 26th Int. Symp. Ind. Electron., IEEE*; 2017, p. 1725–31. doi:10.1109/ISIE.2017.8001508.

Co-authored publications in proceedings with peer review

[C5] Bellido Outeirino F. J., Flores-Arias J. M., Linan-Reyes M., **Palacios-Garcia E. J.**. In-home power management system based on WSN. *Dig. Tech. Pap. - IEEE Int. Conf. Consum. Electron., Las Vegas, NV: IEEE*; 2013, p. 546–7. doi:10.1109/ICCE.2013.6487013.

[C6] Chen A, Gil-de-Castro A., **Palacios-Garcia E. J.**, Flores-Arias J. M., Bellido-Outeirino F. J.. In-home data acquisition and control system based on BLE. *2015 Int. Symp. Consum. Electron., vol. 2015–Augus, IEEE*; 2015, p. 1–2. doi:10.1109/ISCE.2015.7177780.

[C7] Rodriguez-Diaz E., **Palacios-Garcia E. J.**, Savaghebi M., Vasquez J. C., Guerrero J. M., Moreno-Munoz A.. Advanced smart metering infrastructure for future smart homes. *5th IEEE Int. Conf. Consum. Electron. - Berlin, ICCE-Berlin 2015, IEEE*; 2016, p. 29–31. doi:10.1109/ICCE-Berlin.2015.7391260.

[C8] Rodriguez-Diaz E., **Palacios-Garcia E. J.**, Savaghebi M., Vasquez J. C., Guerrero J. M.. Development and integration of a HEMS with an advanced smart metering infrastructure. *2016 IEEE Int. Conf. Consum. Electron. ICCE 2016, IEEE*; 2016, p. 544–5. doi:10.1109/ICCE.2016.7430724.

[C9] Santiago I., Trillo-Montero D., **Palacios-Garcia E.J.**, Moreno-Garcia I. M., Moreno-Munoz A.. Influence of photovoltaic installation angles and geographical dispersion in the smoothing of photovoltaic fleet power fluctuations. *EEEIC 2016 - Int. Conf. Environ. Electr. Eng., IEEE*; 2016, p. 1–6. doi:10.1109/EEEIC.2016.7555459.

[C10] Moreno-Garcia I. M., **Palacios-Garcia E. J.**, Santiago I., Pallares-Lopez V., Moreno-Munoz A.. Performance monitoring of a solar photovoltaic power plant using an advanced real-time system. *2016 IEEE 16th Int. Conf. Environ. Electr. Eng., IEEE*; 2016, p. 1–6. doi:10.1109/EEEIC.2016.7555473.

[C11] Ruiz-Garcia G., Flores-Arias J. M., Bellido-Outeirino F. J., Moreno-Munoz A., **Palacios-Garcia E. J.**, Quero-Corrales MA. Home Lighting controller based on BLE. *2017 IEEE Int. Conf. Consum. Electron. ICCE 2017*, 2017, p. 340–1. doi:10.1109/ICCE.2017.7889346.

[C12] Santiago I., **Palacios-Garcia E. J.**, Moreno-Garcia I. M., Gil De Castro A., Moreno-Munoz A.. Appliances in the residential sector: Economic impact of harmonic losses. *2017 11th IEEE Int. Conf. Compat. Power Electron. Power Eng. CPE-POWERENG 2017, IEEE*; 2017, p. 620–5. doi:10.1109/CPE.2017.7915244.

[C13] Rodriguez-Diaz E., **Palacios-Garcia E. J.**, Anvari-Moghaddam A., Vasquez J. C., Guerrero J. M.. Real-time Energy Management System for a hybrid AC/DC residential microgrid. *2017 IEEE 2nd Int. Conf. Direct Curr. Microgrids, ICDCM 2017, IEEE*; 2017, p. 256–61. doi:10.1109/ICDCM.2017.8001053.

The following PhD Thesis is presented as a collection of papers whose main body is composed of the book chapter [B1], three first authored journal articles [J1-J3], a first authored journal article submitted for consideration to Elsevier's Energy & Building journal and two first authored conference papers published in proceedings with peer review [C2] and [C4].

Contents

List of Tables

List of Figures

List of Acronyms

AMI	Advanced metering infrastructure
ANN	Artificial neural network
API	Application programming interface
BAN	Building area network
CDD	Cooling degree-days
CDF	Cumulative distribution function
CFL	Compact Fluorescent Lamp
CO	Continental
COP	Coefficient of performance
COSEM	Companion Specification for Energy Metering
CRI	Color Render Index
CSV	Comma separated values
CT	Current transformer
DCF	Demand cover factor
DER	Distributed energy resource
DG	Distributed generation
DLMS	Device Language Message Specification
DOD	Deep of discharge
DR	Demand Response
DSM	Demand Side Management
DSO	Distribution system operator
EEF	Exported energy factor
EEPROM	Electrically erasable programmable read-only memory
EMS	Energy management system
ENTRANZE	Policies to Enforce the Transition to Nearly Zero Energy buildings in the EU-27
ETP	Equivalent thermal parameter
EU	European Union
EV	Electrical vehicle
GA	Genetic Algorithms
GISCF	Grid interaction supply cover factor
GUI	General user interface
HAN	Home area network
HC	Hosting capacity
HDD	Heating degree-days
HETUS	Harmonised European time use surveys

HTTP	Hypertext Transfer Protocol
HVAC	Heating, ventilation and air conditioning
ICT	Information and communication technology
IDAE	Diversification and Energy Saving Institute
JSON	JavaScript Object Notation
LED	Light-emitting diode
LOLP	Lost of load probability
MDMS	Meter data management system
ME	Mediterranean
MSE	Mean square Error
MV/LV	Medium voltage/low voltage
NA	North Atlantic
NTP	Network time protocol
NVF	Normalised variation factor
PDF	Probability distribution function
PF	Power factor
PMF	Probability mass function
PQ	Power Quality
PV	Photovoltaic
REE	Red Eléctrica Española (Spanish DSO)
REMODECE	Residential Monitoring to Decrease Energy Use and Carbon Emissions in Europe
RES	Renewable energy source
RESTful	Representational state transfer
RMSE	Root mean square error
RTP	Real time prices
SCEMS	Smart community energy management system
SCF	Supply cover factor
SD	Standard deviation
SG	Smart Grid
SM	Smart Meter
SOC	State of charge
STR	Smooth transition regression
SVM	Support vector machines
TDU	Transmission distribution utility
THD	Total harmonic distortion
TOU	Time of use
TUS	Time Use Survey
UTC	Coordinated Universal Time
VAT	Valued Added Tax
VSI	Voltage source inverter
WD	Weekday
WE	Weekend
XML	eXtensible Markup Language

1

Introduction

1.1 The power grid

The energy system has undergone a radical transformation since its initial conception. This transformation focuses on four main points which include the integration of more efficient and less polluting energy sources, the reduction of final energy consumption, the expansion of the system's control possibilities and the establishment of a bidirectional flow not only limited to energy but also information [1].

This change has been evident for more than ten years in Europe, as well as, to a greater or lesser extent, in other developed countries, where a substantial increase in the penetration of renewable energy sources can be observed, as opposed to a reduction in fossil fuel-based technologies. All this aims to comply with the CO_2 emission limits and the targets established in the Kyoto Protocol [2].

This transformation over time can be clearly seen in the historical annual primary production data collected by the statistical office of the European Union Eurostat [3]. As can be seen in Figure 1.1 (a), between 2005 and 2015, the production generated by renewable energies (hydro, wind, solar and geothermal) in Europe has increased by more than 80%, currently meaning a quarter of the energy in the region as can be seen in Figure 1.1 (b), which represents the net energy generation for 2015.

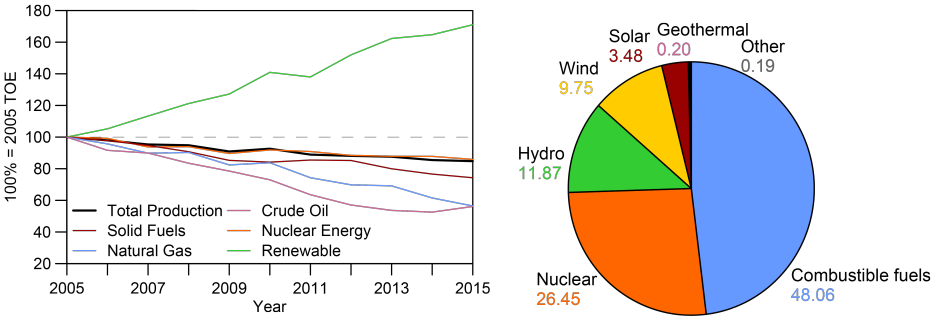

(a) Primary energy production by fuel from 2005 – 2015 **(b)** Distribution of primary energy sources in 2015

Figure 1.1: Primary energy production statistics in the EU28.

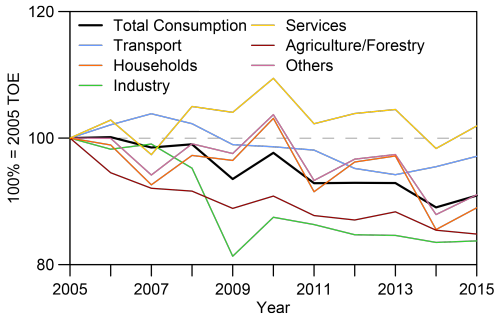

(a) Final energy demand by sector from 2005 – 2015

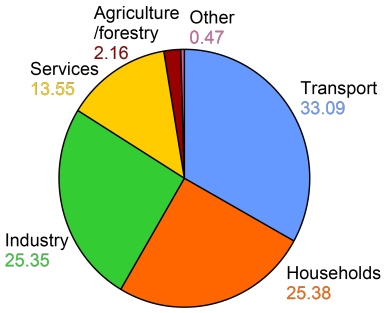

(b) Distribution of final energy consumption among sectors in 2015

Figure 1.2: Final energy consumption in the EU28.

Nowadays, however, the energy produced by combustible fuels is still the main source of generation and supply, accounting for almost half of primary energy production. Nevertheless, from 2005 – 2015, a decrease of around 20% has been achieved in the case of solid fuels, whereas natural gas and crude oil have decreased by 40%. Likewise, although to a much lesser extent, nuclear power plants have also reduced their share of primary energy.

At the same time, on the final consumption side, there is a reduction compared to the figures reached in 2005. Although the economic instability during this period may be responsible for the various increases and decreases observed over the last 10 years, it can be concluded that energy saving measures established in various sectors have also played a significant role in this reduction.

This can be seen in Figure 1.2 (a) where the trend in the annual consumption for different sectors has been represented, referencing all the figures to the consumption observed in 2005. Apart from the services sector, all of the others have shown a decrease in total energy consumption, which has been reduced in key sectors such as residential, industrial and transport by 15%, 17% and 3% respectively.

The significance of these figures can be seen in Figure 1.2 (b), where the percentage of final energy consumption represented by each sector in 2015 has been collected. Thus, a small reduction in sectors such as transport, which accounts for 33% of demand, or the industrial and residential sectors, which together account for half of the final consumption in Europe as a whole, can bring about significant energy, environmental and economic savings.

1.2 The residential sector

Of the various sectors described in the previous section, the residential one, given its flexibility and heterogeneity, may have the greatest potential for improvement. As has been stated, household consumption in some European countries may account for around 30% of the total demand, which is almost entirely covered by fossil fuels.

In the last 10 years, this consumption has experienced a decrease of around 0.9% in the European Union as a whole, with even better results in individual countries such as the UK with a 14% reduction, Germany and Portugal with 10% and the surprising case of Belgium with 28%. Other countries, such as Sweden, Italy and Denmark, showed little significant variation from their situation in 2005.

In contrast, some EU countries presented an opposing trend due to the increase in the number of dwellings and their purchasing power, which has led to higher standard of comfort, and more numerous household appliances. This is the case for countries such as Romania (30%), France (10%) and Spain (12%).

This global consumption is composed of a series of smaller demands that are heterogeneous and difficult to quantify with accuracy. These consumptions are due to elements such as household lighting systems, appliances and general-purpose equipment or heating and cooling devices in their most generic form.

In the particular case of the aforementioned Spain, which will be the main case of study in this Thesis, there has an upward trend in its energy consumption and the division of these consumptions can be established according to Figure 1.3. In this graph, the total consumption of a household has been broken down into its various components dividing them into groups that retain a series of common influence factors and indicating the main appliances found in the country for each group.

Starting from the base of the graph, the consumption due to the lighting system in the dwelling can be found, which accounts for approximately one-fifth of the total demand [4, 5]. The average figure for this consumption in Spain has a typical value of around 470 kWh per year and household. Lighting spots installed in the home are responsible for this demand and they can present different technologies such as (Compact Fluorescent Lamps) CFL, halogen, (Light-emitting diode) LED, fluorescent or incandescent. The latter, despite its purchase having been prohibited after the European directive 2005/32/EC is still present in many homes [6]. The main influence factor, as would be expected, is the availability of daylight in the dwelling when there is an active occupancy which determines the periods during which it will be necessary to use artificial light.

The next consumption that can be seen in the graph is due to heating and cooling systems. The amount of this consumption among the total energy demand of the dwelling is not as easy to evaluate as the previous one, given the drastic climate differences between the different regions. However, as an average, between 15% and 18% of the total electrical consumption can be attributed to these types of devices. This percentage is shared among the heating and cooling systems, in general, the heating one being the largest term [7]. As regards the influence factors, in addition to the active occupancy of the residents, the ambient temperature plays a key role in shaping the daily consumption profile. Nevertheless, parameters such as the insulation of the building or the possible solar gains can have a significant impact on this percentage [8].

Finally, the last five blocks represent what can be denoted as appliances consumption. Its contribution is the most important of the three divisions under consideration, since it covers the energy expenditure associated with food preservation systems such as refrigerators and freezers (18%), cooking systems such as ovens,

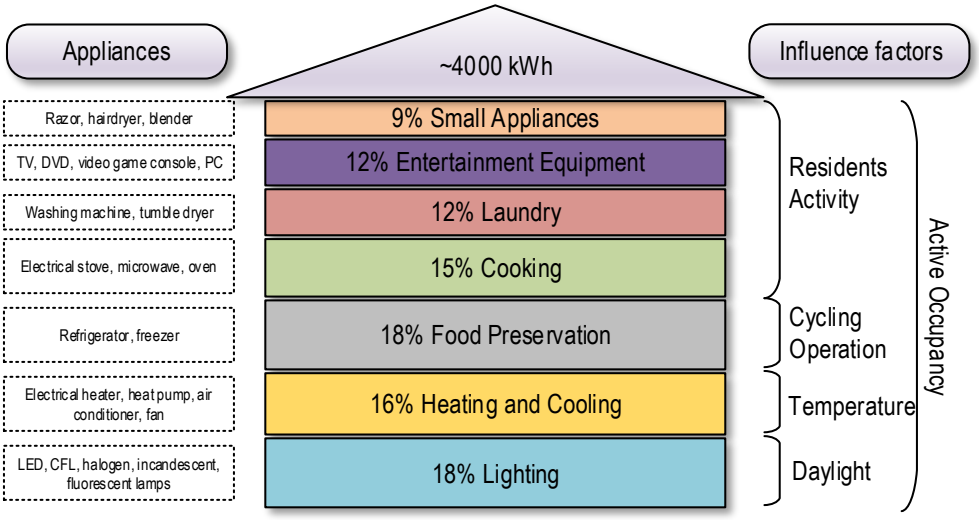

Figure 1.3: Distribution of energy consumption in a household. Associated appliances and main influence factors.

microwaves or electric stoves (15%), laundry equipment (10%), entertainment systems such as televisions and PCs (10%) and other small household appliances (7-9%), The average energy consumption figure for these five groups together is almost 3.000 kWh out of the total 4000 kWh estimated per household and year [9]. Some of these devices operate uninterrupted according to duty cycles regulated by thermostats such as food preservation appliances. Nevertheless, the rest of them depend exclusively on the activities undertaken by the occupants at home, so their consumption is relatively difficult to predict by merely observing the occupancy levels and must be related to additional variables.

1.3 The Smart Grid

The previous sections have clearly explained the problems existing in the current power grid. On the one hand, there is a great penetration of different renewable energy sources that ensure low or even zero carbon emissions, but with disadvantages such as poor manageability and intermittent and unpredictable production. On the other hand, the consumer elements are heterogeneous and difficult to predict which decrease even more the manageability of these renewable sources.

The energy policies and measures developed in this context are committed to reducing global energy consumption, as well as designing advanced demand control or demand response (DR) strategies that can achieve a better balance between generation and consumption. These measures will avoid the overload or collapse of the current electricity system, while looking towards the scenario of an intelligent electricity grid or Smart Grid and advanced consumers [10].

In this way, the classical idea of a centralised production network where users are just passive agents of the system is doomed to failure. Thus, as it is shown in Figure 1.4, the electrical system is evolving from the previous unidirectional flow of energy and information to a complex scheme of two-way energy flows that require exhaustive coordination of the parties and therefore active communication not only from producers to consumers, but also in the opposite direction [11].

What is more important, is this decentralisation of the production gives room for the end-users to have on-site generation systems. These installations can exclusively be used for self-consumption or they may inject the surplus production into the grid taking advantage in some cases of feed-in tariffs. Thus, the end user also becomes an active element in the system that can negotiate with the energy, buying and selling, therefore adopting the role of prosumer [12].

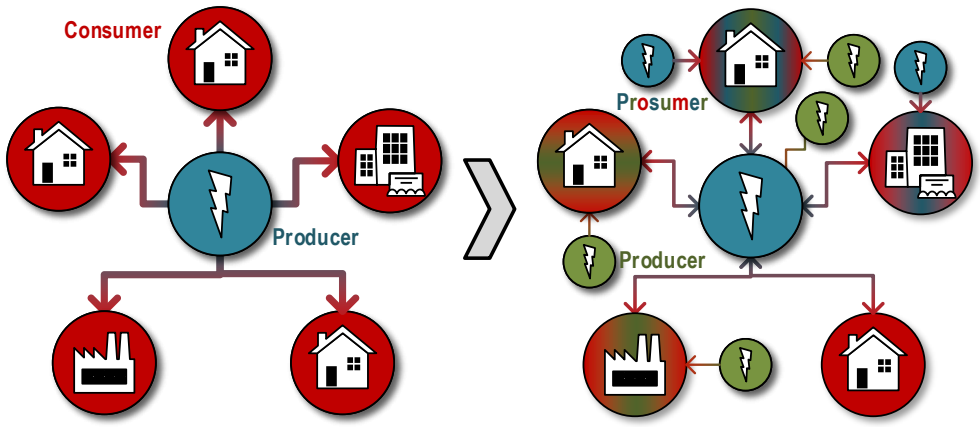

Figure 1.4: Conceptual comparison between the classical power grid and the Smart Grid.

Against this backdrop of technological challenges and difficulties that the paradigm of Smart Grid has introduced, this Thesis raises two main questions which are the cornerstones of the work:

- How can the heterogeneous behaviour of consumers be modelled and predicted with the sufficient time precision needed to interact with variable renewable resources over time?
- What integration actions can be carried out between these elements and what real impact/benefit can they have on the Smart Grid?

1.4 Load modelling and forecasting

Forecasting and assessment models have been used for decades in a multitude of disciplines ranging from medicine to the stock market and weather forecasting. Furthermore, there are already models for planning the production and operation of the power system, as well as optimizing primary resources according to demand, otherwise, it would be impossible to manage the grid. However, few of these works focus on understanding the consumers' side at a low level.

The current context of integration of distributed renewable energy (DER) sources, new equipment and greater end-users participation in the electricity system makes it necessary to develop advanced tools to model this demand. These models can be used both as prediction tools for making decisions concerning the management of the system, as well as evaluation tools that allow the impact that future measures and energy policies may have on the electricity grid to be estimated [13].

Thus, taking into account the perspectives discussed in Section 1.1 and the new Smart Grid paradigm presented in Section 1.2, the focus is now on the end-user due to the development of the aforementioned two-way energy and information flow. This involves the use of modelling techniques with particular characteristics. The following subsections describe the main features that differentiate consumption models, the main impact factors included in the estimations and a brief review of the most used methodologies in this field.

1.4.1 Characteristics of a model

According to the classification work carried out by Kuster *et al.* [14], there are three characteristics in the results provided by load prediction models that differentiate them and define their scope and validity. These characteristics are:

- The **scale** which determines the aggregation level used by the system. In other words, what is the minimum unit being modelled for the predictions. This unit can be a type of appliance, a house or building, a district or even cities and entire countries.
- The **time horizon** that indicates the timeframe in which the model is able to make predictions. Such timing can range from very short-term to long-term or very long-term forecasts.
- The **temporal resolution** which should not be confused with the time horizon or timeframe. While the previous one indicates the period for which predictions can be made, the resolution indicates the minimum time step for which results are obtained using the model. There are models that can provide results below one hour, as well as others whose minimum estimation period is one year.

The influence of these variables is conceptually illustrated in Figure 1.5. As it can be seen, the Y-axis indicates the aggregation scale of the consumption curve which can correspond to a group of dwellings considering that the given unit is MW. On the other hand, the X-axis indicates the time horizon, which for this case is clearly one day. Similarly, the X-axis minimum interval between two consecutive datum can be observed to be less than an hour.

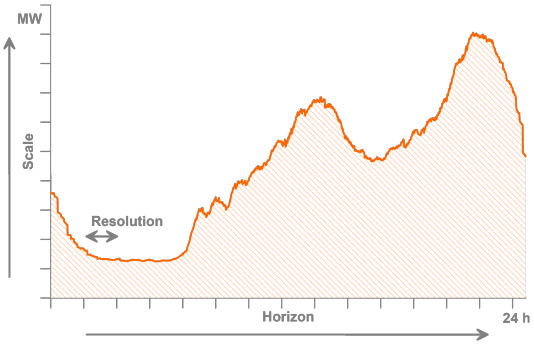

Figure 1.5: Conceptual representation of the output characteristics of a load model.

1.4.2 Influence factors

The previously discussed output characteristics are obtained from models that have a series of influence or input factors. These factors might have different natures and are closely related to the methodology used. In this way, there are cases in which input variables can cover different fields such as physical laws, social behaviour, economic indicators or climatic properties, whereas other methodologies do not even use external or exogenous factors other than the consumption data by themselves.

Different previous studies have shown that, especially in the field of buildings, which naturally concerns the residential sector, five groups of influence factors can be distinguished [15, 16]. These parameters are comprehensively analysed in the review conducted by Ma *et al.* [17] which are summarised as:

- **Building indoor conditions**: They comprise of all of the elements of influence within a building or house. Three entities are generally included in this group which are: (i) consumer devices or elements, which group together appliances, lighting systems and HVAC systems; (ii) occupants, whose interaction with such devices determines the intervals, intensity and duration of the consumption; (iii) the required internal conditions, which may be imposed by the legislation, such as in the case of buildings that develop a regulated economic activity or that will depend on the comfort demanded by users in private homes.

- **Building design characteristics**: This group includes the inherent properties of the building such as construction materials, floor area, façade dimensions, shape and orientation, etc. Their main interest lies in the estimation of HVAC consumption, which is highly dependent on the enclosure, although the window area also has a significant influence on the consumption of lighting systems.

- **District layout**: This element refers to the distribution of activity types in buildings and houses with different characteristics, as well as the physical layout in which they are distributed. Thus, with respect to the first criterion, there may be buildings with varied economic activities or houses with a different number of residents or family types that affect their consumption. In terms of physical distribution, the density of buildings can influence other factors such as weather conditions or limit the interaction between them.

- **Local Climate**: These are the atmospheric variables that influence the studied region. Depending on the main goal of the model, these variables will require a greater or lower granularity and time horizon. Temperature, humidity, solar radiation and wind speed can be pointed out as the most common ones. Sometimes, depending on the purpose of the model, global indicators, such as heating degree-days (HDD) and cooling degree-days (CDD) are employed over the temporal profiles.

- **Social and economic factors**: They refer to the characteristics and capabilities of final consumers. The main variables of influence are monthly incomes, education level and the cost of energy, variables which mainly influence users' behaviour in terms of energy (environmental awareness, energy expenditure) and the availability of resources (number of appliances, types, efficiency, etc.).

1.4.3 Methodologies

These characteristics and influence factors result in a wide range of modelling methodologies. In this context, a large number of attempts have been made to classify these models according to their methodological characteristics [14, 17–22].

Nevertheless, as proposed in Swan and Ugursal's work [18], most classifications concur in distinguishing between the so-called top-down and bottom-up models. This denomination comes from the directionality that exists in the prediction of the final consumption and determines to a certain extent the influence factors that are likely to be used. Moreover, some authors add a third category called hybrid models that collect methodologies that use both principles.

As far as the different subcategories within each group are concerned, a wide variety of alternatives can be found in the literature. In our case, the most comprehensible classification is the one obtained by combining the work of Swan and Ugursal [18] and Fumo [22]. The structure of this classification is shown in Figure 1.6 and will be discussed in the following subsections.

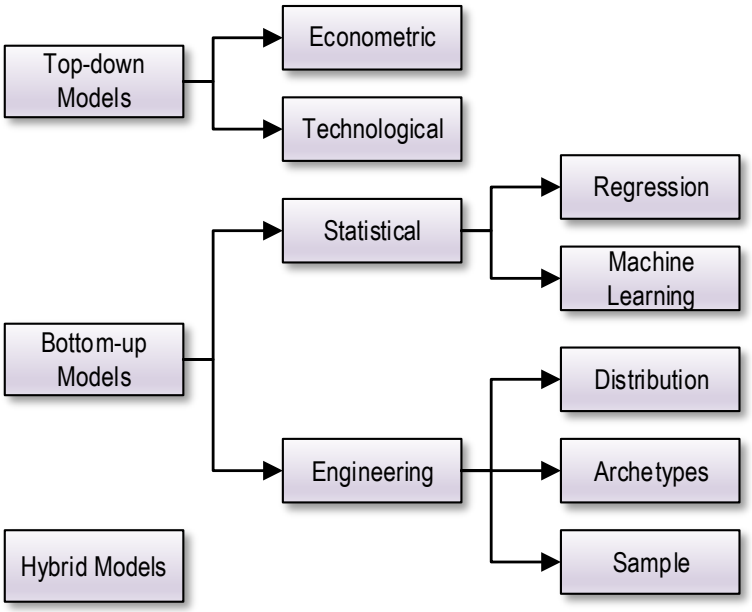

Figure 1.6: Classification of the energy consumption modelling techniques.

1.4.3.1 Top-down models

The consumption estimation of top-down models is based on variables that belong to the whole sector. Therefore, the individual entities are taken as energy sink units without considering the underlying demands that produce these consumptions.

These modelling techniques are mainly used in the planning of the network, as well as in the study of historical trends by means of aggregated consumption data which are widely available. Nevertheless, they lack the resolution and disaggregation to forecast the impact of new energy trends and resources integration.

These models were further divided by Swan and Ugursal [18] into econometric and technological models:

- **Econometric** models are mainly based on energy or appliances prices, and other elements such as the acquisition power of users.

- **Technological** models are focused on general characteristics of the total housing stock, referring to elements such as the percentage of equipment ownership.

It should be mentioned that such models generally use similar statistical data and techniques derived from economic theory. However, in addition to the classical regression and analysis techniques of time series, some authors have applied genetic algorithms with a top-down philosophy. It should also be highlighted that the econometric and technological components are generally used together to improve the quality of the results.

1.4.3.2 Bottom-up models

The estimation of the consumption in bottom-up models is made by means of input data that are located at a level lower than the energy demand. In this way, the total consumption is the result of individual elements that influence and shape it.

Given their great flexibility and the possibility of modelling low-level elements, they are of great interest in the study of the integration of new energy sources, appliances and behavioural changes as they can use a wide range of input variables and methodologies.

As can be seen in Figure 1.6, they can be classified into two large groups that use statistical methods or engineering techniques.

Statistical methods

The existence of a large number of consumption historical records provides a basic source of information for the application of statistical techniques in the demand study. Therefore, statistics-based models are one of the most commonly used.

In the field of building energy modelling, this group is also sometimes referred to as black-box models because they take the whole building as a box of uncertain inner behaviour that has some input variables which result in a final consumption.

Depending on the treatment of this information, two basic types of modelling can be distinguished.

- **Regression**: Using classical statistical techniques, the regression coefficients needed to create a model are determined. This technique aims to predict the consumption with a certain degree of uncertainty based on a series of input parameters, and always seeking the maximum simplicity. In addition, the influence of exogenous parameters such as occupancy profiles can be incorporated. Furthermore, conditional demand analysis (CDA) techniques make it possible to limit the study of the consumption to the presence of certain appliances installed by the user. In this way, it is possible to determine not only the total demand but also the individual consumption of each element.

- **Machine learning**: In addition to the above-mentioned classical statistical techniques, three machine learning techniques stand out in the modelling of energy consumption. These techniques are genetic algorithms (GA), artificial neural networks (ANN) and support vector machines (SVM). The importance of these techniques lies in their ability to solve non-linear problems, even when the amount of training data is limited such as in the case of SVMs.

Engineering methods

The final energy consumption can be also predicted from the behaviour of low-level consumer entities. Thus, bottom-up models based on engineering techniques use the physical modelling of appliances, thermodynamic principles, etc. Hence, they are often called white-box models in relation to building consumption since every element inside the construction must be known and characterised by means of physical laws.

These types of models provide a higher degree of flexibility than the statistics-based ones and the potential to model new types of appliances. In addition, they are the only ones that allow estimations to be made without the necessity of having a previous historical record of the energy consumption. However, they generally make use of variables that are relate to users' behaviour, which is difficult to predict.

Three techniques can be distinguished:

- **Distribution**: These models use appliances distribution data in each home and the usage rates of those appliances to estimate the consumption. Data related to the appliances time of use, consumption values and efficiency are then required for the calculation. Within this division, the models classified as Time of Use models by Grandjean *et al.* can be found [19]. This modelling technique was selected in this Thesis because of its characteristics and flexibility. Further details and justification for their use will be given in Chapter 2.

- **Archetype**: This methodology categorises the dwellings according to a series of characteristics such as age, size, type of house, etc. Next, a series of archetypes are created and used as input variables in the energy model. From these archetypes and the information from their distribution within an area, the extrapolation of the total consumption in the region is possible.

- **Sample**: This technique is based on the monitoring and collection of data from a wide variety of dwellings in an area so that a representative population can be obtained. From these data, different estimation models can be constructed with great precision and detail. Nevertheless, it requires a large sample, investment and the management of a large volume of information.

1.4.3.3 Hybrid models

In many cases, the complexity of a system or the lack of information makes it necessary to combine elements that belong both to a higher and a lower level than the consumption to be predicted. These models, especially applied in the prediction of thermal consumption or related heat transfer problems are denoted as hybrid models [20, 21].

These types of models are also designated in the literature as grey, grey-box, or statistical-engineering models, the latter having a great relationship with their mode of operation. The hybrid models are mainly bottom-up models that use engineering methods whose data have been adjusted by means of statistical elements, which are generally at a higher level than the consumption to be estimated.

In this way, a balance between complexity and accuracy can be achieved. The main reason for that is that knowing all the physical parameters that influence the consumption would lead to an unapproachable or even mathematically unsolvable system. On the other hand, relying only on statistical data provides little information on the origin of the consumption and the measures that could be taken to reduce or improve it. These models are therefore a technical optimal solution in some cases.

Finally, and as a conclusion to this section, it should be noted that, although some models perfectly fit into one of the proposed divisions, in most cases the barriers between them are not clear, and characteristics that fall into more than one category can be found. Nevertheless, they all ultimately seek to achieve the prediction of the energy consumption with the greatest simplicity and precision, always related to a main objective.

1.5 Resources decentralisation

The previous section has shown everything related to energy consumption modelling, one of the fundamental elements of this work. However, this modelling pursues a practical objective within the current energy context and the paradigm of Smart Grid.

The Smart Grid has associated a decentralisation of the typical resources that form part of the network. This concept is currently not only limited to the installation of new DER sources, but it also includes a series of additional measures related to users' behaviour, control and communications systems, and disruptive technologies.

Thus, parallel to the integration of DER, storage systems and the interaction with the main grid, the impact of energy policies and the promotion of certain user behaviour on the network should also be considered. Similarly, the assessment of whether advanced control actions that can be taken to manage energy not only at the production level but also at the end-user level must be studied. Finally, the additional requirements of potential future scenarios should be evaluated.

In all these areas, the previous modelling techniques would be suitable for the evaluation phase as well as prediction tools which might be integrated into control systems. A brief overview of these challenges is included below justifying the key role of models within the Smart Grid.

1.5.1 Distributed generation and storage

As already mentioned, the power grid was originally designed to support unidirectional energy flows. In the new context of the Smart Grid, although the central energy generation will be reduced, the system will have to deal with diverse and concurrent flows from different points and end users.

Likewise, end users may in many cases incorporate storage systems which must be charged and discharged according to the availability of the DER or even based on external price signals provided by the distribution system operator (DSO).

Furthermore, these storage systems can be used not only by the users but also in a cooperative way by the DSO, in order to avoid network congestion taking an active part in the network planning operations. Eventually, given the massive injection of renewable energy at certain periods of the day such as at midday for solar production, the system stability can also be improved and ensured by these means.

Therefore, as shown in Figure 1.7, the combination of production with storage systems and grid interaction must be studied in parallel with the users' consumption. The aforementioned models will provide the estimation of the users' behaviour and will help to understand the complex relationships between all of the elements.

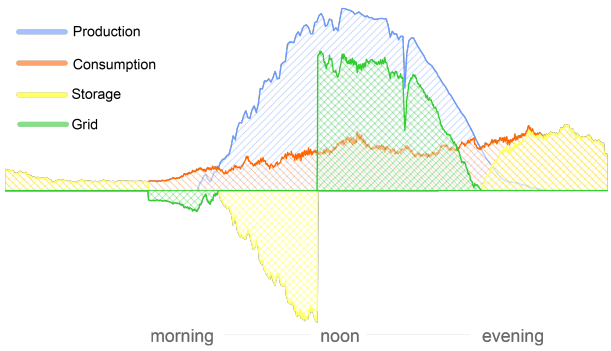

Figure 1.7: Conceptual scenario. Integration of renewable generation and energy storage systems.

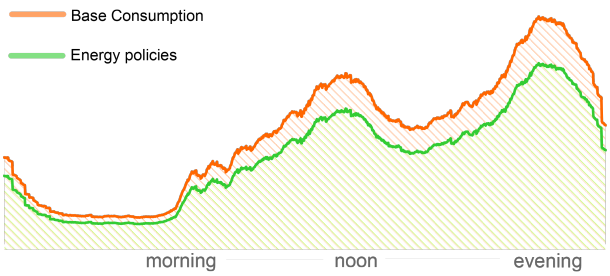

Figure 1.8: CConceptual scenario. Integration of more efficient appliances and energy policies.

1.5.2 Energy efficiency

In spite of the existence of numerous energy measurement programmes that seek to improve the efficiency of the system, its projection over time and the possibilities of adoption by users are difficult to predict and quantify. In addition, most of them are based on the use of innovative technologies and incentives whose benefits must be evaluated.

As presented in Figure 1.8, this strategy aims to go from an aggregate base consumption to a lower one after the integration of new elements and more efficient consumer devices at the individual level. In this context, the predictions that can be generated by consumption models are of great value. First, to assess the base situation and subsequently, to estimate the potential improvement. In order to achieve this goal, the load curve should be generated based on the real profiles of the individual devices which would allow an effective prediction of the real impact of these actions.

1.5.3 Demand Response

In addition to the integration of DER and more efficiency technologies, the new active role of the consumer in the Smart Grid through so-called DR programs is also a key development. Such programs can provide considerable savings for consumers whereas contributing to better network planning. However, there are still factors to be considered.

One of these main factors is the introduction of external signals such as variable energy prices, off-peak and peak tariffs, or curtailment strategies to limit the consumption under certain conditions. This information should be provided by the DSO in a way that allows its integration into the users' planning systems.

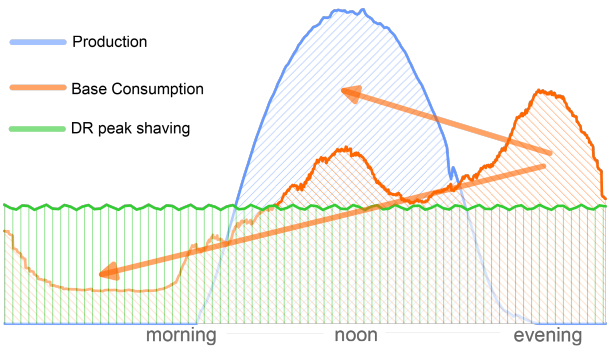

Figure 1.9: Conceptual scenario: Integration of DR strategies for peak shaving.

Likewise, the aggregate impact of such programmes must be also analysed, as not all end-users may either be willing to accept these programs or set the same management criteria, which may be beneficial on an individual basis, but go against the system as a whole.

One of the most popular DR strategies is the peak shaving represented in Figure 1.9. This technique promotes a consumption shift to periods with renewable production or to night-time hours where energy is cheaper. In this way, a final flat load curve is achieved which also eases the planning of the system.

For all the aforementioned reasons, the possibility of having a model that can simulate the DR actions at the individual users level, evaluating how they react to price signals and the influence of their willingness to accept or decline such measures offers a decision tool that can be used in both the evaluation phase and the daily system planning.

1.5.4 Future scenarios

Finally, new elements are being incorporated into the electricity grid whose role has not yet been determined. The clearest case in this context is the electric vehicle (EV), an emerging technology that introduces new management and control possibilities in the network as well as new challenges.

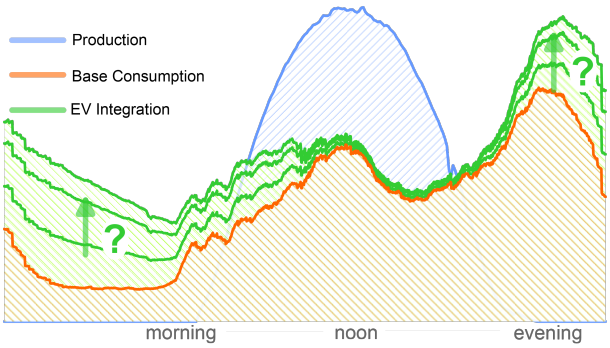

Figure 1.10: Conceptual scenario. Integration of new elements such EVs in the grid and the associated uncertainty.

This disruptive technology can reshape the current consumption curve in many ways as shown in Figure 1.10. Nevertheless, given its recent incorporation, the real impact is not yet unknown. Low-level consumer models can help to include these new technologies as additional loads on the consumer side, so a clearer view of the change and benefits that they will bring can be given, as well as whether it is necessary to reinforce the currently available infrastructures for their incorporation.

This, therefore, makes it clear that the integration of distributed resources goes hand in hand with the knowledge of consumers' behaviour by means of modelling techniques which are the basis for the management and evaluation of the Smart Grid nowadays.

1.6 Smart Meters: Toward energy digitalisation

Up to now the importance of modelling and resource management for the Smart Grid has been highlighted, which justifies the work carried out in this Thesis. However, this development cannot turn its back on the current context and be limited to a mere theoretical tool. Instead it must be able to be integrated into the current ecosystem of massive data intercommunication towards the so-called energy digitalisation.

The most visible element of this trend without any doubt is the incorporation of smart metering systems in households, which have been widely deployed in several countries [23] and are intended to be the standard

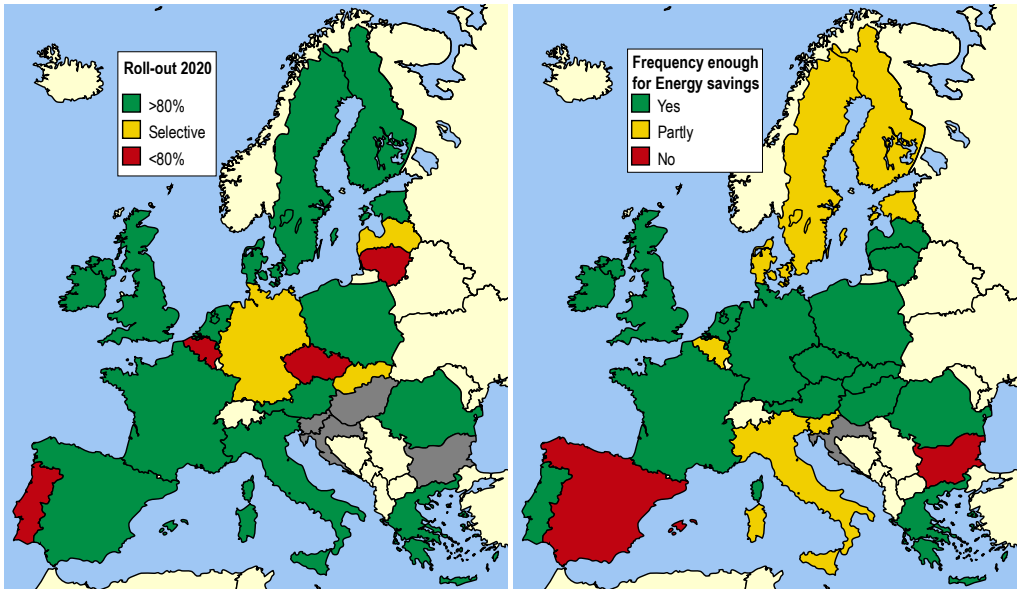

(a) Smart Meters roll-out by 2020

(b) Reading frequency enough for implementing energy saving actions

Figure 1.11: Potential for smart metering infrastructures in the EU28.

for 2020 in the European Union as shown in Figure 1.11 (a). These systems, as presented in the latest report of the European Union Joint Research Centre [24], have in most cases a reporting frequency which is sufficient to allow for the direct implementation of energy saving measures, as can be seen in Figure 1.11 (b). However, even in the cases where this frequency is not enough for direct saving measures, they can indirectly be implemented by means of the data reported by the DSO or the retail electric provider.

These saving measures can be developed due to the advantages that these Smart Meters present over conventional systems that make them to stand out as a key technology in the Smart Grid. Whereas conventional meters were only used for energy measurement in one direction and generally by manual data collection, the new Smart Meters present the following advantages:

- Remote data collection by means of data concentrators and central processing units.
- Bidirectional communication based on international standards: DLMS/COSEM (IEC 62056 53 and IEC 62056-62), M-Bus (EN 13757), SML (IEC 62056-58) or IEC 61850.
- Advanced measurements such as total harmonic distortion (THD), voltage events (Sags and Swells), voltage unbalances, etc.

In this way, as can be seen in Figure 1.12, the energy measurement chain is undergoing a drastic transformation from the classic manual collection (blue area), to automated meter reading (AMR) with no human intervention (pink area), and finally, the novel context of advanced metering infrastructures (AMI).

These systems have direct benefits for end users as they allow the remote collection of consumption data for billing purposes without the need for estimations, as well as the possibility of integrating equipment measurements into the so-called in-home displays, devices that show instantaneous consumption and even make recommendations based on consumption habits.

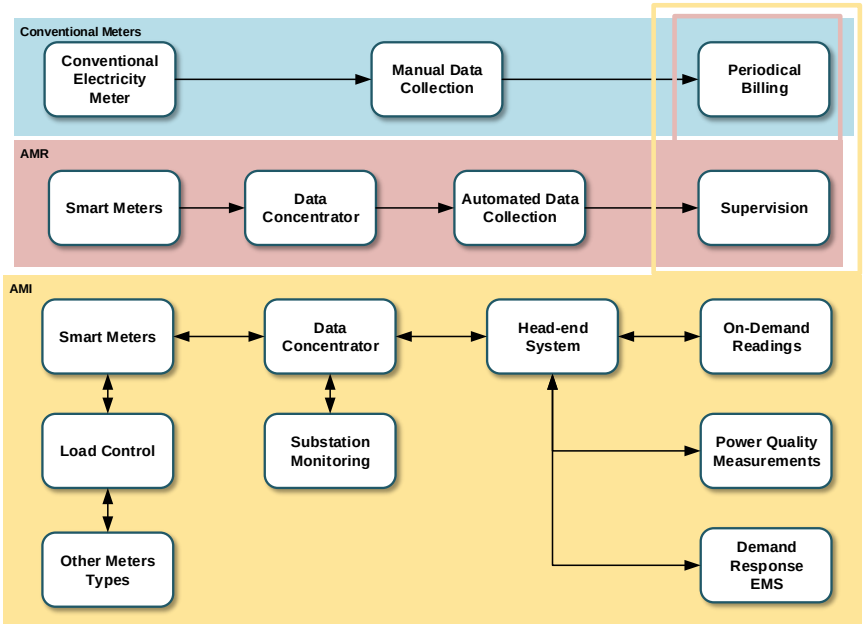

Figure 1.12: Evolution in energy metering systems capabilities.

They also present many advantages from the point of view of the DSO, allowing the integration of dynamic billing with real-time prices as discussed in the previous sections, the remote control of power flows and, in some cases, monitoring various power quality indicators.

Nevertheless, although initially conceived as advanced energy billing tools, they have become active management elements of the Smart Grid. Taking into account the sampling speed of the measurements, which are usually carried out in intervals of 5, 10, 15, 30 or even 60 minutes, their data can be incorporated into energy management systems together with other elements such as the presented models above.

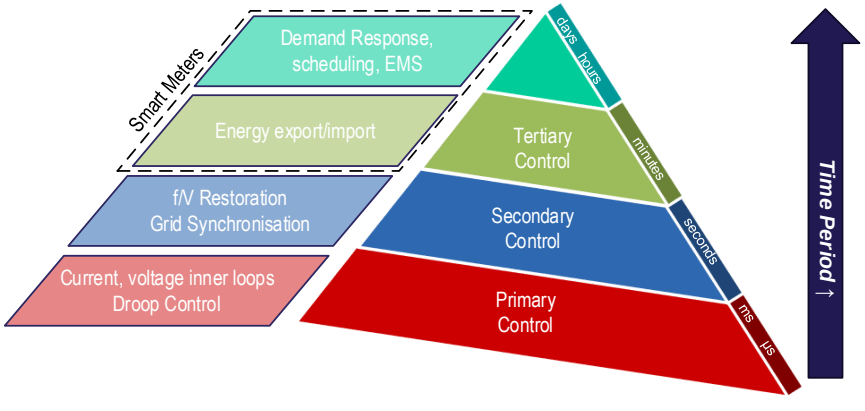

Figure 1.13: Integration of Smart Metering system in the hierarchical control scheme of the grid.

Hence, Smart Meters can be considered to be located in the upper layers of the control scheme, usually denoted as tertiary control, shown in Figure 1.13. In these layers, the Smart Meter data can assist in monitoring and controlling the energy exchanges of each consumer within the electric network, as well as at a higher level, in the development of strategies and algorithms for DR.

This point means the convergence of both the models developed in this Thesis and the study of the integration of DER since the combination of monitored data with the model allows different optimization algorithms to be carried out. For this reason, as will be seen throughout the development, the model has also been equipped with communication mechanisms that allow its data to be seamlessly integrated into the digital architecture of the electricity grid.

1.7 Objectives

Based on all of the points previously discussed, the main aim of this Thesis is the study and development of a simulation model that enables the application and evaluation of the different DR techniques and energy policies, to manage and control the energy supply, in a context of high penetration of distributed energy resources, ensuring the reliability of supply and fulfilment of the customers' needs at all times. This primary objective can be broken down into the following secondary objectives that are presented in this section.

1. To investigate the different energy demand modelling techniques, and to analyse the procedures, algorithms and data used in these models.

2. To study the various existing techniques for the development of DR algorithms.

3. To develop a model for energy consumption simulation in the context of a smart community. This model should provide a high temporal resolution and a high degree of disaggregation so DR techniques can be applied and assessed.

4. To analyse the consumption patterns generated by the model and identify the different actions that might be taken to maximise the use of renewable resources and minimise the energy consumption.

5. To develop and apply the aforementioned techniques for DR.

6. To analyse and validate the behaviour of the developed techniques and to study the impact that their implementation would have on the integration of distributed resources and energy saving actions.

1.8 Methodology

Taking into account all aforementioned objectives, the methodology employed in this Thesis combines the classical modelling approach procedure with assessment strategies, programming and evaluation indices. The guidelines followed are presented in this section.

1. Analysis of the state-of-art energy modelling and DR techniques, with a special interest in stochastic simulation algorithms.

2. Definition of the modelling technique(s) to be used.

3. Specification and collection of data required for the development of the model

4. Implementation of the simulation model using a high-level programming language.

5. Validation of the modelling system.

6. Study of the demand cover and supply usability factors of different types of renewable and distributed energy resources. This will preferably be done by means of historical data from different installations.

7. Location of potential actions to be taken in relation with DR strategies.

8. Implementation of the DR algorithms using a high-level programming language.

9. Integration of these algorithms into the consumption simulation and modelling system.

10. Planning a simulation scenario that integrates modelling, DR strategies and distributed energy resources data to test and assess the measures adopted.

11. Discussion and estimation of the improvements brought about by the adopted techniques and the feasibility of their implementation.

1.9 Outline

This PhD Thesis is presented as a collection of papers. Therefore, the main body is composed of a series of articles, book chapters and peer-reviewed conference papers which have been previously published or that have been submitted for consideration to relevant international journals with impact factor (JCR indexed). The document is organised as follows:

- **Chapter 2** presents the book chapter published in *'Large Scale Grid Integration of Renewable Energy Resources'*, edited by the prestigious and worldwide recognised Institution of Engineering and Technology (IET). In this chapter, a global insight into the development that has been carried out is given. First, the methodology employed for modelling the domestic energy consumption is contextualised among the currently available techniques. Subsequently, the subsystems that compose the demand model are presented in brief, as well as the basic principles that make it possible to implement and evaluate the different DR techniques, energy policies and integration of distributed renewable resources. Those points will be addressed in detail in the following chapters which are focused on the different subsystems of the model.

- **Chapter 3** contains the paper published in Elsevier's *Energy & Buildings* Journal (Q1). This article develops the consumption model for domestic lighting systems, the first piece of the global simulation system. This consumption was simulated by means of a stochastic model whose main input element is the active occupancy of dwellings. This occupancy, together with the availability of daylight and the switch-on period of the devices, made it possible to model the consumption of lighting systems with a resolution of 1 minute. This model was implemented and validated for Spain by comparing the results with previous developments carried out by other authors in other locations, as well as global indicators of energy consumption intensity. Likewise, the ability of the system to take into account the distribution of lighting technologies (LED, CFL, Halogen, Fluorescent and incandescent) and their associated powers, allowed for an impact assessment of the new LED and CFL lighting technologies on the consumption and the power quality, as well as the potential economic savings.

- **Chapter 4** includes the article published in Elsevier's *Energy* Journal (Q1). It addressed the modelling of the consumption of electrical heating and cooling devices in the residential sector. Like the previous model, the fundamental input datasets are the active occupancy profiles. However, in this case, this occupancy is combined with a function that relates the ambient temperature to the energy consumption intensity. The function was obtained by means of smooth transition regression (STR) techniques. This methodology allowed us to model the increment in energy consumption both for temperature increases and decreases from an equilibrium temperature where the consumption is insensitive to temperature.

The combination of both elements made it possible to model the electrical consumption in heating and cooling with 1-minute resolution in the context of Spain. The system was calibrated for the studied location and the results validated with data obtained in submetering campaigns developed in other countries. Finally, the model highlighted the great importance of this consumption in Spain due to the high penetration rate of heating equipment powered by electricity, as well as air conditioning in the southern region. In this way, the load duration curve showed that the annual heating consumption figures are significantly high but distributed over long periods of time. On the other hand, the air conditioning curve showed lower yearly demand figures but with a high concurrence in time that might lead to a system overload if the current upward trend is maintained.

- **Chapter 5** contains the article submitted to Elsevier's *Energy & Buildings* Journal (Q1). This article develops a modelling system for appliances consumption in the residential sector. The demand of these devices was simulated based on the active occupancy of the dwellings and its relationship with the activities carried out by the residents at home such as cooking, doing the laundry, ironing, etc., which have a variable probability distribution throughout the day and are associated with specific energy consumptions. These probabilities were combined with different types of household appliances, which were simulated by means of fixed, variable or periodic operation cycles and with 1-minute resolution. The results, as in the previous cases, were validated with previous work on the subject and indicators of energy consumption intensity in the region of Spain. Subsequently, the model was also combined with a series of DR strategies and energy policies that were implemented in a low level due to the bottom-up methodology and high temporal resolution of the system. Nevertheless, the aggregate results showed the influence and impact of these strategies. The implemented DR strategies were the introduction of 2 types of time of use (TOU) tariffs, peak shaving techniques, the maximisation of renewable energy resources and the reduction of standby consumption. The results demonstrated the impact of consumer acceptance on global aggregate benefits that might be achieved.

- **Chapter 6** presents the article published in MDPI's *Energies* Journal (Q2). This paper makes use of the modelling subsystems presented in chapters 3–6 to implement a global consumption model in the residential sector with a high temporal resolution that is able to simulate the individual energetic behaviour of the consumers in each household. By means of this model, the consumption of a community with a high degree of penetration of photovoltaic solar energy, as well as distributed storage was simulated. This scenario, together with a series of developed indices, allowed us to evaluate the degree of integration of the renewable resources in terms of demand coverage and supply utilisation, as well as the possibility of interacting with the main grid. In this context, the limited hosting capacity of low-voltage networks was quantified by an indicator that account for the loss of produced energy resulting from the application of curtailment techniques. Finally, a 2-level charging strategy was proposed for the distributed battery systems in order to minimise the loss of renewable energy produced in the medial hours of the day, where the simultaneous energy injections might overcharge the network on sunny days.

The book chapter included in Chapter 2, as well as the three articles contained in Chapters 3, 4, 5, and 6 address the objectives proposed in the Thesis report, using the proposed methodology, and, therefore, constitute the central body of this Thesis. Nevertheless, due to its importance in the development and application of the results obtained by means of the model, two peer-reviewed conference papers published at international conferences of recognised prestige are also included. These publications together with some other co-authored documents are the result of close collaboration with the Department of Energy Technology at Aalborg University (Denmark), during two PhD stays of three month each. They address the direct application of the model developed in the previous papers and represent one of the main future themes of this Thesis.

- **Chapter 7** includes the paper presented at the *IEEE 41st International Conference on Industrial Electronics (IECON)*. This paper addresses the integration of advanced energy metering systems or Smart Meters in the context of distributed generation as a Microgrid. This integration was tested by means of a test bed developed at the University of Aalborg, which consisted of three-phase inverters and controllable loads, which made it possible to assess the validity and use of these systems in three scenarios, namely: (i) the measurement of power and energy consumption in households with sub-hourly resolution and without additional equipment, (ii) the detection of certain supply quality events and (ii) the contribution of Smart Meters to the evaluation of the stability in low-voltage grids. Likewise, the ability of these devices to be integrated into an AMI with distributed communications was also presented, highlighting the potential contribution that they will provide to the grid management operations.

- **Chapter 8** contains the paper presented at the *IEEE 26th International Symposium on Industrial Electronics (ISIE)*. This paper presents the integration of an AMI into an intelligent building controlled by an energy management system. This energy management system uses the model developed in the previous works as one of the inputs for the optimisation process and implements different DR strategies to integrate renewable resources and storage. The system was implemented and validated by means of a test bed based on inverters that simulated the consumption of dwellings with stochastic data obtained by the model, the evolution of the renewable production based on weather conditions, as well as the interaction with the electric grid and storage systems. This development demonstrated the contribution of smart metering to the energy management and supply monitoring and how Smart Meters can be combined with other elements in the Smart Grid within the so-called tertiary control or energy management level.

- **Chapter 9** includes the concluding remarks of the Thesis, as well as the future developments and works to which this Thesis might lead.

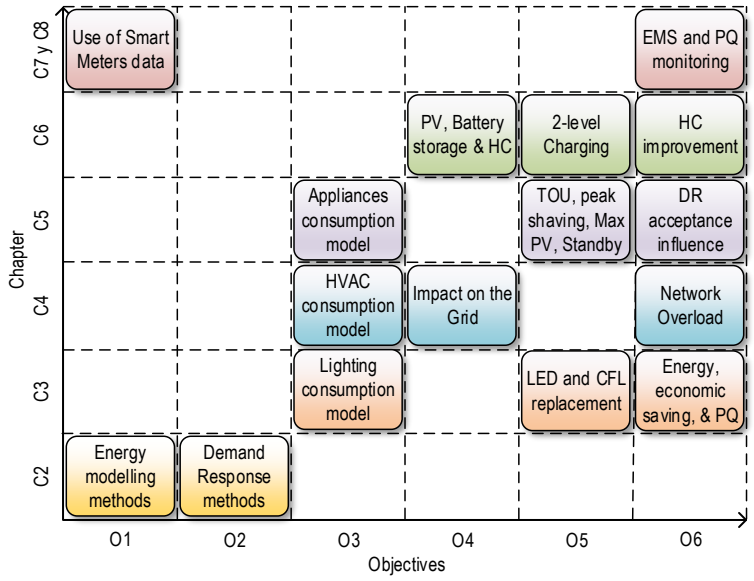

Figure 1.14: Relationship between the Thesis objectives and the chapters with the main findings of each work.

The relationship between the papers included in the Thesis and the objectives proposed in section 1.7 is summarized in Figure 1.14. The X-axis represents the objective number referred to, while the Y-axis indicates the chapter(s) where the objectives are addressed. Within the graph, each colour box corresponds to a Chapter indicating the main developments or findings achieved. The contributions and conclusions drawn from this work will be discussed further in Chapter 9 after presenting the collection of papers that comprises this Thesis.

References

[1] X. Yu, C. Cecati, T. Dillon, M. G. Simões, The New Frontier of Smart Grids, IEEE Industrial Electronics Magazine 5 (2011) 49–63. doi:10.1109/MIE.2011.942176.

[2] UNFCCC, Kyoto Protocol To the United Nations Framework Convention on Climate Change, Review of European Community and International Environmental Law 7 (2) (1998) 214–217. doi:10.1111/1467-9388.00150.

[3] Eurostat, Energy, transport and environment indicators - 2015 edition (2015). URL: http://ec.europa.eu/eurostat/documents/3217494/7052812/KS-DK-15-001-EN-N.pdf

[4] A. de Almeida, P. Fonseca, B. Schlomann, N. Feilberg, Characterization of the household electricity consumption in the EU, potential energy savings and specific policy recommendations, Energy and Buildings 43 (8) (2011) 1884–1894. doi:10.1016/j.enbuild.2011.03.027.

[5] D. Ndiaye, K. Gabriel, Principal component analysis of the electricity consumption in residential dwellings, Energy and Buildings 43 (2-3) (2011) 446–453. doi:10.1016/j.enbuild.2010.10.008.

[6] European Parliament and Council, Directive 2005/32/EC, establishing a framework for the setting of ecodesign requirements for energy-using products (2005). URL: http://eur-lex.europa.eu/legal-content/EN/TXT/?uri=LEGISSUM%3Al32037

[7] IDAE, Análisis del consumo energético del sector residencial en España INFORME FINAL (2011). URL: http://www.idae.es/uploads/documentos/documentos_Informe_SPAHOUSEC_ACC_f68291a3.pdf

[8] L. Pedersen, Use of different methodologies for thermal load and energy estimations in buildings including meteorological and sociological input parameters, Renewable and Sustainable Energy Reviews 11 (5) (2007) 998–1007. doi:10.1016/J.RSER.2005.08.005.

[9] IDAE, Guía Práctica de la Energia. Consumo Eficiente y Responsable. (2011).

[10] I. Vassileva, F. Wallin, E. Dahlquist, Understanding energy consumption behavior for future demand response strategy development, Energy 46 (1) (2012) 94–100. doi:10.1016/j.energy.2012.02.069.

[11] P. Palensky, D. Dietrich, Demand side management: Demand response, intelligent energy systems, and smart loads, IEEE Transactions on Industrial Informatics 7 (3) (2011) 381–388. doi:10.1109/TII.2011.2158841.

[12] T. Strasser, F. Andren, J. Kathan, C. Cecati, C. Buccella, P. Siano, P. Leitao, G. Zhabelova, V. Vyatkin, P. Vrba, V. Marik, A Review of Architectures and Concepts for Intelligence in Future Electric Energy Systems, IEEE Transactions on Industrial Electronics 62 (4) (2015) 2424–2438. doi:10.1109/TIE.2014.2361486.

[13] N. Arghira, L. Hawarah, S. Ploix, M. Jacomino, Prediction of appliances energy use in smart homes, Energy 48 (1) (2012) 128–134. doi:10.1016/j.energy.2012.04.010.

[14] C. Kuster, Y. Rezgui, M. Mourshed, Electrical load forecasting models: A critical systematic review, Sustainable Cities and Society 35 (July) (2017) 257–270. doi:10.1016/j.scs.2017.08.009.

[15] R. Pacheco, J. Ordóñez, G. Martínez, Energy efficient design of building: A review, Renewable and Sustainable Energy Reviews 16 (6) (2012) 3559–3573. doi:10.1016/J.RSER.2012.03.045.

[16] E. Dotzauer, Simple model for prediction of loads in district-heating systems, Applied Energy 73 (3-4) (2002) 277–284. doi:10.1016/S0306-2619(02)00078-8.

[17] W. Ma, S. Fang, G. Liu, R. Zhou, Modeling of district load forecasting for distributed energy system, Applied Energy 204 (2017) 181–205. doi:10.1016/j.apenergy.2017.07.009.

[18] L. G. Swan, V. I. Ugursal, Modeling of end-use energy consumption in the residential sector: A review of modeling techniques, Renewable and Sustainable Energy Reviews 13 (8) (2009) 1819–1835. doi:10.1016/j.rser.2008.09.033.

[19] A. Grandjean, J. Adnot, G. Binet, A review and an analysis of the residential electric load curve models, Renewable and Sustainable Energy Reviews 16 (9) (2012) 6539–6565. doi:10.1016/j.rser.2012.08.013.

[20] H.-x. Zhao, F. Magoulès, A review on the prediction of building energy consumption, Renewable and Sustainable Energy Reviews 16 (6) (2012) 3586–3592. doi:10.1016/j.rser.2012.02.049.

[21] A. Foucquier, S. Robert, F. Suard, L. Stéphan, A. Jay, State of the art in building modelling and energy performances prediction: A review, Renewable and Sustainable Energy Reviews 23 (2013) 272–288. doi:10.1016/j.rser.2013.03.004.

[22] N. Fumo, A review on the basics of building energy estimation, Renewable and Sustainable Energy Reviews 31 (2014) 53–60. doi:10.1016/j.rser.2013.11.040.

[23] S. Zhou, M. A. Brown, Smart Meter Deployment in Europe: A Comparative Case Study on the Impacts of National Policy Schemes, Journal of Cleaner Production 144 (2016) 22–32. doi:10.1016/j.jclepro.2016.12.031.

[24] Joint Research Centre (JRC) Euorpean Comission, Smart Metering deployment in the European Union (2018).

2

Distributed energy resources integration and demand response: The role of stochastic demand modelling

Emilio J. Palacios-Garcia[1], Antonio Moreno-Muñoz[1], Isabel Santiago[1], Jose Maria Flores-Arias[1] and Francisco J. Bellido-Outeiriño[1]

[1]Departamento de Arquitectura de Computadores, Electrónica y Tecnología Electrónica, Escuela Politécnica Superior, Universidad de Córdoba, Córdoba, Spain.

Abstract

One of the main problems with it comes to the integration of distributed energy resources is the estimation and prediction of the energetic demand that those energy sources must be able to supply. This is especially difficult nowadays due to the upward trend observed in all the projections for the energy consumption for major energy end-use sectors (residential, commercial, industrial, and transportation). In this context, stochastic modelling techniques have been presented as the most suitable ones as they are able to create the diversity needed to take into account the behaviour of the residents while keeping the general observed statistical trends. These methods are based on the individual modelling of each appliance and the consumer behaviour patterns so not can only high-resolution profiles be generated, but also the end-use of the energy can be specifically determined. That is not even possible nowadays with the new advanced metering infrastructure, unless non-intrusive load monitoring programmes are applied, which also makes these models a great tool for the assessment of energy policies and the impact of including new appliances at home. In this chapter, the usage and application of stochastic demand models will be addressed, with a focus on the prediction and estimation of the energy consumption, the assessment of different demand response policies and the integration of distributed energy resources at small scale. For this aim, first, a short overview of the main modelling techniques employed in the residential sector will be given to the reader in order to contextualise this type of models. Subsequently, the methodology used in these models will be exposed, showing the different blocks that usually built up the estimation process. Finally, the usability for assessing energy policies and integrating distributed energy resources will be discussed.

This book chapter has been published in *Large Scale Grid Integration of Renewable Energy Sources, A. Moreno-Munoz, Ed. London: The Institution of Engineering & Technology (IET), 2017, p. 336. ISBN: 978-1-78561-162-9. Chapter doi: 10.1049/PBPO098E_ch8*.

2.1 Introduction

One of the main problems with it comes to the integration of distributed energy resources is the estimation and prediction of the energetic demand that those energy sources must be able to supply [1]. This is especially difficult nowadays due to the upward trend observed in all the projections for the energy consumption for major energy end-use sectors (residential, commercial, industrial, and transportation) [2].

From all these end-use sectors, probably the one that presents the greatest interest in the modelling field is the residential one. Whereas the consumption patterns and daily load profiles of the commercial, industrial and transportation sectors might be relatively easy to predict depending on the activity, the wide amount of appliances, household types and consumers' behaviours in the residential sector generate stochastic consumption profiles, being almost impossible to find two households with the same habits [3].

Moreover, in order to accurately estimate the integration of new energy resources, detailed knowledge of the consumption profiles is needed. Nowadays estimations and predictions for the global consumption are available, but the temporal resolution is not enough since the great variety of consumption patterns between the different sectors, as well as within them, makes the task of balancing production and demand not easy, and much less when non-dispatchable energy sources are included in the system [4, 5]. In addition, this higher resolution is justified from the point of view of demand response and energy management as the time granularity needed for the development of the strategies has to be between 5 and 30 min and submetering programmes are not usually carried out, so only aggregated measurement are available [6].

In this context, stochastic modelling techniques have been presented as the most suitable ones as they are able to create the diversity needed to take into account the behaviour of the residents while keeping the general observed statistical trends [7]. These methods are based on the individual modelling of each appliance and the consumer behaviour patterns so not can only high-resolution profiles be generated, but also the end-use of the energy can be specifically determined. That is not even possible nowadays with the new advanced metering infrastructure, unless non-intrusive load monitoring programmes are applied, which also makes these models a great tool for the assessment of energy policies and the impact of including new appliances at home [8].

In this chapter, the usage and application of stochastic demand models will be addressed, with a focus on the prediction and estimation of the energy consumption, the assessment of different demand response policies and the integration of distributed energy resources at small scale. For this aim, first, a short overview of the main modelling techniques employed in the residential sector will be given to the reader in order to contextualise this type of models. Subsequently, the methodology used in these models will be exposed, showing the different blocks that usually built up the estimation process. Finally, the usability for assessing energy policies and integrating distributed energy resources will be discussed.

2.2 Overview of modelling techniques for energy demand prediction

The great diversity of factors that influence the residential energy consumption leads to a wide range of modelling techniques and methodologies. One of the most accepted criteria to classify them is the hierarchical relationship between the consumption that is being modelled and the input data for the model. This classification was first proposed by Swan and Ugursal [9], and it distinguishes basically two types of models named as top-down and bottom-up models respectively, also defining different categories within each of these two types depending on the methodologies employed.

A similar approach was followed by Grandjean *et al.* [10] in a more recent work, nevertheless, the proposed classification of the different load curve models was based on the manner how the diversity among dwellings is obtained. The idea of this basic classification criterion is illustrated in Figure 2.1, where the most usual input data and their relationship with the household consumption estimation are represented together with the two suggested approaches, which will be discussed in the following sections.

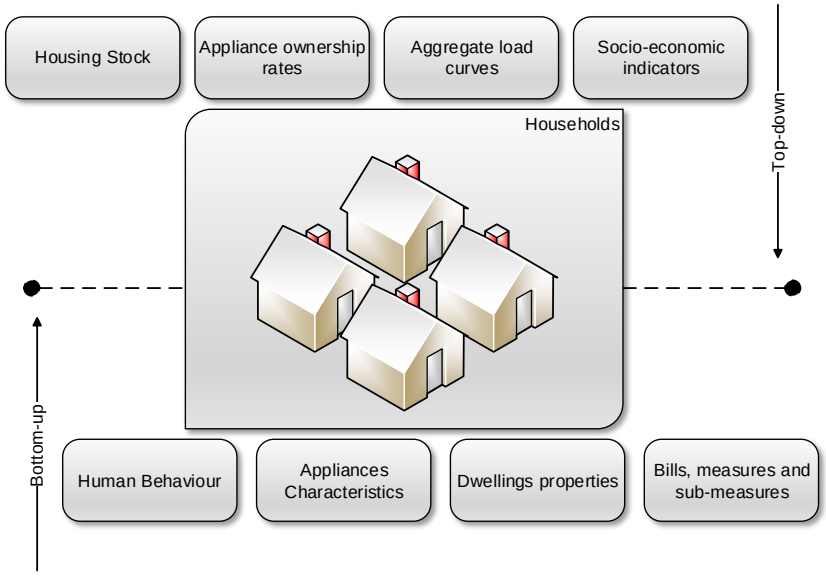

Figure 2.1: Conceptual approach. Top-down vs bottom-up models.

2.2.1 Top-down models

The top-down models are those where the consumption estimation is based on variables or input data that belong to the whole sector. Therefore, the residential consumption is regarded as an energy sink without taking into account the individual characteristics of the demands that account for this consumption. Thus, the main purpose of these modelling strategies is planning and estimating the possible trends and evolution of the sectors by using relatively simple and widely available aggregated data. However, its ability for predicting new emerging end-uses or disruptive technologies is limited.

Among the principal inputs variables or data for these models that can be highlighted we found as follows:

- Socio-economic indicators such as the gross domestic product
- Unemployment rates
- Electricity prices
- Weather conditions
- Housing stock
- Appliances usage rates

Regarding the possible subdivisions in the top-down category, these models were classified by Swan and Ugursal [9] as either Econometric or Technological models, although many times the characteristics are mixed. Econometric models generally make use of prices of electricity or appliances, whereas technological models base their predictions on characteristics such as appliances usage rates or housing stock.

2.2.2 Bottom-up models

With an opposite philosophy, the bottom-up models use input data which are in a lower hierarchical level than the energetic consumption itself. Therefore, it is the aggregation of detailed data what builds up the load demand curve, although some global indicators might also be included for the prediction, such as weather conditions of housing stock in the same line of the top-down models. In contrast with the top-down models, the bottom-up approach has the ability to simulate the occupants' behaviour, as well as the individual consumption of different appliances which makes them very suitable for studying demand response strategies, new energy policies or high-resolution simulations. Nevertheless, the complexity of these models is higher, requiring a large data sample, detailed input information and more computationally intensive tasks.

Some usual input data for this type of models are as follows:

- Human behaviour
- Electricity or energy bills
- Thermal properties of the households
- Appliances characteristics
- Equipment penetration rates
- Daily activities schedules

According to Swan and Ugursal [9] classification criteria, the bottom-up models are divided into two large categories which are statistics-based models and engineering-based models. The first ones make use of regression analysis techniques, conditional demand analysis or neural network for modelling the energy usage, whereas the engineering-based models are focused on appliances ratings, archetypes definitions or detailed sampling of the population. Nevertheless, alternative classifications can be found such as the one proposed by Grandjean *et al.* [10].

2.2.3 Comparison

After this initial categorization, it is clear that the decision of using any of the introduced methodologies will eventually be determined by the end goal. Therefore, when reliable long-term forecasting is needed, without taking into account possible technological disruptions and without knowledge of the explicit end-uses that compose the global consumption, the top-down models are the most suitable. Nevertheless, when an understanding of the energy end-uses is required, as well as the possibility of assessing the impact of new technologies the bottom-up methods are the only ones with this capability.

Subsequently, since the goal of this chapter is to address the usage of modelling techniques for the integration of renewable resources and assessing different demand response strategies and energy policies, the chapter will be focused on the bottom-up modelling techniques. More specifically, the engineering-based bottom-up models that utilise distribution data concerning appliances and usage rates will be the ones exposed, since they will allow simulating the individual appliances, as well as the influence of each dwelling behaviour. Moreover, these models were also classified by Grandjean *et al.* [10] as time of used based bottom-up models, a name that results to complete the definition, since they do not only use distribution data, but they are also based on monitoring campaigns on a sample of households such as the time use surveys (TUSs), where the time devoted to certain activities is recorded.

2.3 Time of use based bottom-up models

The conceptual architecture of the system is presented in Figure 2.2. The system has a set of input parameters such as the number of residents in the household, the type of day, the period of the year or the location.With these inputs, it will generate the daily consumption for the given household distinguishing between the different end-uses.

Each of the grey blocks represents a particular model aiming to estimate the occupancy of the household or the consumption due to appliances, lighting systems, and cooling or heating equipment, having defined a set of appliances, lamps or HVAC (heating, ventilation and air conditioning) systems (red blocks) that are responsible for consuming the energy and that can usually be randomly selected on the basis of distribution statistics or self-defined sets. In addition, some specifics statistics data about the activities performed at home or the occupancy probability (Transition Matrices), as well as meteorological information, is provided (yellow blocks).

This basic structure will be further discussed in the following sections, where the occupancy model and the three mentioned consumption models will be individually addressed, explaining the basic methodology of a real implemented model, the input information required for the model to run, and finally the actual simulation procedure.

2.3.1 Occupancy and consumers' behaviour

The energy consumption in the residential sector is strongly influenced by the occupancy patterns as most of the equipment at home requires the direct intervention of the residents, with only a few exceptions such as refrigerators, freezers, or appliances in standby mode. Therefore, following the previously exposed bottom-up philosophy, it is reasonable that the cornerstone for many of these models is the estimation or simulation of the consumers' behaviour.

However, the occupancy modelling has the main inconvenience of being affected by a wide range of external factors such as the working hours, the day of the week, or the number of residents in each household. Thus, it is almost impossible to find two dwellings with the same occupancy patterns or one dwelling whose occupancy profile is exactly the same for two consecutive days. Nevertheless, when the aggregate occupancy profiles are observed, some general trends can be deducted.

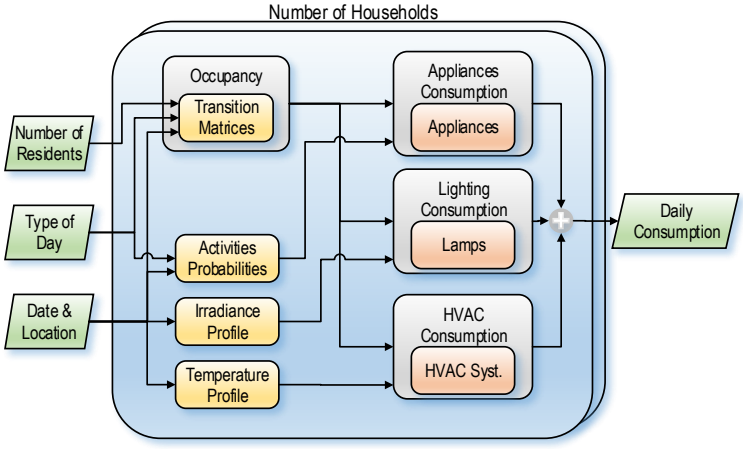

Figure 2.2: Block diagram of the simulation system.

The models for estimating the consumers' behaviour aims to simulate individual households in a deterministic way, but keeping the results statistically accurate. The fundamental of these models, the main input parameters and an example of simulation process will be presented in the next sections.

2.3.1.1 Model basics

In the commercial and industrial sectors, presence control is usually common by means of access cards or other methods. Moreover, even when no control methods exist, the working hours are usually well defined and consequently, the occupancy patterns can be known with a high degree of confidence. Nevertheless, if the occupancy profiles of the residential sector are to be studied, a monitoring campaign is required, using a sample of households as a representative of the entire population. This is commonly performed through surveys, where the residents write down their daily activities and habits.

In the context of Europe, the main effort to collect this information is the harmonised European TUSs. These surveys have been carried out in most of the European countries in different years such as in the United Kingdom (2000), Sweden (2010), and Spain (2010) among others. The surveys include the different activities that the interviewees are performing with 10-min resolution, as well as information about where they were located and whether someone accompanied them.

The information collected in the TUS have been used by several authors aiming to generate daily occupancy patterns statistically consistent that can be employed for energy demand prediction. All of them followed a similar methodology as it can be read in the work of Richardson *et al.* in the United Kingdom [11], Widén and Wäckelgård in Sweden [12], or Lopez *et al.* in Spain [13]. The proposed occupancy models are all built around Markov Chains theory and Monte Carlo simulations.

Markov Chains simulate the random progress of a process between different states whose probability is influenced by the past states of the system. Therefore, this statistical process includes the concept of memory as the previous states or history define in some term the future ones.

Therefore, given a finite number of states, $S = \{s_1, s_2, \ldots, s_n\}$, of a defined process that starts with one of those states and keeps moving only between the space of states S, it is called a Markov process if the probability of moving to another state j in the time $t + 1$ depend on the current state i at time t. This is defined by the probabilities p_{ij} which are included in the so-called matrix of transition probability or transition matrix. If this matrix is constant for any time step t, the process is said to be homogeneous, whereas if the probabilities of the transition matrix depend on the time $p_{ij}(t)$, the process is non-homogeneous and, therefore, for a process with R states and N time steps, there will be N matrices with a size $R \times R$.

In the case of active occupancy simulation, all the studies use the non-homogeneous Markov process for defining the transition probabilities. Specifically, due to the 10-min resolution of the TUS, 144 transition matrices are defined, one for each time step and ranging from 1 to 6 residents. Moreover, additional parameters such as the region, the quarter of the year or the day of week can be and have been used for estimating the transition matrices in different circumstances.

In order to illustrate the transition matrices, an example of one of them can be observed in Table 2.1, where the matrix of transition probabilities for a three-resident household located in Spain during a weekday

Table 2.1: Transition probability matrix for a three-resident household.

Current state (07.30 h)	**Next state (07.40 h)**			
	0	**1**	**2**	**3**
0	0.7288	0.1864	0.0848	0
1	0.0938	0.7500	0.1563	0
2	0.0588	0.2941	0.5294	0.1177
3	0.1429	0.2857	0	0.5714

and in the period from 7.30 to 7.40 h is represented. As it can be seen, there are four possible states ranging from 0 active occupants to 3 active occupants. Depending on the current state, the distribution probability of one of the rows will be considered. Therefore, if the current occupancy is 0, is very likely that it remains 0 in the next step too (p_{00} = 72.88%), whereas if the occupancy in the current state is 2, there are around a half of chances of keeping the same occupancy value (p_{22} = 55.94%), but it is also likely to be increased (p_{23} = 11.77%) or decreased (p_{21} = 29.41%). It should also be pointed out that the sum of each row must be equal to 1 since each row actually represents an individual discrete probability distribution.

2.3.1.2 Input parameters

The input parameters for the occupancy models will mainly depend on the input information available from the TUS. Nevertheless, some of the common information that can be found in all of them is as follows:

- **Number of residents**. Each dwelling in the survey is characterised with the number of residents that share the property.
- **Location**. The location of the households is also accounted in the survey, generally in terms of region, province or municipality.
- **Type of day**. The day of the week is written down by the interviewees in the dairies. Thus, weekdays and weekends can be distinguished in the modelling process.
- **Period of the year**. Some of these surveys distinguish between each quarter of the year, making possible to compare the behaviour in different seasons.
- **Other information**. The survey also collects information about the age, the work sector, the employment status etc. Those data can also be included in the model.

The main concerns when selecting the influence input variables for the transition matrices are two. On the one hand, the increment in the complexity of the model should be justified by an increment in the accuracy or sensibility of the results. On the other hand, a fine characteristic selection can derivate into small data sets of the sample that might not be representative of the population being studied.

2.3.1.3 Simulation algorithm

Using the Markov Chain methodology and the input parameters that have been explained before, the simulation algorithm is implemented as is illustrated in Figure 2.3. This algorithm starts by loading the transition matrices to be used during the process, which are defined depending on the given input information previously commented.

Nevertheless, as was exposed in the Markov Chain methodology, the initial state should be defined before the process starts. For this aim, the occupancy probability distribution for the given starting point is used in order to generate the initial state with a random Monte Carlo sampling.

Once the initial state is defined, the process iterates through all the simulation intervals, first, selecting the appropriate transition matrix for this time step, and subsequently generating a random sampling over the row of the transition matrix corresponding with the current number of active occupants in order to determine the next state of the system. If this process is repeated for the 144 time steps of a day with 10-min resolution, the occupancy profile of a house with a given number of residents and some characteristics can be randomly obtained in a way that the results are completely deterministic, but they represent a significant sample of the population, and, therefore, they can be used in the following models for estimating the different end consumptions.

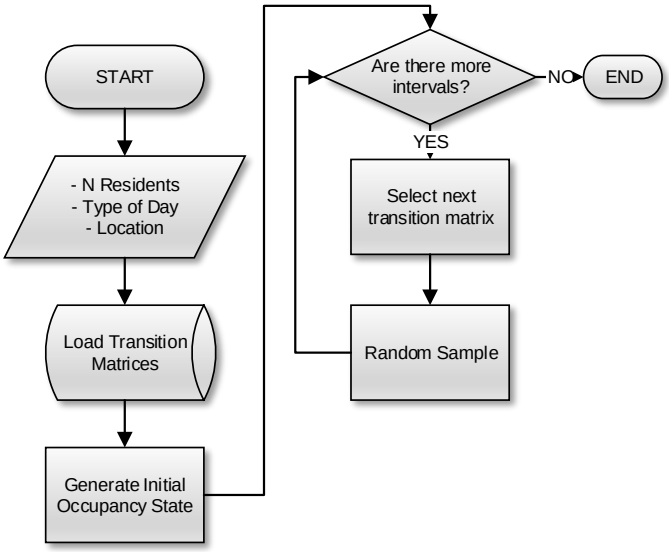

Figure 2.3: Flowchart of residents' behaviour simulation algorithm.

2.3.2 Lighting system consumption

The energy demand due to lighting systems comes to represent around a fifth part of the total electrical consumption in the residential sector [3, 14]. In Spain, the figure is around 470 kWh a year per household, whereas in other countries like the United Kingdom, it might be even higher, 715 kWh a year reported. Due to the importance and the specific influence factors that determine this consumption, many different lighting demand models have been developed by many authors such as Stokes *et al.* [15] and Richardson *et al.* [16] for the United Kingdom, Widén *et al.* [17] for Sweden, and Gago *et al.* [18] and Palacios-Garcia *et al.* [8] for Spain. The methodology for developing a model focused on lighting consumption is subsequently exposed.

2.3.2.1 Model basics

The active occupancy of the household is a necessary condition for the usage of lighting systems, which require the direct intervention of the residents. Nevertheless, it is not enough to determine the period of consumption due to the direct relationship between the daylight availability and the needs of artificial light. Therefore, not only is the occupancy profile necessary for the estimation of lighting consumption, but also the external irradiance along the day or studied period should be known.

This external irradiance profile varies along the day from dawn to sunset and is also influenced by the meteorological conditions such as clouds or precipitations, resulting in different levels of daylight availability during the day. For a given threshold, this irradiance will be so low that the artificial lighting systems must be used. This has been supported by other authors such as Reinhart or Hund in the offices' sector [19, 20], who have set the value for this threshold as normally distributed with mean 60 W/m^2 and standard deviation 10 W/m^2.

Thus, the occupancy and the irradiance can be considered the main factors that influence the lighting consumption and, consequently, the principal input data for the model. Nevertheless, if they are taken into account with no further restrictions the consumption is likely to be overestimated due to two main problems: the relative usage of different lighting spots and the sharing of them between the residents.

The relative usage is related to the fact that some lighting spots are more likely to be turned on than others. For instance, practically, the lamps installed in the living rooms or kitchens are more often used than the ones situated in corridors, bathrooms or bedrooms. Subsequently, each lighting systems should be adequately weighted according to the relative usage within the household.

The other factor, the shared usage, refers to the contribution of each active occupant to the total energy consumption. If the proportion of active occupants is considered to be proportionally related to the energy demand, this would mean that the consumption, when two residents are active, is double than when only a single person is in the household. However, this relation is not linear since some of the lighting systems are shared between the occupants, and it tends to saturate when the number of active occupants is increased.

In order to quantify this, a factor named as effective occupancy is usually inserted into the model, not only for the lighting consumption but in other consumption groups, as it will be seen in the following sections. This factor is calculated on the basis of the energy consumption figure of households with a different number of residents, obtaining the relative increment in the consumption with the increment in the number of people living in the same house.

Finally, if all the parameters determine that the lighting system should be turned on, then it is necessary to establish the period of time that it will remind in this state. Those times can only be determined by means of an experimental study such as the one performed by Stokes [15]. All this methodology has been successfully used by other authors in previous works such as [8, 16, 17] showing accurate results.

2.3.2.2 Input data

Regarding the above-mentioned influence parameters, a set of input parameters for the model can be defined. Some of them have been already used in previous works; others can be used for improving the current results obtained by these models.

- **Active occupancy**. The number of occupants with 10-min resolutions is used for simulating the behaviour based on the previously discussed model.

- **External irradiance**. The global irradiance profile is used for estimating the probability of using the artificial light systems. This irradiance can be extracted from historical databases, or other prediction or forecasting models. Nevertheless, they must have at least the same temporal resolution as the occupancy data, although in some previous works it has been proved that fast irradiance variations due to clouds have a small impact on the residents' behaviour [16].

- **Lighting systems**. Following the bottom-up methodology, the consumption will be generated by the simulation of each lighting spot in the household. Therefore, information about the number of lighting units, their power, as well as additional information such as the technology or the possible grouping has to be defined. Different approaches can be followed for that. In some cases, depending on the type of household or family a set of lighting units can be selected. It is also possible to individually define the lighting units in each household. Finally, another approach can be the development of a statistical model that is able to randomly establish the distribution of lighting technologies and power within the dwellings.

- **Additional information**. As in the case of the occupancy sector, additional information can be included to improve the estimation. Due to the high correlation between the daylight availability and the orientation of the windows in the household, as well as the type of household (detached, semi-detached, block etc.), it might be possible to gain accuracy in the model if parameters such as the geometry of the house or the archetype of the household are taken into account.

2.3.2.3 Simulation algorithm

The simulation process is illustrated in Figure 2.4. As can be observed, the first step performed by the system is the estimation of the active occupancy. This process can be done in advance if a daily occupancy profile is to be generated, but it can also be obtained dynamically for each simulation step. In addition, information about the external irradiance and the characteristic of the lighting spots should also be given using any of the methodologies exposed in the previous section. Once those data are available for the simulation process, the iteration through all the time steps and all the given lighting spot starts.

First, the number of active occupants in the dwelling is obtained since the existence of active occupancy is a necessary condition for the lighting spots to be turned on. Otherwise, all the lighting systems in the household will be considered to be off due to the absence of occupants. That might not be consistent with the reality in some cases when the residents forgot to turn off the lighting system. Hence, the model includes a small percentage of uncertainty to account for this, as was previously proposed by other authors [16].

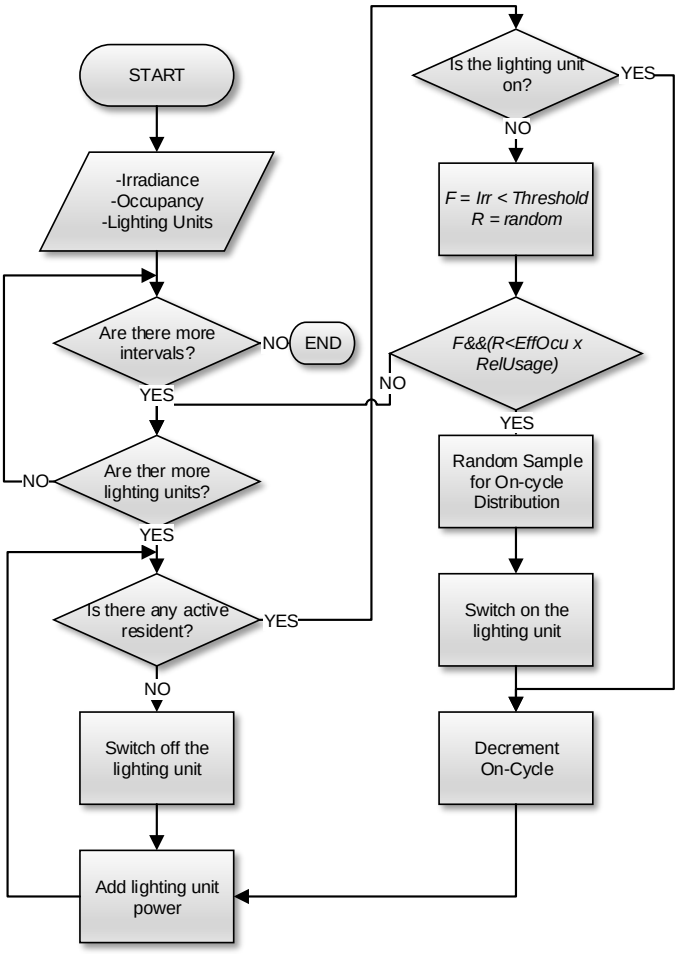

Figure 2.4: Flowchart of the lighting consumption simulation algorithm for each household.

In the case at least one active occupant is at home the algorithmic process continues normally, checking the operation of each installed bulb in the household. If the lighting point is already working and the occupancy is not null, the operation cycle of the bulb is decreased. In contrast, if the light is off, the comparison process of the external irradiance and the internal lighting threshold is performed.

Thus, if the global external irradiance is lower than the selected threshold, the lighting point is likely to be turned on. This threshold is defined as a normally distributed value, so for each household a random value is sampled from the normal distribution in order to define the lighting threshold, emulating with this the random behaviour of different people.

If the comparison in the previous step results to be true, the lighting point will be turned on, providing the relative usage of this lighting spot is high enough and the influence of the effective active occupancy determines that. In addition, a scalar value is usually included in the decision process in order to keep the energy figure comparable with the historical average values of consumption in the studied region.

Finally, if after all the decision process the lamp has to be turned on, the operation cycle has to be assigned. This is usually performed on the bass of a probability distribution of on cycles. The whole process, as it can be seen in the flowchart of Figure 2.4 is then repeated for each lighting spot in the household and for each time interval in order to simulate the lighting consumption profile of a household. Thus, if a given number of households (N) is to be simulated, the above-described process has to be repeated for each house.

2.3.3 General appliances consumption

The following group of sub-consumptions that are generally considered in the bottom-up models is the one related to the general appliances, meaning those that are related neither to the lighting systems nor to the heating or cooling appliances. As far as electrical energy is concerned, these consumptions usually present the highest demand as they cover the appliances devoted to food refrigeration and freezing, cooking systems, laundry appliances, entertainment devices and others additional equipment.

In the European households, this consumption has an average value of 2,600 kWh/year as it was shown in the results of the REMODECE project [21]. Nevertheless, the figures vary significantly from one to another country with maximums of around 3,500 kWh/year for Denmark and Norway, and minimums of around 1,500 kWh/year for the Czech Republic or Romania [3].

This model keeps using the active occupancy as the main input parameter, which determines the probability of using or not some equipment. Nevertheless, in order to associate each appliance with a certain behaviour, the concept of activity is now introduced as it will be exposed in the following section.

2.3.3.1 Model basics

The main concept that is introduced in the equipment consumption model is the idea of activities in the household. Most of the appliances are linked with a determined activity performed in the household, with the exception of some equipment such as refrigerators, freezers or appliances in standby mode, that do not depend on the activity. All these activities together with the active occupancy determine the interval where the different appliances are more likely to be turned on. The activities are linked to the TUS data, where the interviewees wrote down for each 10-min interval the primary and the secondary activity that they were carrying out.

Some of the activities that are recorded in the diaries are ironing, house cleaning, cooking, laundry, personal care, watching TV or PC usage. As it can be depicted, many of those activities are directly linked with some appliances. For instance, an iron is needed in order to perform the activity 'ironing'. On the other hand, some relationships with the energy consumption are not so obvious, but if some laundry activity is performed, either a watching machine or a tumble dryer is likely to be employed. Therefore, most of the appliances usually installed in a household can be related to the activities found in TUS.

The methodology used for obtaining the activity probabilities is illustrated with the example given in Table 2.2. First, for each time interval, the number of households with the selected number of active occupants

Table 2.2: Probability for the activity cooking for a weekday at 13.00 h. Calculation example.

Number of active occupants	Number of households with the given number of active occupants	Number of households where at least one residents perform the activity	Activity probability
1	2,367	822	822/2,367 = 0.35
2	956	429	429/956 = 0.45

has to be determined. As can be observed in Table 2.2, the number of household with one active occupant at 13.00 h are 2,367, whereas for two active occupants the number is 956. After that, the number of households where at least one of the active residents is carrying out the activity has to be accounted. This means that from the 2,367 households where one occupant is active, only in 822 these occupants are performing the activity Cooking. Likewise, from the 956 households with two active residents at the same time, only in 429 of them at least one occupant is carrying out the activity. By means of this calculation, the activity probability for each time step and depending on the number of active occupants can be calculated.

It should be pointed out that this method, as can be observed in the resulting probabilities in Table 2.2, intrinsically takes into account the concept of appliance sharing since the condition is that at least one occupant is performing the activity. So as the results depict, the probability for one active occupant to carry out the activity is 35%, whereas for two active occupants this figure is not the double but only 45%.

2.3.3.2 Input data

The input parameters for this model include again the occupancy profile, but taking also into account the activities and the appliances that are responsible for the energy consumption.

- **Occupancy profile**. As in the previous model, the number of active occupants in the dwelling will be needed in order to estimate the intensity of the power consumption.
- **Activities probability**. For each defined activity from the TUS, the probability distribution is established, distinguishing between the numbers of active occupants, so the probability of performing a selected activity can be determined for any interval of time during the day and depend on additional parameters such as the day of the week, the region or the period of the year.
- **Appliances characteristics**. Following the bottom-up methodology, each appliance consumption is basically defined as an individual power rate (reactive power might also be included) and an on-cycle. In addition, a standby power, as well as an off-delay, can be assigned. For other appliances, such as the dishwasher or the washing machine, the actual working cycle is defined as a variable power along the on period.

2.3.3.3 Simulation algorithm

In Figure 2.5, the simulation process of this specific end-use is illustrated. As in the case of the lighting systems consumption, the estimation iterates over each time interval and for each appliance, deciding if it should be turned on, kept in on state, kept in off state, or switched off, depending on the decision factors. Those decision factors are the active occupancy and the dwelling activities.

Thus, the state of every appliance is first checked. If the appliance has a delay cycle such as the refrigerator, the freezer and other thermostat controller equipment, the first test is to check if it is in the waiting state and, if this is the case, the waiting cycle should be decreased. If the appliance has no waiting time, then the process continues.

In the second stage, the active occupancy is checked, so if the number of active residents is zero either the appliance is turned off if it depends on occupancy and it is active, or the appliance keeps on working with the normal operation if it does not depend on occupancy. Opposite, when there is active occupancy, the state of the appliances is tested.

Subsequently, if the appliance was already turned on, the system will only decrease the on cycle and account for the energy consumed. However, if the appliance is off the stochastic process for determining if it should be switched on starts. In this process, the probability of the activity associated with the appliance $P(Activity)$, together with a calibration scalar z, calculated to keep the annual consumption consistent with the observed historical figures, are compared with a randomly generated number R. The result of this test will decide if the appliance is turned on at this interval or if it should remain in the off state.

In order to clarify the process, all the possibilities are summarised in Table 2.3 depending on the appliance state, the operation cycles the type of equipment and the occupancy, showing the decision that will be taken by the simulation procedure.

Thus, with this process, the individual operation of each appliance is simulated with a given time interval.

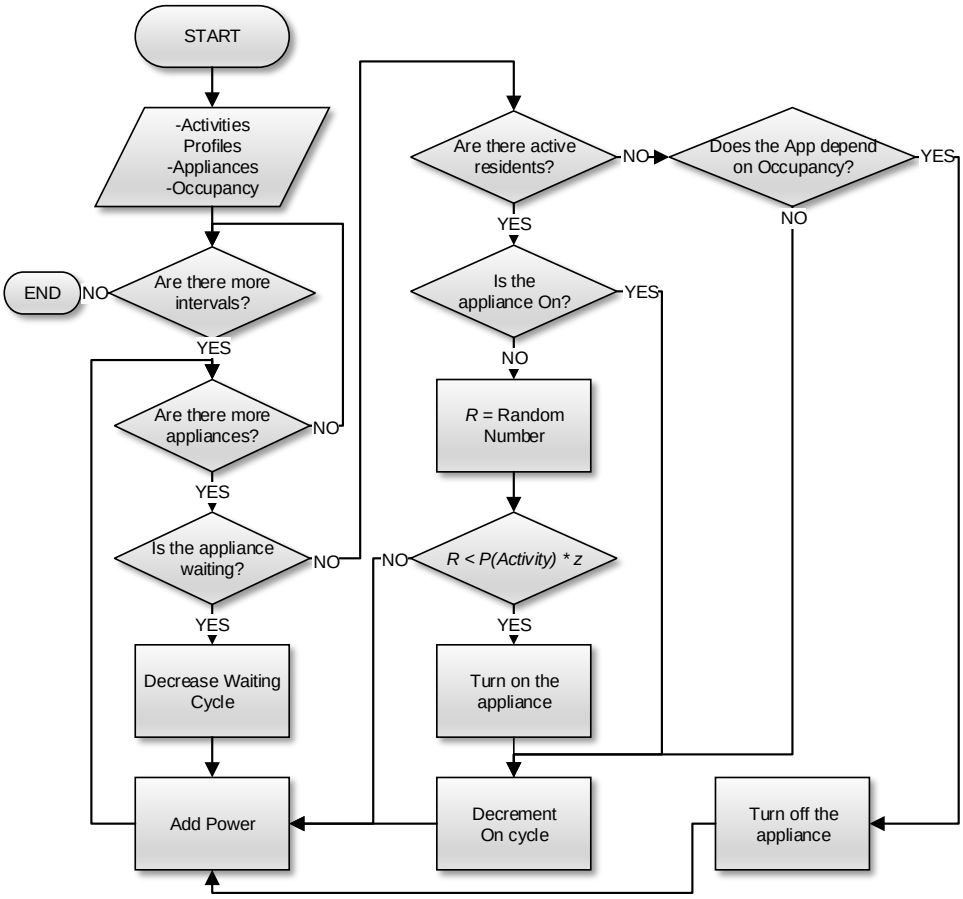

Figure 2.5: Flowchart of the general appliances consumption simulation algorithm for each household.

Table 2.3: Simulation case for the general appliances consumption simulation algorithm.

Appliance state	Activity related	Delay cycle	Occupancy	Decision
OFF	–	$\neq 0$	–	• Decrease delay cycle • Add standby power
OFF	NO	$= 0$	–	• Turn on appliance • Add on power
ON	NO	$= 0$	$= 0$	• Remain ON • Add on power
OFF	YES	$= 0$	$= 0$	• Remain OFF • Add standby power
OFF	YES	$= 0$	$\neq 0$	• Stochastic test with activity probability
ON	YES	$= 0$	$= 0$	• Turn off appliance • Add Standby power
ON	YES	$= 0$	$\neq 0$	• Remain ON • Add on power

This simulation has the main advantages of being based on the relationship between human behaviour and actual devices, which makes possible to define the consumption units with a big degree of details, as well as introduce new technologies, something fundamental in the prediction of new consumption trends due to emerging and disruptive appliances.

2.3.4 Heating and cooling consumption

The last element or simulation block that the proposed model takes into account is the energy demand due to heating and cooling appliances. Those consumptions strongly depend on the climate zone and the season. Therefore, the observed figures vary significantly even inside the same country as it has been exposed in the European ENTRANZE project [22]. For the heating consumption, the values can range from around 40 to 100 kWh/m^2/year for Mediterranean countries up to 160–240 kWh/m^2/year in countries such as Germany, Czech Republic or Finland. In the case of cooling consumption, the trend is opposite with values around 40–70 kWh/m^2/year for Mediterranean cities and almost non-existent demand in countries such as Germany (9 kWh/m^2/year), Czech Republic (5 kWh/m^2/year) or Finland (1 kWh/m^2/year).

In addition, whereas lamps and domestic appliances are mainly supplied with electricity, in the case of the heating systems a wide range of technologies and different energy sources such as natural gas, propane, fuel oil and hot water (district heating) can also be employed. This fact makes the modelling process more complex than for other energy end-uses. The methodology, input data and simulation process, for a proposed modelling technique, will be addressed in the following sections, pointing out its strengths and weaknesses.

2.3.4.1 Model basics

The heating and cooling consumptions are not only linked with the human behaviour but also with the insulation of the households and the geometric characteristics. Subsequently, if an accurate model is to be developed, a large number of variables such as the overall heat transfer coefficients of the building construction elements (U-values), infiltration and other specifications will be needed, also making the modelling process non-applicable to other houses other than the studied. On the other hand, if not information at all is supplied to the model about the characteristics of the household, it might be highly estimative with no useful results.

Depending on the information that is known about the building or house to be simulated, the consumption models for heating and cooling are usually classified as white, black or grey-box models. In the white-box or physic-driven models a wide knowledge of the building structure, as well as the parameters and characteristic of the construction, is needed as they make use of the system physics for modelling the dynamic. On the other hand, the black-box or data-driven models only try to find a relationship between the inputs and the output data usually by means of statistical techniques and with no knowledge about the building itself. Finally, somewhere in between, the grey-box models consider some physical parameters of the building in the estimation, but they also make use of statistical approaches.

The white-box models provide good generalisation capabilities, whereas the black-box models are very accurate. The grey-box models benefit from the characteristic of both of them [23]. In addition to these models, many calculation tools that accurately simulate the building dynamic can be found, which include models of the most used HVAC systems. Some of these programmes are TRNSYS, EnergyPlus, DOE-2 or ESP-r to name a few.

The goal of the proposed modelling methodology is to simulate the diversity of the household in order to generate detailed individual heating and cooling consumption profiles. Therefore, according to the above-mentioned criteria, the model can be classified as a grey-box model, as a few characteristic of the household will me mixed with statistical data in order to generate diversity among the different residents and dwellings, but trying to keep the results statistically consistent.

Thus, the main reference input parameter for the modelling process will be the external temperature. It has been proved that the average external temperature for each day of the year can be used to determine the intensity of the energetic consumption, by comparing the value with a reference comfort temperature. The main problem of this comfort value is that it has to be empirically determined for each region. The flexibility of this figure has been shown in previous works such as the 21 °C (69.8 °F) obtained by Sailor in Florida [24], the 15 °C (59 °F) estimated by Sarak and Satman for heating usage in Turkey [25], the 22 °C (71.6 °F) proposed by Giannakopoulos and Psiloglu for Greece and the 18 °C (64.4 °F) determined by Valor *et al.* for Spain [26]. In addition, a 3 °C hysteresis is observed around these values, where the consumption is insensitive to temperature.

These comfort values are usually used as a reference for the calculation of the heating degree-days (HDD) and the cooling degree-days (CDD) depending on the usage of either heating or cooling appliances respectively. Therefore, using the reference comfort value with the hysteresis term and the deviation of the average temperature from this one, the HDD and CDD can be calculated for a given day and this value subsequently related to the energy intensity needed [27].

However, the degree-days only allow us to account for the energy intensity, but the period of the day where those consumptions take place cannot be determined unless the daily temperature profile is used. This instantaneous temperature together with the insulation level designated for the dwelling will allow us to estimate the heat gains and losses in order to establish the switch on probability or the thermostat cycling operation of the appliances.

If a more detailed knowledge about the specific region or set of household to be simulated is obtained, more constraints can be added to these models such as the division into zones of the dwelling with different temperatures. Nevertheless, the more detailed the model, the more computationally intensive the tasks will be, and probably the diversity generated by the simulation will decrease, what might be a problem when the human behaviour wants to be simulated.

2.3.4.2 Input data

- **Occupancy profile**. As in the other models, the occupancy determines the main periods where the consumption might take place. In addition, when the thermal gains are considered for the cooling consumption, the active occupancy in the dwelling has a direct impact due to the metabolic heat gain from persons.

- **Daily temperature profile**. The external temperature mainly influences the energy needs to be required to maintain the comfort conditions inside the household. The average, minimum and maximum temperatures of the day can help the model to estimate the demand of this day and simulate the seasonality. Nevertheless, due to the high resolution of the model, the daily profile of temperatures is required so the probabilities of turning on the heating and cooling devices can be determined.

- **Heating and cooling appliances characteristics**. In the same line of the appliances consumption model, the appliances characteristics should be defined following the bottom-up methodology. Nevertheless, the wide range of fuels and appliances types sometimes might require the usage of mixed models, where not only electrical energy is considered, but also hot water demand or others fuels, although in the presented case, only the electrical cooling and heating appliances were considered. Moreover, it will also be necessary to distinguish between thermostat controlled and non-thermostat controlled equipment. This means that thermostat controlled appliances, once there are turned on, they will follow a reference temperature without the user operation by means of hysteresis cycles or variable power cycles. Opposite, the non-thermostat controlled equipment will only operate in on or off mode and the change of state will always be determined by the occupants (although it might be possible to have different power levels, which are selectable by the user).

- **Household insulation level**. The heating and cooling appliances produce internal thermal flows that are added or subtracted from the total thermals gains. However, some of those thermals gains will depend on the structural characteristics of the household. Taking into account all the parameters, geometrical structure and construction materials of the stock of houses will require a computational intensive task with a large database. Moreover, those data are not usually widely available. Thus, an alternative might be the definition of the different average levels of insulation and thermal losses, which will determine the probability of activating the heating and cooling equipment. Therefore, in a poor insulated household, the probability of turning on a device or cycling a thermostat controlled appliance is higher than in a good insulated one.

2.3.4.3 Simulation algorithm

The simulation algorithm is shown in Figure 2.6, where, as it can be seen, the same iterative procedure of the previous models is also carried out. Therefore, for each simulation interval and heating or cooling appliance, the consumption is calculated by using the above-exposed methodology and input parameters.

First, the simulation system loads all the input parameters about the dwelling characteristics and the appliances, as well as the active occupancy for each time interval and the temperature data, that must include, as it was exposed, both the daily indicators (mean, maximum and minimum temperature) and the detailed profile for the day.

Next, the degree-days are calculated for the heating (HDD) and cooling (CDD) consumption. These values will determine the overall consumption intensity for the given day, so if the HDD>0, a heating consumption is likely to occur, whereas if the CDD>0, the consumption will be due to the cooling appliances. If both of these values are null or negative, then the zone conditioning system will not consume electrical energy for this day.

Nevertheless, the simulation procedure continues to account the energy in a lower lever following the bottom-up methodology. Therefore, for each time interval and appliance, the active occupancy of the household is checked. If there are no active occupants, the heating and cooling appliance will be turned off, since mainly electrical heating and cooling appliances do not remain on when nobody is at home. However, as it can be observed in Figure 2.6, this condition has an asterisk in the switch off condition as it implements a percentage of exception (around 10% for the studied countries) due to the fact that a relatively significant percentage of heating and cooling appliance might be on during the night by using temporization methods

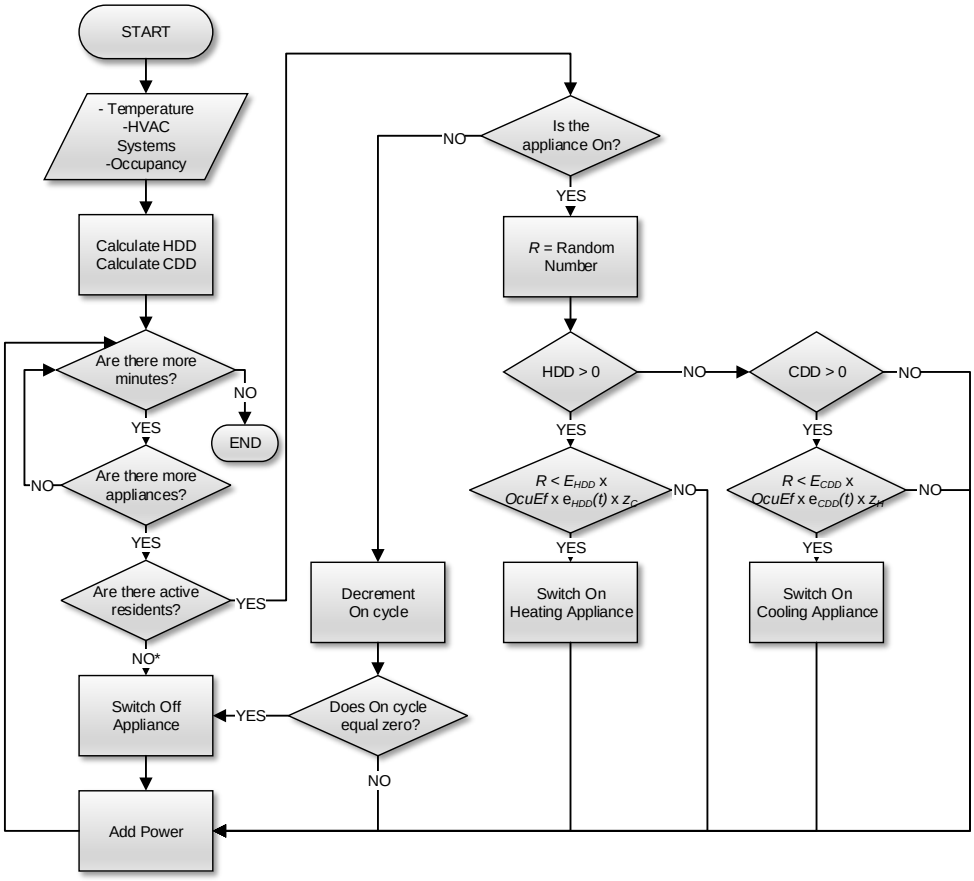

Figure 2.6: Flowchart of the cooling and heating systems consumption simulation algorithm.

and when the active occupancy is null. Thus, although the occupancy might be zero in some cases, the appliances will continue operating until their cycle is finished.

After this, if there is active occupancy, the state of the appliance is tested. If the appliance is already on, the on cycle will continue either until the end of the established average operation time or until the temperature is within the comfort limits in the case of thermostat operated systems. Opposite, when the appliance is off, the possibility of being turned on is checked. This logical and statistical test has two levels.

The first level or step is related to the energy intensity of the day. For this aim, the obtained values of the HDD and CDD are used. These indices relate the deviation from the comfort temperature with the daily energy intensity. Therefore, if any of them is not null, there is a possibility of consuming energy for this day and the logical test continues to the next stage. Otherwise, if both are zero, it means that it is no likely to use the heating or cooling devices for this day.

If the logical test of the first level is true, the system will continue to the second stage, where the possibility of turning on a heating or cooling device is now tested with a higher temporal resolution using the daily temperature profile. For this, a random number, generated in the previous steps is used and compared with the product of three probabilities.

The first one named as E_{HDD} or E_{CDD} relates the deviation from the comfort temperature with the consumption intensity. This can be calculated using the historical temperatures and the consumption figures for each day and then normalising the results as a probability distribution. The second influence factor is the effective occupancy ($OcuEf$), which as well as in the lighting consumption model takes into account the sharing of the heating and cooling appliances. Finally, the last factor is the energy intensity related to the temperature for that simulation interval ($e_{\mathrm{HDD}}(t)$ or $e_{\mathrm{CDD}}(t)$), obtained from the daily profile and the insulation level of the household. In addition, two calibration scalars are introduced in order to keep the results consistent with the annual consumption figures observed in the studied region (z_H or z_C).

Thus, if the result of the test is true, the appliance is turned on, setting either an operation cycle for it, in the case where no thermostat control is implemented by the device, or a comfort thermostat temperature for switching off, when the equipment has a thermostat control. Finally, the power consumption for this interval is accounted for this appliance.

Subsequently, iterating through all the time interval and defined appliance, the energy consumption due to heating and cooling equipment is simulated for a household with the given characteristics having the advantage of individually emulating the behaviour of each device in relation to the human patterns and the external climate conditions.

2.3.5 Remarks on the model

The previous sections have presented a specific model based on the bottom-up methodology and based on time of use data. Thus, it is only a concrete implementation that has been proposed by the authors due to the capabilities that it presents in relation with the integration of energy resources. Nevertheless, as it was pointed out in Section 2.2, the range of possibilities when it comes to the demand modelling techniques is broad, so in case further knowledge about the topic is desired the lecture of the references [9, 10] is recommended.

Some of these capabilities of the model that will be used in the following section to show the possible applications are summarised below:

- **Simplicity of use:** The model has only a few input parameters, some of which can be defined by the user or obtained from third party sources such as the climate condition regarding irradiance and temperature. Therefore, in the most general case, the only input information required by the model will be the number of residents in each house, the number of households to be simulated, the region where they are located and the date (including month, the day of the month and the day of the week). With this information, the climate condition will be loaded from the database based on the date and location, and the household characteristics such as appliances, insulation and income level will be selected randomly on the basis of the observed statistics of the region. Nevertheless, due to the high flexibility of the model, the climate condition, the appliances sets or the household characteristics can also be defined, although deeper knowledge of the system to be modelled will be required.

- **Individual household simulation:** The results of the model are obtained with high temporal resolution (1-min resolution in the results that will be presented) for each defined household. Thus, each consumption profile will simulate the real stochastic behaviour of the residents. It is true that this will be required to perform aggregated simulation in order to obtain significant results. However, it allows us to simulate low-level phenomena such as the distributed integration of PV, micro-wind turbines or batteries at household level or the influence of each house consumption and generation in the feeder (overvoltage, overload etc.) if further details of the distribution system are known.

- **Breakdown of energy end-uses and appliance:** As well as from the distribution point of view, the proposed model has also several advantages from the end-user point of view. The division of the consumption into lighting, general appliances and heating and cooling devices allow determining not only the energy intensity of each of them but the actual daily profiles of this consumptions.

In addition, the modelling of the global consumption as the aggregate of each individual appliance presents significant benefits. On the one hand, energy policies can be tested from the user point of view such as the impact that might have a technological update of lighting systems, the usage of a more efficient appliance or certain energy saving behaviours. On the other hand, the period of usage of the different appliance can be observed along the daily profile, which can be used for the development of demand response strategies that shift some of those consumptions to other period of the day depending on factors such as the variable price of the energy or the integration of non-dispatchable renewable resources.

2.4 Applications of bottom-up stochastic models

After exposing the modelling methodology, as well as the main features of the model, the usage of the system will be addressed for four tasks. First, the characteristics for demand prediction will be commented. After this, the capabilities for the assessment of energy policies and demand response strategies will be exposed. Finally, the usability of the system for energy resource integration will be introduced.

2.4.1 Demand prediction

The possibility of supplying the model with external conditions data and characteristics of the households allows using the system for the prediction of power and energy needs. Nevertheless, it has to be considered that the model methodology is based on a stochastic process, so the simulation of an individual household

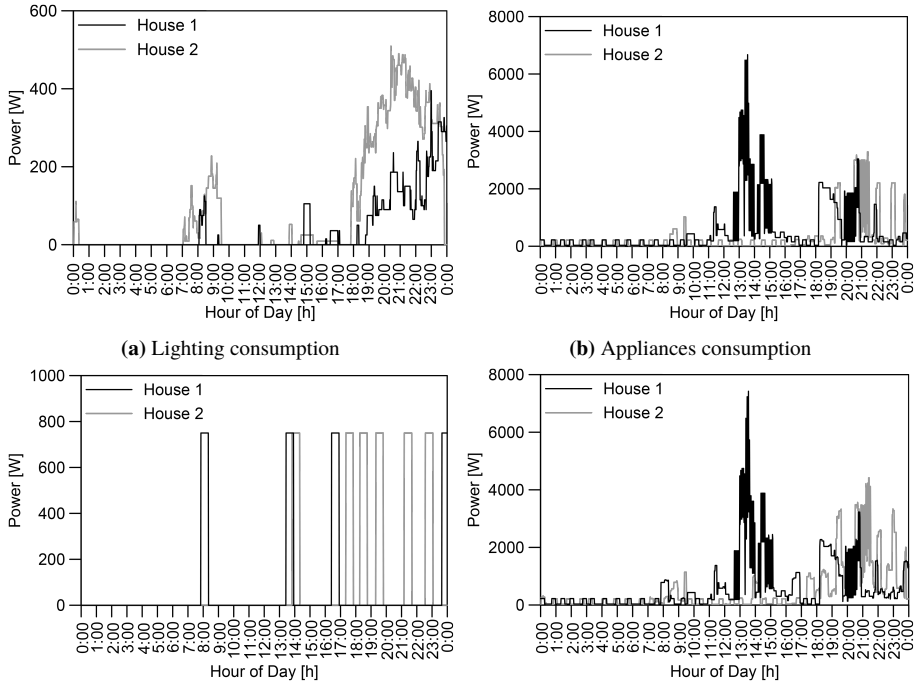

(a) Lighting consumption

(b) Appliances consumption

(c) HVAC consumption

(d) Total consumption

Figure 2.7: Daily simulation. Two households of three residents for a weekday in winter and located in Cordova.

cannot be employed as a forecasting tool, due to the determinism of the simulation. This fact is presented in Figure 2.7 where the instantaneous power consumption with 1-min resolution has been simulated with the model for two households with three residents during a weekday of a winter month and located in Cordova, Spain.

Figure 2.7 includes the different sub-consumptions, (a) lighting, (b) general appliances, (c) heating, as well as the total consumption (d). As it can be observed, the degree of determinism of the results is extremely high as each appliance is represented at a low level. This completely tallies with the actual behaviour of the residents, whose activity is chaotic. Therefore, as the figure depicts, each time the model is run, the curves obtained are different, and subsequently, the results cannot be used for the estimation of the demand.

However, despite the stochastic methodology, the observed statistics of the population are intrinsically implemented in the model. This means that if enough simulations are performed, the results are likely to have a trend and be reproducible. In other words, a number of household with some given characteristics can be simulated, representing a community, neighbourhood or group of users connected to the same network or feeder. With this methodology, each simulated house will present deterministic results almost irreproducible, but the aggregated estimation will produce similar results.

This is observed in Figure 2.8, where the results for 2 groups of 1,000 household as the one previously simulated are represented. As is shown, both groups present similar daily estimations. Therefore, in the same line of the top-down models that aim to estimate the total demand for supply purpose, the aggregated data of bottom-up models can be used for the same task. However, the results have to be calibrated for each zone in order to predict consumption figures consistent with the observed energy in the area or region.

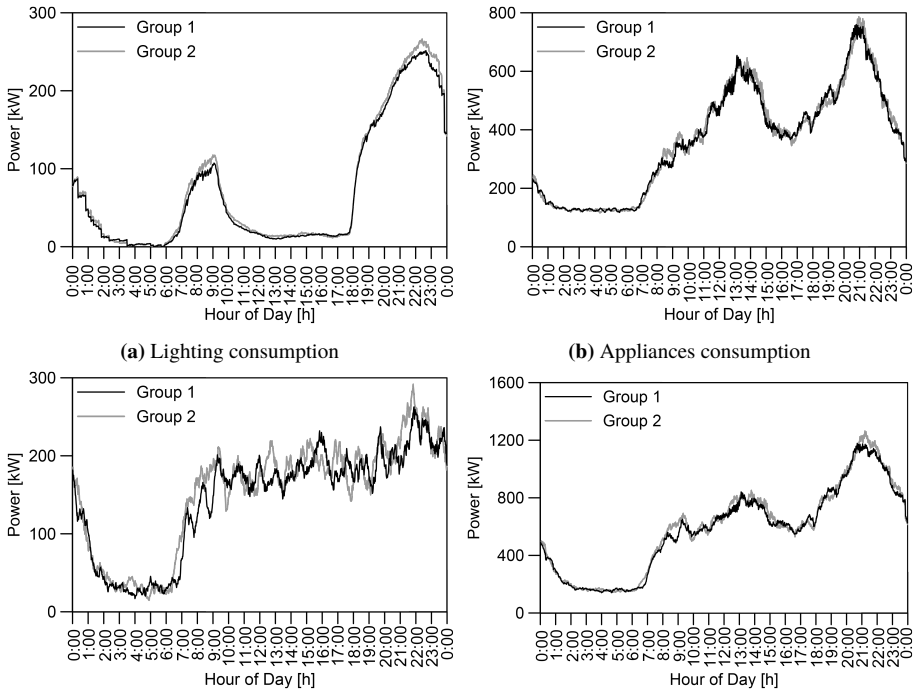

(a) Lighting consumption

(b) Appliances consumption

(c) HVAC consumption.

(d) Total consumption

Figure 2.8: Daily simulation. Two groups off 1,000 households of three residents for a weekday in winter and located in Cordova.

2.4.2 Energy policies and demand response strategies assessment

The previous section has shown the possibility of using the stochastic models for demand prediction. However, they present better and exclusive features in other fields such as the energy policies and demand response strategies assessment. These capabilities are a consequence of the modelling strategies, where each appliance is individually simulated with a given power consumption and operation cycle. Therefore, if the characteristics of these appliances or their relationship with the human behaviour are changed following some policies, the impact on the overall consumption can be observed.

The first element that can be simulated is the adoption of certain energy policies. Energy policies are understood as techniques that aim to address energy issues and they can be composed of legislation, incentives or guidelines. Some of those policies might be a change in the appliance technology with more efficient equipment or consumption reduction with some energy-saving strategies.

Figure 2.9 represents the impact of reducing the consumption of standby equipment in an aggregate of 10,000 households during a winter day. This reduction can be driven by the users' interaction or using specific switches that detect that consumption and deactivate the appliances. Anyhow, the consequence of this is that the consumption of the appliances, when they are off, is reduced from a few Watts to zero. This impact can be observed in the daily profile where a reduction between the base scenario (solid black line) and the action applied (solid grey line) is depicted, especially during the night period.

In energy terms, if the daily energy consumption of the both scenarios is accounted, the reduction is around 8% a day. That means that if the average consumption of a household is around 14 kWh/day, almost 1 kWh can be saved each day if the operation of a certain device in standby is avoided. Other strategies that can be tested are the implementation or update of technologies, as was shown in [8], where the implementation of the new European directive regarding the substitution of lighting technologies was assessed.

Another important field of application is the development of demand response strategies. These techniques aim to manage the different appliances' consumptions in a way that certain optimums or desired objectives are achieved. Some of these objectives are usually the match between generation and consumption when non-dispatchable resources are used or the reduction of the monthly bill in a context where dynamic energy or electricity prices are established.

An example of the usage of the model for simulating these techniques is shown in Figure 2.10. The case of study is a set of 10 000 households with PV production whose objective is to increment the solar energy usage and reduce the night peak, which will have to be supplied either from an energy storage system or from the grid. In order to reduce the peak, a group of loads considered as shiftable during the day have been selected to be moved to the period when the irradiance is maximum. Those loads are washing machines, tumble dryer and washer dryer machines.

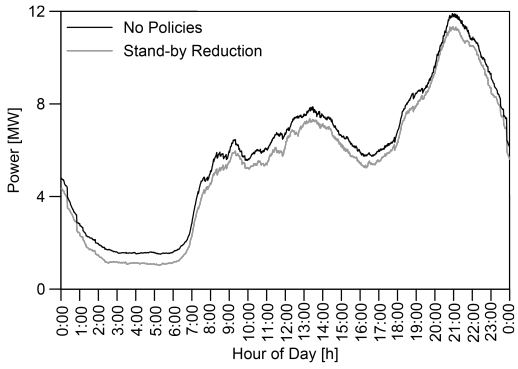

Figure 2.9: Impact of standby reduction policies for an aggregate of 10,000 households.

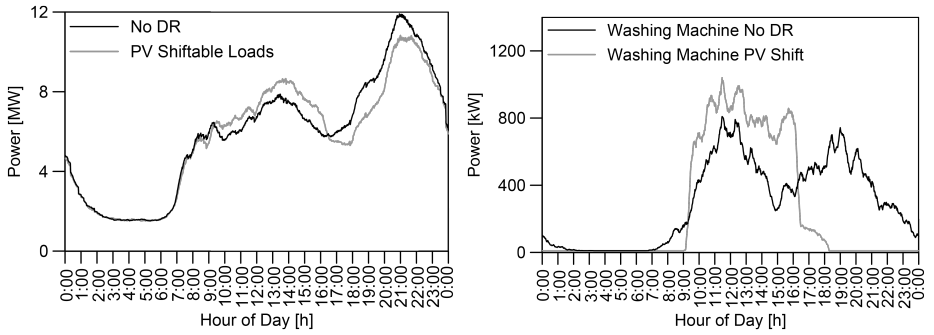

(a) Aggregate consumption **(b)** Washing machine consumption

Figure 2.10: Impact of demand response strategies with shiftable loads to match PV generation. 10,000 households.

The global results of this strategy can be observed in Figure 2.10, where the aggregated instantaneous power consumption of the 10,000 households is represented for the base scenario (solid black line) and for the demand response scenario (solid grey line). As can be observed, the result is as expected, and the demand during the middle hours of the day has been increased, whereas the night demand peak has been reduced around 1 MW in aggregate.

Moreover, as the model is able to simulate each appliance individually the instantaneous power demand only for one of the selected appliances for demand response strategies can be observed at a low level. In this case, the aggregate demand for the washing machines is represented in Figure 2.10 for the base scenario (solid black line) and for the demand response scenario (solid grey line). It should be pointed out that although 10,000 different households are simulated; it does not mean that each of them has installed a washing machine, but they are randomly distributed according to the observed penetration rates include in the model.

The results clarify the demand response strategy. In the base scenario, the consumption due to the washing machines presents two demand peaks one around 12.00 h, and the second one around 19.00 h. The demand response strategy is to centralise these consumptions in the central hours of daylight when the PV generation is the highest, as well as avoiding using those appliances when no solar irradiation exists. Thus, in the demand response scenario the consumption is now limited from 9.00 h to around 18.00 h, increasing the utilisation of the solar resource and eliminating the demand when there is no daylight.

2.4.3 Distributed resources integration

Finally, the last field of application of these models is the evaluation of the integration in the households of distributed energy resources. As the model is able to simulate each individual house independently, the interaction with renewable resources such as PV generation, as well as with different storage systems and the energy exchange with the grid can be simulated. This is especially important when non-dispatchable resources are considered since demand and generation can be non-coincident and, therefore, although enough energy might be generated, some of this energy cannot be utilised unless a storage system is also installed [28].

Thus, at a low level, the individual behaviour can be simulated as is shown in Figure 2.11, where two individual households, located in the same community or neighbourhood, are presented. As can be seen, the consumption profiles are completely different and subsequently the interaction with the PV generation and the storage system. These types of simulations are useful for developing energy management strategies, where the grid interaction can be studied at a low level, sometimes with the possibility of including the influence on voltage and frequency of the injection of the PV excess power. In addition, peer-to-peer energy management can be also studied emulating the wide range of demand profiles and the casuistry that they might generate.

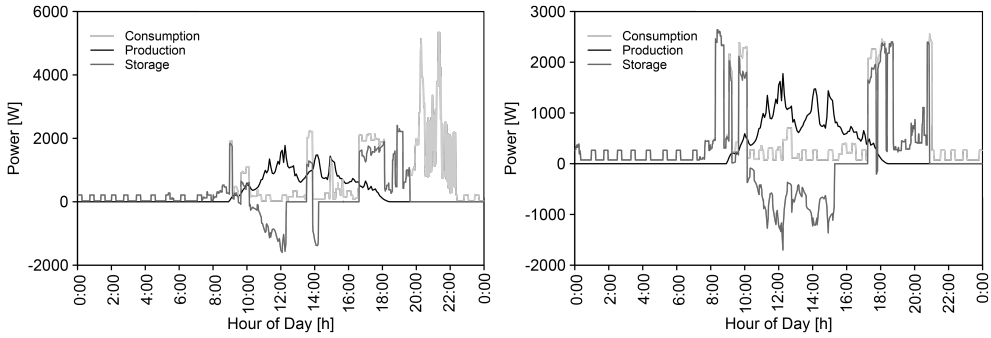

(a) Household 1 **(b)** Household 2

Figure 2.11: Individual simulation of two households with PV production and energy storage system.

Moreover, using the above-mentioned individual profiles, the aggregate curves for demand (a), production (b), grid exchanges (c) and storage (d) can be constructed for a group of households with a high temporal resolution, something that might be interesting for the planning of the distribution network when bidirectional power flows exist. That can be observed in Figure 2.12 where a contour plot has been

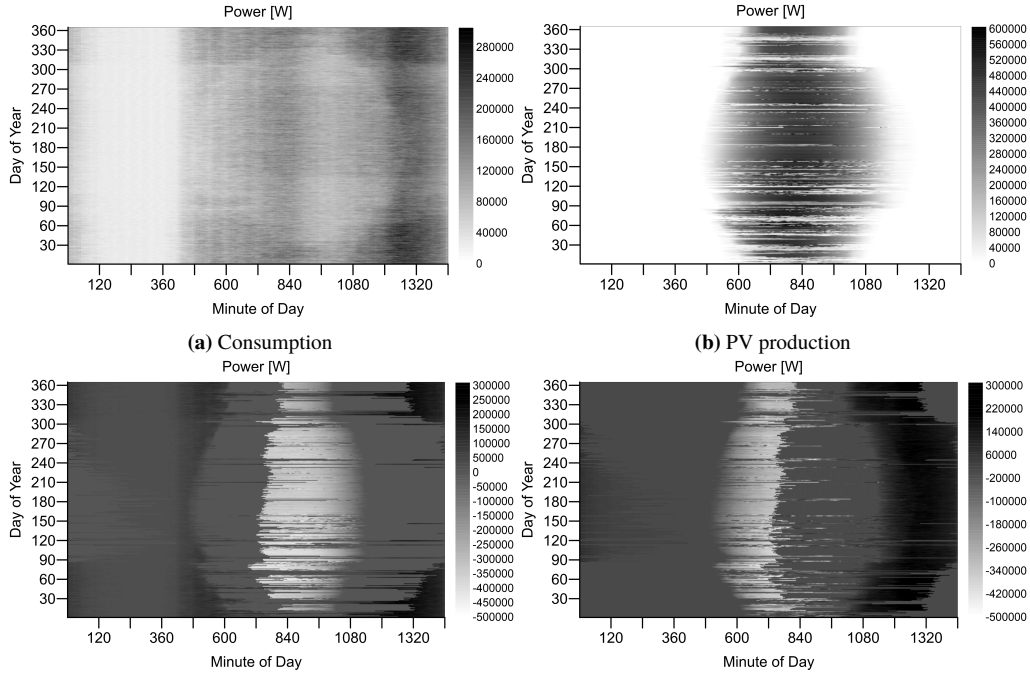

(a) Consumption **(b)** PV production

(c) Grid exchanges **(d)** Battery storage system

Figure 2.12: Interaction with distributed renewable resources of a 200 household community with PV production, energy storage and grid exchanges.

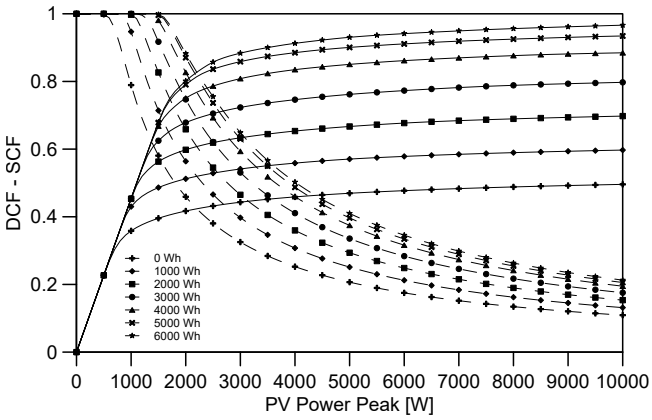

Figure 2.13: Demand cover factor (solid lines) vs supply cover factor (dashed lines).

used for representing a whole year with a 1-min resolution of a community composed of 200 households with integrated PV production and storage located in the south of Spain. The X-axis represents the minute of the day, the Y-axis is the day of the year and the colour scale is the instantaneous power.

The complexity of the information represented in the graph is high, but many conclusions can be obtained. From the consumption plot (a), it can be seen how the power demand varies along the year, but always presenting two consumption peaks around 13.00 (780) and 22.00 h (1,320) corresponding with the lunch and dinner times in Spain. In addition, it can be observed how the demand from 20.00 (1,200) to 24.00 (1,440) increases during the winter months, whereas for the summer months the consumption is increased from 14.30 (870) to 19.00 h (1,140). In the case of the PV production (b), the increment in the hours of light from the winter to the summer months is clearly illustrated too. Moreover, the existence of many days with low irradiance during the winter period is also depicted.

These both profiles have a direct influence in the grid exchanges (positive means power imported from the grid, while negative is power injected in the grid) and the storage system (positive when the battery discharges and negative when it is charged). Therefore, in the grid exchanges (c) figure it is shown how during the winter months it is necessary to buy energy from the grid starting around 22.00 h (1,320) and sometimes early for the days with the worst weather conditions. This tallies with the behaviour of the storage system (d) that cannot be fully charged in the winter days. Opposite, during the summer time, the system can sell energy to the grid for a long time, as well as fully charge the storage system. Thus, almost no energy has to be bought from the grid.

With all this information at such a high level of resolution, it is possible to evaluate the average autonomy and energy utilisation of a given community, neighbourhood or grid area. This can be performed by means of some indicators defined in the literature named as demand cover factor (DCF) and supply cover factor (SCF). The DCF indicates the percentage of demand that can be supplied with the generation system either by direct consumption or by delayed consumption when storage systems are installed. On the other hand, the SCF accounts for the degree of utilisation of the generation system. The formal definition of these two indices can be found in [29].

Using these two indices, the proposed model and different rates of penetration of PV generation and battery storage, Figure 2.13 was constructed where the average DCF (solid lines) and the SCF (dashed lines) can be observed for a household located in the south of Spain and simulated during a year using real irradiance data. The X-axis represents the different PV power peaks that might be installed, whereas the lines with different colours are different capacities of the storage system.

This figure depicts that when more PV power is installed in the household the DCF increases, but with a tendency to saturate. In contrast, the SCF decreases since not all the PV capacity is used every day, but only in the worst scenarios. On the other hand, when the storage capacity is increased both indices are always improved. Nevertheless, the degree of enhancement is major for the DCF, allowing the delayed consumption of the PV generation.

In addition, it should be pointed out that for a given battery capacity value, both the DCF and the SCF intercept. At this point, the energy demand that cannot be covered (1-DCF) equals the portion of energy production that can be neither stored nor consumed (1-SCF). Nevertheless, if a bi-directional power flow interchange with the grid is considered, the net energy exchanged with the grid at that point will be zero and, therefore, if not additional losses are considered, the system will follow a net-zero energy philosophy. Thus, this modelling technique has several advantages as an energy planning tool.

2.5 Conclusion

The chapter has presented the current context of the demand modelling with a focus on the stochastic and bottom-up modelling techniques. In this context, this specific methodology has been contextualised between all the other strategies pointing out the reasons and arguments that make this technique the most suitable in the context of this book.

Next, the methodology for implementing this modelling technique has been shown, addressing the main parts of the system, as well as the basic and fundamentals of each of them. Subsequently, the simulation procedure that is employed for generating the results has been explained by means of detailed flow charts and exposing the main input parameters, and how they can be obtained.

Finally, the application areas have been discussed. The validity of this model for demand prediction has been exposed, although some issues derivate from the stochastic simulation methodology do not make this model the most suitable for accurate energy prediction in aggregate terms. However, they have shown a unique ability in the fields of energy policies assessment, demand response strategies development, and distribute energy resources integration and planning, all of these due to their capability of simulating the appliances at a low level and always in relation to the human behaviour. This emphasises the important role that stochastic modelling techniques can play in the energy planning and management sector.

References

[1] L. Suganthi, A. A. Samuel, Energy models for demand forecasting - A review, Renewable and Sustainable Energy Reviews 16 (2) (2012) 1223–1240. doi:10.1016/j.rser.2011.08.014.

[2] L. Pérez-Lombard, J. Ortiz, C. Pout, A review on buildings energy consumption information, Energy and Buildings 40 (3) (2008) 394–398. doi:10.1016/j.enbuild.2007.03.007.

[3] A. de Almeida, P. Fonseca, B. Schlomann, N. Feilberg, Characterization of the household electricity consumption in the EU, potential energy savings and specific policy recommendations, Energy and Buildings 43 (8) (2011) 1884–1894. doi:10.1016/j.enbuild.2011.03.027.

[4] S. Cao, K. Sirén, Impact of simulation time-resolution on the matching of PV production and household electric demand, Applied Energy 128 (2014) 192–208. doi:10.1016/j.apenergy.2014.04.075.

[5] J. Widén, E. Wäckelgård, J. Paatero, P. Lund, Impacts of different data averaging times on statistical analysis of distributed domestic photovoltaic systems, Solar Energy 84 (3) (2010) 492–500. doi:10.1016/j.solener.2010.01.011.

[6] J. Torriti, Demand Side Management for the European Supergrid: Occupancy variances of European single-person households, Energy Policy 44 (2012) 199–206. doi:10.1016/j.enpol.2012.01.039.

[7] J. Torriti, A review of time use models of residential electricity demand, Renewable and Sustainable Energy Reviews 37 (2014) 265–272. doi:10.1016/j.rser.2014.05.034.

[8] E. J. Palacios-Garcia, A. Chen, I. Santiago, F. J. Bellido-Outeiriño, J. M. Flores-Arias, A. Moreno-Munoz, Stochastic model for lighting's electricity consumption in the residential sector. Impact of energy saving actions, Energy and Buildings 89 (2015) 245–259. doi:10.1016/j.enbuild.2014.12.028.

[9] L. G. Swan, V. I. Ugursal, Modeling of end-use energy consumption in the residential sector: A review of modeling techniques, Renewable and Sustainable Energy Reviews 13 (8) (2009) 1819–1835. doi:10.1016/j.rser.2008.09.033.

[10] A. Grandjean, J. Adnot, G. Binet, A review and an analysis of the residential electric load curve models, Renewable and Sustainable Energy Reviews 16 (9) (2012) 6539–6565. doi:10.1016/j.rser.2012.08.013.

[11] I. Richardson, M. Thomson, D. Infield, A high-resolution domestic building occupancy model for energy demand simulations, Energy and Buildings 40 (8) (2008) 1560–1566. doi:10.1016/j.enbuild.2008.02.006.

[12] J. Widén, E. Wäckelgård, A high-resolution stochastic model of domestic activity patterns and electricity demand, Applied Energy 87 (6) (2010) 1880–1892. doi:10.1016/j.apenergy.2009.11.006.

[13] M. A. Lopez, I. Santiago, D. Trillo-Montero, J. Torriti, A. Moreno-Munoz, Analysis and modeling of active occupancy of the residential sector in Spain: An indicator of residential electricity consumption, Energy Policy 62 (2013) 742–751. doi:10.1016/j.enpol.2013.07.095.

[14] D. Ndiaye, K. Gabriel, Principal component analysis of the electricity consumption in residential dwellings, Energy and Buildings 43 (2-3) (2011) 446–453. doi:10.1016/j.enbuild.2010.10.008.

[15] M. Stokes, M. Rylatt, K. Lomas, A simple model of domestic lighting demand, Energy and Buildings 36 (2) (2004) 103–116. doi:10.1016/j.enbuild.2003.10.007.

[16] I. Richardson, M. Thomson, D. Infield, A. Delahunty, Domestic lighting: A high-resolution energy demand model, Energy and Buildings 41 (7) (2009) 781–789. doi:10.1016/j.enbuild.2009.02.010.

[17] J. Widén, A. Nilsson, E. Wäckelgård, A combined Markov-chain and bottom-up approach to modelling of domestic lighting demand, Energy and Buildings 41 (10) (2009) 1001–1012. doi:10.1016/j.enbuild.2009.05.002.

[18] E. J. Gago, J. O. García, A. E. Estrella, Development of an energy model for the residential sector: Electricity consumption in Andalusia, Spain, Energy and Buildings 43 (6) (2011) 1315–1321. doi:10.1016/j.enbuild.2011.01.016.

[19] C. F. Reinhart, Lightswitch-2002: A model for manual and automated control of electric lighting and blinds, Solar Energy 77 (1) (2004) 15–28. doi:10.1016/j.solener.2004.04.003.

[20] D. R. G. Hunt, The use of artificial lighting in relation to daylight levels and occupancy, Building and Environment 14 (1) (1979) 21–33. doi:10.1016/0360-1323(79)90025-8.

[21] REMODECE project, Residential Monitoring to Decrease Energy Use and Carbon Emissions in Europe (REMODECE) Database (2015). URL: http://remodece.isr.uc.pt/

[22] ENTRANZE project, Heating and cooling energy demand and loads for building types in different countries of the EU (2014). URL: http://www.entranze.eu/

[23] A. Afram, F. Janabi-Sharifi, Review of modeling methods for HVAC systems, Applied Thermal Engineering 67 (1-2) (2014) 507–519. doi:10.1016/j.applthermaleng.2014.03.055.

[24] D. J. Sailor, Relating residential and commercial sector electricity loads to climate - Evaluating state level sensitivities and vulnerabilities, Energy 26 (2001) 645–657. doi:10.1016/S0360-5442(01)00023-8.

[25] H. Sarak, A. Satman, The degree-day method to estimate the residential heating natural gas consumption in Turkey: A case study, Energy 28 (9) (2003) 929–939. doi:10.1016/S0360-5442(03)00035-5.

[26] E. Valor, V. Meneu, V. Caselles, Daily Air Temperature and Electricity Load in Spain, Journal of Applied Meteorology 40 (8) (2001) 1413–1421. doi:10.1175/1520-0450(2001)040<1413:DATAEL>2.0.CO;2.

[27] M. Isaac, D. P. van Vuuren, Modeling global residential sector energy demand for heating and air conditioning in the context of climate change, Energy Policy 37 (2) (2009) 507–521. doi:10.1016/j.enpol.2008.09.051.

[28] E. J. Palacios-Garcia, A. Moreno-Munoz, I. Santiago, I. M. Moreno-Garcia, M. I. Milanes-Montero, Smart community load matching using stochastic demand modeling and historical production data, in: 2016 IEEE 16th International Conference on Environment and Electrical Engineering (EEEIC), IEEE, 2016, pp. 1–6. doi:10.1109/EEEIC.2016.7555885.

[29] J. Munkhammar, P. Grahn, J. Widén, Quantifying self-consumption of on-site photovoltaic power generation in households with electric vehicle home charging, Solar Energy 97 (2013) 208–216. doi:10.1016/j.solener.2013.08.015.

3

Stochastic model for lighting's electricity consumption in the residential sector. Impact of energy saving actions

Emilio J. Palacios-Garcia[1], Aihou Chen[1], Isabel Santiago[1], Francisco J. Bellido-Outeiriño[1], Jose Maria Flores-Arias[1], and Antonio Moreno-Munoz[1]

[1]Departamento de Arquitectura de Computadores, Electrónica y Tecnología Electrónica, Escuela Politécnica Superior, Universidad de Córdoba, Córdoba, Spain.

Abstract

The residential sector represents about 30% of the total energy demand in Europe. Included in this percentage, lighting consumption is one of the basic end uses in all households and it may come to represents 15–20% of the total electricity bill. This figure can be reduced using advanced control techniques or more efficient lighting technologies, requiring previous detailed information about current consumption patterns. In this context, bottom-up stochastic models are established as the main tools to study new energy savings. In this paper, a high-resolution stochastic model for simulating lighting consumption profiles was developed, obtaining both daily active and reactive instantaneous power demand profiles, with a 1-minute resolution. The model takes into account the number of household residents and differentiates between weekdays and weekends. Moreover, the monthly and annual amounts of electricity demanded by lighting in Spanish households were simulated. The proposed model was also used to quantify the impact of LED technology's penetration into domestic lighting systems on consumption patterns. Research has revealed the existence of two consumption peaks matching with morning and evening. Although these peaks are hard to shift since they are due to human behavior, they are easy to reduce through the improvement of lighting systems.

The paper has been published in *Energy & Buildings, 2015, 89 pp. 245-259. doi:10.1016/j.enbuild.2014.12.028*. The layout has been revised.

3.1 Introduction

In the current energy context the residential sector, with an average worldwide energy consumption of around 30% of total consumption [1, 2], represents a key factor in terms of energy supply needs. In Spain, this sector represents 17% of the end energy consumption and 25% of total electricity demand [3]. In addition, this electricity consumption has a broadly upward trend due to the increasing number of households, the higher comfort of occupants and the greater number of appliances at home, with a widespread utilization of new types of electricity loads [4].

Against a backdrop of increasing electricity demand, new policies and measures, focused on optimizing users' consumption, are being studied by researchers and governments. The aim is to achieve a significant impact on aggregate energy saving and to establish a way of meeting the environmental requirements for CO_2 reductions [5]. Along with this environmental factor, higher demand may involve a grid overload. In this situation the ability to withstand the demand peaks could mean the full resizing of the current system which would, in turn, require heavy investment. Thus, not only is the goal to reduce consumption, but also to stimulate the development of strategies for demand response (DR) solutions which would lead to peak shifting and to a better equilibrium between generation and consumption [6, 7], while looking towards a future scenario of smart grids and smart homes [8].

In order to reduce consumption and to achieve load control it is fundamental to know the demand profiles of individual electrical devices in dwellings, instead of merely the total household electricity consumption [8]. Among all domestic appliances, one of the potential devices for focusing the means of action are household lighting systems, whose consumption in some European countries such as Sweden or UK, and in Canada, could amount from 15 to 20% of the total electricity bill [4, 9–12]. Based on these considerations, the first objective of this work was to develop a model which would enable us to deliver a reliable measurement, with high temporal resolution, of the consumption patterns related to the electrical energy demanded, associated with lighting, in the Spanish residential sector, data which were unavailable for this country.

At present, the global estimations of electrical consumption for lighting in Spanish households were supplied by IDAE [3]. In addition, Gago *et al.* [13] have previously developed a lighting consumption model for the residential sector in Andalusia, Spain. However, the demand load profiles provided by these authors, gives only a one-hour resolution. Using the model proposed in this paper, one-minute resolution load profiles can be achieved, differentiating between the number of residents in the household, the type of day (weekdays and weekends) and the month. This higher resolution in the results are justified since most DSM (Demand Side Management) programs require a level of granularity in time-related data of between 5 and 30 min [14]. Information on lighting consumption patterns in the residential sector already exists for other EU countries [10, 15], some of them within the European REMODECE (Residential Monitoring to Decrease Energy Use and Carbon Emissions in Europe) project [4] framework. Nevertheless, Spain was not included in these studies and the different schedule distributions, lifestyles and routines of Spain versus its neighboring countries indicate the importance of this present analysis [16].

Once consumption patterns were modeled and analyzed, the second objective of this paper was to make use of the model developed in order to assess the impact associated with saving policies in domestic lighting systems with regard to the current situation. The use of electric lighting at home, related to the basic comfort of its residents, takes place mainly in the hours associated with higher occupancy and with lower solar irradiance levels. Changing these schedules, by means of implementing demand management techniques, might not be the most suitable solution for this type of loads at home. In contrast, other energy saving measures, such as using regulated lamps [17] or installing more efficient technologies, with a higher lumen per Watt rate, may be more appropriated for this goal. Some European and National policies are focused on this latter proposal to use more efficient lamp technologies [18]. This was the measure analyzed in this paper due to its effectiveness to reduce electricity consumption. Implementing this saving measure through the use of the proposed model enabled to obtain a detailed environmental impact analysis and a reliable economic study.

To quantify the impact of these proposed policies, or other future possibilities, the developed model should exhibit a high degree of flexibility in order to work with low-level individual household data, in order to establish the correct modification that these saving measures would involve in their characteristics. As shown in the Swan and Ugursal classification [2], named bottom-up models are the most suitable tools to perform these studies. This type of energy demand models yield accurate results with high time and spatial resolutions, without any great complexity. These models start with the individual households or just an appliance as a basic consumption unit, and make use of statistical data relative to household characteristics, types of appliances or installed systems, as well as information on their occupants' behavior, highlighting the active occupation patterns of different household types [19–21]. The global consumption in this type of model is then obtained by the aggregation of each individual unit. However, one of the principal issues is to obtain all of the input data required by the model, data which are not always easily available. In addition to other sources, this paper used information from national Time Use Surveys (TUS), conducted in 2009-2010 by the National Statistical Institute in Spain for an annual period, following the EUROSTAT guidelines for harmonizing time use data [22]. Despite the disadvantage of requiring an extensive database of empirical data, this type of model enables us to simulate changes in consumption habits and installed technologies. By comparing the results with the previously existing data, this enables us to analyze the load profile alteration as a consequence of the energy saving policies employed.

For lighting systems, different energy saving options could be the use of regulation in lamps [17], the implementation of demand management techniques, or the installation of more efficient technologies with a higher lumen per Watt rate. European and National policies are focused on this latter proposal (efficient lamp technologies) [18], so the second objective of this paper concentrates on analyzing the economic and environmental impact of applying of this particular energy saving measure.

The structure of the ideas described in this paper is the following: in Section 3.2, the modeling procedure and applied saving policies will be defined. Section 3.3 will present the results obtained with the current scenario and later, the improvement load profiles after applying the proposed saving will be presented. Finally, the conclusions of this work will be discussed in Section 3.4.

3.2 Methods

In order for it to be implemented, the bottom-up model developed required, in the first stage, a number of input parameters to be entered. After that, an algorithmic process to determine the electricity demand profiles automatically was applied. A Graphical User Interface (GUI) was developed to facilitate its implementation. Each of these parameters and the processes for result calculation are described below.

3.2.1 Input parameters

The parameters to be entered into the model using the graphical interface were the number of occupants of the dwellings, their geographic location, the date and the type of day (weekday or weekend). These parameters are not directly introduced in the calculus algorithm of the model, but the application uses them to generate the necessary input information required to determine lighting consumption profiles. This information is the daily active occupancy profiles of houses, the global daily external irradiance profiles and the type and the number of existing lighting points in the households. The procedure to calculate them from user input parameters is detailed below.

3.2.1.1 Active occupancy in households

Active household occupancy is taken to be the number of residents at home and not sleeping at each instant of time. Active occupancy profiles are one of the most influential factors in domestic energy consumption, and therefore constitute the principal input in electricity consumption simulation models. These profiles

were synthetically generated by simulating a stochastic model, grounded in Markov Chain probability theory and Monte-Carlo techniques [23, 24], included inside the general lighting consumption model proposed in this paper. This stochastic model was implemented and validated for Spain by Lopez *et al.* and its bases are described in detail in previous publications [16, 19–21]. It is also based on data extracted from Time Use Surveys (TUS) [22], conducted in Spain of 19,295 people who were at least 10 years old and living in a total of 9,541 homes. To obtain occupancy profiles by using the model, it was established that the number of active occupants for each time step depended on the number of occupants in the previous time instant. The evolution between two states was conditioned by the transition matrices. Due to it being a non-homogeneous Markov Chain process, these matrices were calculated or each of the 144 time instants considered over a whole day, based on TUS information. In TUS surveys the interviewees noted down in a diary, at ten-minute intervals, data concerning the activities that they performed over 24 hours during one random day; the place where the activities took place and whether someone accompanied them. Initial states of the model, corresponding to the active occupancy probability at 00:00 h, were also calculated from these surveys.

As already indicated, the results from this stochastic model of daily active occupancy profiles of Spanish households were obtained with a 10-minute resolution, discriminating between the number of residents in the households, their location in the different regions of the country and the type of day, all of which were parameters required for the simulation [16, 21]. These active occupancy profiles, determined by the model from the parameters initially entered, will finally be used in the calculus algorithm of the lighting consumption model proposed in this paper.

3.2.1.2 External irradiance profiles

Along with active occupancy data, other key information required as input for the lighting model were the global daily external irradiance profiles, corresponding to the location of the households analyzed. These values influence the natural light levels existing inside houses and therefore the probability of switching on lighting systems [15, 25, 26]. Irradiance information was stored in the model as average monthly curves with a 1-minute resolution. The selection of the correct irradiance data was performed automatically by the model, by inserting the date and the location in the user GUI as input parameters. These irradiance profiles were then entered into the calculus algorithm of the model as a decision variable.

The irradiance curves used in this work were requested from the Andalusian Energy Agency's [27] public database and contrasted with the data from the European PVGIS database [28]. In both cases the information supplied was average annual data for each location. Examples of such daily irradiance curves with 1-minute resolution are shown in Figure 3.1, corresponding to an average day for the months of March, June, September and December for the location of Cordova, Andalusia, where most of the results of this paper were developed.

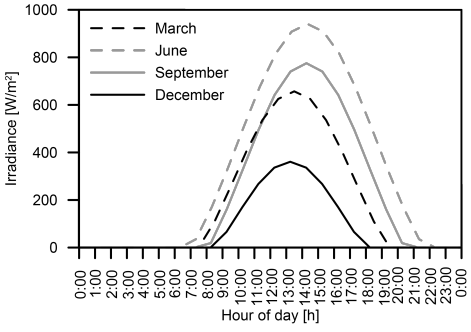

Figure 3.1: Irradiance data for the city of Cordova (Andalusia, Spain).

3.2.1.3 Type and number of lamps

The last sets of data for implementing the model were the number and technology of different lighting points in existing households. The data source used for this purpose was the report on the analysis of energy consumption in the Spanish residential sector for 2010, published by the Diversification and Energy Saving Institute [3] and based on a set of surveys and consumption measures covering the whole country. This report enabled us to define the number of installed lighting units, 23 lamps per household. However, since this value is the average number for the whole country, the standard deviation of light source numbers were determined and fitted into a normal distribution to reproduce the observed diversity in the calculus algorithm.

Next and using the same report [3], technologies probability distribution was obtained for domestic sector lamps. 5 types of technologies were distinguished: incandescent bulbs (35%), halogen (26%), fluorescents (6%), compact fluorescent (CFL) (32%) and lighting emitting diode (LED) lamps (1%). This probability distribution enables the modification of technology percentages for each simulation while preserving the average statistics properties.

With regard to lighting points, the last consideration is their consumption characteristics, namely the nominal active power and the power factor of each lamp, as well as their cost, this last parameter used for the economical approach. Although there are other important parameters which may influence in determining the selection of a certain lamp such as the Color Render Index (CRI) or the Color Temperature, the lamps used in this paper were chosen through a detailed study on the options currently available in the domestic lighting market, taking into account the variability in all these mentioned parameters. Thus, the products offered by 3 main lighting manufacturers [29–31] were analyzed, distinguishing between the above technologies and the availability of their products in the Spanish national market. Finally, both data series were interrelated in order to obtain for each technology a probability distribution which conditioned the power assignation for an individual lamp. The results for each lighting technology obtained from this analysis are shown in Figure 3.2.

Figure 3.2 illustrates that incandescent bulbs and halogen lamps are the technologies with the greatest power consumption since their lumen per Watt ratio is so poor. For incandescent lamps (round symbol), the main power values are 25, 40, 60 and 100 Watts, 60 being the principal power installed. With regard to halogen, the power consumptions are scattered, but there are 3 peaks at 28, 42 and 50 W which should be mentioned. On the other hand, fluorescent lamps (star symbol) are uniformly distributed from 6 W to 58 W. CFL bulbs (square symbol) present a huge variability. Nevertheless 11, 15 and 20 W lamps are the most widely-used. LED technology (triangular symbol) is also included since the impact of this technology in energy consumption will be analyzed later. As can be observed their power values, never more than 20 W, are the lowest.

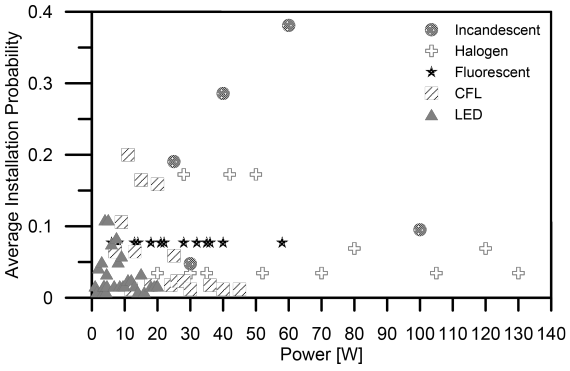

Figure 3.2: Installation probability for each lighting technology.

Table 3.1: Power factor for each lighting technology.

Technology	Power factor
Incandescent	1
Halogen	1
Fluorescent	0.8
CFL	0.5-0.9
LED	0.5-0.9

Along with these data, a power factor was also assigned to each technology. Not only does this enable us to obtain the active power consumed by residential lighting systems but also to obtain the reactive power demand. However, within each technology a certain range of variation can be observed, especially in CFL and LED lamps. In this case, the use of inductive or electronic ballast as well as the type of circuit for the LED driver, may cause variations of almost 40% in power factor. Thus, based on data provided by [32] and the recent improvement of fluorescent lamp technologies implemented in the market [33], a range of power factor values were set up for CFL and LED technologies, enabling the model to simulate the current situation in which a wide range of possibilities can be found. This procedure is only available thanks to the flexibility of the proposed model, which enables to change the power factor within the simulations. The proposed numbers are shown in Table 3.1. Therefore, consumed reactive energy estimations obtained by the model should be considered as a general assessment enabling us to make a comparison between the reactive power consumptions of each kind of lighting technology.

3.2.2 Calculus algorithm

The three previously-calculated data sets were the starting point for the simulation algorithm. The occupancy model provided the activity profile of occupants inside households with a 10-minute resolution. Irradiance curves were extracted from stored data having a 1-minute resolution and finally, light point data were given by the established probability distributions. Output data of the model were the daily lighting consumption profiles for either an individual household or an aggregate of N_h households. With these aims, a stochastic simulation procedure consisting of 4 stages was performed. These 4 stages were the active occupancy profile generation and lamp distribution; the determination of solar lighting availability inside the household; the inclusion of the active occupancy influence; and the switch-on configuration of each lighting point. The first process was performed separately, obtaining an occupancy profile for each simulated household and its lamp point distribution. The three remaining steps, however, were repeated cyclically for every lamp and every minute of the day.

As already indicated, the occupancy profile was determined by the stochastic model previously described, implemented and validated for this country by López *et al.* [16, 21] and which was included in the lighting model programming. Furthermore, the number of lamps in each household was established through a stochastic procedure consisting of the generation of a random number and computing the inverse cumulative distribution function of the fitted normal, obtained from the average number of lamps and their standard deviation. Afterwards, for each light point a technology, a power factor and an active power were assigned. This was undertaken using two new random numbers, the first number was substituted in the technology probability distribution to establish the type of lamp (Incandescent, halogen, fluorescent, CFL or LED), as well as the power factor, while the second was used to determine the power consumption inside the given technology, again using the inverse cumulative probability of the distribution function extracted from lighting manufacturers and the national market.

In the second stage, the calculus algorithm determines solar availability at households, depending on external solar irradiance and its influence on the use of electrical illumination. To achieve this aim, a threshold

of 60 W/m2 was defined as the limit for sunlight usability, establishing a standard deviation of 10 W/m2 following a normal probability distribution. This distribution, defined by Reinhart [25] and Hunt [26] in the context of offices, and also used by Richardson *et al.* [15] for the residential sector, models the variability existing in illumination availability between households of different construction types or orientations. The defined threshold was compared with the external irradiance. If the sunlight values were under this limit, electrical lighting systems would be switched on and the algorithm went to the next step.

The influence of the active occupancy profiles determined was taken into account in the third stage of the calculus algorithm. The results obtained from the previous stage determined only if artificial lighting should be switched on, but the number of active occupants also directly influences lighting consumption. For example, if external irradiance is lower than the usability threshold, but there are no occupants at home, lighting systems would not be switched on. However, if the occupancy level doubles from one occupant to two, light consumption obviously increases, nevertheless the relationship should be considered non-lineal due to the shared use of lighting points. Effective occupancy was defined to take into account this fact and occupancy levels were considered in energy terms. This relationship was proposed by Bladh *et al.* [12] based on household energy consumption data in lighting appliances according to the number of residents, data being extracted from the U.S. Energy Department [34]. Despite the facts that they are data from another country and lighting consumption was treated separately only in 1993 report (nowadays the last available year is 2009, but lighting is included inside the term of other appliances), their use was justified since they are normalized consumption values, considering the type of household by the number of residents. So an increase of energy versus an increase of occupants is related, regardless of the numerical total value of energy. In addition, as well as Bladh *et al.* [12], other authors [15] have used this source for their aim in different location and time, obtaining reliable results which have already been validated.

Another aspect to consider at this stage was the use percentage of each lamp, a concept previously discussed by Boardman *et al.* [35] and Mills *et al.* [36]. This is due to the fact that at the times of greatest occupation of a household, when residents are mainly located in certain rooms in the household, there are lamps whose switch-on probability is higher than the others. Therefore, together with the previously discussed effective occupancy, previously-mentioned relative use of the lighting points of the household should be introduced into the model. Due to the inexistence of statistical data about switch-on probability, a logarithmic distribution was used with the aim of simulating the behavior of a random variable. Using this distribution and generating a random number between 0 and 1, a relative use factor, simulating the weight of the lamp inside the total household electricity consumption [15], was obtained.

Finally in the third stage, a calibration scalar (c), also inserted into the switch on probability decision, was used to calibrate the model so that the simulated energy consumption obtained by the model was equal to the actual energy consumed in the Spanish residential sector. The calibration procedure is a consequence of the stochastic model employed in the simulation. The random process can predict the different instants where the lamps are switched on and off. However, it is not able to obtain an accuracy energy figure without a previous calibration. For this aim the equation (3.1) was used:

$$\left(\frac{1}{N_h}\sum_{h=1}^{h=N_h}\left(E_{\text{year}}\right)_h\right)\times f_s = E_{\text{real/year}} \tag{3.1}$$

where N_h is the number of households, $(E_{\text{year}})_h$ is the simulated annual active energy demanded by each household and f_s is a correction factor. $E_{\text{real/year}}$ is the real average annual consumption of Spanish households, with a value of 474 kWh/year [3], used as a calibration data. Ten simulations (N_s) of 100 households (N_h), covering a whole year, were performed to obtain the calibration scalar value. $(E_{\text{year}})_h$ was averaged for all houses (term in brackets in (3.1)) and then compared with $E_{\text{real/year}}$. The calibration scalar (c) started with a value of one, and for each simulation the correction factor f_s was obtained. Then the previously-calculated calibration scalar was multiplied by the new correction factor, involving an iterative process, as reflected in (3.2):

$$c = \prod_{s=1}^{s=N_s} f_s \tag{3.2}$$

where N_s is the number of simulations, 10 in this case. A final value of 0.007613816 was obtained for the calibration scalar.

Having finished the third stage, the algorithm should now have determined if the lighting point should be switched on. Then, in the fourth stage, a switch-on time was assigned for the lamp through a new stochastic procedure, taking into account that the switch-on time of a light spot has a certain degree of variability, an aspect previously analyzed by Stokes *et al.* [11]. Therefore, a random number was again generated and then compared against the switch-on time distribution function, obtaining a minimum and a maximum time. The final switch-on duration is randomly set between these values.

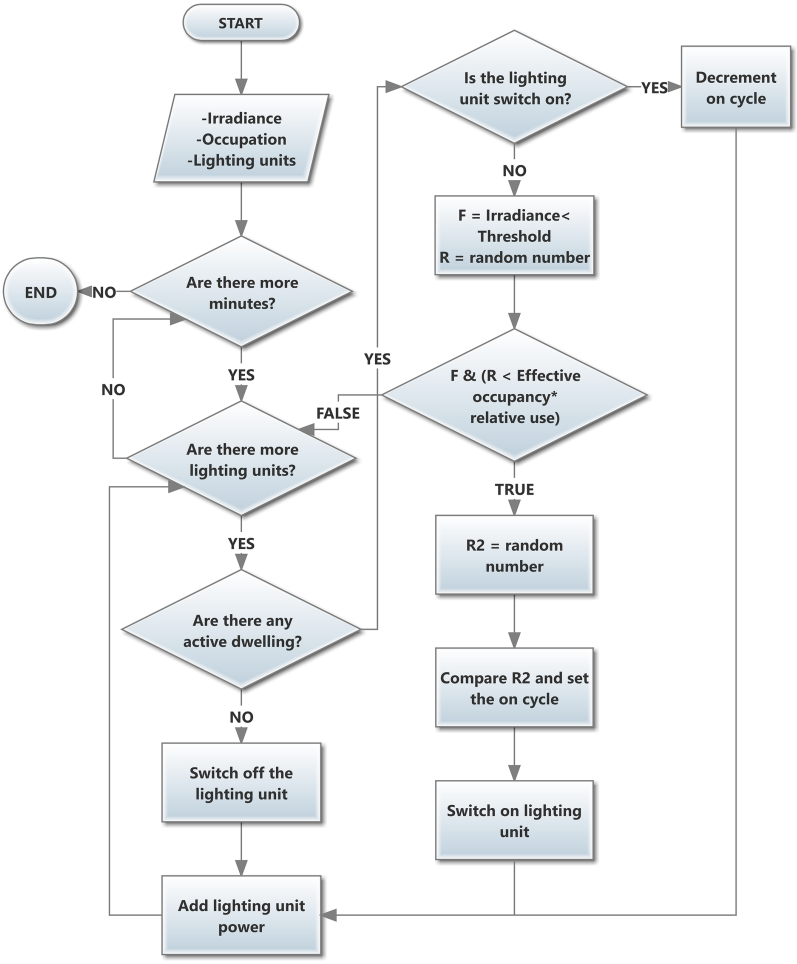

Figure 3.3: Lighting consumption generation algorithm flow chart.

Finally, a set of additional algorithms included in the fourth stage were responsible for maintaining this light spot on for the established time and adding its consumed energy. Furthermore, the algorithm ensures compliance of switch-on time, unless active occupancy becomes null, in which case the switch-on time will set to zero.

Figure 3.3 shows the calculation algorithm implemented in this work in a simple manner. Gathering all the information presented, a switch-on event of a lighting point inside the simulation procedure will take place when both sunlight levels are lower than the set threshold and the product of effective occupancy, relative lighting use, and calibration scalar is higher than a random number generated to simulate the stochastic procedure. In this case, a random switch-on time was assigned to the light spot. After that, the procedure described for a single lighting point was repeated for each remaining lamp in the household and for every minute of the day, finalizing when the whole energy consumption had been calculated. Internally, the energy consumed by each light spot was taken into account for every minute and then added to the total value, building up the daily consumption profile of the entire household. As output data the model simulation provides two vectors, corresponding to active ($\overline{P}_{1440,1}$) and reactive ($\overline{Q}_{1440,1}$) power consumed during the day by lighting systems with 1-min resolution. These vectors have 1440 elements, with the consumption demanded by this house in each minute of the day.

The model also enables us to calculate the consumption pattern of an aggregate of N_h households. In this case, the number of households must be entered by the user. This type of simulation produces interesting results, since individual simulations are as deterministic as they are due to the method of calculation. Thus the system repeats the process of generating an occupancy profile, estimating a lamp distribution and calculates the consumption profile for N_h times, adding in each iteration the energy results of all N_h homes considered, in order to build the overall aggregate curve. Thus, the consumption vector of each house is accumulated to obtain vectors of 1440 elements too, which aggregates for each minute of the day the consumption obtained for each house. This process, for the active power consumed, is expressed in (3.3):

$$\overline{P}_{1440,1}^{N_h} = \sum_{h=1}^{h=N_h} \left(\overline{P}_{1440,1}\right)_h \tag{3.3}$$

where $\overline{P}_{1440,1}^{N_h}$ is a vector with the aggregate active power consumption for N_h houses during a day. An equivalent process is used to obtain the aggregate reactive power consumption, $\overline{Q}_{1440,1}^{N_h}$.

The simulation output profiles obtained differ depending on the selected input parameters: the number of residents, the location of households, the date and the type of day (weekday or weekend).

In addition another scenario, named "Annual Consumption", was established through programming the basic algorithm implemented in the proposed model. Its aim was to determine annual lighting consumption and its variability over the months. In this case the simulation procedure consists of the generation of an occupancy profile for the 365 days of the year, setting a unique irradiance curve for each day, while keeping the same lamp distribution. If this process is repeated for a single household during N_y years, the average annual energy estimation for an installation with the randomly-set characteristic is obtained. Moreover, the possibility of simulating N_y years for N_h different households with their own lamp distribution was added. In this case the results show the aggregate annual and the monthly average consumption through the year for a standard installation. To implement this scenario firstly the monthly consumption for each house and year, $\overline{E}_{12,1}$ is calculated by using the expression (3.4):

$$\overline{E}_{12,1} = \left\{ \sum_{d=1}^{d=D} \frac{1}{60} \left[\sum_{k=1}^{k=1440} (p_d)_k \right] \right\}_{m,1} \tag{3.4}$$

where m represents the twelve months within a year, d denotes each day of a month, D is the last day of each month, which varies during the sum (D = 31 for January, March, May, July, August, October and December, D = 30 for April, June, September and November and D = 28 for February) and k is each minute

of a day. $(p_d)_k$ are the instantaneous terms of the vector $\overline{P}_{1440,1}$ for each minute, k, of a day, d. This vector is previously calculated for each day, d, inside each month, m, of each specific year. Dividing the total value by 60, the active energy consumption is expressed in Watt per hour (Wh). This process is repeated until the last day of the month D, and then the twelve calculated months m, ranging from 1 to 12, conform the vector $\overline{E}_{12,1}$. This process must be repeated for all houses and all years. Then, the average active consumption per each month $\overline{E}^{\text{average}}_{12,1}$ is obtained aggregating the monthly consumption of all houses for all years, as it is expressed in (3.5):

$$\overline{E}^{\text{average}}_{12,1} = \frac{1}{N_h \cdot N_y} \sum_{h=1}^{h=N_h} \left[\sum_{y=1}^{y=N_y} \left(\overline{E}_{12,1} \right)_y \right] \tag{3.5}$$

where N_h is the number of different houses and N_y is the number of years to be simulated for each household. Adding all the terms of this vector average annual consumption values (E_{year}) will be obtained. An equivalent process is also used to obtain the aggregate reactive energy.

The proposed model was implemented in JAVA, a general-purpose and object-oriented programming language developed by Sun Microsystems, currently merged into Oracle Corporation [37], whose main advantages, which have conditioned its use, are concurrent programming, easy connection with database and the fact that it is multiplatform.

3.3 Results

3.3.1 The application developed for energy consumption modeling and results visualization

Figure 3.4 shows a window of the Graphical Interface Guide (GUI) developed in order to facilitate the use of the proposed model. With this interface users can both configure and enter the input parameters for the model and acquire the output data in either graphical or numerical form. Each simulation scenario is situated in the upper tabs named "Consumption Curves" and "Annual Consumption", which correspond to the generation of daily profiles and annual consumption respectively. When a tab is selected, the field for input parameters and the different options for the output data are shown. The fields for input parameters entry are located in the upper left side in the "Household Parameters" panel.

In the first simulation scenario the input parameters required by the system are number of residents, type of day, location, date and the number of simulations which is equivalent in this case to the number of households, N_h, which will be aggregated, the simplest case being one simulation representing the consumption of a single household.

On the other hand, in the second scenario, for obtaining annual consumption and its yearly distribution, the necessary input parameters were the number of residents and the location of the houses, due to the date and the type of day being set automatically in a cyclical process. Together with these parameters, the number of years to be simulated for each household, N_y, should be indicated, as well as the number of different houses, N_h, enabling users to obtain average consumption results for a specific type of household.

The central and right side of GUI window is reserved for output curves and values. This section presents either daily lighting consumption curves of active and reactive power with 1-minute resolution for an individual household or an aggregate of households (in the first scenario) or the bar graph with monthly and annual energy consumption for the second case, depending on the tab previously selected. In addition, total daily or annual values of active and reactive energy obtained by the model are included under the calculated curves.

The last sets of components of note in the GUI are two drop-down buttons located in the toolbar over the tabs. These enable users to switch between the different output graphs generated by the model. Starting from the left, the first button enables the user to switch from occupancy profile to daily consumption curve, while the second enables users to visualize the disaggregate results for an appliance inside a specific consumption

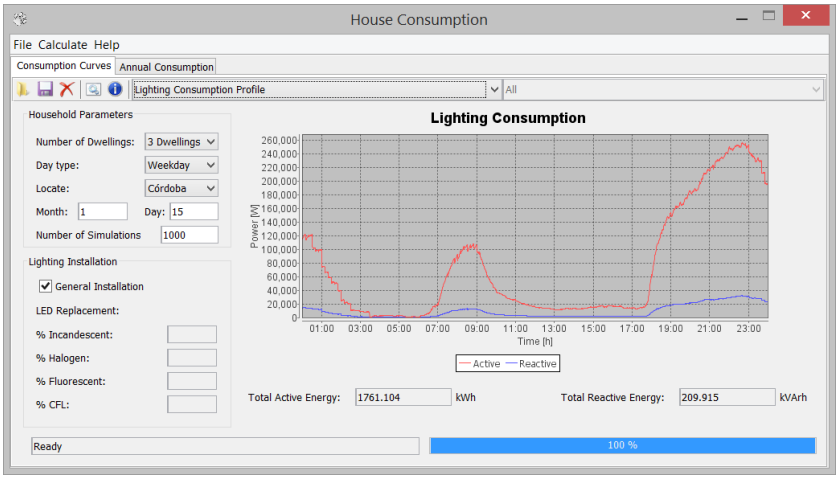

Figure 3.4: Screenshot of the developed GUI.

group. The second drop-down button is not used for this model; it is part of current research on a means of modeling electrical consumption due to general appliances and HVAC systems for either aggregate and disaggregate elements and whose results will be presented in future papers.

The implemented model is flexible enough for it to be able to perform simulations for other geographical areas once their corresponding data has been entered. The data presented in this paper specifically correspond to the city of Cordova, in the autonomous region of Andalusia in southern Spain. However, simulations for other autonomous regions or cities can be performed using the relevant data.

3.3.2 Results for lighting's electricity consumption

Figure 3.5 shows an example in which active and reactive consumption profiles are represented for an aggregate of 1000 three-resident households for January (a) and July (b) , including both weekdays (WD) and weekends (WE). First, from the data shown, two demand peaks should be noted, one of them corresponding

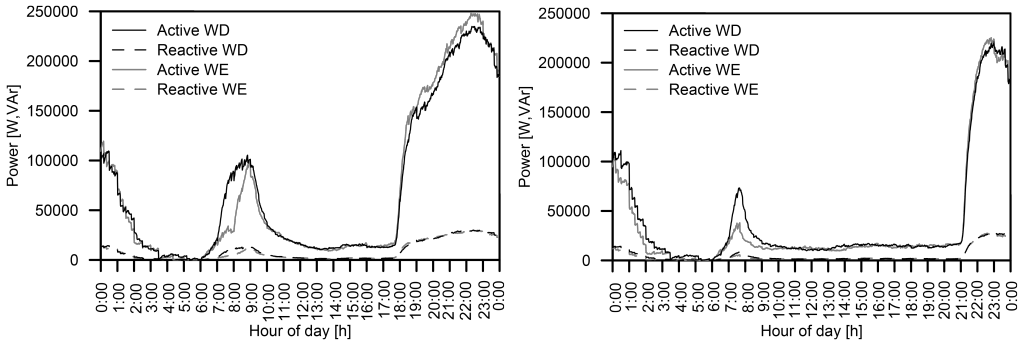

(a) January **(b)** July

Figure 3.5: Weekdays (WD) and weekends (WE) active and reactive power comparison.

Table 3.2: Power factor for each lighting technology.

Nº Occ	Jan	Feb	Mar	Apr	May	Jun	Jul	Aug	Sep	Oct	Nov	Dec	Total	% SD
1	25	20	20	16	14	12	13	15	17	21	24	26	223	3.73
2	41	34	33	26	24	21	22	25	29	35	39	42	370	3.55
3	53	43	43	35	31	28	29	33	38	45	51	55	483	2.74
4	60	50	50	41	38	34	36	39	44	52	57	63	565	2.97

to mornings, starting at 06.00 h and the other corresponding to nights, ranging from 17.00 - 18.00 h in January and to 21.00 h in July. As it can be observed, the times of greatest consumption coincide with lower external irradiance and a higher active occupancy in households [16, 38]. Another fact is that electrical consumption is higher in January than in July due to the high irradiance levels in this latter month, leading to a reduction in lighting consumption in the household. In the middle months of the year, a gradual transition between the curves presented is observed.

With regard to the differences between weekdays and weekends, a reduction in the morning peak is observable since residents wake up later at weekends. Furthermore, nocturnal consumption in occupied hours increases slightly in January during weekends because active occupancy is higher (residents go to bed later), and it decrease in July because of lower occupancy during the holiday period.

Finally, the observed trend in reactive power consumption is similar to active power, always following the same variations – as might be expected – since it is only a small fraction of the active energy, approximately 18% of the active power consumption for current installations.

As already indicated with the second implemented simulation procedure, results for average monthly consumption and annual values can be obtained for a type of household situated in a certain geographical location by simulating a set of N_h households for a time of K years and calculating the mean values for the whole data. The data presented in Figure 3.6 were calculated using this procedure. The bar chart represents monthly lighting consumption for households with 1 to 4 residents. Each set of monthly bars was obtained as the average value calculated from 100 households with a fixed number of residents simulated over a year. The variation of lighting energy consumption throughout the year can be observed. Annual consumption has maximum values in winter months (January and December) and the lowest values in summer (June and July). The seasonality shown for this consumption is a consequence of the variation in sunlight available throughout the year for the specific simulated location, since days are shorter in winter and the irradiance levels are lower, whereas the opposite occurs in summer (Figure 3.1).

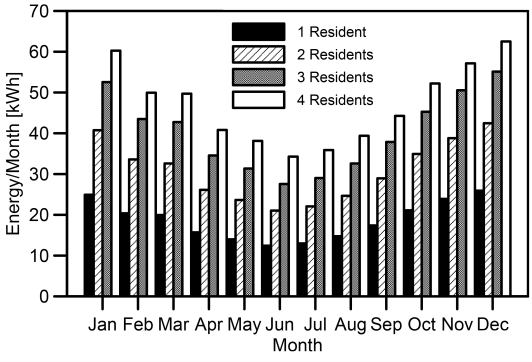

Figure 3.6: Monthly lighting demand for 1–4 residents household.

Moreover, an increase in energy demand in relation to the number of residents was observed. However, the relationship between both variables is neither linear nor uniform, but the increase reduces when occupant numbers rise due to residents sharing the same lighting points. This fact is also reflected in the numerical values, shown in Table 3.2, obtained as the average energy consumption for each month for 100 households over 10 years. The data were stored in a CSV (coma separated values) file, using a feature implemented in the GUI, which enables a further processing of results. As it can be seen, the increase in consumption between a household with a single resident and one with 2 residents is 60%, while the difference in the electricity demand between dwellings with 2 and 3 residents is only 37%. An even lower difference is the 18% increase observed in 3- and 4-resident dwellings.

3.3.3 Comparison with other authors

Because real measures registered in Spanish households are not available in order to validate the developed model, the results obtained using the model were contrasted with those obtained by other authors. The main goal was to determine the coherence and consistency of the synthetic load profiles generated in this work.

First, a comparison between annual electricity values demanded by lighting systems in Andalusia, Spain, obtained using the proposed model and those achieved by Gago *et al.* [13] was undertaken. In Gago *et al.* [13] data concerning the hourly and annual demands for lighting were obtained distinguishing between a set of household archetypes (Detached Houses, Row Houses and Apartment Blocks) and family structures (Couples with children, Couples without children, Parents with children, Single-member families and Multi-member families), as well as studying two periods in the year: winter, from December to March, and summer, from April to November. Data on the type of housing unit were extracted by the above authors from the Directorate General of Economic Programming (Ministry of Public Works) and the household profiles were based on a study performed by the Andalusian Statistics Institute in 2006 [39]. Both housing unit and family types enabled them to quantify the luminous flux needed. This luminous flux enabled the calculation of energy consumption in homes due to lighting, using also data concerning the installed lighting units and their technology, occupant activity and hours during which the light sources in each room consume energy. This latter data were obtained by the authors from surveys undertaken on a selected random sample of Andalusian households. In order to make the data provided by Gago *et al.* [13] comparable to that obtained from the proposed model an intermediate operation was required, which is described as follows.

First, data obtained from the results of Gago *et al.*'s study were calculated for the global aggregate of households in Andalusia, classified by the household types and the family types. This last parameter was linked to the number of household occupants proposed in this work (Table 3.3), trying to establish equivalences among them. For this, the household and family profiles proposed by Gago *et al.* were assigned with a specific household occupant number used as input parameter in the model proposed in this paper, with the exception of profile 5, which would correspond to a complex family type that could have 2 or 3 residents.

Furthermore, individual consumption for each family type and each household type should be obtained from of Gago *et al.*'s global data. The calculus was performed using the equation:

Table 3.3: Established equivalence between Gago *et al.*'s model [13] and the proposed model.

Profile no.	Household profile	Proposed occupant size
1	Couple with children	4
2	Couple without children	2
3	Parent with children	3
4	Single-member family	1
5	Multi-member family	Not used

$$C_{Tij} = \left(\frac{\sum \left(n_L \times C_{Lij} + n_F \times C_{Fij} \right)}{10^9} \right) \times N_{ij} \tag{3.6}$$

proposed by the above authors for the aggregate consumption, C_{Tij}, from a set of N_{ij} households distinguishing between building type i and household profile j.

In this equation, the aggregate consumption was calculated considering the number of working days per year, n_L, multiplied by the energy consumption of a single day, C_{Lij}, plus the number of holidays, n_F, multiplied by the energy consumption of a single non-working day, C_{Fij}. Both consumptions were expressed in Watts per hour and the aggregate consumption obtained in Gigawatts per hour. In this way, the annual consumption for each family profile (j) and each household type (i) could be obtained by dividing C_{Tij} by N_{ij}, which corresponds with the fraction in brackets, thanks to global consumption data and different household numbers given by Gago *et al.* [13].

Moreover, due to the fact that the model proposed in this paper tries to give general results independent of household types, electrical consumptions for each family type should be obtained as the weight average of all the defined household types, enabling the comparison of the proposed result with those obtained by Gago *et al.* [13]. The average weight calculus was valid since the household type data used by Gago *et al.* [13] were obtained from countrywide statistics provided by the Ministry of Public Works and were the same that were used by the IDAE [3] to construct its household distribution, also used in this study.

Table 3.4 presents in columns 2-4 the household number established by Gago *et al.* for each calculus N_{ij}, for the 5 defined family profiles. In columns 5-7 are the annual aggregate consumption results, C_{Tij}. Using this data and the procedure previously mentioned, annual consumption for a household corresponding to each family type and each household type, were calculated and showed in columns 8-10. The household type distribution was then extracted from the number of household data, obtaining a percentage of 8.01% for the detached/semi-detached houses, 18.95% for the row houses/townhouses and 73.04% for the apartment blocks. With this data, and applying a weight average with the above percentages, electricity lighting consumption for each family profile, presented in the data in the last column, was calculated.

These data reflected in the last column of Table 3.4, obtained from the data of Gago *et al.* using the above procedure, are also shown in Figure 3.7 (white bars) versus the results obtained from the model developed in this paper (grey bars), with their respective error bars (column named "% SD" of Table 3.2). The figure illustrates annual average lighting energy consumption for households consisting of 1 to 4 residents. Comparing both data series it can be seen that annual energy predictions are in the same range of magnitude, with a maximal absolute deviation of 36 kWh (14%) for 1-resident houses. The observed discrepancies may

Table 3.4: Annual energy consumption obtained by Gago *et al.*'s model [13].

Prof.	**Number of households, N_{ij}**			**Annual energy consumption, C_{Tij} (GWh/y)**			**Calculated Annual energy consumption/house (kWh/y)**			**Calculated weighed average (kWh/y)**
	Detached house	**Row house**	**Apart. block**	**Detached house**	**Row house**	**Apart. block**	**Detached house**	**Row house**	**Apart. block**	
1	111,503.64	263,707.08	1,016,689.28	58.30	223.15	498.00	522.85	846.20	489.83	559.99
2	35,084.72	82,982.76	319,929.53	14.12	44.72	99.33	402.42	538.91	310.47	361.12
3	20,035.25	47,383.53	182,681.22	9.25	30.58	84.81	461.69	645.37	464.25	498.36
4	35,904.83	84,915.23	327,379.94	11.52	32.02	72.58	320.85	377.08	221.70	259.08
5	3588.88	8487.73	32,723.39	1.55	5.03	12.68	431.89	592.62	378.49	429.91

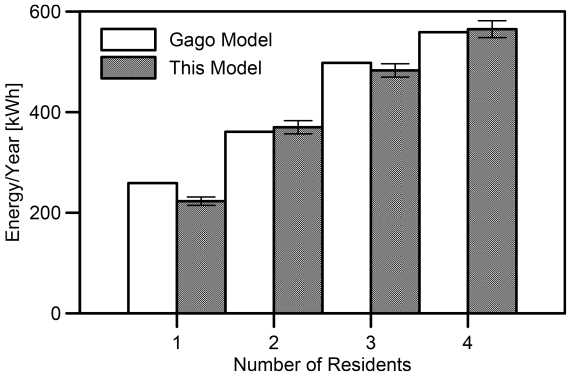

Figure 3.7: Annual comparison of the total annual energy demanded by dwellings in Andalusia, Spain, obtained by the model of Gago *et al.* and by the model presented in this paper.

be a result of the equivalences established between the different family types or the weight average performed to make Gago *et al.*'s data comparable with the results obtained by the proposed model.

In their work, Gago *et al.* [13] also estimated the daily profiles of lighting consumption with a 1-hour resolution for the different family and household types already indicated. In the model proposed in this paper daily consumption profiles were estimated regardless the household type. Thus, a comparison of these profiles were made with those obtained by Gago *et al.* [13] for the household type named "detached/semi-detached" and with family profile number 3 because they are the characteristics of an average household type in this country, as mentioned in the IDAE report [3]. This comparison is reflected in Figure 3.8 and 3.9.

Figure 3.8 illustrates an average winter day estimated by the Gago *et al.*'s model versus an average December day calculated by the proposed model. The results corresponding to both models gives the presence of two main peaks in electricity consumption by lighting points in households, one corresponding to the first morning hours and the other coinciding with nights. Nevertheless, some differences between both models' results were detected, mainly in the hours at which these peaks take place. The most significant is that corresponding to the night peak. Gago *et al.*'s estimation shows a faster rise in consumption during the afternoon, arriving at its maximum value at 21:00 h and suffering a sudden fall from 22:00 to 23:00 h.

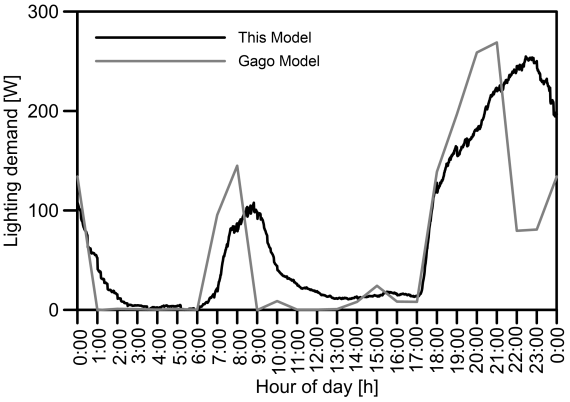

Figure 3.8: Gago model versus this model. Curve comparison for winter weekdays.

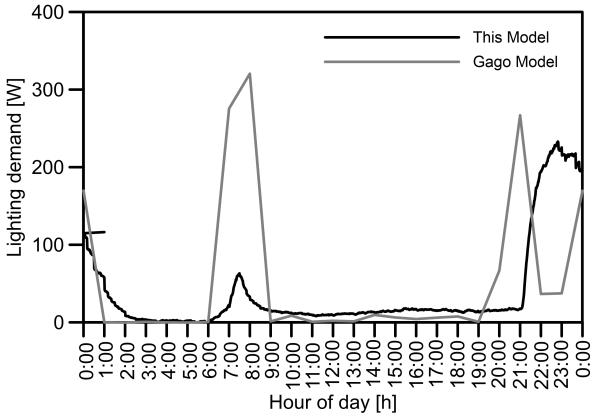

Figure 3.9: Gago model versus this model. Curve comparison for summer weekdays.

However, these results have no consistency with the household occupation profiles obtained for Andalusian households [38], an aspect which is accomplished by profiles given in this paper. This paper's profiles illustrate energy consumption slowly rising from 17:00 to 22:00 h, the steepest gradient occurring between 17:00 and 20:00 h and consumption peaking at 22:00 h. The observed discrepancies can be explained by the lower resolution of Gago *et al.*'s model and by the lower number of households where surveys, used for obtaining the results, were undertaken.

Figure 3.9 shows results for an average summer day estimated by Gago *et al.*'s model versus data calculated by the proposed model for July. Again, the two above consumption peaks can be detected. However, the proposed model estimates lower energy consumption, especially in morning peak, while Gago *et al.*'s model presents an even higher value than that for winter. This fact is curious since higher irradiance levels are reached in summer, obviously leading to a reduction in the consumption of electricity due to artificial lighting. Looking at the night peak, the Gago *et al.*'s model again presents the maximum value at 21:00 h and later an abrupt trough. On the other hand, the proposed model estimated a consumption rising at 21:00 h, the highest figure occurring at 22:30 h, once again matching the maximum occupancy levels.

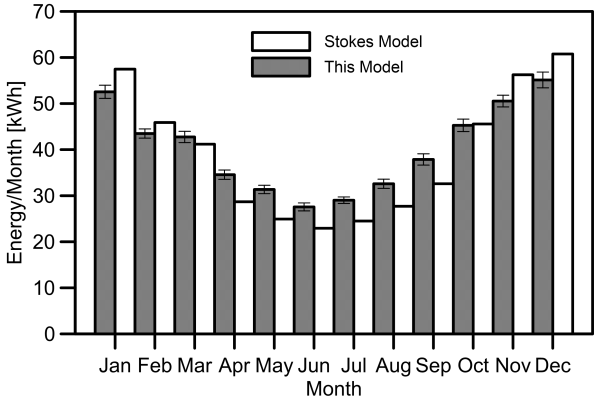

Figure 3.10: Monthly lighting demand. Stokes *et al.* against proposed model.

With regard to consumption curves in other European countries, the results obtained in this work can be compared with those obtained by Stokes *et al.* [11] and by Richardson *et al.* [15], models with similar results developed for the UK. A detailed comparison between Stokes *et al.*'s model and the one proposed here was undertaken. The Stokes model was based on a different methodology to that used in this paper. Stokes *et al.* simulated lighting electricity demand, with a half-hour resolution, as cyclic consumption depending on the solar cycle throughout the year and on established patterns observed during some temporal frames within the day. In this way, lighting electricity consumption for any hour and day is expressed as the sum of two sinusoidal elements –whose amplitude and phase parameters change during the day – and an additional constant term. The parameters were calculated from data collected from 100 households in the UK, fitting the appropriate values by the method of least squares. Later, the values obtained were normalized by the annual peak in order to represent the annual trend.

Figure 3.10 illustrates monthly demand over one year estimated both by Stokes *et al.*'s model (white bars) and the model proposed in this work (dark grey bars). The first layer of Stokes' model was implemented and calibrated so that the annual estimate demand was 474 kWh/y because, as previously mentioned, Stokes' model does not provide energy consumption, but values normalized by the annual average peak demand.

The seasonality observed in the results obtained by both models throughout the year is highly similar. The models estimate an increased trend in lighting consumption in the months between the summer and winter solstices and a decrease during the rest of the year. It can be also observed that values achieved by the Stokes model are higher than those calculated by the proposed model in the winter months with fewer day light hours. In contrast, the summer months have lower consumption values in the Stokes model while the energy estimated by this work is higher. The reason of these deviations could be the discrepancy in sunlight hours existing in the UK as well as the different daily habits since occupants go to bed earlier in the UK than in Spain generally [16].

A further comparison in terms of cumulative energy through the year enables us to represent cumulative energy consumption for each month calculated by the proposed model (X-axis) versus those obtained by Stokes *et al.* (Y-axis), as illustrated in Figure 3.11. The method of least squares was used to fit the values, demonstrating that both models share similar trends during the year, obtaining an R-square value of 0.996458.

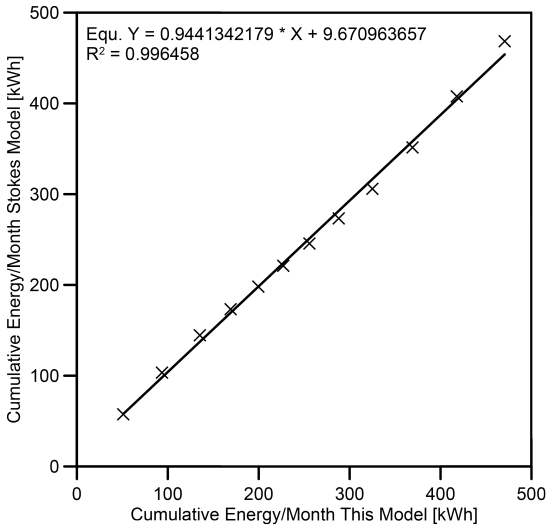

Figure 3.11: Monthly lighting demand minimum squares regression. Stokes *et al.* against proposed model.

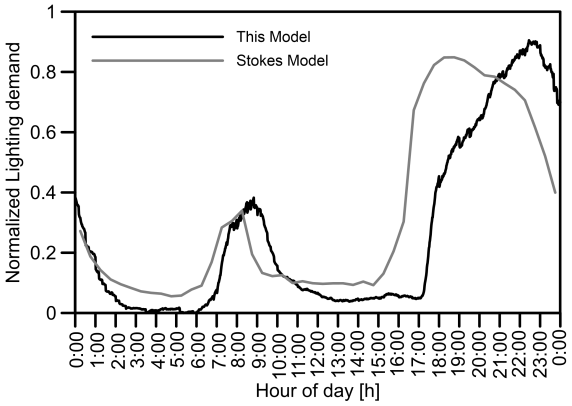

Figure 3.12: Stokes model versus this model. Curve comparison for December.

As in the case of Gago *et al.*'s model, daily consumption profiles can also be compared using normalized values of energy demand, obtained by dividing the annual average peak by the results from the proposed model. Figure 3.12 illustrates this comparison. The results again show two demand peaks in both countries, the night consumption peak being the more significant. The curves are represented in local time corresponding to the Coordinated Universal Time or UTC in the UK and to UTC + 1:00 h in Spain. Therefore this time difference should be taken into account when the data are analyzed. In addition, from the last Sunday in March to the last Sunday in October, local time in the UK is changed to British Summer Time (UTC + 1:00 h), while the same also occurs in Spain (UTC + 2:00 h).

The match between sunlight availability, as well as active occupancy, with consumption curves is notable in both cases. The main discrepancy that arises is due to the different patterns of household activity. Households in the UK experience a significant increase in active occupancy from 16:00 h, while at that time in Spain there is a dip in occupancy and the main active occupancy takes place later on, from 20:00 h [16, 19]. Spanish occupancy profiles, linked to the different habits and schedules, also differ from the rest of the European countries. This fact indicates the reason why the consumption peak in Spain occurs later than in the UK. Moreover, irradiance levels are generally higher in Spain in relation to more northerly countries.

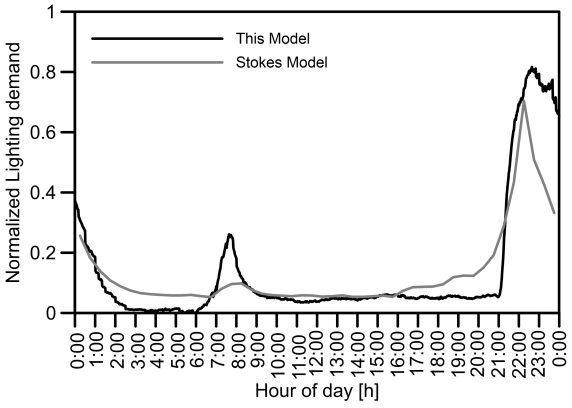

Figure 3.13: Stokes model versus this model. Curve comparison for July.

There are yet more differences between the models such as the higher energy consumption estimated by the Stokes model during the central hours of the day, basically in winter months, which can be associated with lower sunlight availability in the UK. However, in summer (Figure 3.13) the opposite occurs. Due to its latitude, there are more hours of daylight in the UK, so the morning peak is smoother whereas in Spain this peak is still relatively high.

Finally, with regard to consumption profiles due to lighting systems in the residential sector obtained by other authors, the works undertaken by Almeida *et al.* [4] for the European Union, Arghira *et al.* [8] or France and Widén *et al.* [10] for Sweden should be mentioned. In every instance, despite the similar trends with two well-defined consumption peaks, the night peak always appears earlier in the rest of the countries than in Spain, due to the reasons described above.

3.3.4 Saving actions. Impact of LED technology use in residential sector lighting systems

As previously indicated, one of the main goals of this work was to perform a comparison between present lighting consumption and some future situations in which some electricity saving policies could be applied, analyzing the energetic impact of these actions. Based on the consumption profiles obtained, it can be observed that the inclusion of Demand Side Management procedures (DSM) is a difficult task, due to the fact that consumption hours are associated with higher occupancy in households and lower irradiance levels, making it almost impossible to change these schedules. In addition, higher production hours of renewable sources such as photovoltaic energy, one of the best technologies for local generation integrated into buildings, match neither of these peaks.

One possible energy saving measure could be a DSM system having a module which advises users on the efficient use of lighting systems. This can be achieved with smart meters producing acoustic warnings associated with an increase in energy price and/or with an economic penalty on the bill. This measure could be effective since lighting consumption is associated with the presence of occupants in the house [14, 16] and it could help to prevent misuse of the lighting points in households. However, under the premise that illumination is necessary and indispensable for performing the main household activities, the most effective saving action to reduce electricity consumption associated with these types of loads is to use more efficient lighting technologies. Current energy saving policies such as European Directive 2005/32/EC [18], which imposes the phasing-out of incandescent lamps in households, support this technique as the main saving method.

The GUI proposed in this paper enables these saving policies to be implemented easily in the developed model, reaching the goal of comparing the current scenario with the results obtained in hypothetical future contexts. As indicated, the model is based on the statistical distribution of different lighting technologies existing in the market. Nowadays, LED lighting technology in Spanish households represents a marginal percentage of the lighting technologies used [3]. Therefore the proposed future scenario consists of an increase in the penetration percentage of LED technology while the other technologies' share decreases. The modification in the percentages of different lighting technologies enabled us to calculate active and reactive power in the proposed contexts. Choosing LED technology instead of the compact fluorescent lamps (CFL) which have been widespread in the market in recent years, was supported by some significant environmental advantages of LED technology such as its longer useful life, higher lumen per Watt ratio, lower inductive load, instantaneous switching-on and good chromatic reproduction.

Due to the fact that the main disadvantage of LED technology is its higher cost [40], an economic approach to the substitution and energy cost from LED technology versus the current situation , as well as a calculation of the period needed to recoup the initial investment were undertaken. Two different scenarios were studied. First, an average percentage of 50% was fixed for LED technology. Secondly, the simulation was taken to the extreme, fixing a substitution percentage of 80%.The study was performed bearing 3 factors in mind: active consumption reduction, impact in energy quality and economic cost.

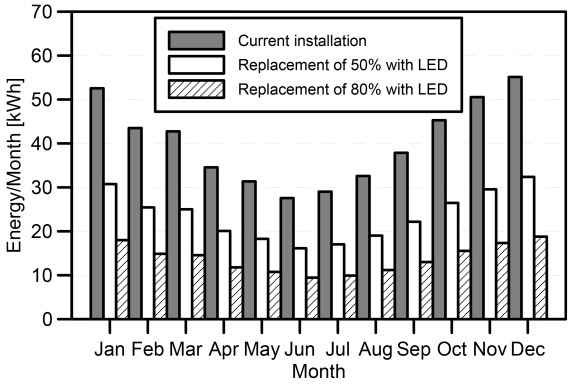

Figure 3.14: Consumption reduction with LED technology for 3 dwelling household.

Figure 3.14 shows the consumption reduction in relation to the current average lighting installation in Spanish homes. For each scenario, monthly consumption over a year is represented. Dark grey bars presents consumption whereas white bars represent the energy consumed with an average replacement of 50% with LED and the light grey ones with a replacement of 80%.

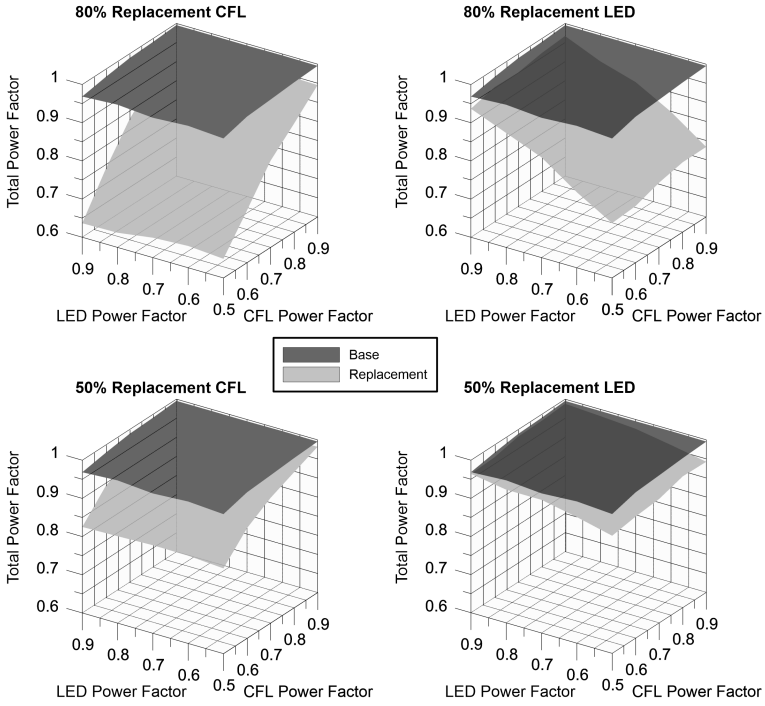

Figure 3.15: Variation of the global lighting installation power factor with the percentage of LED and CFL lamps replacement and the range of power factor.

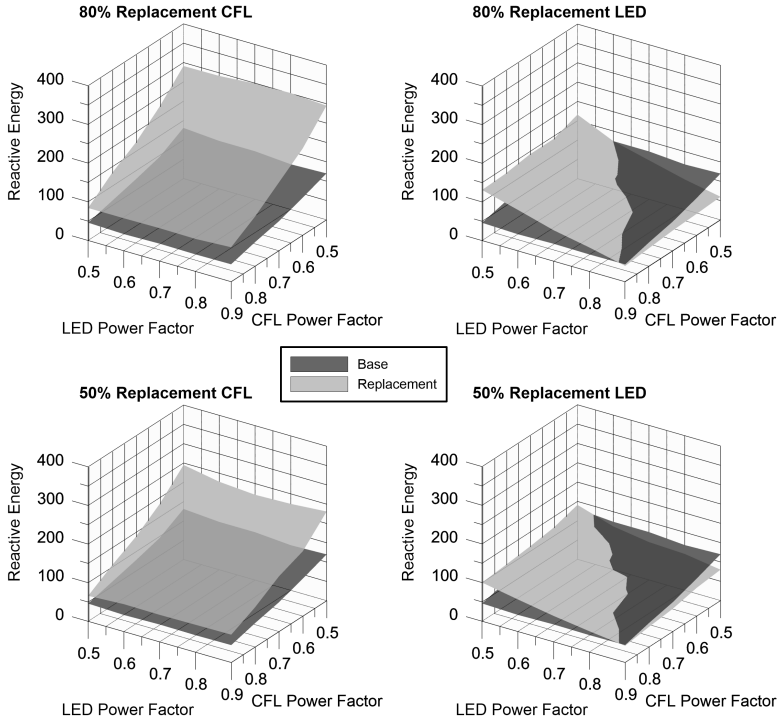

Figure 3.16: Variation of the global lighting installation reactive power with the percentage of LED and CFL lamps replacement and the range of power factor.

The results indicate that current average consumption, established at 474 kWh/y as a mean for the country, could be reduced by 40% by replacing 50% of the current lamps with LED technology. With this action, annual consumption due to lighting systems decreases to 282 kWh. Similarly, if 80% of lamps are replaced, the reduction achieved is 65% of the initial consumption, with 165 kWh for an average household. These figures converted to tonnes/CO_2 and applied over the whole region leads to a reduction of 360,000 tonnes of CO_2 (80% replacement) and 300,000 tonnes of CO_2 (50% replacement) emitted by electricity generation.

The second factor taken into account was reactive power consumption. Nowadays, the power factor of lighting systems in the residential sector is near to one since the incandescent and halogen lamps, with a mainly resistive load, are the most widely installed technologies. The penetration of LED technology into households could decrease this power factor value. To estimate this reduction, Figure 3.15 illustrates power factor variations versus the percentage of replacement with LED or CFL lamp technologies (two alternatives 50% and 80% of replacement were studied) and the range of variation in the power factor for each technology. In both selected cases, a decrement in the power factor of the global lighting installation is observed. However, the obtained values prove that a successfully replacement can be achieved without major impact in the power factor whether good quality lamps are employed. Nevertheless, in the case of lamps with low power factor, values of 0.65 can be observed in the case of CFL lamps and 80% of replacement, or 0.75 for the same case but with LED technology. Therefore, not only is the use of more efficient lighting technology necessary, but also the use of lamps which minor influence in the power factor. Compelling manufacturers and local distributors to provide suitable information about this aspect of the lamps in order to raise users' awareness of this issue may be an important challenge.

In addition, major results can be obtained regarding the reactive energy. In a stationary context where the total installed power remains constant, power factor reductions mean a direct increase in reactive power consumption, involving consequences such as overheating and higher loss in wires, lower capacity of installations and, in short, an increase in the global cost of energy. However, if LED lamps were more widely used, the active power consumption would be lower than in a baseline situation and so the reactive energy would be also reduced, despite the power factor reduction which the use of these lamps supposes. This fact can be observed in Figure 3.16 where the reactive power variations with respect to the baseline or current situation are illustrated versus the percentage of replacement of LED and CFL lamps and versus the variation in the power factor, for the average of 100 households simulated over 10 years. In the case of CFL, due to the lower power factor, reactive power increases despite the reduction in active power. However, for LED technology the reactive power can decrease in reference to the currently situation if lamps with high power factor are used, because of its substantially lower active power consumption. It falls outside of the goals established in this work to study the influence, due to the penetration of this technology in the residential context in harmonic distortion, thus producing other consequences in electricity installations. This field is being currently researched by other authors [41].

Finally, an approach to the economic cost of installing LED technology and to the payback time of the initial investment was undertaken. For this aim, a simple cash flow analysis was carried out, following the guidelines of the European Union for Cost Benefit analysis [42]. The studied parameters were the implementation investment and the operating cost due to the energy consumption. The first value can be easily calculated since each lamp included in the model has a manufacturer's suggested retail price associated. For the second parameter, an energy price of 0.15 €/kWh (0.20 $/kWh), 21% of VAT (Valued Added Tax) and an 11% annual increase were applied, regarding the reports given by "Red Eléctrica de España Co." the sole agent and operator of the Spanish electric system [43].

The results for 80% and 50% of replacement are represented in Figure 3.17. The X-axis shows the time in months since installing LED lamps and the Y-axis shows the economic cost, taking into account the initial installation cost of each situation. The black line represents the current energy cost plus initial installation; the light grey line illustrates the same concept, but with 50% of LED substitution and the dark grey line 80% substitution. As can be observed, monthly energy consumption is reduced to half so the recovery time is 45 months (nearly 4 years) for a substitution rate of 80% whereas in the case of a 50% substitution, it is 69 months. The payback time might appear to be excessively long, yet the energy savings achieved justify the economic investment. Nevertheless, additional factors such as transmission and distribution utility (TDU) delivery charges were omitted, as was a reduction in taxes, when replacing current installations with LED technology, both of which could reduce recovery time. Moreover, since LED technology for residential lighting is relatively new, an increase in the installation rates would produce lower prices and even greater economic savings.

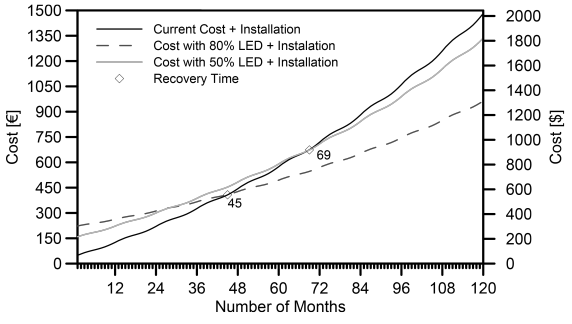

Figure 3.17: Cost analysis of replacement of 80% and 50% of current lamps with LED technology.

3.4 Conclusions

This work has presented the implementation, validation and simulation procedure for a stochastic model which generates synthetic consumption profiles of electricity use in household lighting systems. The model was implemented and calibrated for Andalusia, Spain, although the mechanisms for simulating other locations were discussed.

A strong relationship between sunlight availability and active occupancy of dwellings with electricity consumption for lighting was demonstrated. Two peaks of maximum energy consumption stand out. These peaks occur in the morning and at night when there is little or no sunlight and are also coupled with higher active occupancy rates of the households. This relationship with active occupancy occurs at different times of the day when consumption peaks take place. In Spain peak times differ with regard to those in the UK and other European countries. The dependency on sunlight availability was also observed in the variation of electricity consumption during the year, with maximum values corresponding to winter months and lower sunlight radiation and the minimum values corresponding to summer months.

Subsequently, the model was used to perform a study on the impact of LED technology's penetration into the residential sector. The flexibility of the input parameters for the model enabled us to establish two different future scenarios, the first with a 50% replacement rate of current lamps with LED technology and the second one with a rate of 80%. This showed energy reduction rates of 40% for 50% substitution and 65% for 80% in the average annual lighting consumption of the household. These energy saving policies implicate at an aggregate level a reduction of approximately 360,000 tonnes of CO_2 for the whole of the Andalusian region with a replacement percentage of 80% and without significant impacts on energy quality, since the power factor is only slightly affected and this reduction is compensated by lower active energy consumption.

Finally, an approach to the economic cost, initial investment and recovery time was made, setting the mean time to recoup the initial cost of replacement at 4 years with an 80% replacement rate with LED and 5 and a half years for a 50% replacement rate. Along with the developed model, which has enabled us to perform this work, the final goal is to include this module in a future prediction model. Not only will this future model enable us to calculate electricity consumption due to lighting systems, but also consumption by the whole set of electrical appliances found in households, in order to obtain daily consumption profiles and annual trends. This model, already being implemented and which will be discussed in future papers, will keep the same simulation philosophy as the current one, enabling us to use the predictions practically in order to propose and analyze the impact of new energy saving policies.

Acknowledgements

This work is supported by Feder-Interconecta project TIGRIS under contract no. 12013095 (ITC-20131002).

References

[1] M. Kavgic, A. Mavrogianni, D. Mumovic, A. Summerfield, Z. Stevanovic, M. Djurovic-Petrovic, A review of bottom-up building stock models for energy consumption in the residential sector, Building and Environment 45 (7) (2010) 1683–1697. doi:10.1016/j.buildenv.2010.01.021.

[2] L. G. Swan, V. I. Ugursal, Modeling of end-use energy consumption in the residential sector: A review of modeling techniques, Renewable and Sustainable Energy Reviews 13 (8) (2009) 1819–1835. doi:10.1016/j.rser.2008.09.033.

[3] IDAE, Análisis del consumo energético del sector residencial en España INFORME FINAL (2011). URL: http://www.idae.es/uploads/documentos/documentos_Informe_SPAHOUSEC_ACC_f68291a3.pdf

[4] A. de Almeida, P. Fonseca, B. Schlomann, N. Feilberg, Characterization of the household electricity consumption in the EU, potential energy savings and specific policy recommendations, Energy and Buildings 43 (8) (2011) 1884–1894. doi:10.1016/j.enbuild.2011.03.027.

[5] UNFCCC, Kyoto Protocol To the United Nations Framework Convention on Climate Change, Review of European Community and International Environmental Law 7 (2) (1998) 214–217. doi:10.1111/1467-9388.00150.

[6] I. Vassileva, F. Wallin, E. Dahlquist, Understanding energy consumption behavior for future demand response strategy development, Energy 46 (1) (2012) 94–100. doi:10.1016/j.energy.2012.02.069.

[7] T. F. Sanquist, H. Orr, B. Shui, A. C. Bittner, Lifestyle factors in U.S. residential electricity consumption, Energy Policy 42 (2012) 354–364. doi:10.1016/j.enpol.2011.11.092.

[8] N. Arghira, L. Hawarah, S. Ploix, M. Jacomino, Prediction of appliances energy use in smart homes, Energy 48 (1) (2012) 128–134. doi:10.1016/j.energy.2012.04.010.

[9] D. Ndiaye, K. Gabriel, Principal component analysis of the electricity consumption in residential dwellings, Energy and Buildings 43 (2-3) (2011) 446–453. doi:10.1016/j.enbuild.2010.10.008.

[10] J. Widén, A. Nilsson, E. Wäckelgård, A combined Markov-chain and bottom-up approach to modelling of domestic lighting demand, Energy and Buildings 41 (10) (2009) 1001–1012. doi:10.1016/j.enbuild.2009.05.002.

[11] M. Stokes, M. Rylatt, K. Lomas, A simple model of domestic lighting demand, Energy and Buildings 36 (2) (2004) 103–116. doi:10.1016/j.enbuild.2003.10.007.

[12] M. Bladh, H. Krantz, Towards a bright future? Household use of electric light: A microlevel study, Energy Policy 36 (9) (2008) 3521–3530. doi:10.1016/j.enpol.2008.06.001.

[13] E. J. Gago, J. O. García, A. E. Estrella, Development of an energy model for the residential sector: Electricity consumption in Andalusia, Spain, Energy and Buildings 43 (6) (2011) 1315–1321. doi:10.1016/j.enbuild.2011.01.016.

[14] J. Torriti, Demand Side Management for the European Supergrid: Occupancy variances of European single-person households, Energy Policy 44 (2012) 199–206. doi:10.1016/j.enpol.2012.01.039.

[15] I. Richardson, M. Thomson, D. Infield, A. Delahunty, Domestic lighting: A high-resolution energy demand model, Energy and Buildings 41 (7) (2009) 781–789. doi:10.1016/j.enbuild.2009.02.010.

[16] M. A. Lopez, I. Santiago, D. Trillo-Montero, J. Torriti, A. Moreno-Munoz, Analysis and modeling of active occupancy of the residential sector in Spain: An indicator of residential electricity consumption, Energy Policy 62 (2013) 742–751. doi:10.1016/j.enpol.2013.07.095.

[17] CEDOM, IDAE, Como Ahorrar Energia Instalando Domótica en su Vivienda. Gane Confort y Seguridad (2008). URL: http://www.idae.es/uploads/documentos/documentos_11187_domotica_en_su_vivienda_08_3d3614fe.pdf

[18] European Parliament and Council, Directive 2005/32/EC, establishing a framework for the setting of ecodesign requirements for energy-using products (2005). URL: http://eur-lex.europa.eu/legal-content/EN/TXT/?uri=LEGISSUM%3Al32037

[19] I. Richardson, M. Thomson, D. Infield, A high-resolution domestic building occupancy model for energy demand simulations, Energy and Buildings 40 (8) (2008) 1560–1566. doi:10.1016/j.enbuild.2008.02.006.

[20] J. Widén, E. Wäckelgård, A high-resolution stochastic model of domestic activity patterns and electricity demand, Applied Energy 87 (6) (2010) 1880–1892. doi:10.1016/j.apenergy.2009.11.006.

[21] M. A. López, I. Santiago, F. J. Bellido-Outeiriño, A. Moreno-Munoz, D. Trillo-Montero, Active occupation profiles in the residential sector in Spain as an indicator of energy consumption, in: IEEE International Conference on Consumer Electronics - Berlin, ICCE-Berlin, IEEE, 2012, pp. 1–5. doi:10.1109/ICCE-Berlin.2012.6336472.

[22] National Statistics Institute of Spain. Ministry of Economy and Competitiveness, Time Use Survey (2010). URL: http://www.ine.es/en/prensa/eet_prensa_en.htm

[23] W. R. Gilks, S. Richardson, D. J. Spiegelhalter, Markov Chain Monte Carlo in Practice, Technometrics 39 (3) (1997) 338. doi:10.2307/1271145.

[24] D. Gamerman, L. Hedibert, Markov Chain Monte Carlo: Stochastic Simulation for Bayesian Inference, Vol. 1, Chapmand and Hall, 2006.

[25] C. F. Reinhart, Lightswitch-2002: A model for manual and automated control of electric lighting and blinds, Solar Energy 77 (1) (2004) 15–28. doi:10.1016/j.solener.2004.04.003.

[26] D. R. G. Hunt, The use of artificial lighting in relation to daylight levels and occupancy, Building and Environment 14 (1) (1979) 21–33. doi:10.1016/0360-1323(79)90025-8.

[27] Agencia Andaluza de la Energía, Radiación Solar (2010). URL: http://www.agenciaandaluzadelaenergia.es/Radiacion/radiacion1.php

[28] EC. Institute for Energy and Transport, Photovoltaic Geographical Information System (PVGIS) (2010). URL: http://re.jrc.ec.europa.eu/pvgis/apps4/pvest.php

[29] OSRAM, OSRAM (2013). URL: http://www.osram.com/

[30] Philips, Philips Lighting (2013). URL: http://www.lighting.philips.com/

[31] General Electric, GE Lighting (2013). URL: http://www.gelighting.com/

[32] L. Arsov, M. Cundeva-Blajer, I. Iljazi, Measurement of Power Quality Effects and Energy Efficiency of Various Light Technologies, Renewable Energy and Power Quality Journal 11 (2013) 38–43. doi:10.24084/repqj11.516.

[33] M. Hossen, Z. Rahman, A. Razzak, Study of the improvement of CFL's power factor and beneficiary side of CFL as a replacement of Incandescent Lamp, International Journal of Science, Engineering and Technology Research (IJSETR) 2 (10) (2013) 1982–1987.

[34] U. S. Energy Information Administration, Residential Energy Consumption Survey (RECS) (1993). URL: http://www.eia.gov/consumption/residential/data/1993/

[35] B. Boardman, D. Favis-mortlock, G. Milne, E. Small, Domestic Equipment and Carbon Dioxide Emissions, Tech. rep., Energy and Environment Programme. Environmental Change Unit. University of Oxford, Oxford (1995).

[36] E. Mills, M. Siminovitch, E. Page, Dedicated compact fluorescent fixtures: the next generation for residential lighting (1995).

[37] Oracle, Java (2016). URL: https://www.oracle.com/java/index.html

[38] I. Santiago, M. A. Lopez-Rodriguez, D. Trillo-Montero, J. Torriti, A. Moreno-Munoz, Activities related with electricity consumption in the Spanish residential sector: Variations between days of the week, Autonomous Communities and size of towns, Energy and Buildings 79 (2014) 84–97. doi:10.1016/j.enbuild.2014.04.055.

[39] Instituto de Estadistica de Andalucia, Hogares y familias en Andalucía (2001).

[40] C. J. Humphreys, Solid-state lighting, MRS Bulletin 33 (4) (2008) 459–470. doi:10.1557/mrs2008.91.

[41] A. Gil-de Castro, S. Ronnberg, M. H. J. Bollen, A. Moreno-Munoz, V. Pallares-Lopez, Harmonics from a domestic customer with different lamp technologies, in: 2012 IEEE 15th International Conference on Harmonics and Quality of Power, Ieee, 2012, pp. 585–590. doi:10.1109/ICHQP.2012.6381167.

[42] European Commision. Directorate General Regional Policy, Guide to cost-benefit analysis of investment projects : structural funds and instrument for pre-accession, Tech. rep., European Union (2008). URL: http://ec.europa.eu/regional_policy/sources/docgener/guides/cost/guide2008_en.pdf

[43] Red Eléctrica de España Co., Red Eléctrica de España (2014). URL: http://www.ree.es/en

4

A stochastic modelling and simulation approach to heating and cooling electricity consumption in the residential sector

Emilio J. Palacios-Garcia[1], Antonio Moreno-Munoz[1], Isabel Santiago[1], Jose Maria Flores-Arias[1], Francisco J. Bellido-Outeiriño[1], and Isabel M. Moreno-Garcia[1]

[1]Departamento de Arquitectura de Computadores, Electrónica y Tecnología Electrónica, Escuela Politécnica Superior, Universidad de Córdoba, Córdoba, Spain.

Abstract

Heating and cooling consumption is one of the most significant terms in the total supply, which may come to represent half of the total demand in European countries. These appliances are supplied by a wide range of sources, being electrical devices of special interest in the Smart Grid. Current tools allow the assessment of the consumption with a high accuracy, nevertheless, they lack the temporal resolution or low-level details to study advanced control techniques. In this context, bottom-up stochastic models are a main tool to simulate high-resolution demand profiles. This paper presents a 1-minute resolution model for electricity demand of heating and cooling appliances. The system is based on the simulation of individual households considering variables such as the number of residents, location, type of day (weekday or weekend) and date. It was used to simulate daily profiles which showed two main demand peaks, one during mornings and another during dinner time, for heating, and a high demand during midday for cooling consumption. Moreover, annual simulations depicted the importance of cooling appliances, which despite having a lower annual demand, can overcharge the grid with their concurrent utilisation, highlighting the usefulness of this tool for studying the impact of these devices.

The paper has been published in *Energy, 2018, 144C pp. 1080-1091. doi:10.1016/j.energy.2017.12.082*.

4.1 Introduction

Based on the total energy demand, the residential sector represents on average 30% of the total energy consumption in the worldwide supply [1]. In the case of Spain, this figure is around 17% of the total energy consumption and 25% of the total electricity demand [2]. Moreover, this consumption is increasing in recent years due to the higher level of comfort required by the standards of modern society and by the widespread installation of new domestic appliances. These devices mainly comprise of electronic loads, whose supply quality specifications must also be accomplished [3].

Inside the global domestic electricity demand, different types of consumption can be distinguished such as those from lighting, general appliances, and heating and cooling electrical devices. From all of these sources, the energy demand due to heating and cooling appliances is probably the most significant and variable term [4]. The maximum heating demand in some European countries may come to represent more than half of the total energy consumed in the residential sector [5]. On the other hand, the cooling energy term is significantly lower, but with an upward trend [6]. Specifically in Spain, heating and cooling appliances represent between 15% and 18% of the total electricity consumption for a household, and usually, the heating systems have a higher energy demand than the cooling appliances [7].

Information about heating and cooling demand in the residential sector, as well as daily load profiles for various appliances, already exist for some European countries, specifically inside the REMODECE (Residential Monitoring to Decrease Energy Use and Carbon Emission in Europe) project [8]. However, Spain was not included in this study, and the different schedules of this country [9], as well as the major use of electrical appliances for heating, in contrast with other European countries, reinforce the importance of this analysis. This fact is especially significant in the context of the future Smart Grid. General domestic appliances are supplied with electricity, whereas a wide range of technologies and different energy sources such as natural gas, propane, fuel oil, and hot water (district heating) can be used for the heating systems, making the modelling process more complex than for other energy end uses [10].

In addition, not only do these devices have a heterogeneous distribution and a high demand, but the interdependence between their consumption and the weather conditions is even more significant. What is more, this relationship has been found to be more sensitive in the case of residential buildings due to the higher ratio of building envelope surfaces [11]. These external factors also influence the renewable resources integrated into the grid such as solar or wind power. Hence, to reduce the electricity consumption and provide a better understanding of this type of demand, it is essential to have a high level of resolution in the consumption profiles and a separate treatment of each specific energy end use [12, 13], instead of merely knowing the aggregate figures [14]. This higher resolution of the results is also justified since most demand response (DR) strategies require a level of granularity between 5 and 30 min [15].

Previous works have studied the interdependence of electricity consumption and temperature mainly by means of so-called temperature response functions. A review of these models can be found in Fazeli *et al.* [16]. Pardo *et al.* [17] and Valor *et al.* [18] studied the seasonality of the electricity demand in Spain due to the influence of the temperature using linear symmetric models. Likewise, in the work of Moral-Carcedo and Vicéns-Otero [19], the influence of temperature on consumption was studied, emphasising the existence of a nonlinear relationship and proposing different regression strategies. In addition, some other works can be found in the context of Europe [20]. However, these functions can only estimate the daily trends, but not the actual daily behaviour of each heating or cooling load.

In parallel, a wide range of modelling systems based on information regarding the building structure and/or historical consumption records can also be found in the literature. These models are usually classified as white, black or grey-box. The white-box models or physical driven models require a detailed knowledge of the building structure and parameters. As opposed to, the black-box models or data-driven models establish a relationship between the source and the consumption by means of statistical techniques. Finally, the grey-box models lie somewhere in between, making use of both building parameters and statistical approaches [21].

Currently, many calculation tools that implement some of these models are available on the market and are widely applied such as EnergyPlus, TRNSYS, DOE-2, BLAST or ESP-r among others [22, 23]. However, in the context of electricity consumption and grid impact simulation, they present some problems such as the necessity of a large amount of information regarding the constructions, low temporal resolutions (usually the minimum available time step is an hour), and high computational load. Consequently, if the heating and cooling electrical consumptions of a whole community composed of 500 or 1,000 households are to be simulated, considering the heterogeneity and the residents' behaviour, their use is limited [24].

In this field, bottom-up modelling techniques have shown to be the solution to generate high-resolution energy profiles, while keeping the individual dispersion of the parameters, since they use data corresponding to entities below the global heating and cooling demand. Thus, by using occupancy variations of households, appliances consumption data, and temperature profiles, for instance, the daily electricity demand can be modelled [25].

Different models were previously developed using a bottom-up approach and stochastic techniques. Richardson *et al.* developed a model grounded in the usage of daily occupancy profiles [26], which were subsequently employed as the base data for the estimation of lighting [27] and appliances [28] consumption. Nevertheless, in this paper, only the space heating consumption was considered, relating its use with the occupancy and temperature seasonality. Later, a thermal-electrical model was developed by the same authors, but the heating appliances were supplied with hot water [29]. Likewise, Widén *et al.* also studied the different electricity and hot water profiles for Swedish households, but without specifically focusing on the energy consumed by heating devices [30]. Moreover, none of them considered the air conditioner consumption, due to the different climate characteristics of the locations.

Therefore, based on these considerations, the main objective and the novelty of this work is the development of a model to simulate not only the heating, but also the cooling electricity consumption in the residential sector, with a high temporal resolution, and enough flexibility so it can be adapted to different geographical locations. This model not only takes into account the temperature seasonality, but also some other parameters such as the type of day (weekday or weekend), the number of residents per household and the operation of the actual appliances. The methodology for developing the model, its application to the case of Spain and its capabilities for assessing the impact of cooling and heating appliances on the grid are presented.

The following structure will be used in the paper. Section 4.2 addresses the different data required, the methodology, and the simulation process. Next, Section 4.3 presents and discusses the results obtained using the proposed model, while in Section 4.4 a comparison with other previous studies and an error analysis is performed. Finally, Section 4.5 gives some conclusions of this work and future lines.

4.2 Methodology

The model follows a bottom-up approach and uses a stochastic algorithm to obtain the consumption profiles of the electricity demanded in the residential sector by the use of heating and cooling devices. Moreover, it is not very complex and computationally efficient. However, it previously requires some information related to the cooling and heating electricity consumptions, the appliances, the external weather conditions, and the consumers' behaviour. The following subsections describe the required datasets and the calculation procedure in detail.

4.2.1 Parameters and data

The input parameters comprise a collection of datasets that aims to assist in the energy modelling process. Five main groups of data can be distinguished which are the active occupancy of the dwellings, the external weather conditions, the relationship between external temperature and energy consumption, the type, technology, penetration rate and modelling techniques for the heating and cooling appliances and the household thermal

losses. Each of these datasets mainly depends on the region to be studied. The following subsections explain the methodology employed to obtain and use these data.

4.2.1.1 Active occupancy in households

The occupancy profile is the cornerstone of the model since energy consumption in the residential sector is strongly related to people's activity at home. This occupancy is considered as an active household occupancy, meaning the number of residents at home and not sleeping. The residential daily occupancy profile was generated by simulating a stochastic model based on Markov-Chains theory and Monte-Carlo techniques. This modelling technique was previously implemented and validated by Richardson *et al.* for UK [26], Lopez *et al.* for Spain [9], and Widén *et al.* for Sweden [31]. In addition, the model developed by Lopez *et al.* was already used in a previous work to simulate the lighting consumption in the residential sector showing accurate results [32].

The transition matrices for the Markov-Chain model were obtained from the Time Use Survey (TUS), conducted in Spain during the year 2010 covering 19,295 people living in 9,541 homes [33]. However, similar surveys have been carried out in most of the European countries and their information is periodically collected by the harmonised European time use surveys (HETUS) [15]. In this study, each interviewee wrote information in a diary, during a completed day and with a frequency of 10 minutes, about the daily activities they performed, where these activities took place, and whether someone accompanied them.

The occupancy profile throughout the day was calculated as a transitional procedure, where the next state of occupancy depends on the previous one. In Markov-Chains theory, this is ruled by the so-called transition matrices [34, 35]. Since it is a non-homogeneous Markov process, these matrices were calculated for each of the 144 instances of time (intervals of 10 minutes for a whole day). Using these matrices and the Markov-Chains calculation procedure, the daily active occupancy profiles were obtained, being able to differentiate between different numbers of residents, locations and the types of days (weekday or weekend). Finally, the results are supplied to the main algorithm to estimate the heating and cooling consumption.

4.2.1.2 Nonlinear response between temperature and energy demand. Smooth transition regression (STR)

The use of heating and cooling appliances is directly related to temperatures. Nevertheless, this relationship is clearly nonlinear since both increases and decreases in temperature around a so-called comfort threshold produce a consumption increment. Some authors previously estimated this threshold around 20 °C (68 °F). Sailor *et al.* [36] considered 21 °C (70 °F) for Florida and Giannakopoulos and Psiloglou [37] 22 °C (72 °F) for Greece. However, other authors such as Sarak and Satman [38] obtained 15 °C (59 °F) for Turkey, or in the case of Spain, 18 °C (65 °F) by Valor *et al.* [18].

The Heating and Cooling Degree days, HDD and CDD respectively, daily defined as the difference between the average temperature and a given base temperature T^* [39], are widely-used tools to study this relationship. Nevertheless, as different previous studies depicted, the main problem is the lack of consensus over the comfort reference temperature T^*, which has led to the existence of various bases for the HDD and CDD calculations. Furthermore, the HDD and CDD methods do not take into account the progressive transition between the cooling and heating consumption [20]. Consequently, in this work, the relationship between temperature and energy consumption intensity was studied by means of smooth transition regression (STR) techniques as it was previously done by Moral-Carcedo *et al.* [19].

The STR is based on two linear regression models whose influence is weighted by means of a logistics function that depends on temperature T and limits the cooling and heating trends. The total demand intensity $D(T)$ is obtained as the sum of the linear heating trend of coefficients a_1, b_1 and the cooling regression with coefficients a_2, b_2. Its expression is indicated in (4.1).

$$D(T) = (a_1 + b_1 T)\,(1 - G(T)) + (a_2 + b_2 T)\,G(T) \tag{4.1}$$

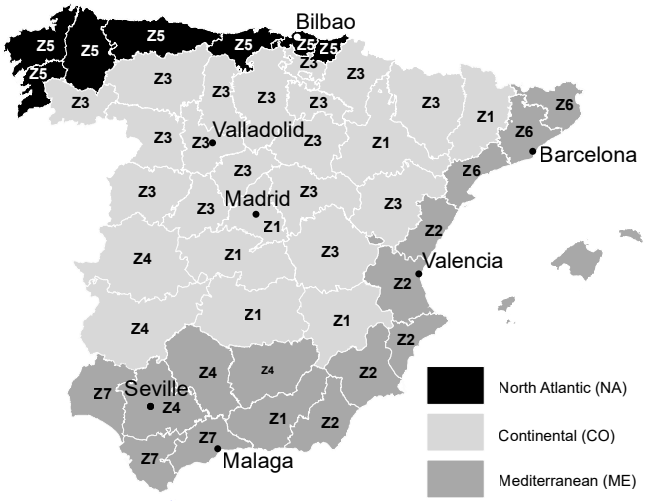

Figure 4.1: Climate zones for the study of temperatures (Z) and for the appliance selection (coloured).

In this equation, $G(T)$ is the logistic function which varies in the interval [0,1] and has two parameters as indicated in (4.2). The parameter γ controls the smoothness of the transition between the heating and the cooling area, whereas c determines the value of T for which the change of state occurs.

$$G(T) = \frac{1}{1 + e^{-\gamma(T-c)}} \tag{4.2}$$

To establish the relationship between the temperature T and the consumption D, both daily temperatures and consumption values were collected for the studied region. The values of the daily temperatures used in this work were specifically obtained from the State Meteorological Agency (AEMET) comprising of hourly values for the years 2014, 2015, and 2016 [40]. Seven representative climate zones were selected based on the cluster analysis performed by Moral-Carcedo *et al.* [19] taking a reference city for the daily temperature profiles. The location of each zone, as well as the referenced cities, are illustrated in Figure 4.1.

As it can be observed each of these climate zones represent a different percentage of the whole population. Thus, a weight factor was assigned to each zone according to the 2015 population census of the country, so the total consumption of the country could be related to the weighted temperatures. The selected data are indicated in Table 4.1.

Table 4.1: Selected climate zones, reference cities and weight factor for the study.

Zone	Weight	Reference City
Z1	0.2391	Madrid
Z2	0.1647	Valencia
Z3	0.1073	Valladolid
Z4	0.1037	Seville
Z5	0.1451	Bilbao
Z6	0.1629	Barcelona
Z7	0.0773	Malaga

As regards the Electricity demand, it was obtained from the national network operator in Spain, Red Electrica Española (REE) [41]. These data include the total aggregate consumption of the country with a 10-minute resolution for the same years as the temperature (2014, 2015, and 2016). Unfortunately, no disaggregate data for the residential sectors were available, so a preprocessing was carried out to eliminate the influence of holiday periods, as well as sectors which are insensitive to the temperature such as large industrial consumers. Therefore, the official holiday periods were eliminated and the daily average consumption of the industrial sector was subtracted from the aggregate figure.

Finally, the historical temperature data indicated above were employed as the input explanatory variable, whereas the consumption data represented the output response variable. The four coefficients of the linear functions for the heating a_1, b_1 and cooling regression a_2, b_2, as well as the two parameters of the logistic function γ and c, were obtained using the non-linear least squares method as proposed by Teräsvirta [42].

4.2.1.3 Cooling and heating appliances percentages

The active occupancy and temperature influence the heating and cooling consumption. Nevertheless, the number and technology of the appliances installed in each household will eventually define the demand. Hence, information about the possession rate of these appliances, as well as their technology and distribution, is necessary for an accurate estimation. Furthermore, this information will be necessary for each one of the geographical locations in which the simulations will be implemented since the rates of possession might vary even within the same country.

The percentages of installed heating and cooling appliances in Spain were obtained from the report published by the Institute of Diversification and Saving of Energy (Instituto para la Diversificación y Ahorro de la Energía, IDAE) [7]. In this report, corresponding to the year 2011, an analysis of the energy consumption in Spain was carried out, distinguishing between the energy source, energy end use, and climate region. Three climate regions were defined: the North Atlantic (NA) area (black), the Continental (CO) region (light grey) and the Mediterranean (ME) region (dark grey). Each of them is represented in Figure 4.1.

Three different figures were used for the simulation model. For simplification, the subscript *H/C* will be employed in all of the expressions meaning that the calculus is performed for both heating and cooling appliances. First, the probabilities of a household having at least one heating p_H and/or one cooling p_C appliance respectively were calculated for each region r. For that aim, from all the households N_h the total number of houses H with one or more heating or cooling appliance $a_{H/C}$ were divided between the total number of households in the studied region. The employed expression can be seen in (4.3).

$$p_{H/C}(r) = \frac{\sum_{h=1}^{N_h} H\left(h, r | a_{H/C}(h) \geq 1\right)}{\sum_{h=1}^{N_h} H(h, r)} \tag{4.3}$$

Subsequently, the average number of appliances per each household with heating or cooling installation $\overline{A_H}$ and $\overline{A_C}$ was determined, by dividing the total number of devices between the number of houses with heating or cooling installation for each case as indicated in (4.4). This means that, whereas some households might not have cooling or heating appliances at all, the ones which possess these kinds of devices might have installed more than one for this purpose.

$$\overline{A_{H/C}} = \frac{\sum_{h=1}^{N_h} a_{H/C}(h, r)}{\sum_{h=1}^{N_h} H\left(h, r | a_{H/C}(h) \geq 1\right)} \tag{4.4}$$

The probability and the average number of appliances for each region can be observed in Table 4.2. The heating systems are installed in almost every house with an average number of devices per household greater than one. The lower percentage of possession is found in the Mediterranean region where winters are softer. Regarding the cooling appliances, the situation is completely different with almost no penetration in the NA

Table 4.2: Percentage use of heating and cooling installation. Average number of appliances per household.

Region	Heating		Cooling	
	Households with installation (p_H)	**Appliances per household ($\overline{A_H}$)**	**Households with installation (p_C)**	**Appliances per household ($\overline{A_C}$)**
NA	0.9275	1.18	0.0112	0.98
CO	0.9505	1.23	0.3986	0.99
ME	0.8615	1.41	0.6765	0.99
Spain	0.9001	1.31	0.4959	0.99

region, while in the CO and the ME areas the percentages are significant but not as high as in the case of the heating equipment.

In addition to the installation rate and the number of appliances per household, the type of each one was studied. The probability of an appliance belonging to a certain technology or type $p_{d_{H/C}}$ was obtained by dividing the total number of each type of appliance d_H or d_C between the total number of appliances installed in each region as expressed in (4.5).

$$p_{d_{H/C}}(r, d_{H/C}) = \frac{\sum_{h=1}^{N_h} a_{H/C}(h, r, d_{H/C})}{\sum_{h=1}^{N_h} a_{H/C}(h, r)} \tag{4.5}$$

Table 4.3 shows the obtained percentages for different types of appliances considered, differentiating between climatological regions. It can be observed that a significant variation is obtained between the values corresponding to the ME region and those corresponding to the others. Specifically, the heating appliances such as the conventional or the condensing boilers, which work mainly with natural gas, have a lower percentage of use in ME climate than in any of the other regions. However, the percentages of electric heating appliances are higher in the ME zone, highlighting the electrical heater and the electric radiator, along with non-reversible heat pumps.

Among all these devices, this paper only considers those appliances which are supplied with electricity, which are the non-reversible heat pumps, reversible heat pumps, electric radiators and electric heaters. That is a key point since, whereas in the NA region the use of heating devices is significantly higher than in the

Table 4.3: Percentage use of each heating and cooling technology.

Appliance	**NA ($p_{d_{H/C}}$)**	**CO ($p_{d_{H/C}}$)**	**ME ($p_{d_{H/C}}$)**	**Spain ($p_{d_{H/C}}$)**
Conventional Boiler	0.4972	0.6098	0.2062	0.3756
Condensing Boiler	0.0144	0.0162	0.0063	0.0106
Not Electric Heater	0.0432	0.0300	0.0375	0.0357
Solar Panels	0.0115	0.0101	0.0052	0.0076
Other Heating	0.0649	0.0572	0.0605	0.0599
Non-reversible Pump (Heating)	0.0025	0.0672	0.2459	0.1571
Reversible Pump (Heating)	0.0078	0.0045	0.0039	0.0046
Electric Radiator	0.2138	0.1152	0.1977	0.1722
Electric Heater	0.1447	0.0898	0.2368	0.1768
Fan	0.6683	0.0890	0.0495	0.0620
Air Conditioner	0.0485	0.2543	0.1215	0.1570
Reversible Pump (Cooling)	0.2832	0.6567	0.8293	0.7810

ME region, as it was observed in Table 4.2, the appliances in the NA region are not usually supplied with electricity, while the ones in the ME are, therefore, their impact on the grid is higher.

As regards cooling appliances, also shown in Table 4.3, the observed percentages within the Mediterranean region are higher too. The use of reversible pump systems for cooling achieves almost 83%, whereas fans and air conditioners represent a relatively small percentage. It should be also emphasised that reversible pump systems could be used for both cooling and heating, nevertheless, they have a marginal usage rate for heating. In this case, all cooling appliances are supplied with electricity, consequently, the three proposed, fans, air conditioners, and reversible pump systems, were considered in the model.

4.2.1.4 Model of an appliance and thermal behaviour

Each heating or cooling electrical device is modelled using a series of parameters that identify its behaviour. The definition combines the operation of the device and the influence of the insulation and external conditions. In this way, each appliance is assigned with an on power P_{on}, a coefficient of performance COP, an on time t_{on}, an off delay t_{off}, a power factor PF and a probability of having a thermostat control P_{Th}, which have associated an average threshold temperature T_{th} that varies with a given standard deviation δ whose value was obtained from [43].

The values for t_{on} and t_{off} were assigned by considering a one-thermal mass equivalent thermal parameter (ETP) model of a household as it was proposed by Smullin [44]. The thermal mass C is coupled with the outdoor temperature T_a by means of the equivalence transmittance radio of the house denoted as H. In addition, a coefficient Q_{loss} has been added to represent the internal gains. The expression of t_{off} in minutes for the cooling case is indicated in (4.6) where $T_{thL} = T_{Th} - \delta$ represents the thermostat low threshold and $T_{thH} = T_{Th} + \delta$ is the upper bound. This expression is only valid when $T_a + \frac{Q_{loss}}{H} > T_{thH}$ since, otherwise, the temperature will be between the comfort limits and no cooling will be necessary, meaning $t_{off} = \infty$. Practically, this value was considered as an hour for the study, a value long enough to allow for further switch-on events.

$$t_{off}(T_a) = \begin{cases} \frac{C}{60 \cdot H} \ln \left[\frac{T_a - T_{thL} + \frac{Q_{loss}}{H}}{T_a - T_{thH} + \frac{Q_{loss}}{H}} \right] & , T_a + \frac{Q_{loss}}{H} > T_{thH} \\ 60 & , T_a + \frac{Q_{loss}}{H} \leq T_{thH} \end{cases} \tag{4.6}$$

In the same way, the t_{on} for the cooling is expressed in (4.7) where Q_c is the heat removed, considered positive for the cooling case and calculated as (4.8). As well as in the previous case, this expression is only valid when the removed heat can compensate the rest of the thermal losses, for the rest of the cases where the operating time will be equal to infinity, again a maximum period of operation of an hour was selected.

Table 4.4: Parameters of the Appliances Considered in the Model.

Appliance	P_{on} [W]	COP	PF	P_{Th} [%]	T_{th} [°C]	δ [°C]
Non-reversible Pump (Heating)	1,142	4.05	0.9	86.46	24.5	4.52
Reversible Pump (Heating)	1,151	4.02	0.9	86.46		
Electric Radiator	2,200	1	1	75.72		
Electric Heater	1,200	1	1	57.81		
Fan	70	1	0.9	0	25.3	5.87
Air Conditioner	1200	3.34	0.9	100		
Reversible Pump (Cooling)	1300	3.75	0.9	100		

$$t_{on}(T_a) = \begin{cases} \frac{C}{60 \cdot H} \ln \left[\frac{T_{thH} - T_a + \frac{Q_c - Q_{loss}}{H}}{T_{thL} - T_a + \frac{Q_c - Q_{loss}}{H}} \right] & , T_a + \frac{Q_{loss}}{H} - T_{thL} < Q_c \\ 60 & , T_a + \frac{Q_{loss}}{H} - T_{thL} \geq Q_c \end{cases} \tag{4.7}$$

$$Q_c = COP \times P_{on} \tag{4.8}$$

The equations (4.6), (4.7), and (4.8) are also valid for the heating case, but the thresholds T_{thL} and T_{thH} are interchanged since the behaviour of the hysteresis band is the opposite and the heat Q_c from the heating appliances has to be considered negative.

In the case of non-thermostat controlled appliances, no t_{off} is assigned and the t_{on} is regulated by the users' behaviour and the external conditions with a continuous operation until the switch-off event. The mean power, COP value, as well as an average estimated power factor, were obtained after a study of the main available products from some heating and cooling manufacturers [45–48]. In addition, the t_{on} of each appliance for the non-controlled cases was selected based on [49], where the use patterns of the domestic appliances within Europe were studied. Table 4.4 lists the selected values.

Table 4.5: Distribution of dwelling stock for the studied region.

Year	Stock (%)	U Floor [W/m^{2}K]	U Walls [W/m^{2}K]	U Ceiling [W/m^{2}K]	U Windows [W/m^{2}K]	Area [m^2]
<1945	13	2.45	2.52	1.75	5.7	87
1945-1969	23	2.45	2.13	1.37	5.7	73
1970-1979	19	2.45	2.13	1.37	5.7	86
1980-1989	12	0.8	1.6	1	3.3	88
1990-1999	12	0.8	1.6	1	3.3	88
2000-2008	20	0.7	0.8	0.54	3.1	99

Regarding the insulation parameters and the type of construction that allows for the calculation of the parameters C and H, the data collected in the European project ENTRANZE [50] were considered. The values are presented in Table 4.5.

4.2.2 Simulation methodology

The simulation process was implemented in two stages. First, each dwelling is assigned a group of heating and cooling devices, as well as thermal characteristics, depending on the climate zone. Furthermore, for the selected period and the number of residents the active occupancy profile is estimated. After this and using the daily temperature profile, the system determines the on/off events of each appliance with 1-minute resolution, consequently, calculating the electrical consumption that they have associated. Figure 4.2 depicts this process whose operation is described in the following subsections.

4.2.2.1 Initialisation process

The initialisation process is carried out for each of the N_h households that will be simulated. In this stage and after loading the probabilities for the selected region, the system defines the heating and cooling appliances, and the insulation characteristics. The appliances are selected using three stochastic processes. First, two random numbers r_H and r_C uniformly distributed between [0,1] are generated and used in an inverse sampling in the cumulative distribution function (CDF) of having heating P_H or cooling P_C devices installed, where $P_{H/C}$ are Bernoulli distributions with $p = p_{H/C}$, calculated as indicated in (4.3).

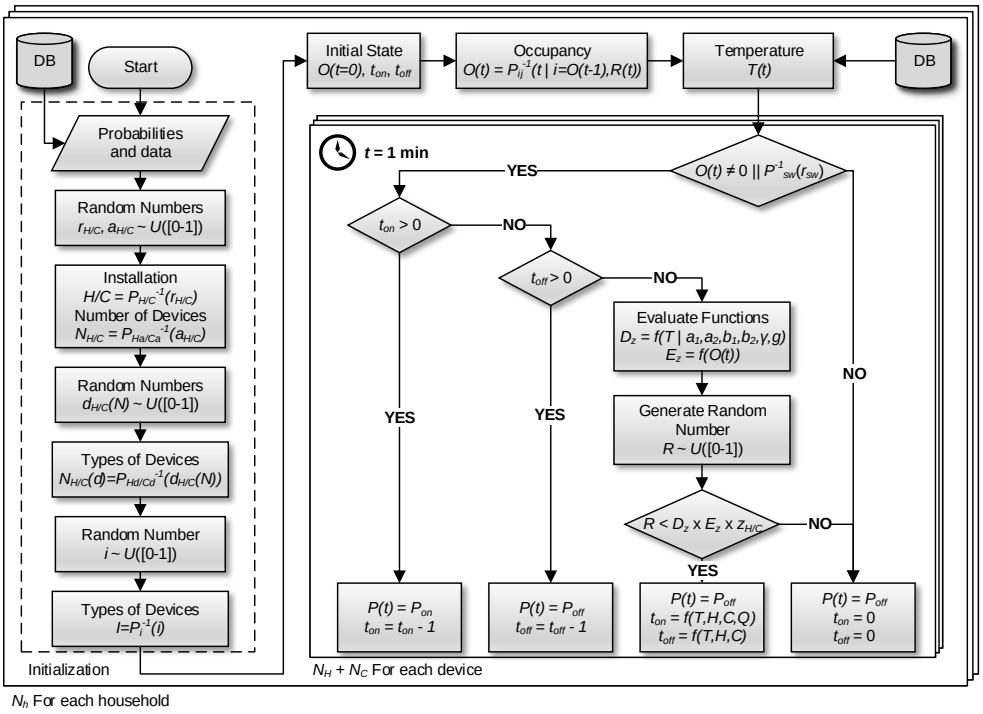

Figure 4.2: Flowchart of the simulation algorithm.

If this operation equals 1 for the heating H and/or the cooling C installation, then the number of devices of each type is determined. In this process, two more random numbers are generated a_H and a_C, and then sampled inversely in the normal distributions P_{Ha}, P_{Ca} with $\mu_{H/C} = \overline{A_{H/C}}$, as in (4.4), and $\sigma_{H/C} = 1$. After this, the number of heating N_H and cooling N_C appliances is calculated.

Subsequently, each appliance is finally assigned to a given technology from the ones considered in Table 4.3. For that aim, a random number $d_{H/C}$ is generated for each of the $N_{H/C}$ appliances and used in an inverse sampling over the discrete CDF of an appliance belonging to a certain technology $P_{d_{H/C}}$, whose probability mass function (PMF) is defined by the columns corresponding to each region in Table 4.3. As it was indicated, the modelling process only considers those appliances supplied with electricity. Thus, in some cases, although the number of heating N_H and cooling N_C devices in the previous stage could be different to zero, if the selected technology in this step does not use electricity, the final number of devices will be zero.

Once the appliances are distributed, the insulation parameters of each house are assigned. This process is performed by means of a random number i uniformly distributed between [0,1], which is used to perform a random sampling over the discrete CDF of households' stock P_i. The PMF p_i in this case is defined in Table 4.5 as the stock of households of each year and insulation characteristics.

After the definition of the household, three steps are carried out before starting the simulation process for each minute. First, the initial conditions of the system are calculated, which means the initial occupancy $O(t = 0)$ as well as the operation point of each appliance. The initial occupancy is assigned based on the discrete CDF of active occupants for the initial minute of the simulation, whereas t_{on} and t_{off} are calculated for each device using (4.6), (4.7), and (4.8), but multiplying the duty cycle by a random number between [0,1].

After that, the occupancy profile for the selected period is calculated with a 10-minute resolution, using the number of residents in the household and the type of day. For each 10-minute instance t_{10}, a random sampled number R_t uniformly distributed between 0 and 1 is generated. After this, the random number is employed to calculate the following state of occupancy $O_n(t_{10})$ by means of the inverse probability sampling of transition matrix P_{ij} for the step t_{10} and considering the previous occupancy state of the dwelling $O_n(t_{10} - 1)$ as indicated in (4.9).

$$O_n(t_{10}) = P_{ij}^{-1}\,(t_{10}|O_n(t_{10} - 1), R_t) \tag{4.9}$$

Since the occupancy profile has a lower resolution than the simulation algorithm, the occupancy is considered constant for each 10-minute interval, an approximation that has no impact on the results since the occupancy changes have a much lower frequency than the appliances' activation and deactivation events.

Finally, before starting the simulation, the temperature profile which is contained in a database, was accessed depending on the date and selected region, and subsequently loaded. The profiles in the database are stored with 1-minute resolution, but they were linearly interpolated from 1-hour resolution data as indicated in Section 4.2.1.2. Nevertheless, the evolution of the temperature during the day is slow and hourly interpolated data were found to be enough to estimate accurate profiles. What is more, the structure of the system allows new data to be stored with more resolution when available.

4.2.2.2 1-minute consumption simulation

The simulation process after the initialisation of each household is performed for every minute of the simulation interval and for every appliance, evaluating the state of them and updating the t_{on}, t_{off}, and $P(t)$ accordingly. The whole process can be observed on the right side of Figure 4.2.

In this way, first, the system checks the active occupancy of the dwelling, being a necessary condition for the activation of the heating and cooling appliances, but not sufficient. Nevertheless, since some appliances can be programmed to operate over periods of inactivity (absent or sleeping residents) an additional condition was added when no occupancy was detected. Thus, when no active occupants are in the dwelling a random number r_{sw} is generated and inversely sampled over the discrete CDF P_{sw} that follows a Bernoulli distribution with $p = 0.05$. This parameter is an average probability obtained from the survey on households and environment [43] where the interviewees indicated if they left the heating and cooling devices activated when they were either absent or sleeping. If the result of this comparison is false, the appliance is deactivated and its P_{off} is added to the 1-minute total power profile $P(t)$.

In case there is active occupancy, the appliance can be in three different states: active ($t_{on} > 0$), waiting ($t_{off} > 0$) or deactivated ($t_{on} = 0$, $t_{off} = 0$). If the appliance is in the active state, its operation cycle is decreased and its active power P_{on} is added to the total power profile. When the appliance is waiting, the off cycle, in this case, is decreased and the inactive power P_{off} is aggregated to the total load. Otherwise, if the appliance is completely deactivated the possibility of turning it on is evaluated based on the temperature profile, the active occupancy and the house insulation parameters. Two stages comprise this evaluation.

First, the relationship between the average daily temperature and the consumption intensity is evaluated by means of the STR function $D(T)$ previously described. This function was normalised (D_z) by dividing the generated values between the demand in the estimated equilibrium temperature (18.7 °C) and depends on the fitted parameters that will be presented in the results. Likewise, the active occupancy is considered but as an effective occupancy [12]. This relationship was obtained from the data provided in U. S. Energy Department in the so-called Residential Energy Consumption Survey [51]. This survey was carried out in 2009 in the United States and includes information about the end uses of each household and their characteristics (number of residents, appliances), allowing to relate the number of residents per household with the equivalent yearly consumption $E(O(t))$. As in the previous case, it was divided between the average consumption for 1-resident houses so it was normalised $E_z(O(t))$. This normalisation also allowed us to use U.S. consumption data although the model is being applied to Spain.

By means of these two indices D_z and E_z and a calibration scalar for each type of appliance, $z_{H/C}$, which is discussed in the following section, a probability is obtained and a comparison is performed with a randomly generated number R. In case this number is lower than the obtained probability the conditions of temperature and occupancy might require the use of heating or cooling appliances respectively. Otherwise, the appliance will remain inactive.

Finally, if the conditions determined that it is possible to use the appliance, the active t_{on} and waiting time t_{off} are assigned based on (4.6) and (4.7). These final equations take into account the household thermal characteristics and the high-resolution temperature profile. Therefore, depending on the values of these parameters the final assigned operation time could also be null, but they allowed for the simulation of the low-level behaviour of the appliances during the day, one of the main novelties of this model.

4.2.3 Calibration

Due to the random and stochastic techniques employed, the power and energy results are not scaled with the real values observed within the region where the simulation was accomplished. Therefore, an iterative process was implemented to calibrate both heating and cooling consumption by means of z_H and z_C variables, which previously appeared in Figure 4.2. To obtain each of these scalars, 10 iterations over 1,000 different households N_h were performed, considering the heating and the cooling appliances separately.

$$f_{H/C}(s) = \frac{E^*_{H/C}}{\frac{1}{N}\sum_{h=1}^{N_h} E_{H/C}(h)} \tag{4.10}$$

$$z_{H/C}(s) = z_{H/C}(s-1) \cdot f_{H/C}(s) \tag{4.11}$$

Before starting the calibration process, a value of 1 is given to $z_{H/C}$. In each of the 10 iterations (denoted by s) $f_{H/C}(s)$ and $z_{H/C}(s)$ are determined by means of (4.10) and (4.11). $f_{H/C}(s)$ is the quotient between the average value of the heating application consumption observed within the studied region $E^*_{H/C}$, taken as reference, and the average result of the 1,000 simulated houses, being $E_{H/C}(h)$ the energy consumed during a year, and for a specific household h. The value of E^*_H was selected as 265.899 kWh and E^*_C equals to 139.311 kWh [2]. $z_{H/C}(s)$ is the updated scalar value obtained for each iteration s, which will be inserted in the next iteration using the equation (4.11). This figure will be employed to update the value of the scalar for each iteration, where $z_{H/C}(s-1)$ is the value of the scalar obtained in the previous iteration (or 1 if it is the first iteration).

4.3 Results

4.3.1 Model implementation

The simulation process was implemented using JAVA programming language. This language and its object-oriented philosophy facilitated a flexible implementation with interoperability between operating systems, and other features required in this development such as database and network connectivity, concurrency and functional programming. The system was developed as a JAVA enterprise application and was provided with a RESTful application programming interface (API) and a database to store the required information as it is illustrated in Figure 4.3. Using this API, the simulation parameters and the results can be sent to the system from any device that implements a network connection and the HTTP protocol which increases the usability and integrability of the system in other simulation platforms. In addition, a general user application (GUI) was developed to ease the use of the system, where the simulation parameters can be configured (Conf. GUI) and the results visualised (Results GUI). This GUI is integrated into the previous one developed in [32].

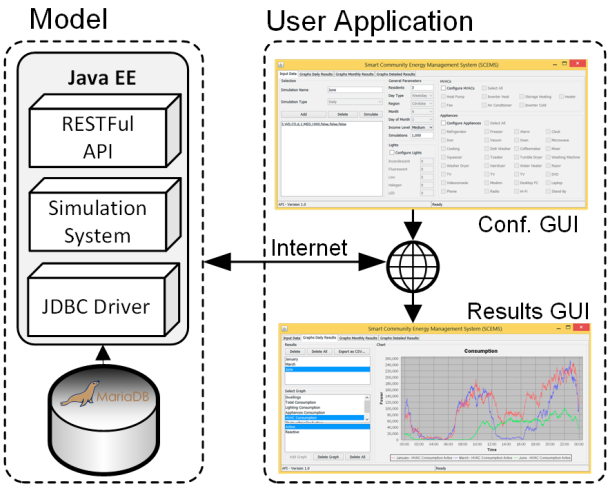

Figure 4.3: Logical implementation of the simulation system and developed GUI.

4.3.2 Temperature-energy STR function

The methodology described in Section 4.2.1.2 used the weighted temperature data by region and the filtered electricity consumption to estimate the STR model by means of the non-linear least squares method as proposed by Teräsvirta [42]. The scatter plot in Figure 4.4 illustrates both the data point (black round symbols) and the fitted values (grey diamond symbols). As can be seen, the estimated trend clearly matched the observed values. An equilibrium temperature was observed with a value of 17.8 °C for which the electricity consumption is insensitive. This value was almost similar to the one previously found by Valor *et al.* [18]. Any value above or below this threshold has associated a consumption increase.

The estimated parameters are listed in Table 4.6 together with their standard errors. It can be seen that the slope modelling the heating consumption b_1 was estimated as zero with no significance for the model. That is due to the deviation of the parameter c, which regulates the transition value for the logistic function, from the equilibrium temperature (17.8 °C). This is caused by the increase that the cooling consumption

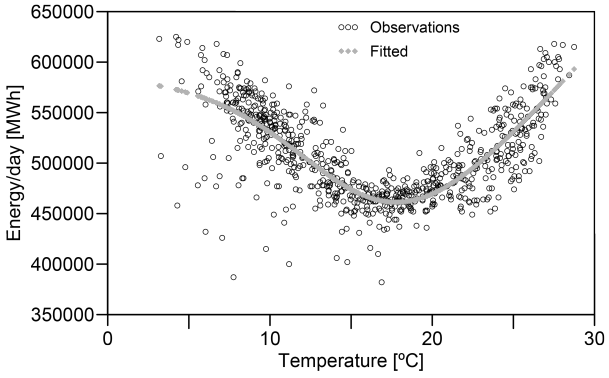

Figure 4.4: Smooth Transition Regression (STR) model for temperature-demand relationship.

Table 4.6: Estimated values for the STR model using nonlinear least squares.

Parameter	Estimate	Std. Error
a_1	589700	18950
b_1	0	7236
a_2	90370	90190
b_2	17500	3224
γ	0.2911	0.06241
c	15.16	1.798

presents. In this way, whereas the heating demand reached a saturation point for lower temperature values, the cooling consumption increased even at high temperatures. This effect confirms the previous observations of Moral-Carcedo and Vicéns-Otero [19] for data from 1995 to 2003. In that study, a small upward trend in the cooling demand was observed throughout the study years. This trend is clearly visible in this study where data from 2014 to 2016 have been used, showing the higher penetration rate of cooling devices.

4.3.3 Daily aggregate trends

The results were obtained using the presented calculation algorithm and with the aid of the developed GUI. The individual daily profiles of an isolated house present a chaotic pattern as might be expected of a stochastic model. Therefore, in order to observe and detect aggregate trends, daily simulations were performed considering a group N_h houses located in different regions and for different dates. The daily consumption vectors of each household P_{1440} were aggregated according to (4.12):

$$P_{1440}^{N_h} = \sum_{h=1}^{N_h} (P_{1440})_h \tag{4.12}$$

Figure 4.5 represents the daily consumption profiles for an aggregate of 10,000 households, simulated for a weekday in the locations of (a) Seville, (b) Madrid and (c) Bilbao and for 4 relevant dates in the year 2015.

As it can be appreciated in Figure 4.5, the shapes and trends of the daily consumption profiles are highly related to the season and consequently with the type of appliances which are used in each case. During the months of January, February, March and part of April, heating appliances are responsible for the daily curve shape, so the highest consumption peaks are associated with the periods of high active occupancy and low temperature. As it can be observed for the 1st January (solid black line), these two peaks take place from 08:00 h to 12:00 h and from 20:00 h to 00:00 h.

Nevertheless, their amplitudes depend on the location. Thus, for (a) Seville, located in the south, the peaks are more pronounced due to the higher temperatures during midday, but the consumption is also larger since mainly electrical appliances are used. In the case of (b) Madrid the installation rate of electrical appliances is lower so the power demand is too. The same trend is observed in (c) Bilbao, which due to the lower temperatures, presents a higher consumption than (b) Madrid even though the installation rate of electrical heating devices is lower.

In the Summer scenario, the 28th June (solid grey line), the daily profile shows the main demand peak from 13:00 h to 18:00 h. This higher demand can only be observed in (a) Seville and (b) Madrid, whereas in (c) Bilbao almost no energy consumption takes place during the summer months as the percentage of cooling appliances is extremely low (around 1%) and the temperatures are moderate. It should also be pointed out that the cooling peak is almost twice the amplitude of the heating peaks. This higher figure is related to the hot and dry summers of the studied locations and the fact that only electrical appliances are employed for cooling purposes.

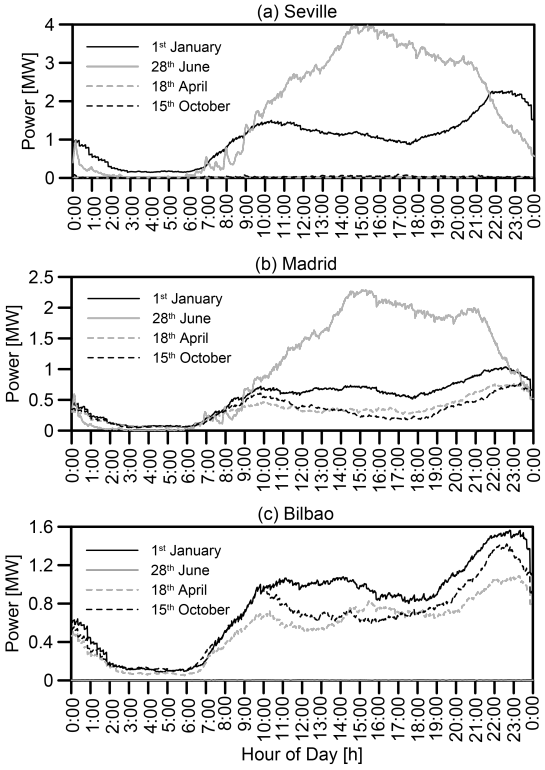

Figure 4.5: Daily Consumption Profiles for Heating and Cooling Appliances.

Finally, two other days, one in spring the 18th April (dashed grey line) and another in autumn the 15th October (dashed black line) were studied. They correspond to transition days between the heating and cooling consumption and vice versa. In the case of (a) Seville, no consumption is observed in these days as the city is located in the south and the temperatures are usually within the comfort limits in these dates. In contrast, both (b) Madrid and (c) Bilbao present consumption for the studied days, although the power demand is not as high as in the winter scenario.

For the 18th April, the consumption has a flat shape during the day once the active occupancy has started. In the case of the 15th October, the consumption figures are almost similar but the morning and night peaks are more pronounced since the thermal amplitude during this month is higher. To visualise this a broader time horizon was studied in the following section.

4.3.4 Annual demand

The daily estimation was extended to a year, although the model allows for simulating even a sequence of years, providing the temperature data are available in the system database. Using the three previous locations Seville, Madrid and Bilbao a cluster of 1,000 households was evaluated for the year 2015. The results are illustrated in Figure 4.6, where the daily energy demand for the whole year is represented. The results were obtained by calculating the daily energy of the aggregate power consumption P_i of each household h for the N_h houses selected for the simulation as expressed in (4.13).

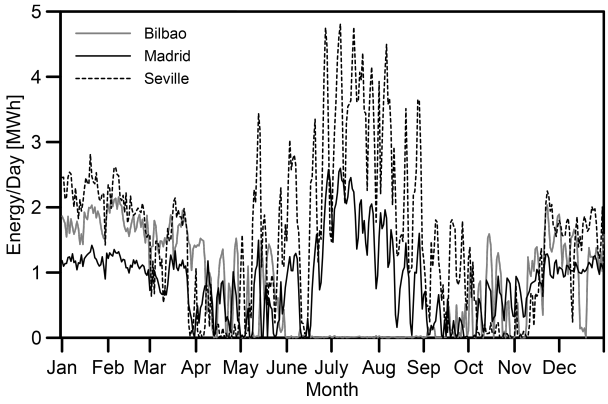

Figure 4.6: Annual Demand Profiles for different locations.

$$E_{365}^{N_h} = \sum_{h=1}^{N_h} \left(\left[\sum_{i=1}^{1440} \frac{1}{60} [P_i] \right]_{365} \right)_h \tag{4.13}$$

The annual profiles show the peculiarities of each climate zone. In the case of Bilbao in the North (solid grey line), the consumption during the winter season is similar to the one found in Seville in the South (dashed black line). Nevertheless, although the temperatures in Seville are higher than in Bilbao the percentage of electrical appliances in Seville is almost twice as high as Bilbao. In the case of Madrid (solid black line), the use of electrical heating appliances is similar to the one in Bilbao but the temperatures are not so cold so the consumption is slightly lower.

Regarding the summer, the trend is completely opposite. Bilbao (solid grey line) shows no consumption at all during this period, whereas Seville (dashed black line) and Madrid (solid black line) have a considerable high energy demand, being the highest consumptions of the year found during the months of July and August. Likewise, if the transition between the heating and cooling consumption is observed, Seville presents a very low or almost null consumption from April to the middle of May and from October to the middle of November, whereas Madrid and Bilbao have a low demand but still not zero.

4.3.5 Impact on the grid

The two previous simulation methodologies were combined to obtain a 1-minute resolution annual power profile. Using this profile, the load duration curve for both heating and cooling demand was calculated. In this way, a simulation of 200 households located in Seville was performed for the year 2015. Figure 4.7 represents the obtained results where the Y-axis indicates the instantaneous power demand for the whole cluster of households and the X-axis is the amount of time that this instantaneous power demand occurs during the studied year.

As it can be observed in Figure 4.7, the cooling load presents higher instantaneous power demand than the heating curve for an equivalent time longer than 50 days a year. However, the heating load has a significant value for almost 110 days whereas the cooling load only presents a high consumption for 70 days. Hence, although the annual cooling energy demand is generally lower than the heating load, the concurrence of a high-power demand in a short period might cause the overcharge of the network. This is of special interest in the current context due to the integration of more renewable energy resources and the purchase of more cooling appliances to increase the comfort level.

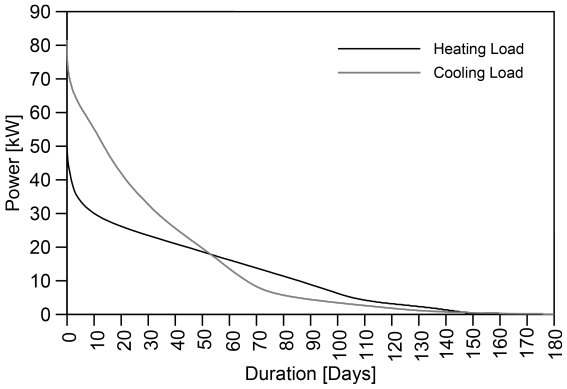

Figure 4.7: Load duration curve for 200 households located in Seville during a year.

4.4 Validation

The accuracy of the proposed model was evaluated by comparing the daily generated profiles with previous works. The main reference in the European context that includes high-resolution disaggregated data is the REMODECE project [52]. This research did not take into account Spain so a direct comparison cannot be performed. Nevertheless, other regions with similar climate characteristics were used in order to evaluate and validate the profiles. For this aim, the database of the REMODECE project was queried [8]. This database includes not only data from the REMODECE project (years 2006-2008) but also data from some other local projects such the Eureco project (years 2000-2001) in the case of Italy.

To allow the comparison of the profiles generated by the proposed model and the individual hourly energy records of the REMODECE project for each household, the model was used to estimate the average curves for one day of winter and one day of summer, calculated for 10,000 households, and weighted between the different studied location of Spain. Subsequently, the hourly energy consumption was calculated and compared with the average results of the REMODECE project for France and Portugal in the case of winter and Italy and Greece for the summer consumption. The results can be seen in Figure 4.8 where the winter profiles are presented in the subfigure (a) and the summer consumption in the subfigure (b).

In the case of the winter profiles (a), a larger energy consumption is presented in the case of France with a consumption peak during the night, which might be justified due to the higher installation rate of

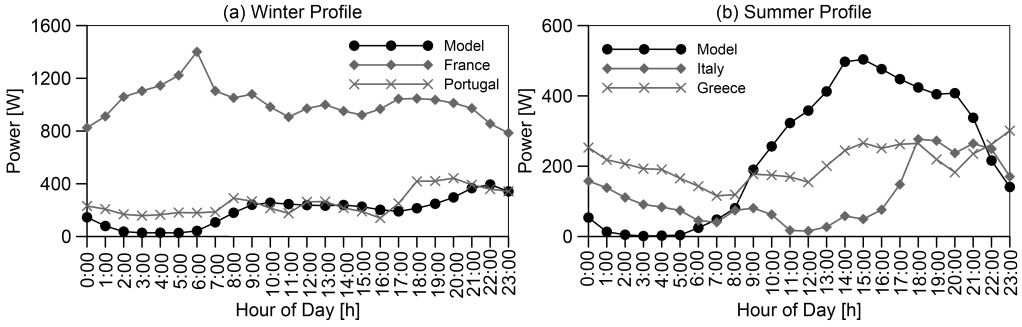

Figure 4.8: REMODECE data for different locations vs Model.

storage heating systems and the colder winters. Nevertheless, the profile obtained for an average Portuguese household almost resembles the one estimated by the model. On the other hand, in the case of the summer profiles (b), the energy estimated by the model is larger than the one obtained for Greece or Italy in the REMODECE project. However, the different daily schedules, as well as the milder temperatures of these countries due to the sea influence, could lead to these different figures and profiles.

$$\mathrm{RMSE} = \sqrt{\frac{1}{n}\sum_{t=0}^{n}\left(P_{Model}(t) - P_{Meas}(t)\right)^2} \tag{4.14}$$

$$\mathrm{NVF} = \frac{\mathrm{MSE}}{\overline{P_{Meas}}^2} = \frac{\sum_{t=0}^{n}\left(P_{Model}(t) - P_{Meas}(t)\right)^2}{n\left(\frac{1}{n}\sum_{t=0}^{n} P_{Meas}(t)\right)^2} \tag{4.15}$$

The profiles were numerically evaluated by means of two indicators, the root mean square error (RMSE) expressed in (4.14), and the normalised variation factor (NVF), a pseudo-variance in which the mean square error (MSE) between the generated profiles $P_{Model}(t)$ and the measured data from the REMODECE $P_{Meas}(t)$ is normalised using the squared mean of the reference measures as indicated in (4.15). The results are listed in Table 4.7 together with the number of measures (N Meas.) that were found in the REMODECE database for each country.

As can be seen, the highest RMSE was obtained between the model winter profiles and the ones found in France. Nevertheless, the climate characteristics also vary significantly. In the rest of the cases, the RMSE and NVF have similar values indicating that although the model does not perfectly match the reference profiles, the estimated power figures are within the expected range. It should also be highlighted that, whereas the IDAE report used in this project [2] is composed of 6,390 interviews and 600 details measurements of 22 appliances, the REMEDOCE database only includes a handful of households and offer a much lower temporal resolution (1-hour) than the one proposed in this model (1-minute).

Regarding how this accuracy compares with other simulation methodologies and previously published works in the field of load modelling [53], it should be considered that the main goal of the proposed model is to study the impact of low-level appliances such heating and cooling devices on the electrical grid for the residential sector. Thus, the chaotic behaviour of the residents and the heterogeneity of the buildings and installed appliances forced us to seek a compromise between precision and diversity.

In the context of energy forecasting, artificial neural network (ANN), autoregressive integrated moving average (ARIMA), and regression models are usually applied to hourly and sub-hourly predictions [54]. These models showed, in general, a higher accuracy than the proposed one [55, 56], but they are limited to the context of a single building [57], mainly commercial ones with fixed schedules and patterns that also conferred them a good robustness [58, 59]. Nevertheless, they lack the flexibility to be applied on a larger scale such as a district, a city or a region [60].

Table 4.7: Comparison between the developed model and REMODECE data for different countries and dates.

	Winter		**Summer**	
Country	**France**	**Portugal**	**Italy**	**Greece**
N Meas.	27	5	10	11
RMSE	849	102	222	172
NVF	0.7009	0.1601	3.5866	0.6905
E/day [kWh]	24.3	6.13	2.82	4.97
E/day [kWh] Model	4.61		5.63	

As opposed to, the bottom-up approach proposed in this article has a stochastic nature that provides a wide diversity of consumptions at the individual household level, but, as depicted by the figures, it presented a good accuracy in the aggregate trends as well as robust results due to the calibration process that is performed. Moreover, it provides a capability that none of the other methodologies has, which is the low-level simulation of the appliances. This feature makes the model especially suitable for studying the impact of the appliances in the grid in two ways. First, the operation of heating and cooling devices at an individual household level can be modified to simulate demand response programs and assess the benefits, both from the economic and the environmental point of view. Secondly, since the rate of possession of heating and cooling devices can be modified, future scenarios can be evaluated such as the increase in the number of cooling appliances and the possible overcharge of the network.

Finally, in terms of speed, the model is mainly designed to operate offline as an assessing tool. However, if the household parameters are known, the environmental variables are measured, and the occupancy patterns are established or given, an online simulation can be carried out, calculating the next consumption step based on the current state of the system.

4.5 Conclusions

This work has presented the development, implementation, along with the capabilities and potentialities, and followed by the validation process, of a stochastic model whose goal is the generation of synthetic high temporal resolution electricity consumption profiles for heating and cooling appliances that can be used to study the impact of these devices in the future Smart Grid. All the input data used in the simulations were obtained in the context of Spain. Nevertheless, the flexibility of the simulation procedure allows for the inclusion of new locations by providing the required input datasets as exposed in the Methods section.

The proposed algorithm was implemented using the high-level programming language JAVA and a server based philosophy so it can be easily integrated into other simulation tools. Likewise, a GUI was built in order to facilitate the selection of the input parameters for the model and the visualisation of the results, allowing the export of the data to CSV files and performing further processing with other software.

The daily profiles have shown the existence of two well-differentiated consumption intervals during the year. From November to the end of March, the energetic consumption can be attributed to the heating appliances, distinguishing two main peaks in the daily consumption profiles: one during the morning hours and another during the dinner time. In contrast, the demand during the middle hours of the day varies within the different regions. In opposition, during May, June, July, and August, cooling appliances account for the energy consumption. Therefore, the consumption was observed to be concentrated during the central hours of the day having a higher demand than the heating consumption in some locations.

That was confirmed by the yearly simulations which showed the ability of the model to simulate the climate characteristic of given locations. Thus, not only is the system able to simulate the daily and yearly variations, but also the peculiarities in the different zones, provided the system database contains the necessary input data.

Combining the 1-minute resolution and the yearly simulations, the impact of the cooling and heating appliances on the grid was assessed by mean of the annual load duration curves. The results depicted the benefits of this tool that allowed the detection of the high instantaneous demand required by the cooling system. These devices, despite having a lower annual energy consumption can overcharge the electrical network due to their concurrent utilisation and their widespread use nowadays.

Finally, the results were validated against previously developed works focused on disaggregated consumption metering. The comparison between the REMODECE curves and the ones obtained by this model showed that the figures estimated by the model are concordant with the observed trends in other countries. Nevertheless, due to the differences in the climate characteristics between the studied region and those included in the REMODECE project the results are not directly comparable and do not perfectly match the reference data.

Therefore, this simulation model together with a previous one regarding lighting consumption simulation [32], are the first steps by the authors to build an assessment tool for the future Smart grid. The final aim is to develop an integrated platform for modelling the electricity consumption in the residential sector. Thus, a general appliances consumption model is being implemented, following the presented stochastic philosophy, and will be discussed in future papers. This will provide an overview of the global electrical consumption for the residential sector and it will also be the base from which to analyse the impact of different energy saving policies, focusing on both DR techniques and more efficient appliances.

Acknowledgements

This work is supported by the Spanish Ministry of Economy and Competitiveness under Research Project TEC2013-47316-C3-1-P; and TEC2016-77632-C3-2-R.

References

[1] M. Kavgic, A. Mavrogianni, D. Mumovic, A. Summerfield, Z. Stevanovic, M. Djurovic-Petrovic, A review of bottom-up building stock models for energy consumption in the residential sector, Building and Environment 45 (7) (2010) 1683–1697. doi:10.1016/j.buildenv.2010.01.021.

[2] IDAE, Análisis del consumo energético del sector residencial en España INFORME FINAL (2011). URL: http://www.idae.es/uploads/documentos/documentos_Informe_SPAHOUSEC_ACC_f68291a3.pdf

[3] A. de Almeida, P. Fonseca, B. Schlomann, N. Feilberg, Characterization of the household electricity consumption in the EU, potential energy savings and specific policy recommendations, Energy and Buildings 43 (8) (2011) 1884–1894. doi:10.1016/j.enbuild.2011.03.027.

[4] D. Connolly, Heat Roadmap Europe: Quantitative comparison between the electricity, heating, and cooling sectors for different European countries, Energy 139 (2017) 580–593. doi:10.1016/j.energy.2017.07.037.

[5] M. Isaac, D. P. van Vuuren, Modeling global residential sector energy demand for heating and air conditioning in the context of climate change, Energy Policy 37 (2) (2009) 507–521. doi:10.1016/j.enpol.2008.09.051.

[6] M. A. McNeil, V. Letschert, Future air conditioning energy consumption in developing countries and what can be done about it: the potential of efficiency in the residential sector (2008). URL: http://escholarship.org/uc/item/64f9r6wr.pdf

[7] IDAE, Consumos del Sector Residencial en España Resumen de Información Básica (2011). URL: http://www.idae.es/uploads/documentos/documentos_Documentacion_Basica_Residencial_Unido_c93da537.pdf

[8] REMODECE project, Residential Monitoring to Decrease Energy Use and Carbon Emissions in Europe (REMODECE) Database (2015). URL: http://remodece.isr.uc.pt/

[9] M. A. Lopez, I. Santiago, D. Trillo-Montero, J. Torriti, A. Moreno-Munoz, Analysis and modeling of active occupancy of the residential sector in Spain: An indicator of residential electricity consumption, Energy Policy 62 (2013) 742–751. doi:10.1016/j.enpol.2013.07.095.

[10] A. Kipping, E. Trømborg, Hourly electricity consumption in Norwegian households - Assessing the impacts of different heating systems, Energy 93 (2015) 655–671. doi:10.1016/j.energy.2015.09.013.

[11] M. A. Brown, M. Cox, B. Staver, P. Baer, Modeling climate-driven changes in U.S. buildings energy demand, Climatic Change 134 (1-2) (2016) 29–44. doi:10.1007/s10584-015-1527-7.

[12] M. Bladh, H. Krantz, Towards a bright future? Household use of electric light: A microlevel study, Energy Policy 36 (9) (2008) 3521–3530. doi:10.1016/j.enpol.2008.06.001.

[13] J. F. Martins, J. A. Oliveira-Lima, V. Delgado-Gomes, R. Lopes, D. Silva, S. Vieira, C. Lima, Smart homes and smart buildings, in: 2012 13th Biennial Baltic Electronics Conference, IEEE, 2012, pp. 27–38. doi:10.1109/BEC.2012.6376808.

[14] N. Arghira, L. Hawarah, S. Ploix, M. Jacomino, Prediction of appliances energy use in smart homes, Energy 48 (1) (2012) 128–134. doi:10.1016/j.energy.2012.04.010.

[15] J. Torriti, Demand Side Management for the European Supergrid: Occupancy variances of European single-person households, Energy Policy 44 (2012) 199–206. doi:10.1016/j.enpol.2012.01.039.

[16] R. Fazeli, M. Ruth, B. Davidsdottir, Temperature response functions for residential energy demand - A review of models, Urban Climate 15 (2016) 45–59. doi:10.1016/j.uclim.2016.01.001.

[17] A. Pardo, V. Meneu, E. Valor, Temperature and seasonality influences on Spanish electricity load, Energy Economics 24 (1) (2002) 55–70. doi:10.1016/S0140-9883(01)00082-2.

[18] E. Valor, V. Meneu, V. Caselles, Daily Air Temperature and Electricity Load in Spain, Journal of Applied Meteorology 40 (8) (2001) 1413–1421. doi:10.1175/1520-0450(2001)040<1413:DATAEL>2.0.CO;2.

[19] J. Moral-Carcedo, J. Vicéns-Otero, Modelling the non-linear response of Spanish electricity demand to temperature variations, Energy Economics 27 (3) (2005) 477–494. doi:10.1016/j.eneco.2005.01.003.

[20] M. Bessec, J. Fouquau, The non-linear link between electricity consumption and temperature in Europe: A threshold panel approach, Energy Economics 30 (5) (2008) 2705–2721. doi:10.1016/j.eneco.2008.02.003.

[21] A. Afram, F. Janabi-Sharifi, Review of modeling methods for HVAC systems, Applied Thermal Engineering 67 (1-2) (2014) 507–519. doi:10.1016/j.applthermaleng.2014.03.055.

[22] M. S. Al-Homoud, Computer-aided building energy analysis techniques, Building and Environment 36 (4) (2001) 421–433. doi:10.1016/S0360-1323(00)00026-3.

[23] D. B. Crawley, J. W. Hand, M. Kummert, B. T. Griffith, Contrasting the capabilities of building energy performance simulation programs, Building and Environment 43 (4) (2008) 661–673. arXiv:0812.0143v2, doi:10.1016/j.buildenv.2006.10.027.

[24] T. D. Pettersen, Variation of energy consumption in dwellings due to climate, building and inhabitants, Energy and Buildings 21 (3) (1994) 209–218. doi:10.1016/0378-7788(94)90036-1.

[25] L. G. Swan, V. I. Ugursal, Modeling of end-use energy consumption in the residential sector: A review of modeling techniques, Renewable and Sustainable Energy Reviews 13 (8) (2009) 1819–1835. doi:10.1016/j.rser.2008.09.033.

[26] I. Richardson, M. Thomson, D. Infield, A high-resolution domestic building occupancy model for energy demand simulations, Energy and Buildings 40 (8) (2008) 1560–1566. doi:10.1016/j.enbuild.2008.02.006.

[27] I. Richardson, M. Thomson, D. Infield, A. Delahunty, Domestic lighting: A high-resolution energy demand model, Energy and Buildings 41 (7) (2009) 781–789. doi:10.1016/j.enbuild.2009.02.010.

[28] I. Richardson, M. Thomson, D. Infield, C. Clifford, Domestic electricity use: A high-resolution energy demand model, Energy and Buildings 42 (10) (2010) 1878–1887. doi:10.1016/j.enbuild.2010.05.023.

[29] E. McKenna, M. Thomson, High-resolution stochastic integrated thermal-electrical domestic demand model, Applied Energy 165 (2016) 445–461. doi:10.1016/j.apenergy.2015.12.089.

[30] J. Widén, M. Lundh, I. Vassileva, E. Dahlquist, K. Ellegård, E. Wäckelgård, Constructing load profiles for household electricity and hot water from time-use data-Modelling approach and validation, Energy and Buildings 41 (7) (2009) 753–768. doi:10.1016/j.enbuild.2009.02.013.

[31] J. Widén, E. Wäckelgård, A high-resolution stochastic model of domestic activity patterns and electricity demand, Applied Energy 87 (6) (2010) 1880–1892. doi:10.1016/j.apenergy.2009.11.006.

[32] E. J. Palacios-Garcia, A. Chen, I. Santiago, F. J. Bellido-Outeiriño, J. M. Flores-Arias, A. Moreno-Munoz, Stochastic model for lighting's electricity consumption in the residential sector. Impact of energy saving actions, Energy and Buildings 89 (2015) 245–259. doi:10.1016/j.enbuild.2014.12.028.

[33] National Statistics Institute of Spain. Ministry of Economy and Competitiveness, Time Use Survey (2010). URL: http://www.ine.es/en/prensa/eet_prensa_en.htm

[34] W. R. Gilks, S. Richardson, D. J. Spiegelhalter, Markov Chain Monte Carlo in Practice, Technometrics 39 (3) (1997) 338. doi:10.2307/1271145.

[35] D. Gamerman, L. Hedibert, Markov Chain Monte Carlo: Stochastic Simulation for Bayesian Inference, Vol. 1, Chapmand and Hall, 2006.

[36] D. J. Sailor, Relating residential and commercial sector electricity loads to climate - Evaluating state level sensitivities and vulnerabilities, Energy 26 (2001) 645–657. doi:10.1016/S0360-5442(01)00023-8.

[37] C. Giannakopoulos, B. E. Psiloglou, Trends in energy load demand for Athens, Greece: Weather and non-weather related factors, Climate Research 31 (1) (2006) 97–108. doi:10.3354/cr031097.

[38] H. Sarak, A. Satman, The degree-day method to estimate the residential heating natural gas consumption in Turkey: A case study, Energy 28 (9) (2003) 929–939. doi:10.1016/S0360-5442(03)00035-5.

[39] J. H. Eto, On using degree-days to account for the effects of weather on annual energy use in office buildings, Energy and Buildings 12 (2) (1988) 113–127. doi:10.1016/0378-7788(88)90073-4.

[40] State Meteorological Agency (AEMET). Spanish Government., AEMET OpenData (2017). URL: http://www.aemet.es/en/datos_abiertos/AEMET_OpenData

[41] Red Eléctrica de España Co., Red Eléctrica de España (2017). URL: http://www.ree.es/en

[42] T. Teräsvirta, Specification, estimation, and evaluation of smooth transition autoregressive models, Journal of the American Statistical Association 89 (425) (1994) 208–218. doi:10.1080/01621459.1994.10476462.

[43] National Statistics Institute of Spain. Ministry of Economy and Competitiveness, Survey on households and the environment 2008 (2008). URL: http://www.ine.es/dyngs/INEbase/en/operacion.htm?c=Estadistica_C&cid=1254736176950&menu=resultados&idp=1254735976601

[44] S. J. Smullin, Thermostat metrics derived from HVAC cycling data for targeted utility efficiency programs, Energy and Buildings 117 (2016) 176–184. doi:10.1016/j.enbuild.2016.02.018.

[45] Daikin, Daikin (2015). URL: http://www.daikinac.com/

[46] Carrier, Home Heating & Cooling Products (2015). URL: http://www.carrier.com/homecomfort/en/us/products/heating-and-cooling/

[47] Fujitsu, Cooling Products (2015). URL: http://www.fujitsu-general.com/eu/products/

[48] Dimplex, Domestic Heating Products (2015). URL: http://www.dimplex.co.uk/products/domestic_heating/portable_heating/index.htm

[49] R. Stamminger, Synergy Potential of Smart Appliances. D2.3 of WP2 from the Smart-A project (2008). URL: http://smart-a.org/WP2_D_2_3_Synergy_Potential_of_Smart_Appliances.pdf

[50] ENTRANZE project, Heating and cooling energy demand and loads for building types in different countries of the EU (2014). URL: http://www.entranze.eu/

[51] U. S. Energy Information Administration, Residential Energy Consumption Survey (RECS) (2009). URL: http://www.eia.gov/consumption/residential/data/2009/

[52] A. de Almeida, P. Fonseca, R. Bandairinha, T. Fernandes, R. Araújo, U. Nunes, M. Dupret, J. Zimmermann, B. Schlomann, E. Gruber, REMODECE-Residential monitoring to decrease energy use and carbon emissions in Europe, Tech. rep., University of Coimbra (2008).

[53] C. Kuster, Y. Rezgui, M. Mourshed, Electrical load forecasting models: A critical systematic review, Sustainable Cities and Society 35 (July) (2017) 257–270. doi:10.1016/j.scs.2017.08.009.

[54] W. Ma, S. Fang, G. Liu, R. Zhou, Modeling of district load forecasting for distributed energy system, Applied Energy 204 (2017) 181–205. doi:10.1016/j.apenergy.2017.07.009.

[55] Y. H. Hsiao, Household electricity demand forecast based on context information and user daily schedule analysis from meter data, IEEE Transactions on Industrial Informatics 11 (1) (2015) 33–43. doi:10.1109/TII.2014.2363584.

[56] S. Jurado, À. Nebot, F. Mugica, N. Avellana, Hybrid methodologies for electricity load forecasting: Entropy-based feature selection with machine learning and soft computing techniques, Energy 86 (2015) 276–291. doi:10.1016/j.energy.2015.04.039.

[57] X. Li, J. Wen, E. W. Bai, Developing a whole building cooling energy forecasting model for on-line operation optimization using proactive system identification, Applied Energy 164 (2016) 69–88. doi:10.1016/j.apenergy.2015.12.002.

[58] R. Platon, V. R. Dehkordi, J. Martel, Hourly prediction of a building's electricity consumption using case-based reasoning, artificial neural networks and principal component analysis, Energy and Buildings 92 (2015) 10–18. doi:10.1016/j.enbuild.2015.01.047.

[59] J. Massana, C. Pous, L. Burgas, J. Melendez, J. Colomer, Short-term load forecasting in a non-residential building contrasting models and attributes, Energy and Buildings 92 (2015) 322–330. doi:10.1016/j.enbuild.2015.02.007.

[60] D. Fischer, A. Härtl, B. Wille-Haussmann, Model for electric load profiles with high time resolution for German households, Energy and Buildings 92 (2015) 170–179. doi:10.1016/j.enbuild.2015.01.058.

5

Stochastic modelling of appliances consumption in the residential sector: The impact of demand response strategies based on consumers' acceptance

Emilio J. Palacios-Garcia[1], Antonio Moreno-Munoz[1], Isabel Santiago[1], Jose Maria Flores-Arias[1], and Francisco J. Bellido-Outeiriño[1]

[1]Departamento de Arquitectura de Computadores, Electrónica y Tecnología Electrónica, Escuela Politécnica Superior, Universidad de Córdoba, Córdoba, Spain.

Abstract

The consumption of electrical appliances in the residential sector accounts for more than half the demand of a single household. This consumption is related to the users' behaviour and, therefore, non-easily predictable and difficult to model. Nevertheless, its significance among the total consumption and the current trend of energy efficiency and saving make it study worthy, especially for the implementation of demand response (DR) strategies aiming to directly control the consumption patterns of some appliances or energy policies that prevent unnecessary demands. Stochastic modelling techniques and the bottom-up methodology can be regarded as the main alternative, estimating the aggregated consumption based on the individual devices demands together with low-level influence parameters such as the occupancy profiles, subsequently, simulating the users' random behaviour. Thus, the aim of this paper is to develop a high temporal resolution simulation system that models each individual appliance influenced by the residents' occupancy patterns and to employ it for the assessment of DR strategies and energy policies, whereas considering the willingness of the users to accept them. The results have shown the close relationship between users' activity and demand peaks and how the individual DR measures can drive to significant aggregate energy savings.

The paper has been submitted to *Energy & Buildings* 2017.

5.1 Introduction

Appliances consumption represents a significant percentage of the total electrical demand in the residential sector, accounting for half of the electrical demand of a single household [1]. At the same time, the residential sector represents around 30% of the total electricity demand in European countries [2]. This consumption is the result of a great variety of individual demands which are difficult to characterise and separate from the whole figures and which have increased in the last years. This increment has been especially influenced by the usage of new technological equipment as well as the major comfort demanded by the users [3].

This increase has both environmental and economic consequences such as more emissions, higher cost for end consumers and larger investment in network infrastructures in order to cope with the total demand. Therefore, different measures and energy policies are being taken and implemented aiming to reduce or minimise the impact of this consumption [4].

From these measures, those denoted as demand response (DR) strategies should be highlighted, which seek to modify the consumption patterns of the end consumer to improve the interaction with the electrical generation [5]. From the consumers point of view, these strategies might help them to take advantage of lower energy costs such as those promoted by the time of use (TOU) tariffs, which encourage the consumption during off-peak hours by means of cheaper energy [6]. In the same way, in the new context of distributed energy resources (DER) integration, the utilisation of renewable resources can be maximised by coordinating the DR strategies with the energy management system (EMS) [7]. Moreover, from the perspective of the DSO, DR strategies can also be employed for improving the planning of the system [8, 9].

A myriad of DR algorithms can be found in the literature ranging from the classical linear programming optimisation [10] to heuristic methods [11], multi-objective systems [12], or multi-agent system [13]. Nevertheless, every DR strategy has two remarkable features, (i) they are driven by one or more elements that allow fulfilling certain objectives such as variable energy prices, integration of DER, etc. and (ii), they have a direct impact on the comfort of the residents since their main working operation is the modification of the behaviour, leading in some cases to the rejection of them and eventually to lower savings than expected [14].

Due to this fact, the first element that must be characterised in order to efficiently evaluate these measures is the consumers' behaviour, treating each end consumption separately [15], instead of the aggregate figures [16]. This will not only allow to analyse the potential improvement and DR strategies that might be carried out, but also the consequences of implementing them. Nevertheless, the extensive ecosystem of domestic appliances installed in each household, as well as the chaotic interaction of the consumers with them make it difficult to have an accurate and general prediction of the behaviour [17]. Moreover, since these measures aim to modify the consumers' habits on a daily basis, a high temporal resolution is needed to observe and assess the results [18].

In this context, the bottom-up consumption modelling techniques can be denoted as the best alternative to deal with this issue [19, 20]. These models are characterised by obtaining the total consumption as the aggregation of low-level consumer entities such as a sole appliance. Starting from a single device and aggregating them for a house, a cluster of household or a region, more complex estimation can be obtained [21]. Nevertheless, since every device is simulated individually, the random behaviour of the users is always considered. What is more, the low-level simulation of each device allows for the analysis of the impact on the demand that the individual modification of the consumption habits might have, by implementing them in each household or even appliance [22].

The validity of these simulation and modelling techniques has been shown in previous works. Richardson *et al.* implemented an occupancy model [23] and later used it as the base for a lighting consumption model [24] and an appliance demand model [25] for the UK. Likewise, Widén *et al.* developed a consumption model for Sweden [26, 27], but instead of using the active occupancy of the consumer as the input parameter, the consumption state and activity of the residents were directly modelled. In the USA, Muratori *et al.* [21] also developed a bottom-up model which combines physical-based approach with activity patterns in order to model the total household consumption. Moreover, works that combine different types of energy sources

can be found in the literature such as Good *et al.* [28] development, where electricity, heat and gas were simultaneously studied for some selected appliances in combination with space heating and hot water, or McKenna and Thomson [29] work that models lighting, appliances and hot water demand.

In line with these developments, authors also implemented and validated an active occupancy model [30] for Spain and used it in a lighting consumption model [31] which also allowed evaluating the impact of LED replacement at households. In the same way, a stochastic simulation approach was used for studying the impact of electricity supplied heating and cooling on the grid [32]. Moreover, a more complex implementation of the system was already employed in the assessment of DER interaction [33], having set the methodological base in a previous related work [34]. Therefore, this work aims to complete the whole simulation and assessment tool with the integration of appliances consumption.

All these studies implemented stochastic models with a high-temporal resolution and having to a greater or a lesser extent disaggregate result of appliances or groups of appliances. However, the potential of combining these models with DR strategies and the simulation of its consequences have never been explored. Therefore, the objective of this paper is the implementation of a high temporal resolution appliance consumption model based on a bottom-up methodology. This model will extend the range of individually simulated appliances as well as the details of their operation curve, being flexible enough so it can be used in the implementation and evaluation of DR strategies. Moreover, it will be combined with optimisation algorithms in order to implement effective DR actions in the individual user level being able to include different levels of acceptance as it may occur in a real context.

The model was implemented for Spain due to its interesting position in the DR field, where despite being one of the first countries to establish a dynamic daily energy price by means of the so-called voluntary price for the small consumer in April 2014 [35, 36], the DR programs are limited to the industrial sector [37, 38]. Nevertheless, the model can easily be adapted to any other location by following the proposed methodology, providing the necessary input data are available for the region. The results of the model were validated and compared with previous works. Likewise, three DR strategies were implemented and analysed, which were based on (i) TOU pricing schemes, (ii) peak shaving strategies, and (iii) DER matching for PV production, as well as an energy policy (iv) of standby consumption reduction. The results showed the potential of these measures for improving the demand and promote energy savings and the impact that the user acceptance can have on the final usefulness of them.

This development is described using the following structure. In Section 5.2, the methodology for implementing and simulating the model is addressed together with the DR strategies and the energy policies that are assessed. Then, in Section 5.3, the results are presented, first showing the flexibility of the system due to its distributed implementation and subsequently describing the simulation results, the validation of them by comparing the daily patterns with previously published works that used the same methods and, finally, analysing the DR response strategies in a selected scenario that represents an average consumer cluster. Section 5.4 is devoted to the conclusions of the work.

5.2 Methods

The methodology consists of three parts. First, the different parameters and datasets which are necessary and take part in the modelling process are described. Then, the simulation algorithm is addressed taking into account additional aspects such as the system initialisation or the calibration procedure. Finally, the DR strategies and the methodology followed in their implementation is explained.

5.2.1 Parameters and data

The appliances consumption model relies upon three basic datasets which are essential to carry out the algorithmic process. These data are the occupancy profile of each household to be simulated, the activities

performed by the occupants along the day, and the appliances available in each household. These elements are addressed in the following subsections.

5.2.1.1 Active occupancy in households

The active occupancy of a household is the main indicator that allows determining the periods of the day with the highest concentration of electrical consumption. Except for some appliances such as refrigerators or freezers that work continuously, the rest of equipment that might be found in a household requires the direct intervention of the occupants in the switch on/off processes.

This idea was already presented in previous works whose main objective was the development of occupancy models for the residential sector. Among these works, those carried out by Richardson *et al.* [23] or Widén *et al.* [27] can be pointed out. In their models, the Markov Chains methodology was employed to simulated the active occupancy and its relationship with the energy consumption in the UK and Sweden respectively. Likewise, in the context of Spain, similar works can be found, some of them implemented by the authors [30].

All of these works are based on the Time Use Surveys (TUS) [39], carried out in most European countries and which have been homogenised under the project HETUS. The surveys include 10-minute resolution information regarding the activities performed by the interviewees during a day, where they took place and whether they performed them individually or someone accompanied them. In Spain, that survey comprised 19,295 individuals, dwelling in 9,541 different households.

By using this information, the transition matrices for the non-homogenous Markov Chains simulation process [40] were obtained distinguishing between the number of residents in the household n_o (from 0 to 5), and the type of day d (weekday or weekend). In that way, for each case of input parameters, 144 transition matrices exist (one for each 10-minute interval in 24 hours) which allow for the calculation of the next occupancy state based on the current one. Likewise, for each 10-minute interval, the discrete probability distribution function (PDF) of active occupants was also obtained for initialisation purposes.

5.2.1.2 Activity of the occupants

The energy consumption that take place in a household has an end purpose that can be categorised and classified according to certain daily activities. Therefore, not only the active occupancy influences the consumption and the periods of time when it is located, but the activities performed by the residents also determine the appliances that are likely to be used for achieving this purpose [22].

As above mentioned, the TUS includes information regarding the activities carried out at home by the interviewees each one assigned with a normalised response code. From all the possible activities included in the survey, the ones selected for this study and their associated fields in brackets are personal care (31,39), cooking (311), doing the laundry (331), cleaning (321,322), ironing (332), watching the TV (821,829), using the phone (514), hearing the radio or HiFi system (831, 832, 839) and using the PC (an individual field is used for this activity).

Using these fields, the probability $P_\alpha(t_{10\text{min}}|n_o, \alpha, d)$ that from a certain number of active occupants n_o at least one of them is carrying out the activity α at the time interval $t_{10\text{min}}$ within the 144 periods of 10 minutes of the model $T_{10\text{min}}$ and the type of day d can be calculated according to (5.1).

$$P_\alpha(t_{10\text{min}}|n_o, \alpha, d) = \frac{N_\alpha(t_{10\text{min}}, n_o, \alpha, d)}{N_o(t_{10\text{min}}, n, d)}, \qquad \forall t_{10\text{min}} \in T_{10\text{min}} \tag{5.1}$$

In this equation, the denominator $N_o(t_{10\text{min}}, n, d)$ represents the sum of households in the TUS survey H_s^{TUS} from the total number included in it N_s^{TUS} where the number of occupants for that interval and house $o^{\text{TUS}}(t_{10\text{min}}|d)$ is equal to a given number of active occupants n_o for a certain type of day d as indicated in (5.2).

Table 5.1: Example of calculation of the activity probability.

			α = Cooking, d = weekday				α = Laundry, d = weekday			
	$N_o(t_{10\text{min}}, n_o)$		$N_\alpha(t_{10\text{min}}, n_o)$		$P_\alpha(t_{10\text{min}}\|n_o)$		$N_\alpha(t_{10\text{min}}, n_o)$		$P_\alpha(t_{10\text{min}}\|n_o)$	
$t_{10\text{min}}\|n_o$	**1**	**2**	**1**	**2**	**1**	**2**	**1**	**2**	**1**	**2**
00:00 h	1876	2488	5	5	0.0027	0.0020	2	3	0.0011	0.0012
14:00 h	2344	1490	533	363	0.2274	0.2436	24	19	0.0102	0.0128
22:00 h	1970	2313	101	133	0.0513	0.0575	10	23	0.0051	0.0099

$$N_o(t_{10\text{min}}, n_o, d) = \sum_{s=1}^{N_s^{\text{TUS}}} H_s^{\text{TUS}} \left[o^{\text{TUS}}(t_{10\text{min}}|d) = n_o \right], \quad \forall t_{10\text{min}} \in T_{10\text{min}} \tag{5.2}$$

On the other hand, the numerator $N_\alpha(t_{10\text{min}}, n_o, \alpha, d)$ is the total number of households where from the n_o active occupants for the time instant $t_{10\text{min}}$, at least one of them is performing the activity α, as stated in (5.3).

$$N_\alpha(t_{10\text{min}}, n_o, \alpha, d) = \sum_{s=1}^{N_s^{\text{TUS}}} H_s^{\text{TUS}} \left[o^{\text{TUS}}(t_{10\text{min}}|\alpha, d) \geq 1 | o^{\text{TUS}}(t_{10\text{min}}|d) = n_o \right], \quad \forall t_{10\text{min}} \in T_{10\text{min}} \tag{5.3}$$

An example of this calculation is indicated in Table 5.1. In particular, the probabilities for the activities cooking and laundry are calculated for three different instants of time in a weekday and for households with 1 and 2 active residents.

As it can be observed, the denominator N_o remains constant for all the activities since it only depends on the active occupants for that instant. The numerator N_α, however, changes for each case. As a rule, the higher the number of active occupants, the more likely is for a certain activity to be carried out. In addition, the probability density differs for each type of activity and instant of time.

5.2.1.3 Appliances model

The activities indicate the behaviour of the residents, nevertheless, this behaviour has to be associated with a specific appliance. This process might be straightforward for some of them such as in the case of the activity 'ironing', which is directly linked to the appliance iron. However, in some other cases, the relationship includes a wide range of appliances. This is the case, for instance, of the activity 'cooking' for which a wide variety of appliances such as ovens, microwaves, electric stoves, etc can be employed. Subsequently, these appliances must be assigned with a probability of possession and use, as well as a model of operation that describes its power consumption profile.

Percentage of appliances of each type

The possession rate of a certain appliance primary depends on the region of study and it might even vary within the same country. In this case, although the model is flexible enough to be implemented in any location, the necessary data for the simulation were obtained from the Institute for diversification and saving of energy IDAE, specifically from the report [41] where a study of the domestic equipment distribution and consumption in Spain was performed. The characterisation of each appliance i is divided into two terms which are the probability of possessing a type of appliance $p_{app}(i)$ and the average number of devices that can be found in a household $\overline{E_{app}}(i)$.

First, the probabilities of a household having at least one type of appliance $p_{app}(i)$ was calculated. For that aim, from all the surveyed households N_s^{IDAE} the total sum of houses H_s^{IDAE} with one or more appliances of a type i were divided between the total number of households in the studied region. The employed expression can be seen in (5.4).

$$p_{app}(i) = \frac{\sum_{s=1}^{N_s} H_s^{\text{IDAE}}(i \geq 1)}{\sum_{s=1}^{N_s} H_s^{\text{IDAE}}} \tag{5.4}$$

Subsequently, the average number of appliances $\overline{E_{app}}(i)$ per household was determined by dividing the total number of devices in the survey between the number of houses having at least one appliance installed as indicated in (5.5).

$$\overline{E_{app}}(i) = \frac{\sum_{s=1}^{N_s^{\text{IDAE}}} i}{\sum_{s=1}^{N_s} H_s^{\text{IDAE}}(i \geq 1)} \tag{5.5}$$

The obtained values are included in Appendix A where the detailed data of each type of appliance are summarised. As it can be observed, in most of the cases, the average number of appliances of each type $\overline{E_{app}}(i)$ is one per household. Nevertheless, for the entertainment appliances, usually denoted as brown goods a multi-equipment takes places, meaning that various appliances of the same type are installed in a single house. This is the case of TVs, PCs or laptops whose average number of devices per households is larger than 1.

Modelling of each appliance type

The model is based on a bottom-up methodology, therefore, each of the previously mentioned appliances is modelled in a low level, having a given operation cycle. In this way, the final consumption of a single household is obtained as the sum of every individual device.

Three types of working cycles are defined for the appliances which can be observed in Figure 5.1. Type I with on and off events controlled by the users (solid black line); the Type II with a periodic operation, not controlled by the user, but usually by thermostat switches (solid grey line); and the Type III which is turned on by the users but operates without their intervention until a cycle is fulfilled (dashed black line).

The Type I includes most of the appliances that might be found in a household. These devices are turned on by the users and maintain this state for a cycle t_c until they are turned off, what happens usually after an

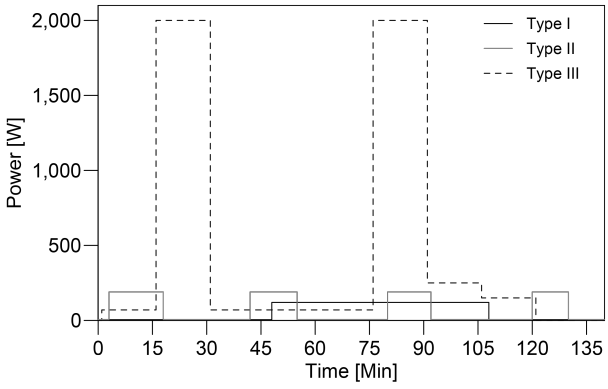

Figure 5.1: Modelling of the three types of working cycles for the appliances.

average operation type T_{on}. During this cycle, these appliances can consume a fixed power P_{on} or have a variable power cycle $P_{on}(c)$. The first ones have been denoted as Type Ia and their expression is indicated in (5.6), whereas the second ones, Type Ib are ruled by (5.7). Since they depend on the presence of the users, if at any time the instant occupancy $o(t)$ turns out to be zero, the appliance is switched off remaining in an inactive or standby status. Some of appliances included in the model having this cycle are TVs, PCs, laptops, irons, vacuum cleaners, ovens, microwaves, electric stoves, hairdryer, DVD, Modems.

$$P(t_c, o(t)) = \begin{cases} P_{on} & 0 < t_c \leq T_{on} \cap o(t) \neq 0 \\ P_{off} & t_c = 0 \end{cases} \tag{5.6}$$

$$P(t_c, o(t)) = \begin{cases} P_{on}(1) & 0 < t_c \leq T_{on}(1) \cap o(t) \neq 0 \\ P_{on}(2) & T_{on}(1) < t_c \leq T_{on}(2) \cap o(t) \neq 0 \\ \vdots & \\ P_{on}(c) & T_{on}(c-1) < t_c \leq T_{on}(c) \cap o(t) \neq 0 \\ P_{off} & t_c = 0 \end{cases} \tag{5.7}$$

Type II comprises those appliances which are continuously connected and perform a periodic working cycle. Generally, the appliances that have this operation are those devoted to food preservation such as refrigerators or freezers. These appliances have an active cycle t_c and an inactive or delay cycle t_d where they consume a P_{on} or P_{off} power respectively. These powers are maintained for an average T_{on} and T_{off} as indicated in (5.8). Nevertheless, these average working periods might be altered by external events such as door openings or extreme external weather conditions.

$$P(t_c, t_d) = \begin{cases} P_{on} & 0 < t_c \leq T_{on} \\ P_{off} & 0 < t_d \leq T_{off} \end{cases} \tag{5.8}$$

Finally, Type III includes all those appliances that only require the intervention of the user when they are turned on, but after that, they operate autonomously until they complete a certain cycle. In most of the cases, they have a variable power cycle, so their behaviour is similar to the Type Ib, but without the dependence on the active occupancy for their operation as it can be seen in (5.9). The appliances defined in this group are dishwashers, washing machines, tumble dryers, and washer dryers.

$$P(t_c) = \begin{cases} P_{on}(1) & 0 < t_c \leq T_{on}(1) \\ P_{on}(2) & T_{on}(1) < t_c \leq T_{on}(2) \\ \vdots & \\ P_{on}(c) & T_{on}(c-1) < t_c \leq T_{on}(c) \\ P_{off} & t_c = 0 \end{cases} \tag{5.9}$$

The operation cycles of the appliances were obtained from a previous work, the Smart-A project where a submetering campaign of the most installed equipment was carried out [42]. These data were combined with the previously mentioned regional report published by the IDAE from where additional information regarding the operational power and times of some other appliances was extracted.

5.2.2 Simulation methodology

The simulation algorithm is composed of two main stages. First, an initialisation process takes place, which determines the base state of the occupants, and appliances. This action is performed only once for each household to be simulated. After this, the system iterates over each house and set of appliances for each

minute of the day. The details of the whole algorithm are subsequently discussed together with the calibration technique that adjusts the annual energy figures provided by the model to the ones observed in the studied region.

5.2.2.1 Model initialisation

The initialisation process is performed for each household to be simulated. After loading the probability of possession and the different appliances included in the model for a given region, the number of devices of each type installed per household is determined by means of a stochastic procedure. For this aim, two random numbers r_i^h and a_i^h uniformly distributed between [0-1] are generated for each appliance type i in each household h. Subsequently, r_i^h are employed in an inverse sampling from the CDF P_{app} of having installed a certain type of appliance app_i, which follows a Bernoulli distribution $Be(p)$ with parameter $p = p_{app}(i)$, calculated as it was indicated in (5.4).

If this operation results in the possession of this type of appliance for the given house, the number of devices of this type is calculated for those case where a multi-equipment can appear. Therefore, for the appliances with a probability higher than 1, the number of devices is modelled as a normal distribution $N(\mu, \sigma)$ of mean $\overline{E_{app}}$ and standard deviation 1. From this CDF and using the previously generated random numbers a_i^h, an inverse sampling is performed. The result of this operation determines the final number of installed devices of each type N_i that might be higher than 1 in some cases or 0 in some others, accounting for the wide variety of casuistry that can be found in a real scenario.

Once the number and type of installed appliances per household have been assigned, their initial operation state is established. Nevertheless, for this aim, the occupancy state must be known. Therefore, the initial occupancy of each household is calculated with an inverse sampling in the CDF of active occupants P_0^{-1} for the initial instant of time t_0. This represents the initial occupancy for each household $o^h(t_0)$ and the first state of the Markov Chains algorithm.

Being known the occupancy in the instant t_0, the operational state of each appliance for that moment can also be established. This process is performed for each appliance app_i and household h by means of another stochastic algorithm hinging on the activity probability distribution for that instant of time $P_\alpha^{-1}(t_0|o^h(t), \alpha[app_i], d)$ associated with the initial occupancy $o^h(t_0)$ and linked activity $\alpha[app_i]$ in a given type of day d. The calibration scalar z_i is also taken into account for each appliance, whose significance will be explained in detail in Section 5.2.2.3.

After this stage, although the state of each device has been determined, the instant of the operation cycle, in which they are, still needs to be assigned. In order to calculate this, a weighting of the cycle is carried out by means of two random numbers uniformly distributed between [0-1] c_i^h and d_i^h generated for each appliance type i in each household h, which scale the active time t_c and inactive time t_d respectively.

With this last operation, the set of appliances in each dwelling, as well as the state of each one of them, have been assigned. Therefore, the following step is to calculate the rest of the occupancy profile which will be used as an input data for the iterative algorithm that calculates the consumption of each appliance and each household h. For that aim, the following states $o^h(t)$ after t_0 are calculated in 10-minute intervals using the previous occupancy state $o^h(t-1)$, which determines the row of the transition matrix P_{xy} that has to be considered for the next time interval. Subsequently, a random number $m^h(t)$ is used in an inverse sampling over the discrete cumulative distribution function created by the selected row x.

Finally, before entering in the iterative algorithm, the daily probability profile of each activity is recalculated if needed when DR strategies where selected. The optimisation algorithm and the calculation of the new activity probability curves for the households accepting this measure are discussed in the DR methodology in Section 5.2.3.

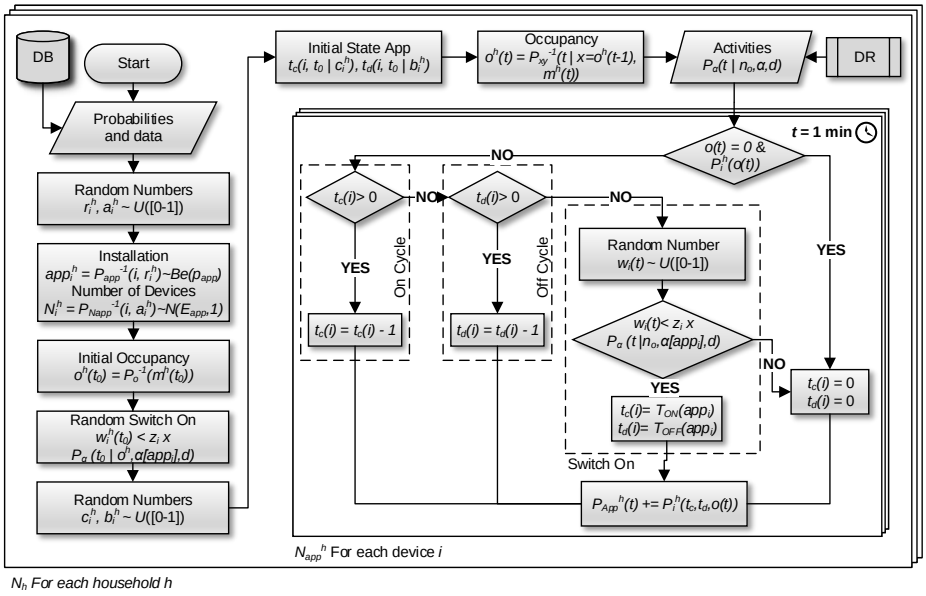

Figure 5.2: Flowchart of the algorithmic process.

5.2.2.2 Simulation algorithm

Right after the initialisation of each household, the individual simulation of each installed appliance app_i for each household h with 1-minute resolution is carried out. For this aim, the parameters stated in Section 5.2.1.3, the active cycle t_c, the on delay t_d, and the power $P(t_c, t_d, o(t))$, are evaluated. This higher temporal resolution is fully justified since, whereas the occupancy transitions take place at a relatively low pace, the switch on/off events have a higher frequency being even possible to activate and deactivate the same appliance within the same period of occupancy.

In this process, first, the active occupancy of the household $o^h(t)$ is checked. If the number of active occupants is null and the appliance type i depends upon the presence of the residents such as the Type I, it is turned off, meaning that both operation times t_c and t_d are established as zero. This causes that the output power accounted by the model $P(t_c, t_d, o(t))$ equals zero or the standby power depending on the type of appliance. On the contrary, if the occupancy is not equal to zero, the algorithm continues.

In this second step, and once it has been determined that the appliance type i either is not dependent on the occupancy such as Types II and III, or the occupancy is not null, the state of it is checked. If the device is active ($t_c > 0$) the on cycle is decreased and its active power P_{on} accounted for the total power consumed by the household $P_{App}^h(t)$. This power is fixed for appliances Types Ia and II, or variable for Type Ib and III. If the appliance is not active, but it belongs to the Type II and the on delay is not zero ($t_d > 0$), the delay time is decremented and the inactive power P_{off} added.

If after all these comparisons, both times t_c and t_d results to be zero, the appliance is in the inactive state and it should be checked if the conditions of occupancy $o^h(t)$ and activity probability P_α are suitable for its activation. In order to perform this operation, a random number $w_i(t)$ is generated for each instant of time and appliance i and subsequently compared with the activity probability function linked to this appliance for given number of active occupants n_o, associated activity α, type of day d and instant of time t, taking into consideration the appliance calibration scalar z_i. If the result of this logical test is the activation of the appliance, the on cycle is assigned as T_{on} and the delay time, if needed, as T_{off}.

5.2.2.3 Calibration

Due to the randomness of the simulation process, the energy consumption figures generated by the model for each appliance might not be coincident with the ones observed in the studied region. Thus, a calibration method is necessary. This process takes into account the average occupancy of the dwelling, the mean activity probability along the year and the appliances characteristics so an adequate average number of annual cycles according to the observed energy consumptions can be established.

To consume an annual energy E_{year} an appliance has to complete n_{cycles} average working cycles in which it will demand and average P_{on} power for an average T_{on} time and, if belonging to the type II, a mean P_{off} power for an average delay time T_{off}. The number of these cycles can be calculated as indicated in (5.10).

$$n_{\text{cycles}} = \frac{E_{\text{year}}}{T_{on} \cdot P_{on} + T_{off} \cdot P_{off}} \tag{5.10}$$

Nevertheless, the simulation algorithm establishes the switch on events with 1-minute resolution, therefore, the number of potential minutes in a year where a switch on event might occur has to be determined. For this aim, the total number of minutes where the appliance is operating is subtracted to the total number of minutes in a year scaled by the average probability of at least one resident being active during the year $\overline{P_{ocu}}$. From this operation, the total number of minutes in a year where a switch-on event for this appliance might occur T_{sw} is determined, as indicated in (5.11).

$$T_{sw} = (365 \cdot 1440) \cdot \overline{P_{ocu}} - \left(T_{on} + T_{off}\right) \cdot n_{\text{cycles}} \tag{5.11}$$

Finally, the scalar z is obtained as a result of distributing the start of these n_{cycles} within the available switch-on time in a year T_{sw}. In addition, it should be considered that each activity probability function has a different density, therefore, the average activity probability $\overline{P_\alpha}(\overline{n_o}, \alpha)$ for a given activity α and considering the mean occupancy of the year $\overline{n_o}$ has to be included in the denominator to equalise the influence of both the cycling of the appliance and the distribution of the activity throughout the day. The final expression can be seen in (5.12).

$$z = \frac{n_{cycles}}{T_{sw} \cdot \overline{P_\alpha}(\overline{n_o}, \alpha)} \tag{5.12}$$

Thus, after all this calibration process and the above-explained initialisation and simulation process the modelling of the appliance consumption is fully described. With this process, the 1-minute resolution profile of a N_h number of household can be determined having each one a given number of residents from 1 to 5, considering a certain type of day (weekday or weekend) and being able to obtain the aggregate load curve as well as the individual demand of a type of appliances, a house or an individual device. The next section, therefore, will be focused on the application of DR strategies over the simulation environment established by this model.

5.2.3 Demand response strategies

From the wide variety of DR techniques, moving the consumption of cyclic loads or load shifting, as it will be referred from now, is one of the most useful strategies in the domestic sector, due to its simplicity and minimum impact on the occupants' comfort [43]. This work is focused on the DR actions applied to shiftable loads, which are defined as those whose consumption is cyclic and well-known in both energy and duration, and that can be distributed within the day with a minimum impact on the dwelling habits. The appliances selected to be shiftable in this model where those belonging to Type III.

This load reallocation is performed by means of additional hardware and communication equipment, therefore, not all the users might be willing to adopt them. Moreover, the criteria for selecting the time periods where the loads are to be shifted might vary depending on the end goal. This section will present

the novel implementation of these DR strategies to assess different optimisation criteria while taking into account the acceptance of the users.

5.2.3.1 Global methodology for DR implementation

The main novelty of this methodology relies on the application of the DR strategies. The model allows simulating the individual behaviour of both residents and appliances in each household. Therefore, the shifting strategies can individually be implemented in the lowest level of the model in order to evaluate the impact on the aggregate figures. The calculation process consists of two steps.

First, since the individual results of a single house are randomly calculated, the possible DR strategies are extracted from the study of a cluster of households representing an average community in the region where the model was implemented. The selected number of households was 200 with the distribution of residents per house that can be observed in Table 5.2 which was extracted from the Household Budget survey carried out by the Spanish National Institute of Statistics [44]. Regarding the type of day, it is chosen depending on the given input parameters.

Once the periods of shifting are determined, the activity probability associated with these shiftable load is modified to emulate the action of an external control that will perform the switch on events over these appliances. This modification is not implemented in all the households, but an acceptance ratio was included so the impact of the gradual adoption of these measures can be studied.

Therefore, for a given cluster of households N_h each of them with N_{app} different types of appliances and using a 1-day temporal horizon, (1440 minutes), the aggregated consumption of the cluster $\sum_{h=0}^{N_h} P^h_{App}(t)$ will be equal to the sum of each individual consumption of each appliance $P^h_i(t)$ as indicated in (5.13).

$$\sum_{h=0}^{N_h} P^h_{App}(t) = \sum_{h=0}^{N_h} P^h_1(t) + P^h_2(t) + \cdots + P^h_i(t), \qquad \forall t \in T_{1\min}, i \in N_{app} \tag{5.13}$$

This expression can be rewritten dividing the appliances into two main groups. On the one hand, those that cannot be shifted since they will impact the comfort or the routines of the residents $\sum_{h=0}^{N_h} P^h_{fix}(t)$, which will be named as non-shiftable loads. On the other hand, the consumption of the appliances that have a shifting potential and whose operation cycle can be displaced along the day $\sum_{h=0}^{N_h} P^h_{shift}(t)$. Thus, (5.13) can be now expressed as in (5.14).

$$\sum_{h=0}^{N_h} P^h_{App}(t) = \sum_{h=0}^{N_h} P^h_{fix}(t) + P^h_{shift}(t), \qquad \forall t \in T_{1\min} \tag{5.14}$$

This shiftable power $P^h_{shift}(t)$ can be reallocated to a power $P^h_{DR}(t)$ representing the new profile if every household had adopted the DR strategy. Moreover, since it is only a reallocation of consumptions, the total daily energy will remain constant and so will do the aggregate shiftable power as indicated in (5.15).

Table 5.2: Distribution of households according to the number of residents in the studied country and in the sample cluster used in the model.

Number of residents	Houses in the country(%)	Number of houses in the model
1	25.30	51
2	30.33	61
3	20.97	42
4	17.64	35
5	5.76	11

$$\sum_{h=0}^{N_h} P_{DR}^{h}(t) = \sum_{h=0}^{N_h} P_{shift}^{h}(t), \qquad \forall t \in T_{1\text{min}} \tag{5.15}$$

However, the DR actions are taken individually in each household as previously mentioned, therefore, this power density $P_{DR}^{h}(t)$ cannot be directly used, but it has to be transformed into an activity probability function. Since the daily energy must remain constant, the total average activity probability must be equal too, before and after the redistribution of the probability density. To achieve that, this probability is redistributed in a newly modified activity probability within the day $P_{\alpha}^{DR}(t|\alpha)$ following the pattern of the new calculated $P_{DR}^{h}(t)$, using a weighted scaling as it is shown in (5.16).

$$P_{\alpha}^{DR}(t|\alpha) = \sum_{t=0}^{T} \overline{P_{\alpha}}(t|\overline{n_o}, \alpha, d) \cdot \frac{P_{DR}(t)}{\sum_{t=0}^{T} P_{shift}(t)}, \qquad \forall t \in T_{1\text{min}} \tag{5.16}$$

In addition, the initialisation and simulation processes are modified to account for the acceptance ratio of the users. In this way, during the initialisation of the appliances, and based on the selected acceptance ratio, each of the simulated households is assigned with a boolean flag Acc_{DR} which indicates if the residents have chosen to implement DR strategies. This flag is calculated by means of an inverse sampling with a uniformly distributed random number over the probability distribution function of implementing DR actions. This probability follows a Bernoulli distribution of parameter $p = p_{ACC}$, where p_{ACC} is the selected acceptance ratio. This is expressed in (5.17).

$$Acc_{DR}^{h} = P_{DR}^{-1}(r_{DR}^{h}) \tag{5.17}$$

If the residents have decided not to implement the DR strategies, the switch on process of the shiftable loads will be the previously exposed one, based on the activity probability distribution for a given number of active occupants, activity, type of day and time $P_{\alpha}(t|n_o, \alpha, d)$. Nevertheless, when the DR actions are accepted these appliances are ruled by the new distribution $P_{\alpha}^{DR}(t|\alpha)$ which only depends on the activity and the instant of time and it is calculated after one of optimisation process stated in sections 5.2.3.2 to 5.2.3.4. The new definition of the decision process for the switch on event is indicated now in (5.18).

$$\begin{cases} w_i < z_i \cdot P_{\alpha}(t|n_o, \alpha, d) & Acc_{DR} = 0 \\ w_i < z_i \cdot P_{\alpha}^{DR}(t|\alpha) & Acc_{DR} = 1 \end{cases} \tag{5.18}$$

5.2.3.2 Day-ahead pricing

The first optimisation process is based on the energy price. In the current context, some new methods for billing energy such as TOU tariffs or RTP have appeared [36]. This means that the cost of 1 kWh of energy varies within the day and it might sometimes be known by the user on a day-ahead basis. As a general rule, these tariffs tend to promote the consumption during off-peak hours, whereas penalising the energy demand during peak hours. Therefore, given a certain prices profile $c(t)$ and an available amount of shiftable energy $E_{shift}(t)$ the distribution of the newly allocated $E_{DR}(t)$ that minimise the cost can be obtained according to the linear programming problem stated in (5.19).

$$\begin{aligned} \text{minimise} \quad & \sum_{t=0}^{T} c(t_{30\text{min}}) \cdot E_D(t_{30\text{min}}) \\ \text{subject to} \quad & \sum_{t=0}^{T} E_{DR}(t_{30\text{min}}) = \sum_{t=0}^{T} E_{shift}(t_{30\text{min}}) \\ & E_D(t_{30\text{min}}) - E_{DR}(t_{30\text{min}}) = E_{fix}(t_{30\text{min}}), \qquad \forall t_{30\text{min}} \in T_{30\text{min}} \\ & E_D(t_{30\text{min}}) \leq E_{\text{Max}}, \qquad \forall t_{30\text{min}} \in T_{30\text{min}} \end{aligned} \tag{5.19}$$

As it can be observed, the optimisation is carried out with a 30-minute granularity. Taking into account that the prices usually vary on an hourly basis, this temporal resolution is more than enough in this case. The different 30-minute energy figures in this and the following cases will be obtained by aggregating the 1-minute resolution power as in (5.20).

$$E_x(t_{30\text{min}}) = \sum_{t=t_{1\text{min}}}^{t_{1\text{min}}+30} \frac{P_x(t_{1\text{min}})}{30} \tag{5.20}$$

5.2.3.3 Peak shaving

The second criterion was the peak demand shaving, minimising the variability of the load curve along the day. This presents advantages from the DSO point of view since the consumption is more predictable and static so the generation resources can be scheduled more effectively. Although some of the previously presented tariffs indirectly aim for this, this study has been implemented independently to observe the differences. The linear programming problem can be stated now as in (5.21).

$$\begin{aligned}
\text{minimise} \quad & \sum_{t=0}^{T} \Delta E_D^{Abs}(t_{30\text{min}}) \\
\text{subject to} \quad & \sum_{t=0}^{T} E_{DR}(t_{30\text{min}}) = \sum_{t=0}^{T} E_{shift}(t_{30\text{min}}) \\
& E_D(t_{30\text{min}}) - E_{DR}(t_{30\text{min}}) = E_{fix}(t_{30\text{min}}), \quad \forall t_{30\text{min}} \in T_{30\text{min}} \\
& E_D(t_{30\text{min}}) \leq E_{\text{Max}}, \quad \forall t_{30\text{min}} \in T_{30\text{min}} \\
& E_D(t_{30\text{min}}) - E_D(t_{30\text{min}} - 1) = \Delta E_D^{+}(t_{30\text{min}}) - \Delta E_D^{-}(t_{30\text{min}}), \quad \forall t_{30\text{min}} \in T_{30\text{min}} \neq 0 \\
& \Delta E_D^{Abs}(t_{30\text{min}}) = \Delta E_D^{+}(t_{30\text{min}}) + \Delta E_D^{-}(t_{30\text{min}}), \quad \forall t_{30\text{min}} \in T_{30\text{min}} \neq 0
\end{aligned} \tag{5.21}$$

As it can be seen in (5.21) the objective of this system is the minimisation of the absolute energy gradient ΔE_D^{Abs} using again a 30-minute resolution. Since the function to calculate the absolute value is nonlinear, two auxiliary variables strictly positive ΔE_D^{+} and ΔE_D^{-} where used to account for the positive and the negative changes keeping the system as a linear problem.

5.2.3.4 Renewable matching

Finally, in those households having installed any renewable energy resources (RES), a suitable option is to concentrate all these shiftable consumption in the hours with the highest generation so the degree of utilisation of the renewable energy source is also maximised. For that aim, the temporal coincidence of production and demand was studied by means of the supply cover factor proposed by [45] and employed in previous works [34, 46]. Its expression is indicated in (5.22), where $P_{DER}(t)$ is the renewable production of the DER and $P_D(t)$ is the user demand.

$$SCF = \frac{\sum_{t=0}^{T} \min(P_{DER}(t), P_D(t))}{\sum_{t=0}^{T} P_{DER}(t)} \tag{5.22}$$

The conceptual significance of this expression is the degree of utilisation, so the closer this value is to one, the more production is directly consumed in the household. If (5.22) is written in terms of 30-minute energy resolution, the optimisation problem can be sated as in (5.23), where the SCF is maximised in this case by the reallocation of the shiftable energy $E_{shift}(t)$ in new temporal periods as $E_{DR}(t)$.

$$
\begin{aligned}
\text{minimise} \quad & \frac{\sum_{t=0}^{T} E_{\text{Min}}(t_{30\text{min}})}{\sum_{t=0}^{T} E_{DER}(t_{30\text{min}})} \\
\text{subject to} \quad & \sum_{t=0}^{T} E_{DR}(t_{30\text{min}}) = \sum_{t=0}^{T} E_{shift}(t_{30\text{min}}) \\
& E_D(t_{30\text{min}}) - E_{DR}(t_{30\text{min}}) = E_{fix}(t_{30\text{min}}), \quad \forall t_{30\text{min}} \in T_{30\text{min}} \\
& E_D(t_{30\text{min}}) \leq E_{\text{Max}}, \quad \forall t_{30\text{min}} \in T_{30\text{min}} \\
& E_{\text{Min}}(t_{30\text{min}}) \leq E_D(t_{30\text{min}}), \quad \forall t_{30\text{min}} \in T_{30\text{min}} \\
& E_{\text{Min}}(t_{30\text{min}}) \leq E_{DER}(t_{30\text{min}}), \quad \forall t_{30\text{min}} \in T_{30\text{min}}
\end{aligned}
\tag{5.23}
$$

Since the minimum function employed in the calculation of the SCF is nonlinear, an auxiliary variable $E_{\text{Min}}(t_{30\text{min}})$ which takes only positive values was used together with the last two constraints to perform the same operation, but keeping the linearity of the system.

5.2.3.5 Standby reduction

An additional strategy not related to the shiftable loads but that can be included in the study to show the broad possibilities of the proposed model is the reduction of the standby consumption. Since every device is modelled with an associated P_{off} that in many cases corresponds with the standby operation, the impact of cutting this consumption during the inactive hours was also considered. The methodology employed in this case is far simpler than in the other cases and consists in the modification of the power equation of each appliance so if the DR action has been accepted, the inactive power equals to zero as stated in (5.24).

$$
P(t_c) = \begin{cases} P_{off} & t_c = 0 \cap Acc_{DR} = 0 \\ 0 & t_c = 0 \cap Acc_{DR} = 1 \end{cases}
\tag{5.24}
$$

These actions represent only a small sample of all the available strategies, nevertheless, they clearly illustrate the potential of the model for assessing future scenarios in the grid that might be impossible to implement if it was not by means of these tools. Moreover, they point out a new methodology for evaluating the global impact on the system of individual measures taken by the end users.

5.3 Results

The results obtained by applying the above-exposed methodology are divided into four parts. First, the implementation of the simulation system is described. After this, the main results are presented and discussed. Subsequently, the model consumption profiles are compared with a previous work in order to assess their validity. Finally, the application of the model for the assessment of the presented DR strategies is indicated, discussing the main results and implications.

5.3.1 Model implementation

The model has been implemented by means of the high-level object-oriented programming language JAVA. This language provided interconnectivity, database communication, and APIs with third-party software, as well as concurrent programming and interoperability between platforms and OS, which made it the most suitable option for our application.

As it can be observed in Figure 5.3 the system was divided into two main modules. On the left side, the simulation and data system is observed. This part was deployed on a JAVA EE server and it is accessible through a RESTful web service. The selected implementation implies flexibility and scalability of the resources depending on the computational load which might be very significant. On the right side of the same figure, the user application is shown. This general user interface (GUI) is the main tool for configuring

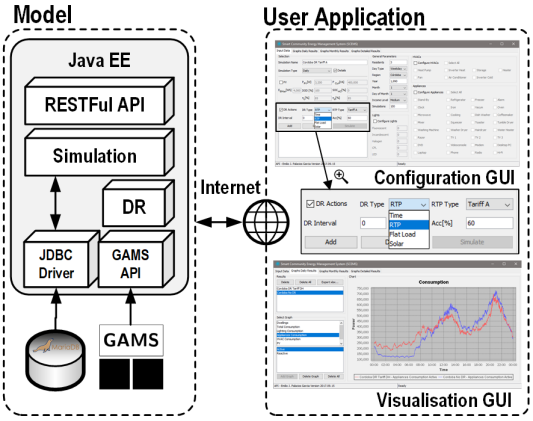

Figure 5.3: Conceptual implementation of the simulation system.

the simulation options, requesting the calculations to the server and retrieving the information for a suitable representation and storage in CSV and EXCEL files for further postprocessing. Nevertheless, it should also be pointed out that this GUI program was developed to ease the operation with the system according to our needs, however, thanks to the RESTful web service the system can be integrated into other third-party software such as MATLAB, LabVIEW or any programming tool implementing an HTTP communication.

Regarding the model itself, the deployment was divided into three functional blocks as it can also be observed in Figure 5.3. The simulation logic was integrated as part of the JAVA EE server. This logic interfaces with the database storage system, implemented with the MariaDB engine, by means of a JDBC (Java Database Connector) driver. In the optimisation side used for the DR strategies, the linear programming problems where coded and solved using the software GAMS whose intercommunication with the simulation logic was established by using the API provided by the manufacturer.

5.3.2 Model results

Using the previously exposed implementation different results were obtained. As indicated in the methodology section, the simulation system was implemented in Spain. Nevertheless, the model is flexible enough, so following the given guidelines it can be adapted to any other region with little effort, providing the necessary data are available.

5.3.2.1 Individual simulations

The basic block of the model is the simulation of an individual house with a given number of residents and for a type of day (weekday or weekend). This house has a certain number of appliances selected based on the possession rates observed in the region and which are individually simulated with 1-minute resolution. Therefore, these consumption profiles represent the chaotic behaviour of the residents with highly deterministic switch on/off events and pronounced spikiness.

This fact can be observed in Figure 5.4 where the daily profiles of two individual households of 3 residents for a weekday are represented. As it can be seen, the high temporal resolution (1-minute) allowed visualising details such as the thermostat cycles of refrigerators and freezers (during the whole day), as well as other high power demanding appliances such as the oven curve from 19:00 to 20:00 for household 2 or the stove for household 1, both characterised by the first preheating period and the thermostat cycles.

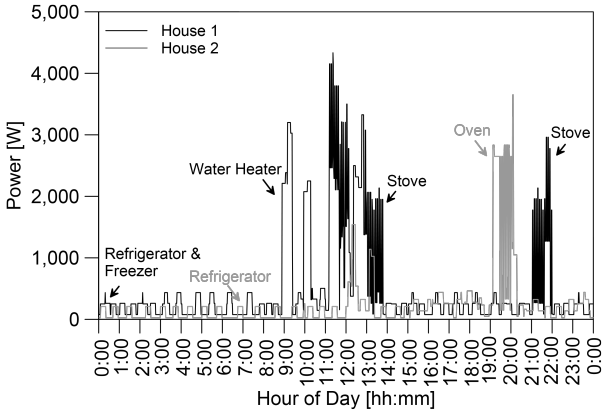

Figure 5.4: Consumption profile of 2 single households for one weekday.

5.3.2.2 Aggregate daily results

Although the individual profiles are essential to accurately simulate the low-level behaviour of each household, the information that they provide is extremely variable. Thus, if usage patterns are to be studied, an aggregate cluster of households must be considered to obtain significant results. In addition, not only the number of elements that are simulated can be extended, but also the temporal horizon, ranging from daily profiles to annual simulations while keeping the 1-minute resolution.

An example of these aggregate results can be observed in Figure 5.5 where 1,000 households for a weekday (solid black line) and a weekend (solid grey line) are represented. The aggregate profile showed two main consumption peaks which temporally matched the lunchtime in Spain (13:00 to 15:00h) and the dinner (20:30 – 22:30h). Likewise, two low-consumption areas took place, one during the night time due to the inactivity of the residents and other from 15:00 to 20:00h although with higher consumption figures. Regarding the differences between weekdays and weekends, it can be seen that the morning consumption was delayed around an hour during the weekend and the lunch peak presented a slighting higher value.

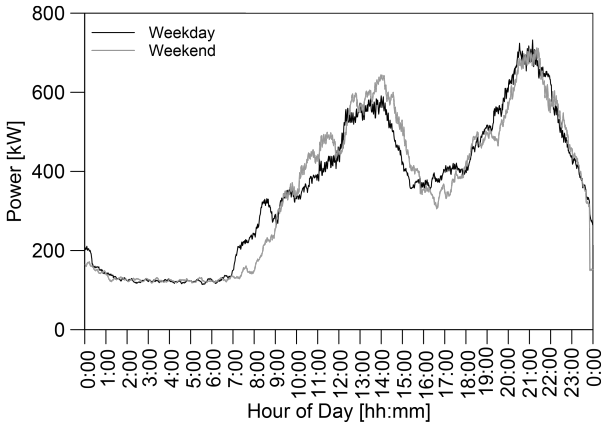

Figure 5.5: Aggregate daily simulation for 1,000 households.

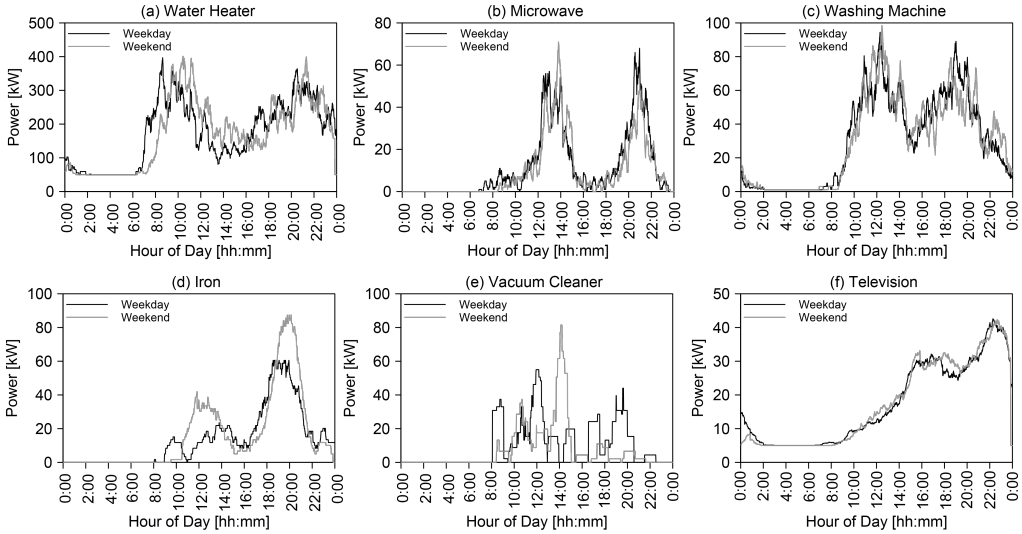

Figure 5.6: Aggregate results for 1,000 households. Selected appliances disaggregation.

Nevertheless, the possibilities of the proposed model are not limited to the aggregated load curve, but the pattern of each appliance can be individually observed. In this way, the devices with the major consumptions can be studied localising the hours of high demand and the possible energy policies to be taken.

This can be seen in Figure 5.6 where the aggregate consumption of 1,000 households for 6 selected appliances was represented distinguishing between weekdays (solid black lines) and weekends (solid grey lines). It can be observed, that each appliance presented a characteristic profile, which is not only related to the active occupancy but to the activities distribution within the day.

For the water heater (a), two consumption peaks were observed, one during the first hours of the morning and other during the night, beginning a few hours before the dinner time. It should also be pointed out that the morning peak was delayed 1 hour on the weekends. In the case of the microwave (b), its consumption was concentrated in the meals hours being almost zero during the rest of the day. For the washing machine (c), the major demand could be seen around mid-morning and mid-afternoon.

The same behaviour was observed for the iron (d) whose peaks were located in the same periods as the washing machine. However, the afternoon peak was almost three time the morning one. Moreover, in the weekend the iron demand was nearly twice as high as during the week. As far as the vacuum cleaner is concerned, its consumption was located in the central hours of the day and it was also higher for the weekend. Finally, regarding the TV usage, the major consumption peaks could be seen in the afternoon and after dinner. Likewise, the standby demand of this appliance produced a relatively significant consumption during the night hours.

Therefore, this model allowed us to study not only the aggregate consumption of each household but also the individual impact on it of each appliance. Moreover, this study can be carried out with different time horizon but keeping the 1-minute resolution.

5.3.3 Comparison with previous works

The validation process of the model is limited due to two main reasons. First, there is a lack of studies in the selected area and the main ones only took into account annual or daily figures which are not enough to validate the 1-minute resolution profiles. Second, a validation based on real consumption data extracted from smart

metering devices might not be accurate since this demand also includes lighting, heating, and cooling devices that are not considered in this appliances model and were studied separately in other works [31, 34]. Only a submetering campaign could solve this, nevertheless, no data were available to perform this comparison.

Therefore, in order to assess the accuracy of the proposed model without the complexity and time-consuming process of submetering, a direct comparison with a previous study was performed. The selected model was the one carried out by Richardson *et al.* [25]. This model was validated with submetered data from 22 households showing a good accuracy. The methodology employed in the proposed model is similar to the one used by Richardson *et al.*, although some differences should be pointed out such as the selected appliances, the modelling process of the devices, the inclusion of DR strategies, and probably the most important one, the location, since our model was implemented for Spain, whereas Richardson *et al.* model was applied to the UK. Nevertheless, taking into account the same operation principle, both models should present consistent results with the particularities of each location and simulation system.

The result of this comparison can be seen in Figure 5.7 where the aggregate result of 1,000 households with 3 residents for the proposed model (solid black line) and Richardson *et al.* model (solid grey line) are represented for a weekday (a) and a weekend day (b). As it can be observed, there are noticeable differences between both profiles, especially in the time periods where the consumption peaks are located. Nevertheless, the night consumption, as well as the average daily consumption figures are similar in both cases.

Therefore, the mismatch in the consumption peaks might be caused by different occupancy patterns. This assumption is backed up by the profiles observed in Figure 5.8 where the occupancy profile for the same aggregate of 1,000 households is illustrated. As can clearly be seen, the occupancy profiles differ for each region and follow a trend similar to the one observed in the consumption profile. Subsequently, although each profile has a different shape due to the schedules and users' behaviour in each country, the power figures are within the same range, being even coincident for those periods of similar occupancy.

The mean power consumption is 355 kW for the proposed model, whereas Richardson *et al.* model predicted 391 kW for a weekday. During the weekend, this model predicted 352 kW, which is lower than the 420 kW, predicted by Richardson *et al.* Nevertheless, if the occupancy profiles are observed, it can be noticed that the Spanish occupancy profile has almost the same shape and amplitude for weekdays and weekend. In contrast, the UK profiles differ greatly from weekdays, where the period from 09:00-15:00 h presents a very low occupancy, to the weekends, where the occupancy profile is almost similar to the Spanish one in the same period.

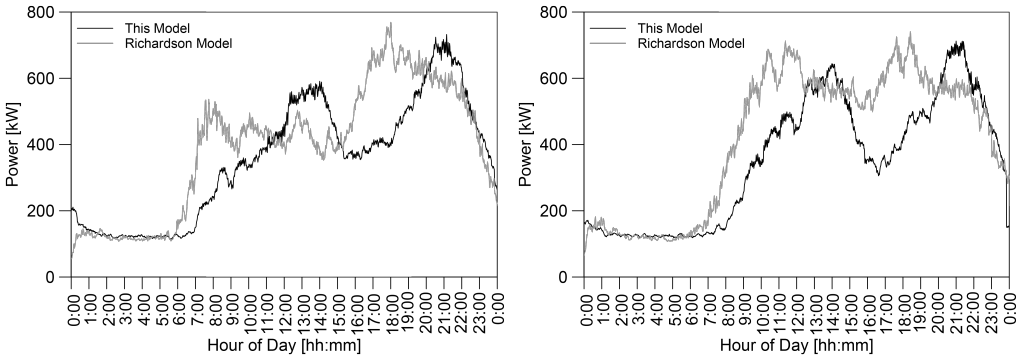

(a) Weekday **(b)** Weekend

Figure 5.7: Power consumption comparison between this model and Richardson *et al.* model for an aggregate of 1,000 households.

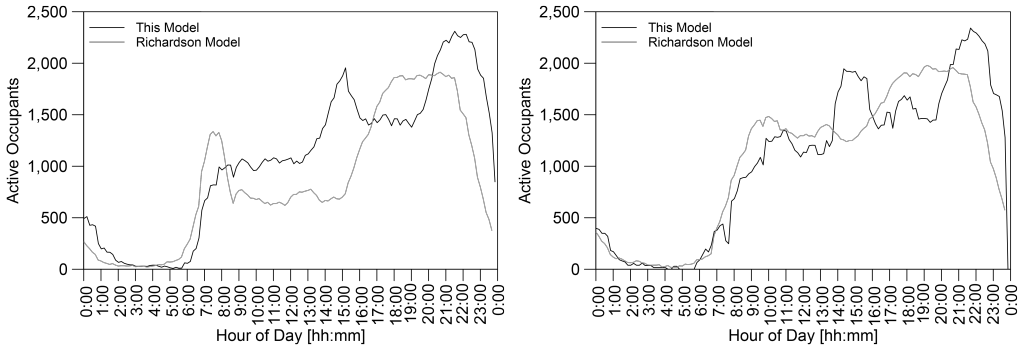

(a) Weekday **(b)** Weekend

Figure 5.8: Active occupancy comparison between this model and Richardson *et al.* model for an aggregate of 1,000 households.

Additional conclusions can be drawn if Table 5.3 is observed. In this table, the root mean square error (RMSE) and the normalised variation factor (NVF) were listed for the consumption and the occupancy profiles predicted by both models taking into account the different type of days. The RMSE is calculated as indicated in (5.25), where $P_M(t)$ is the instant power or occupancy predicted by the proposed model, $P_{Ref}(t)$ is the power or occupancy estimated by Richardson *et al.* model and n is the number of instants for a day, being 1440 in the case of the consumption and 144 for the occupancy.

$$\text{RMSE} = \sqrt{\frac{1}{n}\sum_{t=0}^{n}\left(P_M(t) - P_{Ref}(t)\right)^2} \tag{5.25}$$

As it can be seen in Table 5.3, for both types of days the RMSE is very similar in the case of the consumption. If we consider that the daily power span is around 600 kW, the obtained values are quite significant, nevertheless, as previously stated, the users' schedules vary greatly between the countries. For the occupancy profile, the RMSE values are also relatively large, presenting a higher error in the weekday case.

The second indicator, named as NVF is a pseudo-variance where the mean square error (MSE) is normalised by means of the average value of the reference sample, in this case, the Richardson *et al.* model estimations. Its expression can be seen in (5.26).

$$\text{NVF} = \frac{\text{MSE}}{\overline{P_{Ref}}^2} = \frac{\sum_{t=0}^{n}\left(P_M(t) - P_{Ref}(t)\right)^2}{n\left(\frac{1}{n}\sum_{t=0}^{n}P_{Ref}(t)\right)^2} \tag{5.26}$$

The results in Table 5.3 indicate that, although the total RMSE figures are significant, the instantaneous average variations between the values predicted by Richardson *et al.* and the ones estimated by this model

Table 5.3: RMSE and NVF values. Comparison between this model and Richardson *et al.* Model.

	Consumption		**Occupancy**	
	WD	**WE**	**WD**	**WE**
RMSE	123.5 kW	132.1 kW	510	374
NVF	0.0996	0.0989	0.3586	0.1283

are not very dispersed. Moreover, it depicted that the occupancy profiles present a higher instantaneous mismatch than the power consumption curve, for which the NVF values are around 0.10. Therefore, although with differences in the schedules, the estimations of both models are consistent.

5.3.4 DR strategies

As indicated in the methodology section, one of the main applications of the model is the assessment of DR strategies implemented to reallocate the consumption of shiftable loads or standby reduction. For this study, a cluster of 200 households as the one described in section 5.2.3.1 was used, which represents a type community in the selected area. In this group of households, a percentage of acceptation of the DR strategies was established between the users so the influence of the gradual adoption of the measure could be observed.

It should be highlighted that all the DR strategies or stand-by reduction measures are taken individually in each simulated household, so the aggregate results are the consequence of a modification in individual behaviour, which supposes a novelty in the approach of this work.

5.3.4.1 Day-ahead prices

The objective of the first DR strategy is to reduce the daily energy cost. In this context, two electricity pricings were studied. These tariffs are offered by the DSO in the selected region [47], nevertheless, a similar pricing structure can be found in other European countries. The first type of tariff, named as tariff A presents an hourly price variation based on the electricity demand, usually denoted as TOU tariffs. The second one follows the same criteria but using two ranges of pricing, one for the so-called peak hours and other for the off-peak hours. This tariff is identified as DHA. The simulation system is able to obtain the daily prices from an API provided by the DSO where the information is posted following a 1-day ahead philosophy [48].

The results for the tariff A are illustrated in Figure 5.9 for a cluster of 200 households in the studied location and for an average spring day. The central chart represents the aggregate power consumption of the whole community in kWh in the Z-axis, whereas the X-axis indicates the hour of the day, and the Y-axis the percentage of acceptance of the DR strategies among the users. In addition, for a better understanding, the pricing profile is illustrated in the bottom graph, whilst the average individual cost per household related to the percentage of acceptance is represented in the right chart.

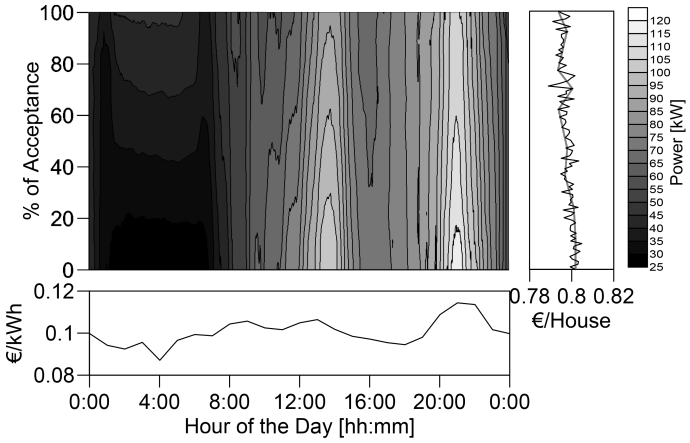

Figure 5.9: Impact of DR actions according to day-ahead pricing with a conventional tariff (Tariff A).

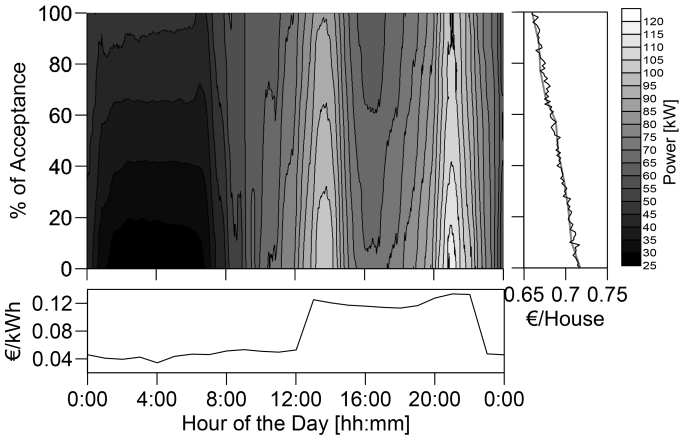

Figure 5.10: Impact of DR actions according to day-ahead pricing with off-peak and peak prices (Tariff DHA).

As it can be observed in the central chart, the two main consumption peaks between 12:00-15:00h and 20:00-22:00h were reduced with this measure, while increasing the night (00:00-06:00h) and afternoon (15:00-17:00h) demands. This reallocation of consumption matches the daily pricing profile. Nevertheless, the span of the price is small (< ±0.02 €), so the final cost reduction is not very significant in average terms.

In contrast with the tariff A, the DHA pricing scheme represented in Figure 5.10 did not only decrease the main consumption peaks but also achieved a lower average energy cost. In this case, the difference between the off-peak prices, around 0.04 €/kWh, and the peak prices 0.12 €/kWh was significant. Therefore, from the average base situation of 0.72 € per household and day, a reduction of 8% in the daily cost could be achieved if the whole community takes part in the DR program.

A numeric comparison of the selected tariffs is included in Table 5.4 for the base scenario, 50%, and 100% of acceptance. As it can be seen, both pricing schemes reduced the maximum power peak in around 5% (50% of acceptance) and 11% (100% of acceptance). This indicates that through the indirect influence of prices, the tariffs aim to shave the consumption peaks. Even though, the tariff DHA brought larger cost reductions (8%) than the tariff A (<1%) when moving the shiftable consumptions to the night time.

5.3.4.2 DR peak shaving

The A and DHA tariffs showed how pricing schemes can influence the daily consumption profiles to indirectly shave the demand peaks. Nevertheless, the second DR strategy aims to assess policies only focused on the minimisation of the demand variability along the day, so it can be more predictable, easing the production planning. The results of this DR strategy are found in Figure 5.11, where again the central figure represents

Table 5.4: Comparison between both tariff. Cost decrement and peak power reduction.

	Cost [€/House]		**Power Peak [kW]**	
Acc_{DR} [%]	**A**	**DHA**	**A**	**DHA**
0	0.8018	0.7175	121.3	120.0
50	0.7995	0.6893	115.8	113.4
100	0.7936	0.6595	107.6	107.1

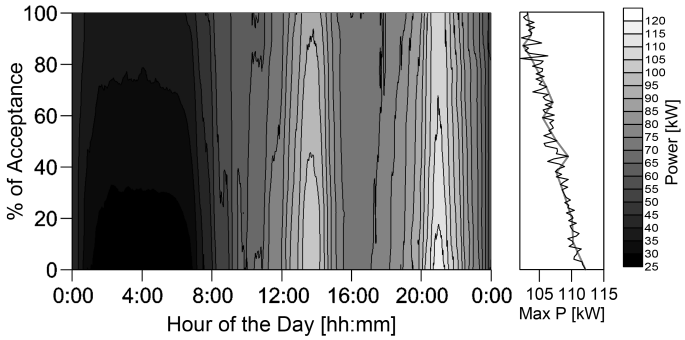

Figure 5.11: Impact of DR actions for peak shaving.

the aggregate power consumption profile of the whole cluster. The right chart, in this case, shows the maximum daily demand peak, which was located at 21:00h for all the cases.

The results showed a peak reduction similar to the TOU tariffs. Nevertheless, although the daily curve modification may resemble the one obtained in Figure 5.9 and Figure 5.10 there is a small peculiarity that distinguished price based strategies from this one. In the TOU DR strategies, a high electricity cost was found from 15:00 to 19:00h so the afternoon consumption was reduced leading to a high variation between the peak and the off-peak power. In contrast, for the load shaving strategy, the afternoon power figures remained almost constant so the midday and night peaks are not accentuated, but the average load is flatter.

This improvement can be clearly observed in Figure 5.12 where the load duration curve for 0%, 50% and 100% of acceptance is represented. This graph presents in the Y-axis the instantaneous power demand, whereas the X-axis accounts for the cumulative duration of this consumption. Therefore, this curve is of special interest for distribution planning since the consumption intensity and its duration can be observed at the same time.

The graph showed the previously mentioned reduction in the peak demand. However, it also indicated an increase in the base load to reduce the total variation along the day. Thus, from the base scenario where the absolute maximum power difference is 96 kW for the whole community, this variation is reduced to 84 kW for 50% of acceptance and 75 kW for 100%, which means 12% and 25% less variability respectively. This flattened load curve provides better management and planning of the distribution network from the DSO point of view.

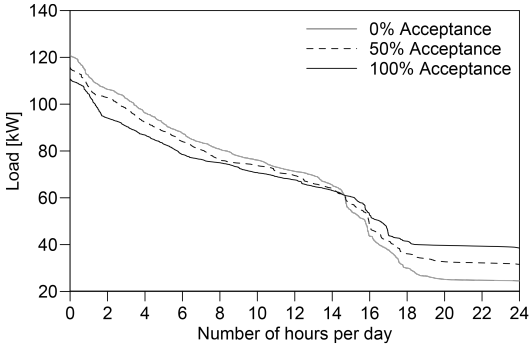

Figure 5.12: Impact of DR actions to flatten de daily profile in the load duration curve.

5.3.4.3 DR renewable matching

The last scenario related to DR strategies for shiftable loads is focused on the maximisation of the utilisation rate when DERs are available. For this aim, due to the widespread installation in the studied region, the integration of photovoltaic energy was considered in this case. This resource also has an additional planning potential since its production is always located during the central hours of the day and, consequently, more predictable than other renewable energies. For the simulation, the same cluster of 200 households was maintained but including now a distributed PV production of 4 kW peak per house. In order to carry out the DR strategies in a realistic environment, real production data of a rooftop installation located in the south of Spain were used for the simulation of the generation, previously employed in other works [33, 46].

Figure 5.13 includes the obtained results for the aggregate community. The central graph maintains the same meaning as in the two previous scenarios, whereas the bottom chart represents the individual PV production of each household for the selected spring day. As it can be observed, this production is located between 8:00-20:00h having its maximum value around 13:00h. On the other hand, the right graph illustrates the loss of load probability (LOLP). This index indicates the percentage of hours in a day, in which the demand cannot be supplied by the RES and its expression is given as the quotient of the energy deficit E_{deficit} and the total daily demand E_{total} as indicated in (5.27).

$$\text{LOLP} = \frac{E_{\text{deficit}}}{E_D} \tag{5.27}$$

As it can be seen in Figure 5.13, this strategy involved a displacement of the night peak (20:00 – 22:00h) to the central hours of the day (12:00 – 16:00h) in order to use the maximum available solar production. This increased the self-consumption rate and decreased the LOLP as it can be observed in the right chart where the base scenario with 27.9% was improved down to 26.7%.

As regards the maximum demand peak, as can be seen in Table 5.5, the base night peak around 21:00h is moved to 13:30h to match the maximum PV production. In this way, the night peak is reduced 15% whereas the midday consumption is increased an 11%.

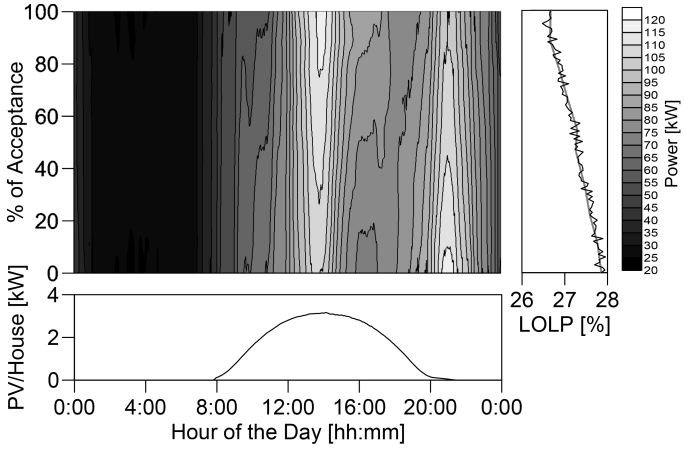

Figure 5.13: Impact of DR actions to match renewable production.

Table 5.5: Change of the time and the value of daily power peaks to match PV production.

	Peak 1		Peak 2	
Acc_{DR} [%]	Time	Power [kW]	Time	Power [kW]
0	13:30	109	21:00	126
50	13:30	116	21:00	114
100	13:30	123	21:00	107

5.3.4.4 DR standby reduction

Finally, and despite not being a load shifting measure, the impact of standby reduction was analysed. The results can be observed in Figure 5.14 where the aggregate daily consumption of the community has been represented together with the average energy consumption per household and day in the right chart.

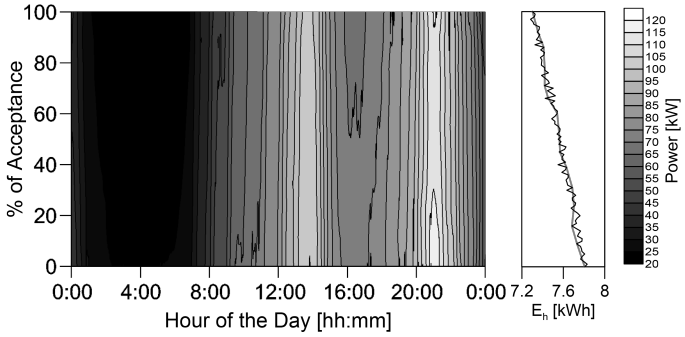

Figure 5.14: Impact of DR actions to reduce Stand-by consumption.

The results showed the relatively significant percentage of consumption that the standby might come to represent, compared to the total demand. As it can be seen, the initial daily average demand of 7.8 kWh per household can be reduced down to 7.3 kWh with a 100% of acceptance, which means an average of 500 Wh per household. If this figure is extrapolated to the whole community the saving can rate up to 100 kWh a day, leading to a daily reduction of 74 kg/CO2, a figure significant enough to be taken into account.

5.4 Conclusions

This work has presented the methodology, implementation and results of a high temporal resolution modelling system aiming to simulate the electricity consumption of general appliances in the residential sector. The model was based on stochastic probability theory and the provided profiles can be used to assess the impact of new DR strategies and energy policies, following a novel implementation where each measure is taken individually in each simulated household also considering the acceptance of the users.

The main simulation algorithm was implemented by means of the high-level object-oriented programming language JAVA, which allowed the integration with other systems such as a database engine for the input data of the model, or the third-party software GAMS for performing the linear optimisation algorithms for the DR strategies. Moreover, the server-based deployment allowed an easy integration with any other systems through the provided RESTful API.

The individual simulations showed the possibilities of the model for simulating the chaotic behaviour of the users and the spikiness of the load profile in which each appliance was simulated with a given power cycle. This power cycle enabled us to reproduce the actual operation of the main household loads, with three different defined categories of equipment, operating by user decision, cyclically or following a power pattern for a certain period of time. The aggregated results and the input parameters such as the type of day (weekday or weekend) also demonstrated the aggregated trend followed by a cluster of household and how although having a random behaviour in the low level, as a whole, defined patterns were obtained.

This property of the model was used for implementing a novel approach to the assessment of DR strategies and energy policies. In this way, each selected measure was individually implemented in the appliances of each household. This provided the possibility of including an acceptation rate among the users, so not all the residents of a certain area might be willing to adopt DR actions. This methodology was applied to 3 different DR strategies, TOU tariffs, peak load shaving and RES integration, as well as to an energy policy, standby power reduction, showing not only the operation of the novel approach but also the impact of these measures according to the rate of acceptance.

The TOU DR strategy proved that shifting the consumption to the night periods can bring not only economic advantages from the user point of view but also an indirect smoothing effect in the load profile that is advantageous for the DSO. Similar results were found for the peak shaving strategy, where the suppression of the price constraint allowed a higher minimisation of the power profile variability. In the case of the RES integration, the DR strategy provided a better utilisation of the PV resource, while decreasing the dependence on the main grid. Finally, the standby reduction strategy pointed out the relatively high amount of energy consumed for that aim a how these energy policies can drive to significant energy savings.

Therefore, the model showed to be not only flexible an accurate with the chaotic environment of the residential sector, but also useful for energy planning and assessment of new strategies in uncertain contexts. In this way, future developments will be focused on two lines. On the one hand, this system together with the previously published one for the lighting, heating and cooling consumption will be integrated into a whole platform with new DR strategies. On the other hand, not yet characterised loads such as the electric vehicle or at home storage systems will be implemented using the appliance model in order to predict the impact on the grid of this potential future scenarios.

Acknowledgements

This work was supported by the Spanish Ministry of Economy and Competitiveness under Research Project TEC2013-47316-C3-1-P; and TEC2016-77632-C3-2-R.

Nomenclature

Basic Variables

t	Time interval with 1-minute resolution
$t_{10\text{min}}$	Time interval with 10-minute resolution
$t_{30\text{min}}$	Time interval with 30-minute resolution
$T_{1\text{min}}$	Group of time intervals spaced 1 minute
$T_{10\text{min}}$	Group of time intervals spaced 10 minutes
$T_{30\text{min}}$	Group of time intervals spaced 30 minutes
d	Type of day (weekday or weekend)
h	Household
n_o	Number of active occupants (0 – 5)
s	Interviewee number

Activities

α	Activity
$P_\alpha(t_{10\text{min}}\|n_o,\alpha,d)$	Activity PDF
$N_o(t_{10\text{min}},n_o,d)$	Number of households with n_o active occupants
$N_\alpha(t_{10\text{min}},n_o,\alpha,d)$	Number of households with n_o active occupants. At least one performs α
N_s^{TUS}	Total number of households in TUS
H_s^{TUS}	Household of the Interviewee s in TUS
$o^{\text{TUS}}(t)$	Occupancy in the TUS

Appliances Model

i	Type of appliance
$p_{app}(i)$	Appliance installation probability
$\overline{E_{app}}(i)$	Average number of an appliance type per house
N_s^{IDAE}	Total number of households in IDAE survey
H_s^{IDAE}	Household s in IDAE survey
$P_{on}, P_{on}(c)$	Appliance ON power. Fix operation and cyclic
P_{off}	Appliance OFF power.
$T_{on}, T_{on}(c)$	Appliance average ON cycle. Fix operation and cyclic
T_{off}	Appliance average OFF power
t_c	Active cycle
t_d	Inactive or delay cycle
P	Appliance Power equation

Simulation Process

N_{app}^h	Number of appliances per household
N_h	Number of household in the simulation
r_i^h	Random numbers for installation probability
app_i^h	Selected appliances in a household
a_i^h	Random numbers for the number of appliances of a type
N_i^h	Number of appliances of type in a household
$m^h(t_{10\text{min}})$	Instantaneous random numbers for the occupancy profile
$o^h(t_{10\text{min}})$	Instantaneous occupancy profile of a household
$P_o(t_{10\text{min}})$	Initial occupancy CDF
c_i^h	Random numbers for the initial active cycle of each appliance
d_i^h	Random numbers for the initial inactive cycle of each appliance
$P_{xy}(t_{10\text{min}})$	Occupancy transition matrix for the instant $t_{10\text{min}}$
$w_i(t)$	Random number for switch on process of appliance i in an instant t
$P^h(t)$	Aggregate power profile of a household

Calibration

E_{year}	Average annual energy consumption of a given appliance
n_{cycles}	Number of operation cycles of an appliance in a year
$\overline{T_{sw}}$	Number of potential switch on minutes in a year for an appliance
$\overline{P_{ocu}}$	Probability of mean active occupancy in a year.
$\overline{n_o}$	Average number of occupants in a year
$\overline{P_\alpha}(\overline{n_o},\alpha)$	Mean activity probability
z	Calibration scalar for each appliance

Demand Response

$P^h_{fix}(t)$	Fixed power demand
$P^h_{shitf}(t)$	Shiftable power demand
$P^h_{DR}(t)$	Shifted power demand profile
$\overline{P_\alpha}(t_{10\text{min}}\|\overline{n_o}, \alpha, d)$	Average daily activity profile
$P^{DR}_\alpha(t_{10\text{min}}\|\alpha, d)$	Reallocated activity PDF after DR actions
$E_D(t_{30\text{min}})$	Total energy demand
$E_{DR}(t_{30\text{min}})$	Energy profile after DR optimisation
$E_{shift}(t_{30\text{min}})$	Shiftable energy profile
$E_{fix}(t_{30\text{min}})$	Fixed energy profile
$\Delta E^+_D(t_{30\text{min}})$	Positive variations in the demand
$\Delta E^-_D(t_{30\text{min}})$	Negative variations in the demand
$\Delta E^{Abs}_D(t_{30\text{min}})$	Absolute variations in the demand
SCF	Supply cover factor
$E_{DER}(t_30min)$	Renewable resources energy profile
$E_{\text{Min}}(t_30min)$	Minimum energy between generation and demand
E_{Max}	Maximum allowed energy per household
$c(t_{30\text{min}})$	Variable energy price
P_{DR}	Acceptance ration CDF
r^h_{DR}	Random number of DR acceptance per household
Acc^h_{DR}	Acceptance of the DR measure per household

Validation

$P_M(t)$	Power profile simulated by the proposed model
$P_{Ref}(t)$	Power profile simulated by the reference model
MSE	Mean square error
RMSE	Root mean square error
NVF	Normalised variation factor

Results

E_{Deficit}	Energy imported from the grid when interacting with RES
LOLP	Loss of load probability

References

[1] D. Ndiaye, K. Gabriel, Principal component analysis of the electricity consumption in residential dwellings, Energy and Buildings 43 (2-3) (2011) 446–453. doi:10.1016/j.enbuild.2010.10.008.

[2] M. Kavgic, A. Mavrogianni, D. Mumovic, A. Summerfield, Z. Stevanovic, M. Djurovic-Petrovic, A review of bottom-up building stock models for energy consumption in the residential sector, Building and Environment 45 (7) (2010) 1683–1697. doi:10.1016/j.buildenv.2010.01.021.

[3] A. de Almeida, P. Fonseca, B. Schlomann, N. Feilberg, Characterization of the household electricity consumption in the EU, potential energy savings and specific policy recommendations, Energy and Buildings 43 (8) (2011) 1884–1894. doi:10.1016/j.enbuild.2011.03.027.

[4] UNFCCC, Kyoto Protocol To the United Nations Framework Convention on Climate Change, Review of European Community and International Environmental Law 7 (2) (1998) 214–217. doi:10.1111/1467-9388.00150.

[5] P. Siano, Demand response and smart grids - A survey, Renewable and Sustainable Energy Reviews 30 (2014) 461–478. doi:10.1016/j.rser.2013.10.022.

[6] X. Ayón, J. K. Gruber, B. P. Hayes, J. Usaola, M. Prodanović, An optimal day-ahead load scheduling approach based on the flexibility of aggregate demands, Applied Energy 198 (2017) 1–11. doi:10.1016/j.apenergy.2017.04.038.

[7] G. Aghajani, H. Shayanfar, H. Shayeghi, Demand side management in a smart micro-grid in the presence of renewable generation and demand response, Energy 126 (2017) 622–637. doi:10.1016/j.energy.2017.03.051.

[8] M. Uddin, M. F. Romlie, M. F. Abdullah, S. Abd Halim, A. H. Abu Bakar, T. Chia Kwang, A review on peak load shaving strategies, Renewable and Sustainable Energy Reviews In press. doi:10.1016/j.rser.2017.10.056.

[9] S. Bahrami, M.H. Amini, M. Shafie-khah, J.P.S. Catalao, A Decentralized Electricity Market Scheme Enabling Demand Response Deployment, IEEE Transactions on Power Systems PP (99) (2017) 1–1. doi:10.1109/TPWRS.2017.2771279.

[10] F. Babonneau, M. Caramanis, A. Haurie, A linear programming model for power distribution with demand response and variable renewable energy, Applied Energy 181 (2016) 83–95. doi:10.1016/j.apenergy.2016.08.028.

[11] G. Graditi, M. L. Di Silvestre, R. Gallea, E. R. Sanseverino, Heuristic-based shiftable loads optimal management in smart micro-grids, IEEE Transactions on Industrial Informatics 11 (1) (2015) 271–280. doi:10.1109/TII.2014.2331000.

[12] M. A. Fotouhi Ghazvini, J. Soares, N. Horta, R. Neves, R. Castro, Z. Vale, A multi-objective model for scheduling of short-term incentive-based demand response programs offered by electricity retailers, Applied Energy 151 (2015) 102–118. doi:10.1016/j.apenergy.2015.04.067.

[13] M.H. Amini, B. Nabi, M.-R. Haghifam, Load management using multi-agent systems in smart distribution network, in: 2013 IEEE Power Energy Society General Meeting, IEEE, (2013) 1–5. doi:10.1109/PESMG.2013.6672180.

[14] D. Geelen, A. Reinders, D. Keyson, Empowering the end-user in smart grids: Recommendations for the design of products and services, Energy Policy 61 (2013) 151–161. doi:10.1016/j.enpol.2013.05.107.

[15] M. Bladh, H. Krantz, Towards a bright future? Household use of electric light: A microlevel study, Energy Policy 36 (9) (2008) 3521–3530. doi:10.1016/j.enpol.2008.06.001.

[16] N. Arghira, L. Hawarah, S. Ploix, M. Jacomino, Prediction of appliances energy use in smart homes, Energy 48 (1) (2012) 128–134. doi:10.1016/j.energy.2012.04.010.

[17] M. Pipattanasomporn, M. Kuzlu, S. Rahman, Y. Teklu, Load profiles of selected major household appliances and their demand response opportunities, IEEE Transactions on Smart Grid 5 (2) (2014) 742–750. doi:10.1109/TSG.2013.2268664.

[18] J. Torriti, Demand Side Management for the European Supergrid: Occupancy variances of European single-person households, Energy Policy 44 (2012) 199–206. doi:10.1016/j.enpol.2012.01.039.

[19] A. Grandjean, J. Adnot, G. Binet, A review and an analysis of the residential electric load curve models, Renewable and Sustainable Energy Reviews 16 (9) (2012) 6539–6565. doi:10.1016/j.rser.2012.08.013.

[20] L. G. Swan, V. I. Ugursal, Modeling of end-use energy consumption in the residential sector: A review of modeling techniques, Renewable and Sustainable Energy Reviews 13 (8) (2009) 1819–1835. doi:10.1016/j.rser.2008.09.033.

[21] M. Muratori, M.C. Roberts, R. Sioshansi, V. Marano, G. Rizzoni, A highly resolved modeling technique to simulate residential power demand, Applied Energy 107 (2013) 465–473. doi:10.1016/j.apenergy.2013.02.057.

[22] U. Wilke, F. Haldi, J. L. Scartezzini, D. Robinson, A bottom-up stochastic model to predict building occupants' time-dependent activities, Building and Environment 60 (2013) 254–264. doi:10.1016/j.buildenv.2012.10.021.

[23] I. Richardson, M. Thomson, D. Infield, A high-resolution domestic building occupancy model for energy demand simulations, Energy and Buildings 40 (8) (2008) 1560–1566. doi:10.1016/j.enbuild.2008.02.006.

[24] I. Richardson, M. Thomson, D. Infield, A. Delahunty, Domestic lighting: A high-resolution energy demand model, Energy and Buildings 41 (7) (2009) 781–789. doi:10.1016/j.enbuild.2009.02.010.

[25] I. Richardson, M. Thomson, D. Infield, C. Clifford, Domestic electricity use: A high-resolution energy demand model, Energy and Buildings 42 (10) (2010) 1878–1887. doi:10.1016/j.enbuild.2010.05.023.

[26] J. Widén, A. Nilsson, E. Wäckelgård, A combined Markov-chain and bottom-up approach to modelling of domestic lighting demand, Energy and Buildings 41 (10) (2009) 1001–1012. doi:10.1016/j.enbuild.2009.05.002.

[27] J. Widén, E. Wäckelgård, A high-resolution stochastic model of domestic activity patterns and electricity demand, Applied Energy 87 (6) (2010) 1880–1892. doi:10.1016/j.apenergy.2009.11.006.

[28] N. Good, L. Zhang, A. Navarro-Espinosa, P. Mancarella, High resolution modelling of multi-energy domestic demand profiles, Applied Energy 137 (2015) 193–210. doi:10.1016/j.apenergy.2014.10.028.

[29] E. McKenna, M. Thomson, High-resolution stochastic integrated thermal-electrical domestic demand model, Appl. Energy, Applied Energy 165 (2016) 445–461. doi:10.1016/j.apenergy.2015.12.089.

[30] M. A. Lopez, I. Santiago, D. Trillo-Montero, J. Torriti, A. Moreno-Munoz, Analysis and modeling of active occupancy of the residential sector in Spain: An indicator of residential electricity consumption, Energy Policy 62 (2013) 742–751. doi:10.1016/j.enpol.2013.07.095.

[31] E. J. Palacios-Garcia, A. Chen, I. Santiago, F. J. Bellido-Outeiriño, J. M. Flores-Arias, A. Moreno-Munoz, Stochastic model for lighting's electricity consumption in the residential sector. Impact of energy saving actions, Energy and Buildings 89 (2015) 245–259. doi:10.1016/j.enbuild.2014.12.028.

[32] E. J. Palacios-Garcia, A. Moreno-Munoz, I. Santiago, J. M. Flores-Arias, F. J. Bellido-Outeirino, I. M. Moreno-Garcia, A stochastic modelling and simulation approach to heating and cooling electricity consumption in the residential sector, Energy 144C (2018) 1080–1091. doi:10.1016/j.energy.2017.12.082.

[33] E. J. Palacios-Garcia, A. Moreno-Muñoz, I. Santiago, I. M. Moreno-Garcia, M. I. Milanés-Montero, PV Hosting Capacity Analysis and Enhancement Using High Resolution Stochastic Modeling, Energies 10 (10) (2017) 1488. doi:10.3390/en10101488.

[34] E. J. Palacios-Garcia, I. Santiago, A. Moreno-Munoz, J. M. Flores-Arias, F. J. Bellido-Outeiriño, Distributed Energy Resources Integration and Demand Response. The Role of Stochastic Demand Modelling, in: A. Moreno-Munoz (Ed.), Large Scale Grid Integration of Renewable Energy Sources, The Institution of Engineering and Technology (IET), London, 2017, Ch. Chapter 8:, p. 300.

[35] J. M. Roldán Fernández, M. B. Payán, J. M. R. Santos, Á. L. T. García, The voluntary price for the small consumer: Real-time pricing in Spain, Energy Policy 102 (November 2016) (2017) 41–51. doi:10.1016/j.enpol.2016.11.040.

[36] Eurelectric, Dynamic pricing in electricity supply (2017). URL: http://www.eurelectric.org/media/309103/dynamic_pricing_in_electricity_supply-2017-2520-0003-01-e.pdf

[37] SEDC, Explicit Demand Response in Europe Mapping the Markets 2017, Tech. rep., Smart Energy Demand Coalition (2017).

[38] A. Conchado, P. Linares, O. Lago, A. Santamaría, An estimation of the economic and environmental benefits of a demand-response electricity program for Spain, Sustainable Production and Consumption 8 (2016) 108–119. doi:10.1016/j.spc.2016.09.004.

[39] National Statistics Institute of Spain. Ministry of Economy and Competitiveness, Time Use Survey (2010). URL: http://www.ine.es/en/prensa/eet_prensa_en.htm

[40] W. R. Gilks, S. Richardson, D. J. Spiegelhalter, Markov Chain Monte Carlo in Practice, Technometrics 39 (3) (1997) 338. doi:10.2307/1271145.

[41] IDAE, Análisis del consumo energético del sector residencial en España INFORME FINAL (2011). URL: http://www.idae.es/uploads/documentos/documentos_Informe_SPAHOUSEC_ACC_f68291a3.pdf

[42] R. Stamminger, Synergy Potential of Smart Appliances. D2.3 of WP2 from the Smart-A project (2008). URL: http://smart-a.org/WP2_D_2_3_Synergy_Potential_of_Smart_Appliances.pdf

[43] I. Laicane, D. Blumberga, A. Blumberga, M. Rosa, Reducing Household Electricity Consumption through Demand Side Management: The Role of Home Appliance Scheduling and Peak Load Reduction, Energy Procedia 72 (2015) 222–229. doi:10.1016/j.egypro.2015.06.032.

[44] National Statistics Institute of Spain. Ministry of Economy and Competitiveness, Household Budget Survey (2016). URL: http://www.ine.es/dyngs/INEbase/en/operacion.htm?c=Estadistica_C&cid=1254736176806&menu=resultados&secc=1254736194790&idp=1254735976608

[45] J. Salom, A. J. Marszal, J. Widén, J. Candanedo, K. B. Lindberg, Analysis of load match and grid interaction indicators in net zero energy buildings with simulated and monitored data, Applied Energy 136 (2014) 119–131. doi:10.1016/j.apenergy.2014.09.018.

[46] E. J. Palacios-Garcia, A. Moreno-Munoz, I. Santiago, I. M. Moreno-Garcia, M. I. Milanes-Montero, Smart community load matching using stochastic demand modeling and historical production data, in: 2016 IEEE 16th International Conference on Environment and Electrical Engineering (EEEIC), IEEE, 2016, pp. 1–6. doi:10.1109/EEEIC.2016.7555885.

[47] Red Eléctrica de España Co., Red Eléctrica de España (2017). URL: http://www.ree.es/en

[48] Red Electrica De España, ESIOS (2017). URL: https://www.esios.ree.es/en

Appendix A. Appliances characteristics

Appliance i	α	Type	T_{on} [min]	T_{off} [min]	P_{on} [W]	P_{off} [W]	p_{app}	$\overline{E_{app}}$	E_{year} [kWh]	DR
Refrigerator	No	II	15	30	190	6	1	1	665	No
Freezer	No	II	15	30	180	6	0.228	1	612	No
Iron	Ironing	Ia	90	0	1,680	0	0.959	1	130	No
Vacuum cleaner	Cleaning	Ia	60	0	2,200	0	0.308	1	74	No
Oven	Cooking	Ib	60	0	1,933	0	0.794	1	202	No
Microwave	Cooking	Ib	15	0	1,000	0	0.81	1	96	No
Stove	Cooking	Ib	60	0	686	0	0.386	1	426	No
Dish Washer	Cooking	III	120	0	556	0	0.362	1	230	Yes
Coffee Maker	Cooking	I	45	0	750	0	0.291	1	55	No
Blender	Cooking	I	30	0	400	0	0.845	1	37	No
Squeezer	Cooking	I	10	0	30	0	0.48	1	2	No
Toaster	Cooking	I	10	0	1,000	0	0.679	1	61	No
Tumbler Dryer	Laundry	III	90	0	1,633	0	0.313	1	260	Yes
Washing Machine	Laundry	III	138	0	408	1	1	1	260	Yes
Washer Dryer	Laundry	III	228	0	1,020	2	0.075	1	511	Yes
Hair Dryer	Washing	I	10	0	1,600	0	0.819	1	97	No
Water Heater	Washing	II	30	0	2,000	50	0.376	1	1638	No
Razor	Washing	I	15	0	4	0	0.322	1	0	No
TV	TV	I	60	0	120	5	1	2.19	160	No
DVD	TV	I	180	0	25	1	0.753	1	24	No
Video Console	TV	I	180	0	200	4	0.292	1	135	No
Modem	PC	I	300	0	30	3	0.373	1	76	No
PC	PC	I	300	0	150	7	0.507	1.20	202	No
Laptop	PC	I	300	0	65	4	0.507	1.30	175	No
Cordless Phone	Phone	I	10	0	2	1	0.3	1	9	No
Radio	Radio	I	240	0	15	3	0.8	1	48	No
Hi-Fi	Radio	I	200	0	75	2	0.592	1	91	No

6

PV hosting capacity analysis and enhancement using high resolution stochastic modeling

Emilio J. Palacios-Garcia[1], Antonio Moreno-Munoz[1], Isabel Santiago[1], Isabel M. Moreno-Garcia[1], and Maria I. Milanés-Montero[2]

[1]Departamento de Arquitectura de Computadores, Electrónica y Tecnología Electrónica, Escuela Politécnica Superior, Universidad de Córdoba, Córdoba, Spain.
[2]Power Electrical and Electronic Systems Research Group, Escuela de Ingenierías Industriales, Universidad de Extremadura, Badajoz, Spain

Abstract

Reduction of CO_2 emissions is a main target in the future smart grid. This goal is boosting the installation of renewable energy resources (RES), as well as a major consumer engagement that seeks for a more efficient utilization of these resources toward the figure of 'prosumers'. Nevertheless, these resources present an intermittent nature, which requires the presence of an energy storage system and an energy management system (EMS) to ensure an uninterrupted power supply. Moreover, network-related issues might arise due to the increasing power of renewable resources installed in the grid, the storage systems also being capable of contributing to the network stability. However, to assess these future scenarios and test the control strategies, a simulation system is needed. The aim of this paper is to analyze the interaction between residential consumers with high penetration of PV generation and distributed storage and the grid by means of a high temporal resolution simulation scenario based on a stochastic residential load model and PV production records. Results of the model are presented for different PV power rates and storage capacities, as well as a two-level charging strategy as a mechanism for increasing the hosting capacity (HC) of the network.

The paper has been published in *Energies, 2017, 10(10) pp. 1488. doi: 10.3390/en10101488*.

6.1 Introduction

Electrical energy is one of the main elements for the development of modern society, where higher quality and reliability are requested by the consumers whilst reducing emissions and increasing efficiency. In the current context, this has led to the integration of large renewable resources in the electrical grid, meaning a high percentage of the total production in many countries. In the European Union (UE), renewable energies represented 25.4% of the total primary energy production in 2015, and among these sources, solar energy accounted for 4.17% of the total annual renewable production [1].

Nevertheless, the variability and uncertainty associated with these types of sources prevent them from taking part in the electricity market, due to their low dispatchability and the perturbations that they might cause in the grid [2]. Therefore, the effective management of these resources is one of the current challenges, usually solved by means of electrical storage systems [3]. However, storage systems have a considerable cost, and they must be combined with advanced control strategies that maximize their utilization without negatively impacting the lifespan [4].

Opposed to the classical unidirectional grid conception where the end user is simply a consumer, the new context of distributed resources integration is leading towards the major participation of users, who have acquired the role of "prosumers" that might interact bi-directionally with the electrical network [5]. This change has been promoted thanks to the use of advanced metering infrastructures (AMI), advanced communications and demand response (DR) programs [6, 7]. Those programs, despite causing sometimes discomfort, may represent substantial economic and energetic savings [8].

Therefore, users are provided with energy management systems (EMS) that ensure the network stability and an uninterrupted supply, all of these by controlling the charging cycles, as well as the possible interactions with the main grid when either an energy surplus or shortage take place [9]. Likewise, this interaction with the grid might contribute to the improvement of the network stability by means of the intercommunication between EMSs. This is particularly useful in decentralized installations or communities with a distributed generation where a global smart community energy management system (SCEMS) is needed to avoid an uncontrolled energy injection that might lead to the overload of the network, exceeding the so-called hosting capacity (HC) [10, 11].

In order to assess the future scenarios and develop effective control strategies that overcome these issues, simulation systems are highlighted as an essential tool. Between all the different alternatives, those modeling techniques that provide a high-temporal resolution are regarded as the most suitable ones due to the random nature of the end users' consumption and the renewable sources [12, 13].

In this context, stochastic models can be pointed out as the main tools for high temporal resolution simulations since they are able to emulate the chaotic consumers' behavior whilst keeping the aggregate trend. A wide range of previous works can be found in the literature regarding these models. In [14, 15], Widen *et al.* modeled the electricity and hot water demand of Swedish households using a bottom-up methodology. Likewise, Richardson *et al.* developed various models to simulate the residential lighting consumption [16] and the appliances demand [17]. In addition, Mckenna and Thomson [18] implemented the simulation of heating consumption in terms of hot water demand. What is more, the authors have previously developed various models based on the active occupancy, which are able to simulate the lighting [19], appliances andheating, ventilation and air conditioning (HVAC) systems' consumption [20].

Together with the consumption simulation, the estimation of the instantaneous power produced by the RES must also be done with a high-temporal resolution in order to study the interplay between both elements. In the particular case of PV power, previous authors have based their works on the modeling of irradiance components by means of historical records [21]. Nevertheless, in addition to the global irradiance, some other factors highly influence the PV production such as the technology, the degradation of the components, the energy losses of the installation, the inverters' performance, etc. [22, 23]. In this way, and taking into account the wide available amount of historical records of domestic PV installations and large solar fields, the use of these logs as the main input for the evaluation of future scenarios is one of the most accurate and

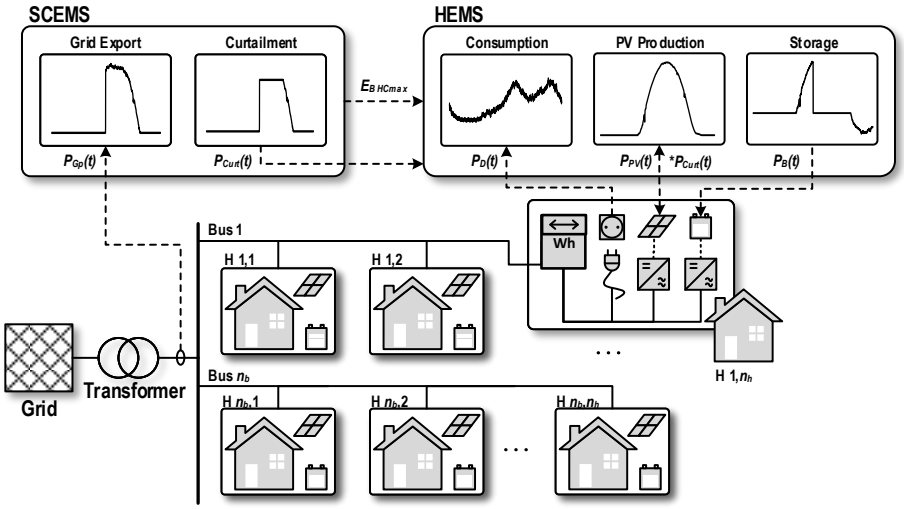

Figure 6.1: Conceptual architecture of the modeling and simulation system. HEMS, home EMS.

realistic alternatives [24].

Using this consumption model together with the production records, different scenarios that represent a future grid or installation can be assessed to plan the electrical network, introduce energy management strategies or develop new algorithms. However, it is also necessary to introduce a series of indicators that take into account this high temporal resolution. Previous authors have proposed different quantifiers of the interplay between demand and production such as Sartori *et al.* [25] and Salom *et al.* [26], especially in the context of net-zero energy buildings and production-consumption matching. Nevertheless, no additional indicators have been developed to study the integration of distributed energy production in a grid with limited HC.

Therefore, this paper aims to implement a simulation system that allows assessing the integration of PV production and energy storage in a residential context, with a high temporal resolution (1 min) and taking into account the interaction with the grid and the limitations in terms of injected power. Moreover, an indicator of the network interaction with limited HC is introduced, finally, proposing a mechanism for using the distributed storage from the distribution system operator (DSO) point of view to avoid the network overload and enhance the HC in the peak production hours.

The paper is structured as follows. Section 6.2 presents the main parts of the system and the methodology used to model them, the control strategies, the developed indexes for quantifying the integration and the simulation process. Subsequently, the results obtained using the system are presented in Section 6.3, first showing the novel characteristics of this simulation system and, posteriorly, evaluating three different scenarios, islanded, grid-connected and grid-connected with HC enhancement operation. Finally, the conclusions are addressed in Section 6.4.

6.2 Methodology

The simulation system aims to represent a low voltage grid composed of n_h households that have distributed renewable production and energy storage systems. Each household is connected to a low-voltage bus n_b that is simultaneously interfaced with the main grid through a medium voltage/low voltage (MV/LV) transformer. The system architecture is shown in Figure 6.1.

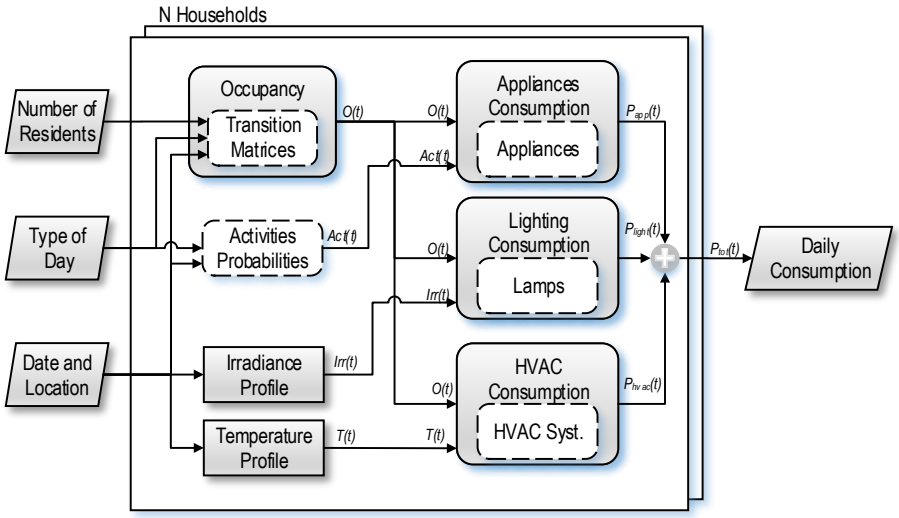

Figure 6.2: Conceptual architecture of the modeling and simulation system.

The AC loads are responsible for the power consumption ($P_D(t)$), and their behavior is modeled by means of a stochastic model. Regarding the PV production ($P_{PV}(t)$), the panels are considered to be connected through a unidirectional DC/AC converter to the household network. In the case of the batteries ($P_B(t)$), the converter is bi-directional, so they can interact with the production, as well as with the grid, aiding in the HC process. Moreover, each house is supposed to have a bi-directional smart electricity meter that quantifies the energy flow to and from the grid and sends information to the home EMS (HEMS) and the SCEMS that control the power interchanged with the grid ($P_{GP}(t)$) and establish the production curtailments ($P_{Curt}(t)$) when needed.

The HEMS controls the charging/discharging process of each battery in each household taking into account only the local PV production and the instantaneous consumption. On the top of that, the SCEMS possesses global information about the network status in order to guarantee the stability of the grid and perform the HC enhancement actions when needed using a percentage of the distributed batteries in each dwelling ($E_{B\,HCMax}$) and reducing the PV production homogeneously between the households ($*P_{Curt}(t)$), according to the curtailment, to avoid the network overcharge.

6.2.1 Households Simulation

As can be seen in Figure 6.1, the households are composed of three modeling blocks, which are the AC loads, the PV production and the energy storage system. The characteristics, modeling methodology and simulation of each system are described below.

6.2.1.1 AC Load

The consumption profiles of each household were calculated using a stochastic model. The estimation uses Monte Carlo simulation techniques and it is based on Markov chains probability theory. The model is composed of four algorithmic blocks that estimate, first, the daily occupancy profiles and, subsequently, the lighting system demand, the consumption due to general home appliances and the needs of HVAC systems, respectively. The general structure of this model is illustrated in Figure 6.2.

As can be observed, the residents' behavior is the common influence factor since the activity of the users at home determines the periods when the higher consumption takes place. Thus, the calculation of the daily occupancy profile is the lower level block of the system, denoted as Occupancy in Figure 6.2. The model has three inputs parameters, which are the number of residents of the household, the type of day (weekday or weekend) and the date and location.

The occupancy model is based on non-homogeneous Markov Chains and has a 10-min resolution. Therefore, for each 10-min interval (144 in a day), the probability transition matrices were calculated. For this aim, the Time Use Survey (TUS) was employed [27]. This survey has been carried out in most European countries, and includes information regarding the interviewees' activities during the day, where these activities took place and whether the interviewees were accompanied. These matrices determine the different transitions between occupancy states based on a random sampling over the associated discrete probability distribution for a given time and the current state of occupancy [28, 29].

Above this block, and using the generated occupancy profile $O(t)$ as an input dataset, the power demand was calculated applying the three other blocks, each one with specific influence factors and with 1-min resolution. This higher temporal resolution in the consumption patterns is fully justified since, whereas the occupancy transitions occur within a longer interval, being unlikely to have occupancy transitions below 10–15 min, the on/off events of appliances are faster.

From the consumption blocks, the lighting demand block (Lighting Consumption) is influenced by the solar irradiance profile $Irr(t)$, which determines when the home lighting system are likely to be used. This profile is combined with the occupancy $O(t)$, so the higher the occupancy level, the higher the probability of switching on the lighting systems when no daylight is available. In addition, by means of a probability distribution of lighting technologies and powers, the lamps that are installed in the household are randomly selected. Further details regarding this model can be found in a previous work [19].

In the case of the appliances consumption block (Appliances Consumption), besides the occupancy profile, the daily probability for different activities $Act(t)$ was taken into account. These activities were also extracted from the TUS [27], and they are: doing the laundry, ironing, cleaning the house, watching the TV, washing and dressing, cooking and using the PC [29]. Those activities are directly or indirectly related to some energy consumption and subsequently with the probability of turning on the associated appliances. For instance, ironing is directly linked to the use of an iron, whereas the activity cooking can be related to a microwave, an oven or an electric stove.

Finally, the block that estimates the HVAC consumption (HVAC Consumption) uses the annual seasonality and the daily ambient temperature profiles $T(t)$ as influence factors. The first one relates the energy intensity consumption of each day with the temperature deviation from the comfort one [30] using the regression methodology proposed by Moral-Carcedo and Vicéns-Otero [31], whereas the daily temperature regulates the cycling of the appliances during the day according to the insulation and the devices technology [32]. It should be pointed out that only the electrical demand was studied. Consequently, only those heating appliances supplied with electricity were considered.

The daily consumption profile $P_{tot}(t)$ for each household n is finally calculated as the sum of the appliances consumption $P_{app}(t)$, the lighting consumption $P_{light}(t)$ and the HVAC consumption $P_{HVAC}(t)$. This confers the model an additional flexibility since not only the global consumption can be studied, but also a specific component can be separated and disaggregated from the rest.

6.2.1.2 Battery Storage

As was indicated in Figure 6.1, each household has an energy storage system. A simplified battery model was selected for the study. Its basic operation is ruled by Equation (6.1).

$$E_B(t) = \begin{cases} E_B(t-1) + \frac{P_B(t)}{60} \cdot \eta_c & P_B(t) \geq 0 \\ E_B(t-1) + \frac{P_B(t)}{60} \cdot \frac{1}{\eta_d} & P_B(t) < 0 \end{cases} \tag{6.1}$$

In this equation t represents the simulation time in minutes, $E_B(t)$ is the stored energy for each simulation step in Wh and $P_B(t)$ is the instant power applied to (+ charging) or supplied by (− discharging) the storage system for a given time in Watts. The process has an associated charge efficiency η_c and a discharge efficiency η_d, which depend on the storage technology and can be provided as input parameters. For this study, since no specific storage technology was selected a 0.85 charging and discharging efficiency was assumed. In addition, the energy $E_B(t)$ is measured in Wh, whereas the instant power is calculated for each minute, so the $1/60$ factor was included.

The stored energy is also limited by the operative range that is expressed in (6.2). In this equation, E_{Bmin} is the depth of discharge and E_{Bmax} is the charging threshold. These limits are established by the technology of the battery and the selected operation.

$$E_{Bmin} < E_B(t) < E_{Bmax} \tag{6.2}$$

6.2.1.3 PV Production

The photovoltaic production was emulated using historical records of a rooftop PV installation located in Cordova (Córdoba), Spain, during 3 years, from 2011–2013. The studied system is composed of 3 similar sectors, each of them containing 36 solar modules. The peak power of each module is 165 W, resulting in a total of 5940 W per sector.

At the same time, each sector is associated with an inverter of 5,000 W. The inverter is capable of monitoring parameters such as the input DC voltage (V_{DC}) and DC current (I_{DC}), output AC voltage (V_{AC}) and AC current (I_{AC}), frequency (f) and power (P_{PV}). In addition, a calibrated cell measures the tilted global irradiance ($Irr(t)$) that is collected by the modules. All of these magnitude are recorded with a 5-min resolution [23].

$$P_{PV}(t) = \eta_{inv} \cdot \eta_{inst} \cdot \eta_G \cdot Irr(t) \tag{6.3}$$

The final production of the PV installation is influenced by a wide range of factors. As indicated in (6.3), the final power $P_{PV}(t)$ produced by the PV installation for a given irradiance $Irr(t)$ mainly depends on the efficiency of the inverter (η_{inv}), the installation (η_{inst}), meaning wiring losses, diodes losses and inhomogeneous irradiance, and the generator (η_G). In order to take into account all of these elements, the output AC power recorded by the inverters was used in the simulations.

$$P_{PV}^{peak}(t|P_{peak}) = \frac{P_{peak}}{P_{peak}^*} \cdot P_{PV}(t) \tag{6.4}$$

Using the expression indicated in (6.4) the output AC power $P_{PV}(t)$ was linearly scaled using the quotient between the selected PV peak per household P_{peak} and the original installation peak $P_{peak}^* = 5,940$ W, obtaining the scaled curve P_{PV}^{peak}, which is used as the input for the simulation. In addition, the power profiles were linearly interpolated to achieve a 1-min resolution from the original 5-min records. Taking into account the 1-min resolution of the consumption profile, this interpolation does not imply a significant error since large power gradients are mainly associated with events slower than 5 min usually associated with large clouds' shading, although fast-moving clouds and scattered skies might cause faster variations.

6.2.2 Hosting Capacity

The HC is defined as the amount of renewable energy that can be integrated into the existing electrical grid without impacting the reliability, quality or performance of the network. The variation of these parameters is studied by means of a series of indicators that must remain between a given threshold such as the voltage, the frequency or the current injected into the grid.

For low voltage grids, the main phenomena that limit the HC of the network are overvoltages and overloads in the system. The first one appears due to the higher R/X (resistance to reactance) radio in low-voltage grids, which might lead to overvoltages when a large amount of current is injected. Nevertheless, the detection of this type of event requires detailed knowledge of the particular network, and its influence is usually small thanks to the oversize of the feeders [33].

On the other hand, the network overload is a more common phenomenon since the distribution transformers are designed to cope with users' demand, but not with the uncontrolled injection of renewable production into the grid. This leads to the overload of the MV/LV transformers whose protections are usually very slow. Subsequently, as proposed by Etherden and Bollen [10], a coordinated curtailment strategy has to be developed.

In this paper, the phenomenon of the HC was analyzed in the context of the system overload, directly relating the issue with the power ratio of MV/LV transformer represented in Figure 6.1, which limits the maximum instantaneous power that can be handled. This power can be imposed by the network protections, the capacity of the electrical conductors or even the DSO. Moreover, it might be defined with different levels of reliability and hysteresis ranges.

Two different control schemes in order to reduce the impact of large distributed energy resources' integration without reinforcing the grid were studied. The so-called soft curtailment and hard curtailment strategies, proposed by Etherden and Bollen [10], were analyzed in this work. These strategies were implemented by the Equations (6.5) and (6.6).

$$P_{G_{soft}}(t) = \begin{cases} P_{Gp}(t) & P_{Gp}(t) < P_{Curt} \\ P_{Curt} & P_{Gp}(t) \geq P_{Curt} \end{cases} \tag{6.5}$$

$$P_{G_{hard}}(t) = \begin{cases} P_{Gp}(t) & P_{Gp}(t) < P_{Curt} \\ 0 & P_{Gp}(t) \geq P_{Curt} \end{cases} \tag{6.6}$$

In these two equations, $P_{Gp}(t)$ is the instantaneous aggregate PV power injected by the smart community, whereas P_{Curt} is the maximum power flow allowed through the MV/LV transformer. In addition, $P_{G_{soft}}(t)$ and $P_{G_{hard}}(t)$ indicate the real power injected into the grid when either soft or hard curtailment strategies respectively are applied.

As can be derived from (6.5) and (6.6), the strategies differ in the amount of power that is allowed to be injected into the grid when a potential overload is detected. The soft curtailment represents the most favorable case, whereas the hard curtailment is the worst case scenario. Within these two strategies, a wide range of alternatives can be chosen with different levels of coordination.

In the case of soft curtailment, the system has enough control capabilities, so the power exported is limited to the maximum power ratio. This situation is completely feasible in the study case, since the distributed PV production units can be selectively disconnected for this aim.

On the other hand, when a hard curtailment is applied, the entire power injection is disconnected under an overload situation. This strategy requires lower control capabilities in the system, but the amount of energy that is exported is also dramatically decreased. For our study, since a 200-household community was studied, considering an average 2,000 W consumption per house, the power ratio of the transformer P_{Curt} was selected to be 400,000 VA.

6.2.3 Smart Community Energy Management System

The last block of the simulation is the SCEMS that controls the power interchange between the different units and implements the above-mentioned curtailment strategies.

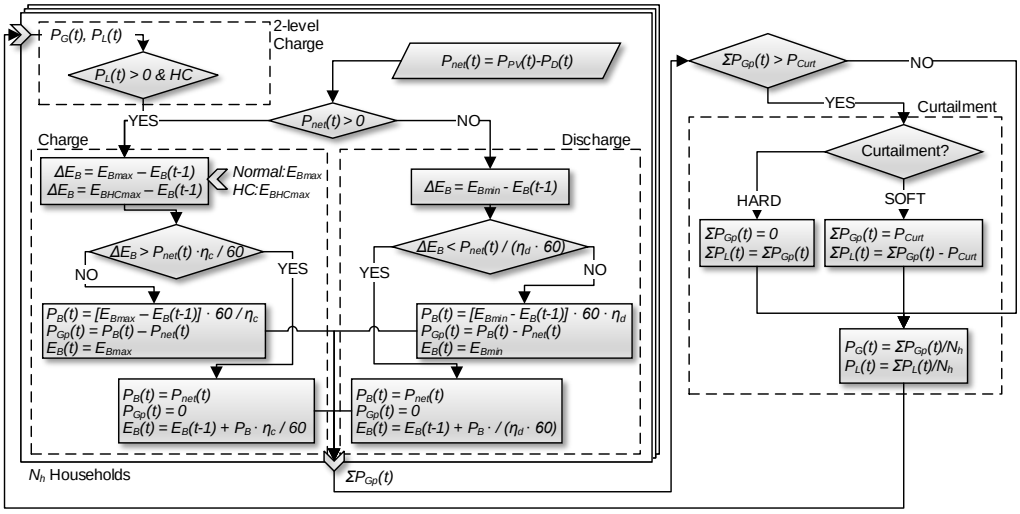

Figure 6.3: Flowchart of the interaction between the PV generation, the demand, the storage system and the main grid.

6.2.3.1 EMS: Self-Consumption Maximization

The EMS in each household aims to maximize the autonomy of the dwelling. Therefore, the distributed storage is charged as soon as the PV production exceeds the consumption to accumulate energy for the non-production period. Once the batteries are fully charged, the production surplus is injected into the grid considering the HC limits. Finally, when the available PV production is too low, the demand is supplied by the batteries until they are discharged, and then, the demand has to be covered by importing energy from the grid.

The interaction between the elements is indicated in Figure 6.3, where the flowchart of the process can be seen. As can be observed, the difference $P_{net}(t)$ between the production $P_{PV}(t)$ and the demand $P_D(t)$ is used to charge or discharge the battery between the energy limits E_{Bmin} and E_{Bmax}. Subsequently, the deficit or excess of power that must be taken or injected into the grid $P_{GP}(t)$ is calculated for each household.

Nevertheless, in case the sum of the power injected by the N_h households exceeds the maximum power that can be injected into the grid P_{Curt} for a given type of Curtailment, the above-mentioned strategies indicated in (6.5) for the soft curtailment and (6.6) for the hard curtailment are applied. The power that is lost and must be reduced in the PV production (P_L) due to the impossibility of being neither injected into the grid nor stored is also calculated for each curtailment.

Finally, the actual power applied to the battery system of each household $P_B(t)$ is lastly calculated sharing the grid capacity $P_G(t)$ and the power lost due to the curtailment $P_L(t)$ between all the households.

6.2.3.2 SCEMS: PV HC Enhancement

The improved algorithm that is proposed in this work to increase the amount of production that can be integrated into the smart community is based on a two-level charging scheme, which is of special interest for PV installations. The danger of incurring in a network overload when PV generation is injected into the grid increases in the central hours of the day due to the higher levels of irradiance; therefore, an algorithm that allows two thresholds of charge might improve the utilization of the PV generation.

The first charging threshold is ruled by the same conditions as the previously exposed mechanism, storing energy when the PV production exceeds the demand. Nevertheless, in this case, the battery is not fully

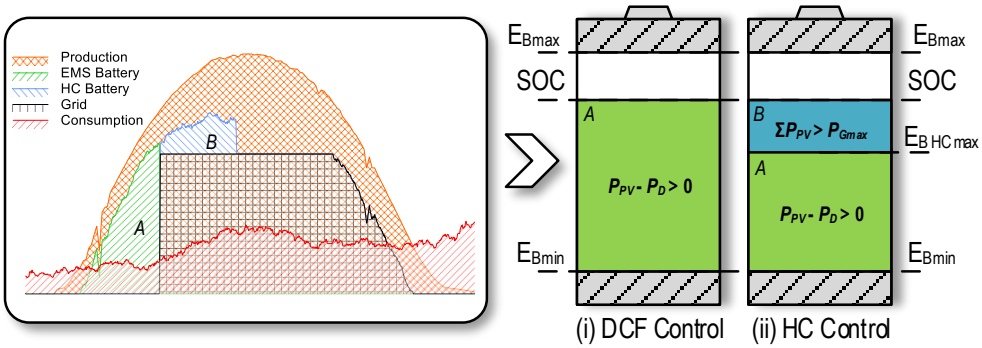

Figure 6.4: Control strategies for the SCEMS when soft curtailment. Daily profile and battery levels.

charged during this period, but only until a set limit $E_{B\,HCmax}$. In this way, a selected percentage $\%SOC_{HC}$ is reserved. This percentage $\%SOC_{HC}$ is used when a potential overload situation is detected, so the injected power is reduced. For this aim, part of the PV production is employed to charge the batteries, whereas the maximum power allowed by the DSO is exported into the grid.

$$\%SOC_{HC} = E_{Bmax} - E_{B\,HCmax} \tag{6.7}$$

The proposed control strategy is illustrated in Figure 6.4 where the instantaneous daily profile together with the charging structure is shown. As can be seen, during the normal operation, the battery is charged as soon as the production exceeds the consumption, until the maximum allowed energy E_{Bmax}, as is depicted in (i), and the green area A is reached.

Using the new strategy proposed in (ii), the battery is divided into two levels. From E_{Bmin} to $E_{B\,HCmax}$, the operation is the usual one illustrated by the green area A. However, a percentage $\%SOC_{HC}$ is reserved for the overload situation, as indicated by the blue area B. As can be observed in Figure 6.4 where the soft curtailment strategy is considered, under an overload situation, the power injected into the grid is set to the maximum allowed by the DSO, whereas the battery is charged for the blue area B.

The algorithmic behavior of the control system is almost similar to the one presented for the individual HEMS. Nevertheless, in this case, an additional charging operation is performed after calculating the production excess $P_L(t)$ as can be observed in the flowchart of Figure 6.3. What is more, the first charging limit in the normal operation is replaced by the new threshold $E_{B\,HCmax}$.

6.2.4 Evaluation Indexes

The performances of the system and the charging strategies were analyzed for different values of PV power and storage capacities with a set of indicators. Four indexes were selected to study the variations in the supply utilization, the percentage of self-consumption and the amount of energy that can be injected into the grid.

The first index was the demand cover factor (DCF), which aims to evaluate the percentage of self-consumption that can be achieved with the installed PV power. The second one was the supply cover factor (SCF) that indicates the percentage of utilization of the local generation. These two indexes are well defined in the literature, although different names can be found for them [25, 26].

Their equations are indicated in (6.8) and (6.9) respectively, where $P_{PV}(t)$ is the instantaneous PV production, $P_B(t)$ is the instantaneous power supplied by ($P_B < 0$) or applied to ($P_B > 0$) the battery and $P_D(t)$ is the power demand. In addition, t_0 and t_f define the temporal period for which the indexes are calculated. Therefore, different periods of time can be studied using the same expression and, in this case, the 1-min resolution power data in order to keep the temporal coincidence between production and demand.

$$DCF[t_0, t_f] = \frac{\sum_{t=t_0}^{t_f} \min\left[P_{PV}(t) - P_B(t), P_D(t)\right]}{\sum_{t=t_0}^{t_f} P_D(t)} \tag{6.8}$$

$$SCF[t_0, t_f] = \frac{\sum_{t=t_0}^{t_f} \min\left[P_{PV}(t) - P_B(t), P_D(t)\right]}{\sum_{t=t_0}^{t_f} \left(P_{PV}(t) - P_B(t)\right)} \tag{6.9}$$

However, those indexes do not take into account the interaction with the grid. Subsequently, a redefined SCF named as the 'grid interaction supply cover factor' (GISCF) is proposed by the authors. As is denoted in (6.10), this index includes a new parameter $P_G(t)$, which represents the instantaneous power exchange with the grid.

$$GISCF[t_0, t_f] = \frac{\sum_{t=t_0}^{t_f} \min\left[P_{PV}(t) - P_B(t), P_D(t) + P_G(t)\right]}{\sum_{t=t_0}^{t_f} \left(P_{PV}(t) - P_B(t)\right)} \tag{6.10}$$

This parameter $P_G(t)$ is substituted by $P_{G_{soft}}(t)$ or $P_{G_{hard}}(t)$ when a curtailment is applied. Thus, the degree of utilization of the PV production can be studied not only under self-consumption conditions, but also when considering power injection into the electrical network.

$$EEF[t_0, t_f] = GISCF - SCF \tag{6.11}$$

Finally, another indicator is proposed in (6.11), extracted from the combination of the SCF and the GISCF. Named as the 'exported energy factor' (EEF), it accounts for the difference between the maximum amount of energy that can be injected into the grid and the percentage of production that is used for self-consumption. Therefore, this index indicates the net amount of PV production that can be sold, having economic connotations since the balance between PV size and maximum injected energy along the year can be obtained using this index.

6.3 Results

Once the methodology of the system has been described, the obtained results are shown and discussed. First, the high temporal resolution simulations provided by the model are addressed from both the individual and the aggregate point of view. After this, the variation of the daily indexes proposed for studying the interplay between production, consumption and the main grid is illustrated. Finally, three different scenarios are presented on a yearly basis to study how the above-mentioned indexes vary with the PV power, the storage capacity and the proposed control strategies.

The simulation process was implemented using the JAVA programming language. This language and its object-oriented philosophy allowed a flexible implementation with interoperability between operating systems and other features required in this development such as database and network connectivity, concurrency and functional programming. The system was developed as a JAVA enterprise application and was provided with a RESTful application programming interface (API) and a database to store the required information illustrated by the dashed line boxes in Figure 6.2.

Using this API, the simulation parameters and the results can be sent to the system from any device that implements the HTTP protocol, increasing the usability and integrability of the system in other platforms such as MATLAB/SIMULINK for further network topologies' processing. In addition, a general user application (GUI) was developed to ease the use of the system, where the simulation parameters can be configured using the configuration tab from Figure 6.5 and the results visualized as shown in Figure 6.6. This GUI is integrated into the previous one developed in [19].

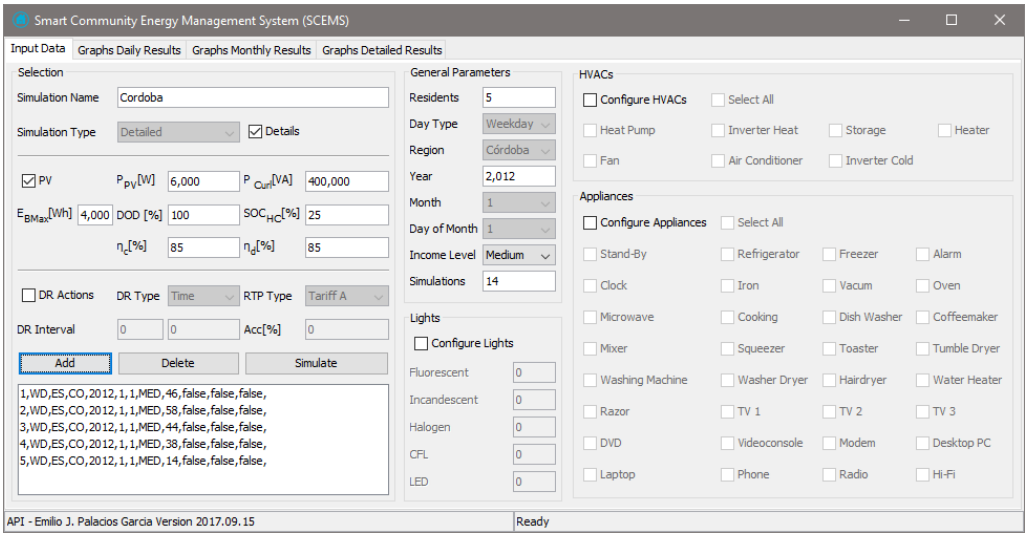

Figure 6.5: GUI for configuring the simulation parameters of the system.

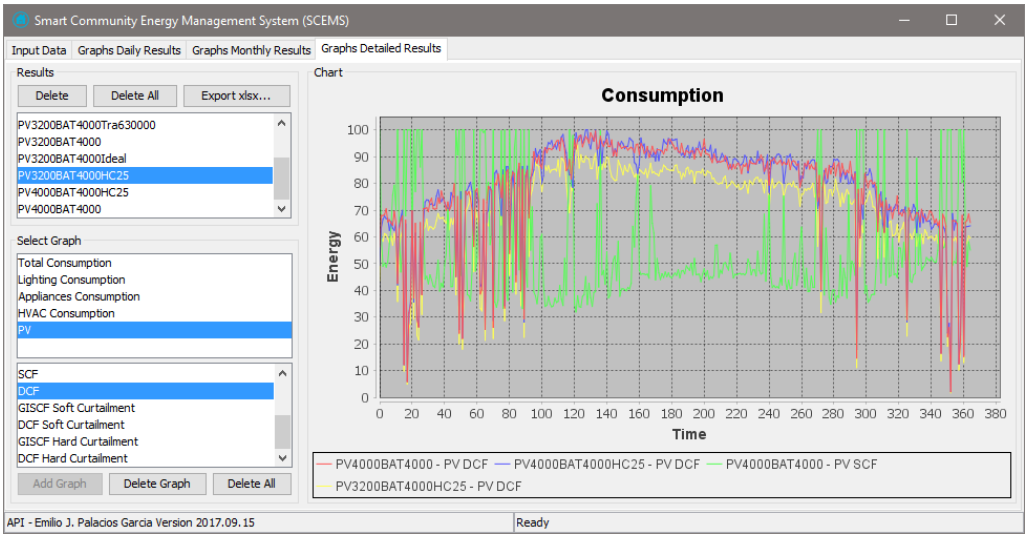

Figure 6.6: GUI for visualizing and analyzing the result of the simulation system.

6.3.1 High Temporal Resolution Simulations

The high temporal resolution of the model allowed analyzing the interplay between the consumer demand, the PV production, the energy storage system and the main grid with 1-min resolution. Moreover, as was indicated in the Methodology, the consumption model simulates each household individually so the daily profile of each dwelling can be observed, as well as the aggregate behavior.

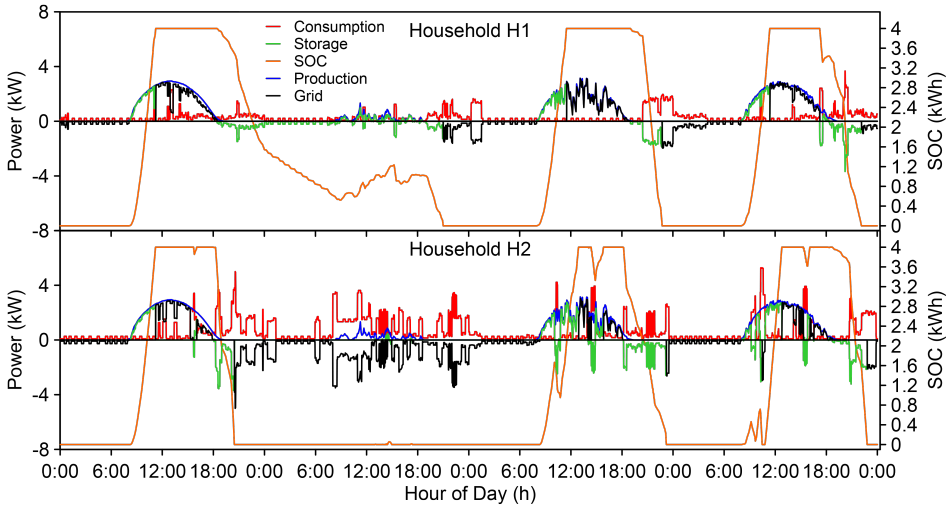

Figure 6.7: Individual results of two households with 3,200 W of PV peak and 4,000 Wh of energy storage installed. Simulation from 18 March–21 March with 1-min resolution.

This fact is illustrated in Figure 6.7, where two individual households are represented from 18 March–21 March. Each household has the same 3,200-W PV installation and 4,000 Wh of energy storage, and they can interact with the main grid using the energy management strategy without HC enhancement.

As can be seen in Figure 6.7, the production profiles were similar since the two households are considered to be located in the same area. Nevertheless, the consumption profiles generated by the model were completely random, yet representing the aggregate trends observed in the region. This is one of the essential features and novelties of the model since each household has its individual and unique profile with a 1-min resolution, which even allows visualizing the on/off cycles of thermostat-controlled appliances such as refrigerators.

This has also a crucial impact on the calculation of the proposed indexes. In Table 6.1, the DCF and the SCF, as well as the daily energy demand E_D and production E_{PV} are indicated for the two households (H1 and H2) without taking into account the grid interaction. Some important conclusions can be drawn by observing both Table 6.1 and Figure 6.7.

For 18 March, the DCF of H1 was higher than the DCF of H2, whereas the SCF of H2 was higher. This means that the self-consumption rate of H1 was higher as might be expected due to the lower demand for the day. However, the direct utilization rate of the PV production was higher for H2, since demand and production were coincident in time, even though the demand was almost double for H2. The same trend was observed for 19 March.

Table 6.1: Indicator and energy figures for individual simulations. Comparison of 2 households. H, household.

Date	DCF (%)		SCF (%)		E_D (kWh)		E_{PV} (kWh)	
	H1	H2	H1	H2	H1	H2	H1	H2
18 March	86.6	61.1	30.7	43.5	6.5	14.0	21.0	21.0
19 March	69.4	11.6	100	100	5.2	23.0	2.7	2.7
20 March	49.1	78.9	28.6	64.2	8.8	12.0	16.5	16.5
21 March	69.61	74.0	33.5	61.5	8.7	14.7	19.4	19.4

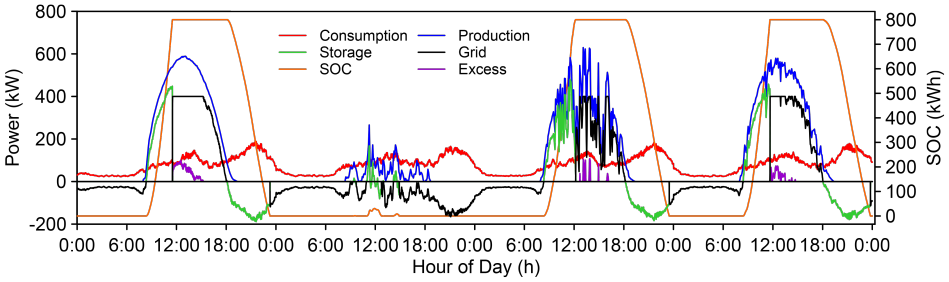

Figure 6.8: Aggregate results of 200 households with 3,200 W of PV peak and 4,000 Wh of energy storage installed each. Simulation from 18 March–21 March with 1-min resolution.

For 20 and 21 March, in contrast to the previous results, the DCF of H2 was higher than the DCF of H1 even when the demand of H2 was almost double. In addition, the utilization rate (SCF) was higher for H2. That points out the importance of high-resolution simulations since, although the demand of H2 was higher, it temporally matched the production, and subsequently, both indexes were improved. This situation could not have been observed if merely the daily energy figures had been taken into account.

Additional conclusions can be obtained if a cluster of 200 households similar to the previously studied ones is simulated for the same range of dates (18–21 March). As can be seen in Figure 6.8, although the consumption profiles were stochastically obtained, the aggregate trend presented the expected behavior with two consumption peaks located during middays and evenings.

Regarding the aggregate PV production, when the whole system was taken into account, an overload occurs for 18, 20 and 21 March. In this case, a soft curtailment strategy was selected, and no HC enhancement was used, so a certain amount of energy E_L is lost.

The figures of the cluster of households are presented in Table 6.2 using the GISCF since the interaction with the main grid is considered. The results show that for good days, the self-consumption factor DCF might achieve values in the range 80–85%. However, for very low production days, it might decrease down to 1/4, making it necessary to import a large amount of energy from the grid. Regarding the percentage of exported energy, even when the soft curtailment is considered, the percentage was higher than 90%.

Table 6.2: Indicator and energy figures for the aggregate simulation of 200 households.

Date	DCF (%)	GISCF (%)	E_D (MWh)	E_{PV} (MWh)	E_{Buy} (MWh)	E_{Sell} (MWh)	E_L (MWh)
18 March	85.0	92.7	1.936	4.191	0.329	2.222	0.100
19 March	27.8	100	1.896	0.541	1.370	0	0
20 March	83.0	98.8	1.957	3.298	0.333	1.396	0.017
21 March	84.6	98.3	1.920	3.890	0.297	1.971	0.034

6.3.2 Evaluation Indexes

The previous results showed the novel features of the model, but they only represent some specific days of a whole year. Therefore, the annual simulation of the proposed indexes was performed using different rates of installed PV peak and storage capacity per household, as well as different curtailment strategies. Again, a cluster of 200 households that represents the average users connected to an MV/LV transformer in the studied region was used, each of the households having the same PV power and storage capacity.

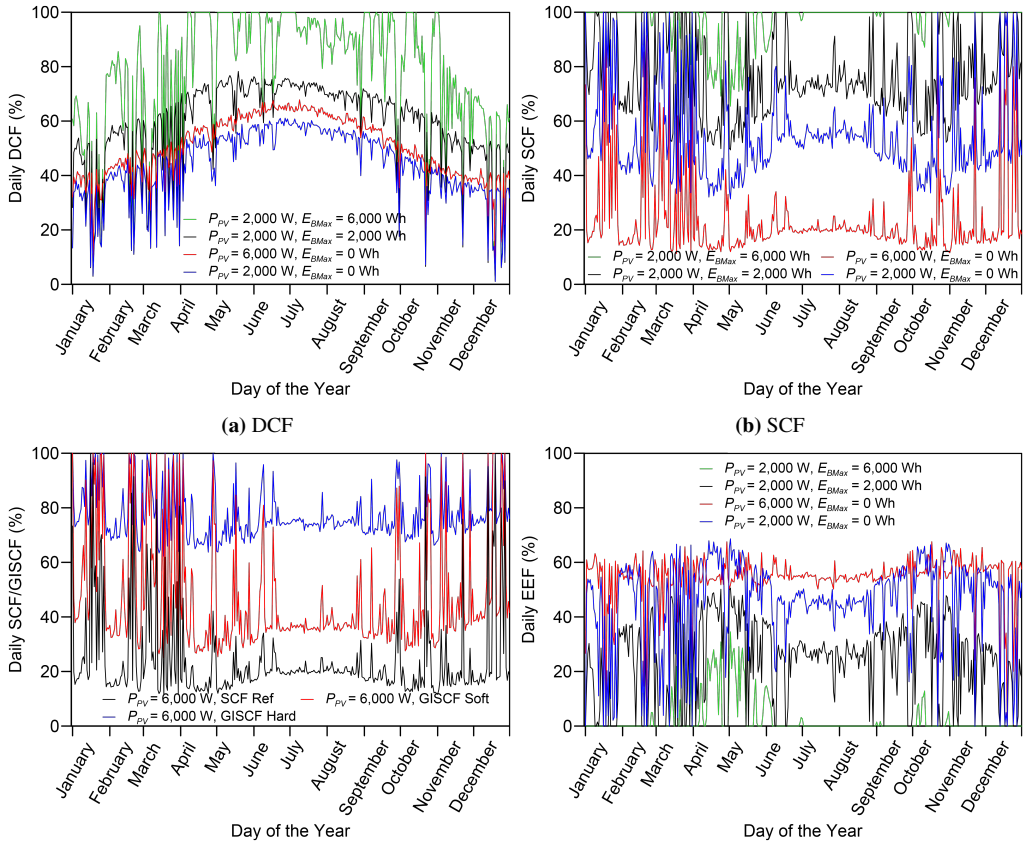

(a) DCF **(b)** SCF

(c) SCF and GISCF **(d)** EEF

Figure 6.9: Daily evaluation indexes for 200 households with different installed PV power and storage capacity per household.

In Figure 6.9, the daily proposed indexes for a whole year are represented. In Figure 6.9 (a), the DCF is illustrated for different values of PV power and storage per household. As can be seen, an increase in the battery capacity produced a far more significant improvement in the DCF than a larger PV installation. Regarding the SCF in Figure 6.9 (b), large PV installations always worsened and decreased the degree of utilization, whereas, on the contrary, high values of battery storage improved the index.

Figure 6.9 (c) presents the SCF when no interaction with the grid is allowed (black line). It depicts the low degree of utilization of the solar resource in islanded installations due to the non-temporal coincidence of production and consumption. When the excess of PV production was allowed to be injected in the grid according to some curtailment strategy, the increment in the utilized energy was 20% for the hard curtailment (red line) and 60% for the soft curtailment.

Finally, as regards the EEF in Figure 6.9 (d), it decreased when the battery capacity was increased, since more energy could be locally collected instead of being injected into the grid. However, when the PV power was increased such as in the case of the red solid line, the EEF mainly increased during the summer months with good production days, yet for some days, the values were lower since the energy injected had to be curtailed.

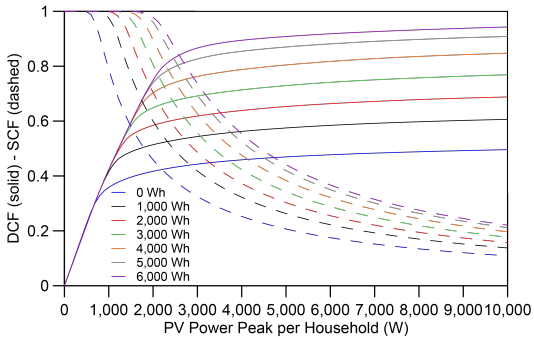

Figure 6.10: Annual DCF (solid lines) and SCF (dashed lines) variation with the installed PV power and storage capacity per household.

6.3.3 Yearly Calculated Index Scenarios and EMS Strategies

The previous calculations have shown some initial results about the influence of the PV power and the storage capacity in the proposed indexes. Nevertheless, another interesting feature of the model is that Expressions (6.8)–(6.11) can be extended to different periods of time such as a whole month or year by modifying the limits t_0 and t_f for the instantaneous calculus. In this way, the annual average evolution of these figures was observed in three scenarios using the same cluster of 200 households and varying the installed PV power and storage capacity per household.

6.3.3.1 Off-Grid System

The base scenario without grid interaction was analyzed. The obtained results are shown in Figure 6.10, where the X-axis represents the installed PV power peak per household, whereas the Y-axis indicates either the annual DCF (solid lines) or the annual SCF (dashed lines). In addition, the different storage capacities per house are illustrated in different colors.

Figure 6.10 depicts how the DCF (solid lines) increased when the PV power peak increases, whereas in the case of the SCF (dashed lines), the opposite trend was observed. In contrast, for a given PV power peak, if the capacity of the storage system was increased, both the DCF and the SCF were improved, but not by the same percentage.

6.3.3.2 Grid Interaction

The base scenario exposed that in the case of off-grid systems, both a high amount of installed PV power and storage capacity were required in order to cover the energy demand along the year, whereas a great amount of produced energy was lost, as well. However, when considering the interaction with the grid, part of this excess might be injected always considering the HC limitations.

This interaction can be studied with the proposed GISCF as illustrated in Figure 6.11. The solid lines represent the soft curtailment strategy, whilst the hard curtailment situation is shown with dashed lines. As in the previous case, different storage capacity and PV power per household were studied considering an MV/LV transformer with a rated power of 400,000 VA.

As can be seen, the utilization degree was dramatically impacted by both HC strategies, but especially in the case of hard curtailment, where the energy lost due to the operative limits of the network was 40% higher. In addition, it can be pointed out that, although a higher storage capacity increased the degree of utilization, its impact was not very significant with an improvement of only 5% per 1,000 kWh of installed capacity.

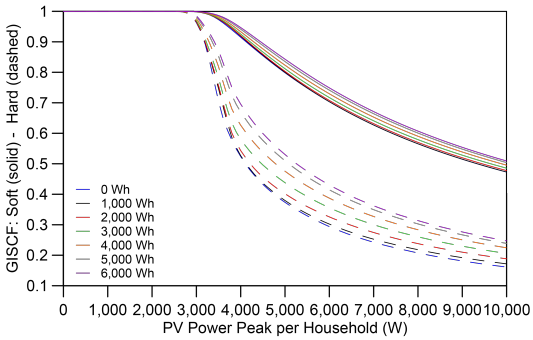

Figure 6.11: Annual GISCF variation with the installed PV power and storage capacity for soft curtailment (solid lines) and hard curtailment (dashed lines).

Further conclusions can be drawn if the EEF is studied. Figure 6.12 represents the proposed index to quantify the amount of injected PV production (EEF). Again, the soft curtailment situation is represented by the solid lines, whereas the dashed lines illustrate the hard curtailment strategy.

Figure 6.12 depicts that the injected generation was not directly proportional to the PV installed power, but under the curtailment situation, a given amount of PV power existed for which the energy exported to the grid was maximum, which was in fact slightly different for each curtailment situation. This result is especially relevant for planning PV installations, since the exported energy can be maximized and, subsequently, the benefits obtained from feed-in tariffs, whilst minimizing the initial investment and the payback period.

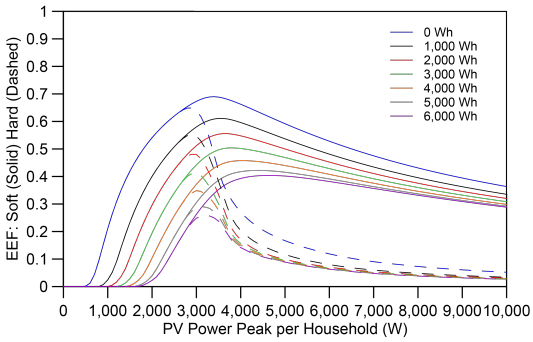

Figure 6.12: Annual EEF vs. installed PV power and storage capacity when soft curtailment (solid lines) or hard curtailment (dashed lines) are applied.

6.3.3.3 PV HC Enhancement

Finally, the third scenario illustrates the impact of control strategies focused on the enhancement of the HC. Since this control strategy depends on the battery capacity, three situations were considered, which are 4,000 Wh of storage capacity per household and no enhanced control, 6,000 Wh per household and no enhancement and 4,000 Wh per household with two-level control using 75% of the capacity for individual control (HEMS) ($E_{B\,HCmax}$), whereas keeping a 25% available for HC strategies of the whole smart community (SCEMS).

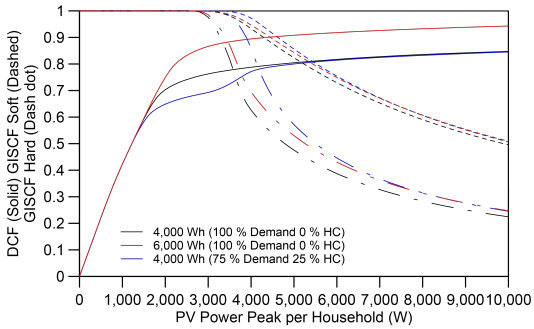

Figure 6.13: Comparison between the increase in the storage capacity and the application of grid interaction optimization techniques.

The results can be seen in Figure 6.13 where the three situations were represented. Black lines correspond to the 4,000 Wh storage system with no enhancement; the red lines represent the 6,000-Wh storage and no enhancement; and the blue lines are the proposed control algorithm to improve the HC. On the X-axis, different PV power peaks per household are illustrated, whereas the Y-axis accounts for the value of the indexes, which are the DCF (solid lines) and the GISCF both for the soft-curtailment situation (dashed lines) and the hard-curtailment strategy (dash-dot lines).

As can be seen in Figure 6.13, increasing the individual battery capacity improved the DCF by around 10%. However, the GISCF was almost unaltered showing an extremely small improvement. Nevertheless, when the HC enhanced algorithm was applied, the GISCF improved around 15% in the case of hard curtailment and around 5% for the soft curtailment when the values of PV power installed were not excessively large. If high installation rates of PV power are to be controlled with this strategy, a large percentage of battery should be devoted to the HC strategy or it should also be combined with an increase in the storage capacity.

In addition, as is shown in Figure 6.14, the amount of energy that can be prevented from lost for a year in the whole cluster of households is very significant, especially in the case of hard curtailment situations. Using a larger local capacity saved around 50 MWh for the soft curtailment and 100 MWh for the hard curtailment. Opposed to this, with the new two-level charging strategy, the same savings were achieved for the soft curtailment with almost half of the PV power. In the case of the hard curtailment, a peak of

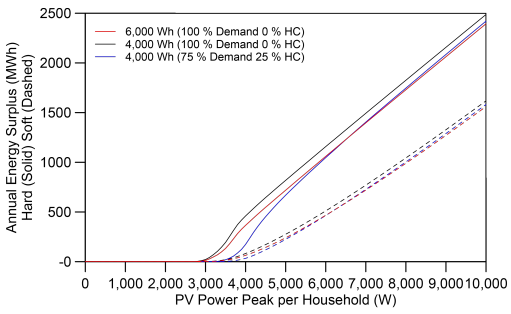

(a) Annual energy surplus

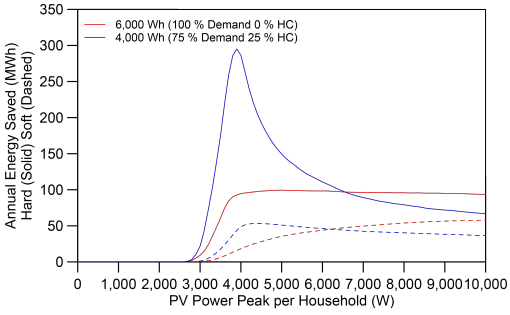

(b) Annual energy savings

Figure 6.14: Annual energy surplus and energy saved for a cluster of 200 households when soft curtailment (dashed lines) or hard curtailment (solid lines) is applied.

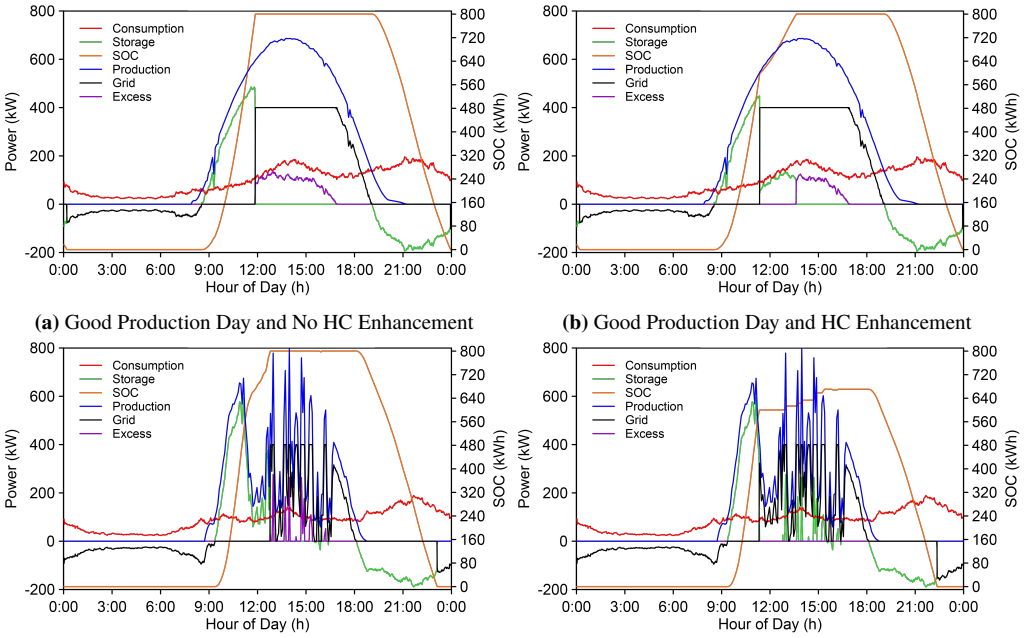

(a) Good Production Day and No HC Enhancement

(b) Good Production Day and HC Enhancement

(c) Bad Production Day and No HC Enhancement

(d) Bad Production Day and HC Enhancement

Figure 6.15: Daily simulation for and a cluster of 200 households with 4,000 W of PV power and 4,000 Wh of energy storage each. Comparison of HC enhancement strategies.

300 MWh was reached when 4,000 W of PV power per household were considered, which means around 25% of the total annual consumption of the whole cluster of households.

It can also be noticed that the DCF was affected by PV power values that do not cause a serious energy surplus in the main grid (0–3,000 W). Regarding this, two options can be adopted. On the one hand, a variable $E_{B\,HCmax}$ can be calculated so the fixed 75% value proposed in Figure 6.13 can be dynamically changed along the year depending on the irradiance forecasting. On the other hand, the enhanced algorithm can be chosen to be applied only for large PV powers.

The reason for the DCF decrease can be seen in the high temporal resolution results represented in Figure 6.15 for a good production day (a) and (b) and a bad production day (c) and (d).

As can be seen when comparing Figure 6.15 (a) and (b) for a good production day, the two-level battery management algorithm allowed reducing the energy that is lost due to the soft curtailment, whilst the storage was fully charged. Thus, almost the same DCF cover factor was reached in both cases as can be seen in Table 6.3, whereas the GISCF was increased in the enhanced case and the energy lost E_L reduced to zero. However, in the bad production day, shown in Figure 6.15 (c) and (d) the selected $E_{B\,HCmax}$ prevented the storage system from being fully charged during the day for the enhanced strategy (d), and therefore, the DCF was lower. Nevertheless, the amount of lost energy was null as indicated by the GISCF of 100%.

If both the energy imports from the grid E_{Buy} and the energy lost due to the soft curtailment E_L, indicated in Table 6.3, are taken into account, it can be observed that the balance is positive or zero. In the case of a good production day, when the enhanced strategy was applied, the energy saved was 199 kWh, while the energy that needed to be imported from the grid was the same for both controls. Likewise, in the bad production day, although 110 kWh extra had to be imported from the grid in the enhanced strategy, 87 kWh were prevented from being lost, compensating the decrease in the DCF.

Table 6.3: Indexes and energy for 2 days with and without HC enhancement strategy.

Type of Day	DCF (%)		GISCF (%)		E_{Buy} (kWh)		E_L (kWh)	
	No HC	HC	No HC	HC	No HC	HC	No HC	HC
Good Production	87.5	87.4	90.6	94.6	292.2	292.8	470.5	271.3
Bad Production	77.0	71.6	96.8	100	477.3	587.5	86.7	0

Therefore, although the proposed two-level charging control might have an impact on the DCF, if the whole cluster of households and its interaction with the main grid are considered, the stability of the network will not only be guaranteed, but the utilization rate of the PV installation will also increase.

6.4 Conclusions

A high temporal resolution simulation environment has been presented that allows assessing the integration of distributed renewable energies and storage systems in households, whilst interacting with the main grid, by means of a stochastic demand model and historical data from a PV installation.

Various evaluation indexes have also been proposed in this work. Along with the previously defined DCF and SCF, the authors have developed and used two new indicators named GISCF and EEF. The first index allows assessing the renewable production utilization when the system interacts with the main grid under some constraints such as the HC of the network. This index has been shown to be valid to quantify the impact of curtailment strategies when both the PV production and the capacity of the battery storage system are incremented.

The second index, EEF, has proven its application in the context of energy planning for assessing the most suitable combination of PV power and storage capacity that might allow maximizing the power injected into the grid. Therefore, in a context where feed-in tariffs are applied, it would help choose the initial investment and minimize the payback period.

Using the models and the evaluation indexes, a series of high-temporal simulations have been performed, showing the possibilities of the system from the individual and the aggregate point of view. Likewise, the yearly evolution of the proposed indicators has been studied for different rates of PV power and storage capacity per household.

Based on the previous results, three scenarios were evaluated for a whole year and for different rates of PV power and storage. The off-grid scenario showed the influence of the PV power and the battery capacity in the SCF and the DCF. Larger capacities always improved the both indexes, but the installation of more PV power only helps increase the DCF, whereas the SCF is worsened. The same results were obtained in the grid connected scenario, the newly developed indexes GISCF and EEF comprising a key point to assess the soft and hard curtailment strategies when interacting with the grid.

Finally, a novel two-level charging strategy has been proposed aiming to maximize the renewable energy utilization, while preventing the network overload. The algorithm has shown a substantial improvement of the GISCF, and although the DCF is worsened in some cases, the amount of energy that is prevented from being lost fully justified its use.

This DCF decrease can be corrected with the use of a dynamic $E_{B\,HCmax}$, taking into account the energy demand prediction, as well as the production forecast and the capacity of the transformer itself. In this way, not only the GISCF will be improved, but the DCF will also remain almost unaltered. Therefore, future works will be focused on the development of a predictor for the $E_{B\,HCmax}$ based on the irradiance and the demand estimation.

Acknowledgement

This work was supported by the Spanish Ministry of Economy and Competitiveness under Research Project TEC2013-47316-C3-1-P and TEC2016-77632-C3-2-R.

Nomenclature

n_h	Number of households
n_b	Number of electrical bus
$P_D(t)$	Power demand
$P_{PV}(t)$	PV power production
$P_B(t)$	Battery power
$P_{GP}(t)$	Power interchanged with the grid if no curtailment
$P_G(t)$	Power interchanged with the grid with curtailment
$P_L(t)$	Power lost due to the curtailment strategies
P_{net}	Difference between the PV power $P_{PV}(t)$ and demand $P_D(t)$
P_{Curt}	Global power curtailment of the household cluster
$*P_{Curt}$	Local power curtailment of each PV installation
$P_{G_{soft}}(t)$	Power when soft curtailment is applied
$P_{G_{hard}}(t)$	Power when hard curtailment is applied
$Curt$	Type of curtailment being applied
$Soft$	Soft curtailment strategy
$Hard$	Hard curtailment strategy
$E_B(t)$	Instantaneous energy stored in the battery
E_{Bmin}	Maximum depth of discharge of the battery
E_{Bmax}	Charging threshold of the battery
$E_{B\,HCmax}$	Charging threshold for HC strategies
$\%SOC_{HC}$	Percentage of charge reserved for HC strategies
E_D	Energy demand
E_{PV}	Energy produced by the PV system
E_{Buy}	Energy bought from the grid
E_{Sell}	Energy sold to the grid
E_L	Energy lost due to curtailment strategies
$O(t)$	Active occupancy profile
$Irr(t)$	Solar irradiance
$Act(t)$	Activity probability
$T(t)$	Ambient temperature
P_{light}	Consumption of the lighting system of a household
P_{app}	Consumption of the appliances of a household
P_{HVAC}	Consumption of the HVAC system of a household
P_{tot}	Total consumption of a household
η_{inv}	Solar inverter efficiency
η_{inst}	Solar installation efficiency
η_G	Solar generator efficiency
P_{peak}	PV power peak per household
P^*_{peak}	PV power peak of the reference installation

References

[1] Eurostat, Energy, transport and environment indicators - 2015 edition (2015). URL: http://ec.europa.eu/eurostat/documents/3217494/7052812/KS-DK-15-001-EN-N.pdf

[2] I. M. Moreno-Garcia, A. Moreno-Munoz, V. Pallares-Lopez, M. J. Gonzalez-Redondo, E. J. Palacios-Garcia, C. D. Moreno-Moreno, Development and application of a smart grid test bench, Journal of Cleaner Production 162 (2017) 45–60. doi:10.1016/j.jclepro.2017.06.001.

[3] S. Zhou, M. A. Brown, Smart Meter Deployment in Europe: A Comparative Case Study on the Impacts of National Policy Schemes, Journal of Cleaner Production 144 (2016) 22–32. doi:10.1016/j.jclepro.2016.12.031.

[4] B. D. Olaszi, J. Ladanyi, Comparison of different discharge strategies of grid-connected residential PV systems with energy storage in perspective of optimal battery energy storage system sizing, Renewable and Sustainable Energy Reviews 75 (2017) 710–718. doi:10.1016/j.rser.2016.11.046.

[5] A. Moreno-Munoz, F. Bellido-Outeirino, P. Siano, M. Gomez-Nieto, Mobile social media for smart grids customer engagement: Emerging trends and challenges, Renewable and Sustainable Energy Reviews 53 (2016) 1611–1616. doi:10.1016/j.rser.2015.09.077.

[6] E. J. Palacios-García, Y. Guan, M. Savaghebi, J. C. Vásquez, J. M. Guerrero, A. Moreno-Munoz, B. S. Ipsen, Smart metering system for microgrids, in: IECON 2015 - 41st Annual Conference of the IEEE Industrial Electronics Society, IEEE, 2015, pp. 3289–3294. doi:10.1109/IECON.2015.7392607.

[7] E. J. Palacios-Garcia, E. Rodriguez-Diaz, A. Anvari-Moghaddam, M. Savaghebi, J. C. Vasquez, J. M. Guerrero, A. Moreno-Munoz, Using smart meters data for energy management operations and power quality monitoring in a microgrid, in: 2017 IEEE 26th International Symposium on Industrial Electronics (ISIE), IEEE, 2017, pp. 1725–1731. doi:10.1109/ISIE.2017.8001508.

[8] P. Siano, Demand response and smart grids - A survey, Renewable and Sustainable Energy Reviews 30 (2014) 461–478. doi:10.1016/j.rser.2013.10.022.

[9] P. Palensky, D. Dietrich, Demand side management: Demand response, intelligent energy systems, and smart loads, IEEE Transactions on Industrial Informatics 7 (3) (2011) 381–388. doi:10.1109/TII.2011.2158841.

[10] N. Etherden, M. H. Bollen, Overload and overvoltage in low-voltage and medium-voltage networks due to renewable energy - Some illustrative case studies, Electric Power Systems Research 114 (2014) 39–48. doi:10.1016/j.epsr.2014.03.028.

[11] N. Etherden, M. H. J. Bollen, Dimensioning of energy storage for increased integration of wind power, IEEE Transactions on Sustainable Energy 4 (3) (2013) 546–553. doi:10.1109/TSTE.2012.2228244.

[12] S. Cao, K. Sirén, Impact of simulation time-resolution on the matching of PV production and household electric demand, Applied Energy 128 (2014) 192–208. doi:10.1016/j.apenergy.2014.04.075.

[13] J. Widén, E. Wäckelgård, J. Paatero, P. Lund, Impacts of different data averaging times on statistical analysis of distributed domestic photovoltaic systems, Solar Energy 84 (3) (2010) 492–500. doi:10.1016/j.solener.2010.01.011.

[14] J. Widén, E. Wäckelgård, A high-resolution stochastic model of domestic activity patterns and electricity demand, Applied Energy 87 (6) (2010) 1880–1892. doi:10.1016/j.apenergy.2009.11.006.

[15] J. Widén, M. Lundh, I. Vassileva, E. Dahlquist, K. Ellegård, E. Wäckelgård, Constructing load profiles for household electricity and hot water from time-use data-Modelling approach and validation, Energy and Buildings 41 (7) (2009) 753–768. doi:10.1016/j.enbuild.2009.02.013.

[16] I. Richardson, M. Thomson, D. Infield, A. Delahunty, Domestic lighting: A high-resolution energy demand model, Energy and Buildings 41 (7) (2009) 781–789. doi:10.1016/j.enbuild.2009.02.010.

[17] I. Richardson, M. Thomson, D. Infield, C. Clifford, Domestic electricity use: A high-resolution energy demand model, Energy and Buildings 42 (10) (2010) 1878–1887. doi:10.1016/j.enbuild.2010.05.023.

[18] E. McKenna, M. Thomson, High-resolution stochastic integrated thermal-electrical domestic demand model, Applied Energy 165 (2016) 445–461. doi:10.1016/j.apenergy.2015.12.089.

[19] E. J. Palacios-Garcia, A. Chen, I. Santiago, F. J. Bellido-Outeiriño, J. M. Flores-Arias, A. Moreno-Munoz, Stochastic model for lighting's electricity consumption in the residential sector. Impact of energy saving actions, Energy and Buildings 89 (2015) 245–259. doi:10.1016/j.enbuild.2014.12.028.

[20] E. J. Palacios-Garcia, I. Santiago, A. Moreno-Munoz, J. M. Flores-Arias, F. J. Bellido-Outeiriño, Distributed Energy Resources Integration and Demand Response. The Role of Stochastic Demand Modelling, in: A. Moreno-Munoz (Ed.), Large Scale Grid Integration of Renewable Energy Sources, The Institution of Engineering and Technology (IET), London, 2017, Ch. Chapter 8:, p. 300.

[21] E. Akarslan, F. O. Hocaoglu, A novel method based on similarity for hourly solar irradiance forecasting, Renewable Energy 112 (2017) 337–346. doi:10.1016/j.renene.2017.05.058.

[22] G. Chicco, V. Cocina, P. Di Leo, F. Spertino, A. Massi Pavan, Error assessment of solar irradiance forecasts and AC power from energy conversion model in grid-Connected photovoltaic systems, Energies 9 (1) (2016) 8. doi:10.3390/en9010008.

[23] D. Trillo-Montero, I. Santiago, J. J. Luna-Rodriguez, R. Real-Calvo, Development of a software application to evaluate the performance and energy losses of grid-connected photovoltaic systems, Energy Conversion and Management 81 (2014) 144–159. doi:10.1016/j.enconman.2014.02.026.

[24] I. M. Moreno-Garcia, E. J. Palacios-Garcia, V. Pallares-Lopez, I. Santiago, M. J. Gonzalez-Redondo, M. Varo-Martinez, R. J. Real-Calvo, Real-Time Monitoring System for a Utility-Scale Photovoltaic Power Plant, Sensors 16 (6) (2016) 770. doi:10.3390/s16060770.

[25] I. Sartori, A. Napolitano, K. Voss, Net zero energy buildings: A consistent definition framework, Energy and Buildings 48 (2012) 220–232. doi:10.1016/j.enbuild.2012.01.032.

[26] J. Salom, A. J. Marszal, J. Widén, J. Candanedo, K. B. Lindberg, Analysis of load match and grid interaction indicators in net zero energy buildings with simulated and monitored data, Applied Energy 136 (2014) 119–131. doi:10.1016/j.apenergy.2014.09.018.

[27] National Statistics Institute of Spain. Ministry of Economy and Competitiveness, Time Use Survey (2010). URL: http://www.ine.es/en/prensa/eet_prensa_en.htm

[28] M. A. Lopez, I. Santiago, D. Trillo-Montero, J. Torriti, A. Moreno-Munoz, Analysis and modeling of active occupancy of the residential sector in Spain: An indicator of residential electricity consumption, Energy Policy 62 (2013) 742–751. doi:10.1016/j.enpol.2013.07.095.

[29] I. Santiago, M. A. Lopez-Rodriguez, D. Trillo-Montero, J. Torriti, A. Moreno-Munoz, Activities related with electricity consumption in the Spanish residential sector: Variations between days of the week, Autonomous Communities and size of towns, Energy and Buildings 79 (2014) 84–97. doi:10.1016/j.enbuild.2014.04.055.

[30] A. Pardo, V. Meneu, E. Valor, Temperature and seasonality influences on Spanish electricity load, Energy Economics 24 (1) (2002) 55–70. doi:10.1016/S0140-9883(01)00082-2.

[31] J. Moral-Carcedo, J. Vicéns-Otero, Modelling the non-linear response of Spanish electricity demand to temperature variations, Energy Economics 27 (3) (2005) 477–494. doi:10.1016/j.eneco.2005.01.003.

[32] S. J. Smullin, Thermostat metrics derived from HVAC cycling data for targeted utility efficiency programs, Energy and Buildings 117 (2016) 176–184. doi:10.1016/j.enbuild.2016.02.018.

[33] G. Hoogsteen, A. Molderink, V. Bakker, G. J. M. Smit, Integrating LV network models and load-flow calculations into smart grid planning, in: 2013 4th IEEE/PES Innovative Smart Grid Technologies Europe, ISGT Europe 2013, IEEE, 2013, pp. 1–5. doi:10.1109/ISGTEurope.2013.6695427.

7

Smart metering system for Microgrids

Emilio J. Palacios-García[1], Yajuan Guan[2], Mehdi Savaghebi[2], Juan C. Vásquez[2], Josep M. Guerrero[2], Antonio Moreno-Munoz[2], and Brian S. Ipsen[3]

[1]Departamento de Arquitectura de Computadores, Electrónica y Tecnología Electrónica, Escuela Politécnica Superior, Universidad de Córdoba, Córdoba, Spain.
[2]Department of Energy Technology. Aalborg University. Aalborg, Denmark.
[3]Kamstrup A/S. Denmark.

Abstract

Smart meters are the cornerstone in the new conception of the electrical network or Smart Grid (SG), providing detailed information about users' energy consumption and allowing the suppliers to remotely collect data for billing. Nevertheless, their features are not only useful for the energy suppliers, but they can also play a big role in the control of the Microgrid since the recorded power and energy profiles can be integrated in energy management systems (EMS). In addition, basic power quality (PQ) disturbances can be detected and reported by some advanced metering systems. Thus, this paper will expose an example of Smart Meters integration in a Microgrid scenario, which is the Intelligent Microgrid Lab of Aalborg University (AAU). To do this, first the installation available in the Microgrid Lab will be introduced. Then, three different test scenarios and their respective results will be presented, regarding the capabilities of this system and the advantages of integrating the Smart Meters information in the Microgrid control.

This conference paper has been published in *IECON 2015 - 41st Annual Conference of the IEEE Industrial Electronics Society, Yokohama, 2015, pp. 003289-003294. doi: 10.1109/IECON.2015.7392607*.

7.1 Introduction

The concept of Smart Grid (SG) has completely changed the conception of the electrical network, where the classical chain of centralize energy production, transmission, and end users' consumption has been substituted by a bi-directional power flow, with distributed generation (DG) and consumption, and new emerging types of energy resources. In this context the Smart Meters play a main role, not only giving the suppliers access to accurate data for billing, but also collecting information of the end users, and establishing a two-ways communication [1].

This new approach has been possible due to the implementation of new communication protocols and a complex metering infrastructure. In consequence, the direct manual billing has been substituted by a metering network composed of communication hubs, data concentrators, central system units and different control centers, defining a new Grid architecture [2].

In the beginning, these protocols were mainly proprietary and the development of an advanced measuring network had to face a wide range of issues. Nevertheless, a standardization process has been promoted to assure the interconnection between different Smart Meter units. In this context, protocols such as DLMS/COSEM (IEC 62056-53 [3] and IEC 62056-62 [4]), SML (IEC 62056-58 [5]), M-Bus (EN 13757 [6]) or IEC 61850 [7], are today ones of the most common implemented standard for Smart Meters and substations data collection [8].

This standardization process has implied significant benefits from the point of view of system integration and control in Microgrid networks. A Microgrid can be described as an electrical system where a bi-directional flow of energy exits. It is usually composed of many DG units (renewable or not) and the whole system can be either isolated or connected to the main grid [9]. Therefore, to control this shared energy flow, a well-developed communication infrastructure is an essential part of the Microgrid conception [10].

Likewise, another important feature of the Microgrid networks is the usage of a hierarchical control strategy. The primary control is focused on the inner control of each DG unit (droop control), the secondary control is supposed to restore frequency and voltage amplitude deviations due to the inertias. The tertiary control regulates the power flows between the Microgrid [11], [12].

The reported frequency of the Smart Meters measures is usually slow, 5 to 15 minutes, to be integrated into the primary or secondary control. However, they can be employed in a higher level for matching production and demand in the Microgrid network. Thus, it is in the so-called tertiary control level of the Microgrid where the Smart Meters can provide measures for the EMS, allowing the implementation of demand response (DR) techniques [13], [14].

In addition, some advanced Smart Meter systems report not only information about energy consumption, but also basic power quality (PQ) indices, with increasing importance due to the proliferation of non-linear loads. These PQ measures can range from voltage profile measurement to harmonic distortion calculations [15, 16].

In this paper, the benefits of the Smart Meter systems for the Microgrid will be addressed, showing a real example in a lab-scale Microgrid. For this aim, the structure of this paper is as following: in Section 7.2 the installation available in Aalborg University Microgrid Lab for emulating a Microgrid network is presented. Section 7.3 will provide different test scenarios defined to evaluate the operation of the Smart Meters and the obtained results will be commented. In Section 7.4, future works in the Microgrid Lab are described. Finally, Section 7.5 is dedicated to the conclusions about the systems and tests.

7.2 System Overview

The Smart Meter system is integrated into the Aalborg University (AAU) Intelligent Microgrid Lab [17]. The whole system is composed of 6 workstations that can be supplied using a central DC source of up to 80 kW, PV panels, Wind Turbines or flywheel storage. The general schema of the Lab can be observed in

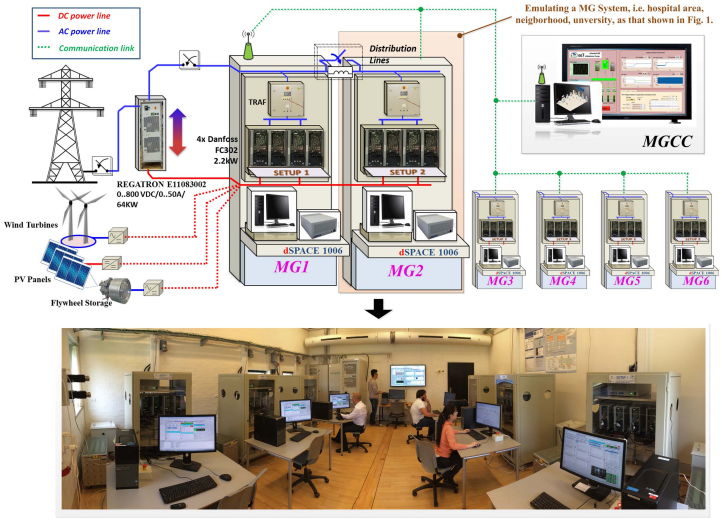

Figure 7.1: Overview of the Intelligent Microgrid Lab facilities.

Figure 7.1. Each set-up includes four DC-AC three phase converters with LCL output filters, monitored switches for load operation and two Smart Meters from Kamstrup Company.

The four three phase converters can be individually controlled using a dSPACE real-control platform managed from a desktop PC. In addition, the different switches on the system can be operated from this PC, enabling the remote control of the whole system, that can be connected to a wide range of load types.

7.2.1 Smart Meters

As mentioned before, each workstation contains two Kamstrup Smart Meters, each one with a different purpose. The industrial Smart Meter 351B is used to measure the energy flow of the whole workstation, so it can measure DG, whilst the other model the 382L is attached to the load consumption, and therefore it can be regarded as an individual consumer.

Both models of Smart Meters are for three-phase measurements. They measure active positive energy (EN 50470-1 and EN 50470-3 [18]), reactive energy, and active negative energy (IEC 62052-11 [19], IEC 62053-21 and IEC 62053-23 [20]). In addition, average and maximum power values during the billing period and different tariffs can be configured in the Smart Meter, recording individual information in each tariff period.

Along with these basic features, as can be desirable in any Smart Meter, additional characteristic are provided by these models. The two employed Smart Meters have a built-in EEPROM memory where the load profile information can be stored. The amount of data that can be recorded depends on the number of energy variables and integration period selected for the energy. Thus, the number of days range from 450 days when only the positive active energy is recorded every 60 minutes, down to 17 days, when positive and negative active and reactive energy is monitored with 5 minutes of integration period.

Another common feature of the two models is the measurement of the voltage quality. The Smart Meter is able to record deviations in the nominal voltage within a given range and during a defined period of time. The default characteristic of this function is minimum ±10% voltage deviation detection for events longer than 10 minutes.

Finally, an additional characteristic only available in the 382L model is the possibility of defining a customized analysis logger. This logger can register up to 16 different variables with sampling periods of 5, 15, 45 or 60 minutes. Depending on the number of variables and the selected resolution, the logger's depth can range from 2 days up to 520 days. Therefore, in this model, not only the load profile is available, but also the average voltage, current, power, etc. can be recorded in different intervals [21].

7.2.2 Communication

Another important feature of the Smart Meters is the implemented communication protocol. The Kamstrup meters installed in the Microgrid Lab are compliance with the IEC 62056 standard [3], which is the International Standard version of the DLMS/COSEM specification (Device Language Message Specification/Companion Specification for Energy Metering). In particular, these Smart Meters support the DLMS/COSEM specification over TCP/IP, GSM or over a serial communication through an optical port.

From these three options, the communication procedure implemented in the Lab is the TCP/IP connection since it provides a scalable solution, where all the Smart Meters installed in the Lab can be accessed using the TCP/IP protocol over the same network structure. In addition, a ZigBee Communication is implemented between the 382L Smart Meter and an In-Home display only for global energy monitoring. However, since the goal of the experiments is to study the real detailed measures of the Smart Meters it has not been used.

7.3 Test Scenarios and Results

In order to test the capabilities of the installed Smart Meters, a simulated scenario was developed using one of the workstations in the Microgrid Lab of Aalborg University. As it can be observed in Figure 7.2, the test set-up was composed of one of the four three-phase DC-AC converters working as a Voltage Source Inverter

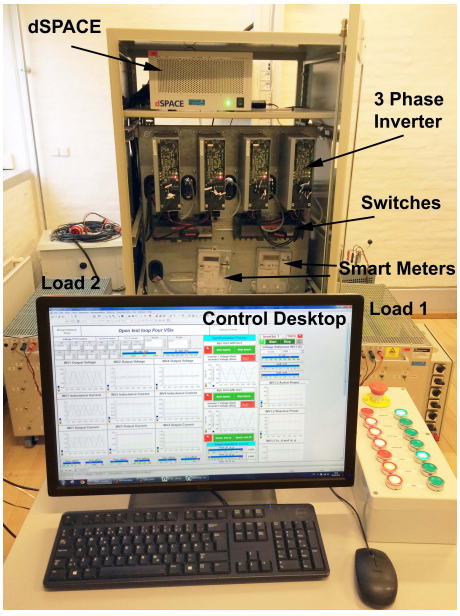

Figure 7.2: Workstation configuration for the tests.

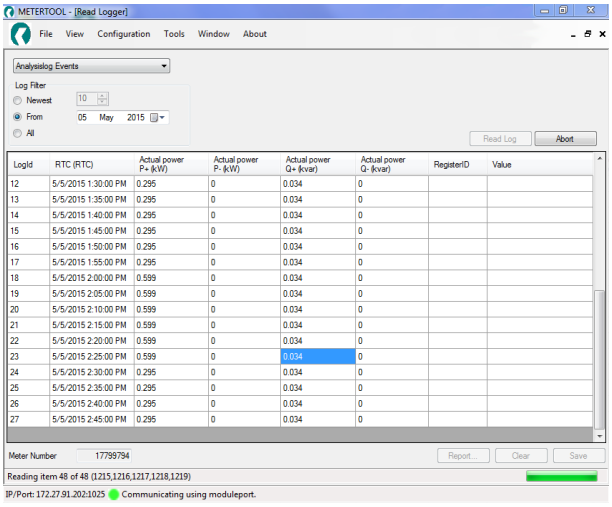

Figure 7.3: Screenshot of Kamstrup MeterTool software.

(VSI). This converter was supplying two different loads (in both sides of the cabinet) connected in parallel throw two individual monitored switches. In addition, two system Smart Meters were monitoring the energy flow between the converter and the two loads. Finally, all the system was controlled from the desktop PC and the dSPACE, whereas the Smart Meters data were collected using a TCP/IP communication and over an Ethernet connection.

Using this configuration, three different test scenarios were analyzed. First, the possibilities of the Smart Meters to record the power and energy demand profile were studied by means of switching the two loads on and off. Secondly, the capability of these Smart Meters to detect voltage quality events was tested by changing the voltage reference of the three-phase converter. Finally, the possibility to detect changes in the network parameters due to the droop control strategy was tested.

To obtain the data recorded by the Smart Meters, the MeterTool software, provided by Kamstrup, was used. A screenshot of the application is shown in Figure 7.3. This screenshot corresponds to the Analysis logger of the Smart Meter where each column corresponds to a monitored variable. In addition, these data can be exported in a wide range of format. For the performed tests, the data were exported as CSV files (Comma Separated Values) in order to build the different graphs that will be subsequently shown.

7.3.1 Load Profile Measurement

The first scenario aims to simulate a power demand variation, to test the capability of the Smart Meters for measuring and recording the load profile of the system. For this purpose, two different load were used, named as Load 1 and Load 2. Load 1 was an inductive load with 460 Ω and 50 mH per phase, whereas Load 2 was a pure resistive load with 460 Ω per phase.

Using the two loads with different characteristic a simulated power demand change was forced in the system. The VSI was started together with Load 1 and after a defined period of time, Load 2 was turned on. Finally, after 30 minutes, Load 2 was switched off again.

The obtained results were recorded by the Smart Meter using the load profile memory and were extracted in CSV format using the MetorTool Kamstrup Software. The load profile logger recorded four variables: active positive and negative energy, and reactive positive and negative energy. However, since the energy is

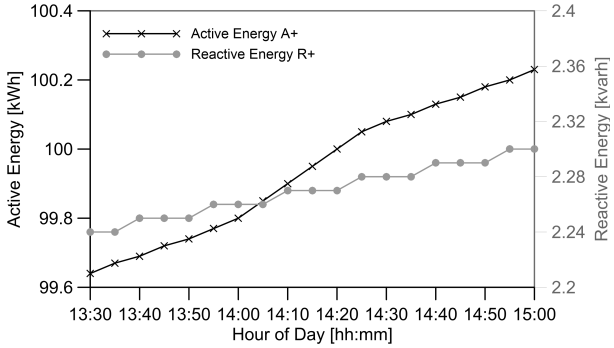

Figure 7.4: Scenario 1. Active and Reactive Energy during a Load Disturbance.

only sunk by the loads the active and reactive negative energy do not present any variation, so they are not represented in Figure 7.4. It should also be denoted that the energy is an aggregated variable and therefore, the initial value at the beginning of the experiment was not zero due to the previous usage of the Smart Meter. Another important consideration is that all the results will be represented as a line-scatter plot where the real values of the Smart Meter correspond to the points, whilst the line is just a linear interpolation between adjacent measures.

As it can be seen in Figure 7.4, the active energy (solid black line with cross symbols) at the start of the test had a value of 99.7 kWh (left Y-axis), whereas the reactive energy (solid grey line with point symbols) equals to 2.24 kvarh (right Y-axis). Three different zones can be observed in the active energy profile, characterized by a different slope. One from 13:30 h to 14:00 h, the second one from 14:00 h to 14:25 h and the third one from 14:25 h until the end of the experiment. In contrast, the reactive energy profile seems to have an average constant slope.

These three zones clearly correspond with three different power intensities in the active power consumption. This power can be easily obtained from the energy profile since the integration period is known (5 minutes). However, due to the existence of an analysis logger in the 382L Smart Meter, the system was configured to store the average active and reactive power during each integration period. The different measures obtained by the Smart Meter are graphically represented in Figure 7.5.

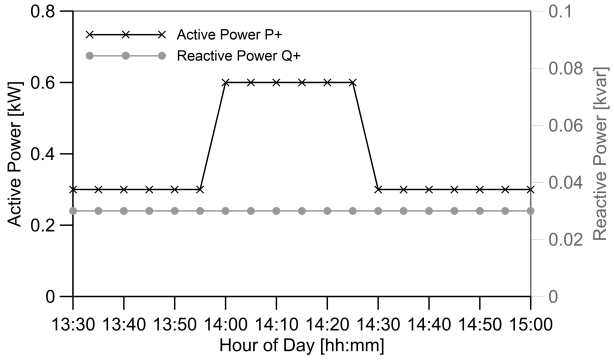

Figure 7.5: Scenario 1. Active and Reactive Power during a Load Disturbance.

Now, the load variation can be observed in terms of power consumption. As it was expected, after switching on the Load 2, the active power measured by the Smart Meter rose up from 0.295 kW to 0.599 kW, whereas the reactive power kept a constant value, since Load 2 was pure resistive. The opposite happened between 14:25-14:30 h when Load 2 was turned off.

7.3.2 Voltage Quality Events Detection

The second test scenario was focused on the detection of voltage quality events using the Smart Meter system. For this aim, the DC-AC three phase converter was operated again as a VSI, but changing now the voltage reference value for the control loop. With this configuration two perturbations in the voltage were generated, firstly an undervoltage and secondly an overvoltage.

The detection of voltage quality events is recorded in a logger inside both 351B and 382L Smart Meters. This logger stores not only the deviations of the supplied voltage outside the normal operation range, but it also detects and notice the power cut off and the switch on events of the meter system. In order to illustrate this behavior, a screenshot of the voltage quality logger of one of the Smart Meters during the Test is shown in Table. 7.1.

The previously presented test and this second one were carried out approximately from 13:30 h to 16:20 h. Before this time, the Smart Meters were off and after the two scenarios the system was again turned off. This can be perfectly seen in the report of the voltage quality logger, where a power enabled event was detected at 13:28 and a power cut off at 16:19.

Nevertheless, two additional events were also recorded in between. One of the lines of the system seems to have a undervoltage during approximately 30 minutes. Thus, to validate the occurrence of the event, before the start of the simulation the 382L Smart Meter Analysis logger was also configured to store the voltage in the 3 lines of the system.

Figure 7.6 illustrates the evolution of the three phase voltages during the test period where the voltage perturbation was introduced. Again the real measured data are shown as different points, whereas the line is just an interpolation. In addition, two dashed lines have been represented to indicate the maximum and minimum thresholds of the system, which for these case were $\pm 10\%$ of the nominal voltage (230 V).

Figure 7.6 shows that at the start of the test, the voltages of the three phases of the system are within the admissible range. Furthermore, a small unbalance can be observed between three-phase, that can be justified since the real resistance and inductance values of the load are not perfectly similar for all the phases.

After approximately 10 minutes, the voltage of the system was slowly decreased. This operation promoted that the voltage in line 3 reached a value outside the nominal range. The first sampled value outside range was reported to be 203 V at 13:15 h. However, regarding Table 7.1 and Figure 7.6 it can be noticed that the event occurs before the refresh of the register. This depicts an important fact in the behavior of the system. In spite of updating the measuring registers after the integration period (5 minutes), the instantaneous values of voltage and current are measured to calculate power and energy, otherwise it would have been impossible to have reported the undervoltage event with a precision of seconds.

The undervoltage situation is maintained during approximately 30 minutes. After this time, the voltage is restored to the nominal value. As it was illustrated in Figure 7.1, the system is also able to detect and record the instant when the voltage is again between the limits.

Table 7.1: Smart Meter Voltage Quality Events Logger.

RTC (RTC)	Hour counter (h)	Voltage extremity (V)	Voltage event
5/5/2015 1:28:42 PM	66	0	System L1,L2,L3: Power enabled - above cutoff threshold
5/5/2015 3:12:14 PM	68	0	System L3: Voltage below limits
5/5/2015 3:41:51 PM	68	91	System L3: Voltage within limits from minimum
5/5/2015 4:19:25 PM	69	0	System L1,L2,L3: Power cut off

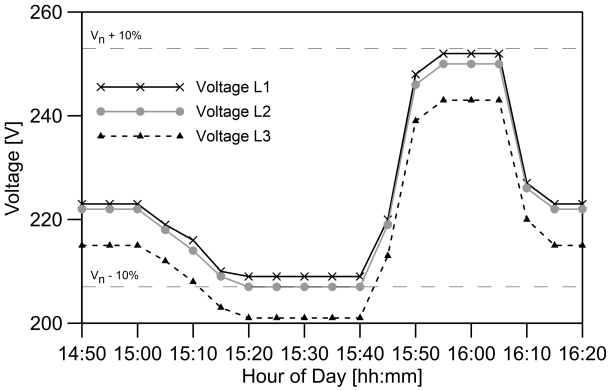

Figure 7.6: Scenario 2. Voltage per phase during a variation in the reference voltage of the VSI.

Subsequently, an overvoltage situation is forced. However, in this case, the voltage was selected so that it was still within the limits to prove the behavior of the system tolerance for voltage quality event detection. As it can be observed in Figure 7.6, the voltage in line 1 reached a value near to the maximum threshold. The value of this voltage is equal 252 V, a figure which is inside the limits since 230+10% is 253 V. Thus, as it was expected no voltage quality event is reported in Table 7.1 during this period.

7.3.3 Monitoring of Droop Control

The third and final scenario was focused on the detection of deviations in the system parameters, due to the control operations of the Microgrid, specifically the droop control. This control strategy is employed to regulate the active and reactive energy power flow by means of changing the frequency and voltage of the DGs respectively, a behavior that can be clearly observed in the Microgrid when it is working in islanded mode, which means without connection to the main grid, and no voltage and frequency restoration strategy (secondary control) are implemented.

The operation mode of the droop control is summarized by the equations (7.1) and (7.2), where ω is the angular frequency of the DG, E is the voltage, and P and Q are the active and reactive power exchanged with the Microgrid. On the other hand, k_p and k_v are the droop coefficients, which determine the slope of the control strategy and, therefore, the frequency and voltage deviation for achieving a determined power exchange.

$$\Delta\omega = -k_p \cdot P \tag{7.1}$$

$$\Delta E = -k_v \cdot Q \tag{7.2}$$

Since the Smart Meters installed in the Lab are not able to measure frequency, only the droop control strategy for reactive power exchange was tested. For this aim, the same loads of the Scenario 1 were used, but activating now the droop control in the DC-AC converter, which works as a VSI emulating a DG unit. In addition, the switch on sequence was inverted, so now the Load 2 (pure resistive load) is first turned on, and subsequently Load 1 (inductive load) is activated to cause a change in the demanded reactive power.

The obtained results are shown in Figure 7.7, where the three-phase voltages are represented together with the demanded reactive power. As it can be seen, from 12:50 h to 13:05 h, only Load 2 is activate, so no reactive power consumption is observed, and therefore the voltage of all the lines is around the reference, which was set to be 220 V.

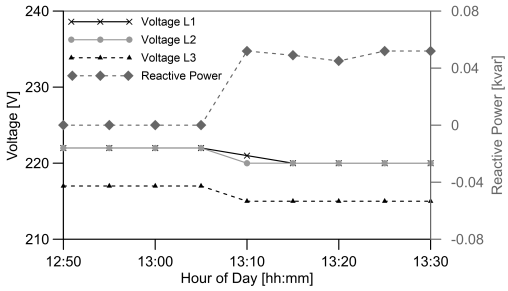

(a) Voltage and Reactive Power Profiles

RTC (RTC)	Actual power P+ (kW)	Actual power Q+ (kvar)	Average Voltage L1 (V)	Average Voltage L2 (V)	Average Voltage L3 (V)
5/11/2015 12:50:00 PM	0.306	0	222	222	217
5/11/2015 12:55:00 PM	0.306	0	222	222	217
5/11/2015 1:00:00 PM	0.306	0	222	222	217
5/11/2015 1:05:00 PM	0.306	0	222	222	217
5/11/2015 1:10:00 PM	0.596	0.052	221	220	215
5/11/2015 1:15:00 PM	0.596	0.049	220	220	215
5/11/2015 1:20:00 PM	0.596	0.045	220	220	215
5/11/2015 1:25:00 PM	0.596	0.052	220	220	215
5/11/2015 1:30:00 PM	0.596	0.052	220	220	215

(b) MeterTool Analysis Logger Screenshot

Figure 7.7: Scenario 3. Voltage and Reactive Power during a load disturbance, using droop control.

However, Load 1 is activated between 13:05-13:10 h, so the DG needs to supply now reactive energy. Since the droop control is activated, the system starts to decrease the nominal voltage in order to fulfill the requirements of the load.

The voltage deviation can be observed in Figure 7.7, where a screenshot of the analysis logger of the MeterTool software is shown. The average deviation in all the phases was observed to be 2 V, whereas the average change in the reactive power demand was 50 var. Thus, the theoretical droop coefficient k_v, that was selected to be equal to -0.05, can be compared with the measured value. This is illustrated in (7.3).

$$k_v = \frac{\Delta E}{\Delta Q} = \frac{-2}{50} = -0.04 \tag{7.3}$$

As it can be seen this value is very near to the theoretical one, and the observed error might be due to the resolution of the measures of the Smart Meter. Therefore, the Smart Meters have demonstrated to be able to detect not only load disturbance and voltage quality issues, but they can also notice the influence of the different control strategies employed in the Microgrid context, when neither frequency nor voltage restoration strategy is implemented, and the Microgrid is working in islanded mode.

7.4 Future Work

The presented metering infrastructure inside the Microgrid Lab will be soon substituted by a more advanced and powerful system which will be based on the OMNIA Suite of Kamstrup. OMNIA Suite is an advanced metering infrastructure (AMI) which includes Smart Meter units, data concentrators, network communication and data management and storage, so the Lab will be able to emulate a SG [21].

As it is shown in Figure 7.8, all the Smart Meters within the system will be connected using the Wireless standard (EN 13757-5 [6]) using the radio mesh communication version. In addition, others Smart Meter systems regarding district heating and water will be implemented, using Wireless M-Bus Standard (EN 13757-4 [6]), to have a complete simulation of a real system.

The data from the Smart Meter will be collected in a data concentrator using the radio mesh communication. As well, this data concentrator will be connected to a PC using Ethernet, GPRS or 3G, and the DLMS/COSEM standard. Inside the PC a software called UtiliDriver® will be responsible for integrating the data from the Smart Meter with the rest of the system.

This central software will not store any data, but it will allow the intercommunication with the Smart Meters using an Open Web Service API (Application Protocol Interface). Thus, the protocol complexity is simplified, so the Smart Meter measurements can be integrated into others systems with a relatively low complexity.

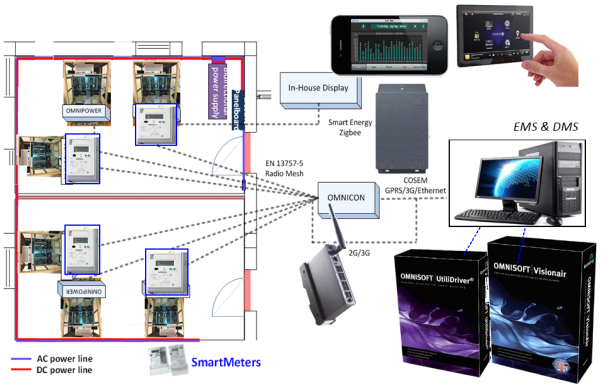

Figure 7.8: Conceptual schema of the future Smart Metering Infrastructure in the Microgrid Lab of Aalborg University.

7.5 Conclusions

The work has presented the benefits of integrating Smart Metering systems inside the electrical grid and specifically in Microgrids. A real application of the Smart Meters to monitor a workstation in the Aalborg University Microgrid Lab was commented, showing three test scenarios for studying the load profile measurement, the voltage quality events detection, and the droop control strategy, and having discussed their respective results.

The Smart Meters have demonstrated their capability to report in the most basic case at least the energy consumption profile and in other more advanced systems the power, voltage and current, too. All of this is due to the wide range of communication possibilities offered by the Smart Meter, which have allowed us to monitor the system from a central PC.

In addition, the report frequency for these energy and power measurements has been observed to range between 5 minutes and 1 hour integration interval, a period that can be fast enough for implementing EMS and DR strategies in a tertiary control level without additional equipment and investment.

The system has also shown the possibility of detect voltage quality events with a resolution of 1 second. This depicts that the real sampling frequency of the system to measure current and voltage is much faster. Therefore, the Smart Metering system can be seen as the most suitable part of the system to implements not only power and energy monitoring but also to detect some basic PQ issues.

Furthermore, although the measures from the Smart Meters cannot be directly used for the inner control loops, the system has shown to be able to detect voltage deviations due to the operations strategies of the Microgrid, such as the Droop control for the regulation of reactive power flow.

Regarding these ideas, the future implementation that will be carried out in the Microgrid Lab has been exposed. This new Smart Metering system will provide a centralized communication and data collection, more advanced PQ measurement and the integration with other systems.

Acknowledgment

This work was supported by the Technology Development and Demonstration Program (EUDP) through the Sino-Danish Project "Microgrid Technology Research and Demonstration" (meter.et.aau.dk).

References

[1] J. Zheng, D. W. Gao, L. Lin, Smart meters in smart grid: An overview, in: IEEE Green Technologies Conference, 2013, pp. 57–64. doi:10.1109/GreenTech.2013.17.

[2] K. D. Craemer, G. Deconinck, Analysis of State-of-the-art Smart Metering Communication Standards, in: Proceedings of the 5th Young Researchers Symposium, 2010, pp. 1–6. doi:10.1109/TSG.2012.2218834.

[3] IEC 62056-53, Data exchange for meter reading, tariff and load control. Part 53: COSEM application layer (2006).

[4] IEC 62056-62, Data exchange for meter reading, tariff and load control. Part 62: Interface Classes (2006).

[5] IEC 62056-58, Data exchange for meter reading, tariff and load control. Part 58: Smart Message Language (2006).

[6] EN 13757, Communication system for meters and remote reading of meters (2008).

[7] IEC 61850, Communication networks and systems in substations (2003).

[8] S. Feuerhahn, M. Zillgith, C. Wittwer, C. Wietfeld, Comparison of the communication protocols DLMS/COSEM, SML and IEC 61850 for smart metering applications, in: 2011 IEEE International Conference on Smart Grid Communications, SmartGridComm 2011, 2011, pp. 410–415. doi:10.1109/SmartGridComm.2011.6102357.

[9] F. Katiraei, R. Iravani, N. Hatziargyriou, A. Dimeas, Microgrids management, IEEE Power and Energy Magazine 6 (3) (2008) 54–65. doi:10.1109/MPE.2008.918702.

[10] Y. Yan, Y. Qian, H. Sharif, D. Tipper, A survey on smart grid communication infrastructures: Motivations, requirements and challenges, IEEE Communications Surveys and Tutorials 15 (1) (2013) 5–20. doi:10.1109/SURV.2012.021312.00034.

[11] J. M. Guerrero, M. Chandorkar, T.-L. Lee, P. C. Loh, Advanced Control Architectures for Intelligent Microgrids—Part I: Decentralized and Hierarchical Control, IEEE Transactions on Industrial Electronics 60 (4) (2013) 1254–1262. doi:10.1109/TIE.2012.2194969.

[12] J. M. Guerrero, P. C. Loh, T.-L. Lee, M. Chandorkar, Advanced Control Architectures for Intelligent Microgrids—Part II: Power Quality, Energy Storage, and AC/DC Microgrids, IEEE Transactions on Industrial Electronics 60 (4) (2013) 1263–1270. doi:10.1109/TIE.2012.2196889.

[13] S. Mohagheghi, J. Stoupis, Z. Wang, Z. Li, H. Kazemzadeh, Demand Response Architecture: Integration into the Distribution Management System, in: 2010 First IEEE International Conference on Smart Grid Communications, IEEE, 2010, pp. 501–506. doi:10.1109/SMARTGRID.2010.5622094.

[14] D. Kathan, Assessment of Demand Response and Advanced Metering, Tech. rep., Federal Energy Regulatory Commission (2012).

[15] M. Music, A. Bosovic, N. Hasanspahic, S. Avdakovic, E. Becirovic, Integrated power quality monitoring system and the benefits of integrating smart meters, in: 2013 International Conference-Workshop Compatibility And Power Electronics, IEEE, 2013, pp. 86–91. doi:10.1109/CPE.2013.6601134.

[16] S. Ali, K. Weston, D. Marinakis, K. Wu, Intelligent meter placement for power quality estimation in smart grid, in: 2013 IEEE International Conference on Smart Grid Communications (SmartGridComm), IEEE, 2013, pp. 546–551. doi:10.1109/SmartGridComm.2013.6688015.

[17] Research Program in Microgrid. Aalborg University, Denmark. URL: http://microgrids.et.aau.dk

[18] EN 50470-3, Electricity Metering Equipment (A.C.). Part 3: Particular requirements - Static meters for active energy (class indexes A, B and C) (2007).

[19] IEC 62052, Electricity metering equipment (A.C.). General requirements, test and test conditions. (2003).

[20] IEC 62053, Electricity Metering Equipment (A.C.). Particular requirements. (2003).

[21] Kamstrup A/S. URL: https://www.kamstrup.com/

8

Using Smart Meters data for energy management operations and power quality monitoring in a Microgrid

Emilio J. Palacios-Garcia[1], Enrique Rodriguez-Diaz[2], Amjad Anvari-Moghaddam[2], Mehdi Savaghebi[2], Juan C. Vasquez[2], Josep M. Guerrero[2], and Antonio Moreno-Munoz[1]

[1]Departamento de Arquitectura de Computadores, Electrónica y Tecnología Electrónica, Escuela Politécnica Superior, Universidad de Córdoba, Córdoba, Spain.
[2]Department of Energy Technology. Aalborg University. Aalborg, Denmark.

Abstract

Smart metering devices have become an essential part in the development of the current electrical network toward the paradigm of Smart Grid. These meters present in most of the cases, functionalities whose analysis capabilities go further beyond the basic automated meter readings for billing purposes, integrating home or building area networks (HAN/BAN), alarms and power quality indicators in some cases. All those characteristics make this widely spread equipment a free, accurate and flexible source of information that can replace expensive and dedicated devices. Therefore, this paper presents the integration of a commercial advanced metering infrastructure (AMI) in the context of a smart building with an energy management system (EMS). Furthermore, power quality monitoring based on this AMI is explained. All the details regarding the implementation in a laboratory scale application, as well as the obtained results, are provided.

This conference paper has been published in *2017 IEEE 26th International Symposium on Industrial Electronics (ISIE), Edinburgh, 2017, pp. 1725-1731. doi: 10.1109/ISIE.2017.8001508*.

8.1 Introduction

Nowadays, smart meters (SMs) are rapidly spreading among the European Countries, as well as the United States due to a global consensus about the necessity of decreasing the electrical consumption and changing the centralized paradigm of the grid to a distributed architecture. This trend is being promoted in some cases by national or international commissions, as in the case of Europe, and, although the penetration rate is not homogeneous [1], these devices are playing and will play a main role in the new smart grid [2].

The advanced features that they add to the electrical grid fully justify the success and significance of the SMs against the classical metering equipment, where the periodic manual billing has been replaced by a bidirectional information flow between customers and utilities [3]. All of these, mainly due to the development of a vast network infrastructure and specific international communication standards [4].

In this context, the advanced metering infrastructures (AMI) have found two principal fields of application that go beyond the simple energy billing. Those fields are the energy management systems (EMS) [5] and the system state monitoring, specifically in terms of power quality (PQ).

In the first case, for the development of EMS or demand response (DR) strategies, additional metering devices were to be installed to successfully implement the control and energy reduction measures [6]. Nevertheless, the SMs provide now power measurements of each household or even a whole buildings with time intervals that range from 5 minutes up to 1 hour. This is fast enough for performing the optimization tasks [7]. Moreover, it is even possible to disaggregate each appliance used by the dwellings, although this operation requires advanced processing and higher sampling rates [8].

Likewise, the assessment of the network state, although performed in a relatively simple way, can be provided by the SMs [9]. Thus, not only have these devices benefits for the end users, but the network operator can take advantage of the distributed measures. Therefore, the basic PQ capabilities of the meters can be used in order to have real-time information of the whole system with a minimum investment [10].

Therefore, this paper describes the integration of an AMI in a microgrid to perform energy management operations and power quality monitoring. This integration is addressed with a proposed network topology and using a commercial AMI that was implemented in different scenarios employing a laboratory scale simulation of an actual microgrid applied to a building.

8.2 System Architecture

In order to contextualize the integration of the SMs in a microgrid regulated by an EMS, the system is described first from the hardware point of view and, subsequently, from the information and communication technology (ICT) viewpoint.

8.2.1 Hardware Installation

The proposed framework is shown in Figure 8.1. As it can be seen, an AC/DC microgrid was selected, where the individual consumers (Apartments) have an AC connection, whereas the distributed energy resources (Wind Turbine and Solar PV Panels), the common facilities (Load) and other elements such as electrical vehicles (EV) are connected to a DC bus.

This DC side is interfaced with the AC grid of the building so all the individual proprietaries can benefit from the energy generation in order to decrease the amount of energy that must be supplied by the main grid, whilst the DC side reduces the number of necessary converters. Therefore, as proposed in [11] this architecture has been selected since it increases the efficiency of the whole system.

In this framework, if energy management operations, as well as power quality supervision, are to be implemented, the SMs can be used at different points of the system. First, since the whole building or community is operating as a microgrid that is able to exchange energy with the grid, and this energy has to be billed, a metering device should be placed in the connection represented by the green circle A.

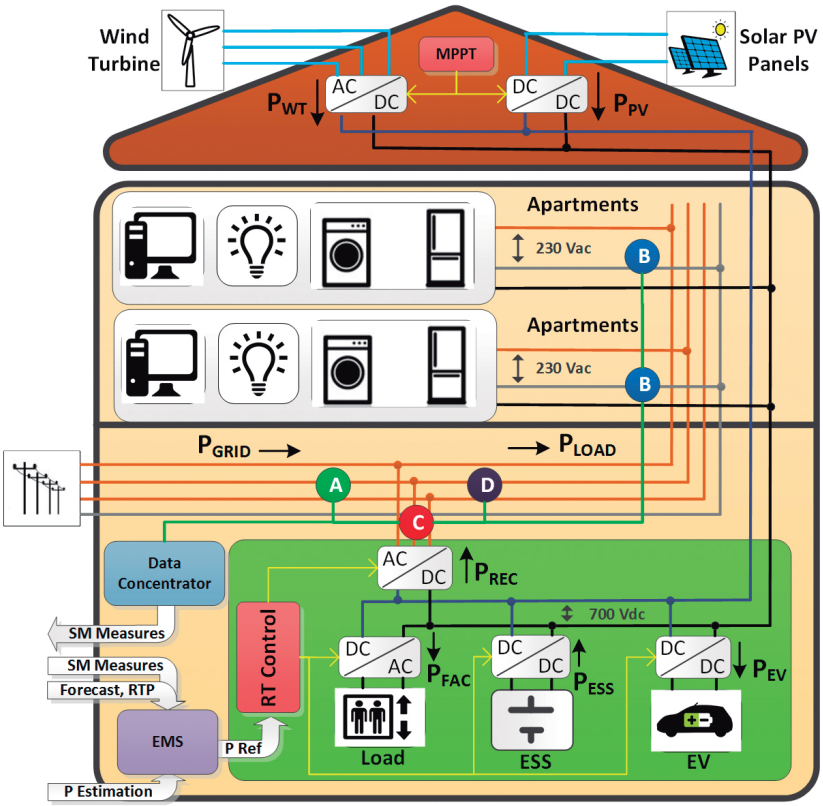

Figure 8.1: Architecture of a AC/DC microgrid for a residential building.

In addition, each household has a different consumption pattern, so an individual SM is needed to account for this, as it is shown in Figure 8.1 by the blue circles named B. If SMs are installed in A and B, both the individual consumption and the energy exchanged with the grid can be measured for billing purposes. Furthermore, information about the individual consumption is available for the EMS, as well as global (A) and individual (B) indicators for PQ monitoring.

Nevertheless, additional SMs can be installed in the interface between the building AC grid and the rectifier (red circle C) if additional information about the energy exchanges and the PQ of the power injected into the AC building network want to be collected. Moreover, for more detailed information, an additional SM can be placed in the common AC bus of the building, represented in Figure 8.1 by the purple circle D. This SM might not send new information to the EMS since it measures the aggregate demand of each individual SMs B, but it will provide information about the global state of the AC bus, and can help to detect PQ issues such as voltage events or total harmonic distortion (THD).

8.2.2 Communications and logical architecture of the system

From the communication point of view, as it can be seen in Figure 8.2, the system consists of three main logical blocks, which are the AMI, composed of the physical devices, as well as the software for obtaining the measurements, the meter data management system (MDMS), and the EMS.

The AMI is divided into two levels. In the first layer, the AMI physical Network can be found (red block). This part comprises all the physical SMs, as well as the data concentrator that collects their measures periodically, and it is permanently connected to a Network Time Protocol (NTP) server to synchronize the timestamps. The communication between the SMs and the data concentrator is based on the standard EN 13757-5 that implements a radio mesh topology. Moreover, they are compliance with the IEC 62056, the international standard of the DLMS/COSEM specification (Device Language Message Specification/Companion Specification for Energy Metering).

Regarding the electrical measures, all the model of Smart Meters being used (3-phase meters, single-phase meters and CT-Meters), belonging to the Kamstrup OMNIA suite, are compliance with international standards. They measure active positive energy (EN 50470-1 and EN 50470-3), reactive energy, and active negative energy (IEC 62052-11, IEC 62053-21 and IEC 62053-23), as well as PQ according to EN 50160.

The second layer (gray block) integrates the logical software provided by the manufacturer to ensure efficient interoperability with the AMI network. This software communicates over Ethernet with the data concentrator and implements all the back-end processes that are necessary to configure the system, perform on-demand operation readings and capture the periodic records. In parallel with this, the data concentrator is also able to forward the alarms produced with the AMI network. For that aim, a service is constantly listening and capturing these events that can subsequently be sent by email or posted to a web service.

The MDMS block is responsible for capturing the data, store them and make them accessible. Therefore, it is the key connection point between the AMI and additional features to be implemented. It is composed of two layers. The first one is the management unit (blue block). This software was implemented using the LabVIEW visual programming language and is composed of two main systems. On the one hand, a RESTFul server was built using the NI WebServer in order to capture the Alarms that are forwarded by the Alarm Server. The information contained in these alarms, sent as an XML packet, is read by the LabVIEW program and subsequently stored. On the other hand, a desktop application with a general user interface (GUI) was developed for performing two tasks: to query on-demand readings from the AMI Network and to read the periodic measurements stored in the SMs' loggers.

It should by pointed out that although the head-end software is connected to a local MongoDB database, it is a temporal storage with a maximum deep of 3 days and with a fixed structure that cannot be modified. Moreover, the alarms triggered in the system are not recorded by this database. Thus, the second layer of the MDMS is the storage system (green block), implemented using the database engine MariaDB. This database is structured in a flexible way, so new meters and types of measurements can be added. Furthermore, it is not limited to a specific manufacturer, since the measured variables are defined by their standard OBIS codes (IEC 62056).

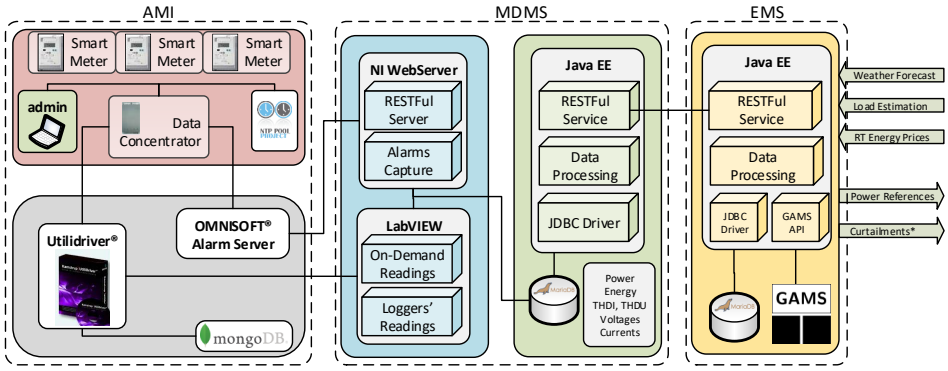

Figure 8.2: Logical Architecture of the System.

On top of this, the JAVA application implements a RESTful service for reading the data with various layers of security for the measures, allowing a simple communication using the HTTPS protocol and JSON or XML format. This makes the system compatible with any other third-party software.

Finally, the EMS (yellow block) queries the necessary measurements from the SMs to the data management system and together with additional information such as weather forecast, real-time energy prices or load estimation generates the power references that can be used by the converters. Another JAVA EE server is used for this task, connected to GAMS software for running the optimization process.

Regarding the PQ supervision, the MDMS is able to record global indicators such as current and voltage THD (THDI, THDU) and power factor, as well as different PQ events (voltage variations, unbalances, etc). Those indicators can be read using the web service and also by means of the LabVIEW application that will be described in the subsection 8.3.2.

8.3 Experimental Results

The system was tested using a small scale laboratory setup that can emulate different element of the building microgrid such as the households consumption, the battery charger or the rectifier. This setup is equipped with the SMs.

8.3.1 Setup installation

The test bench for the experiments can be visualized in Figure 8.3, as well as the central system and data concentrator for the AMI (block in the top-right corner). This setup is part of the Microgrids Research Laboratory at Aalborg University [12].

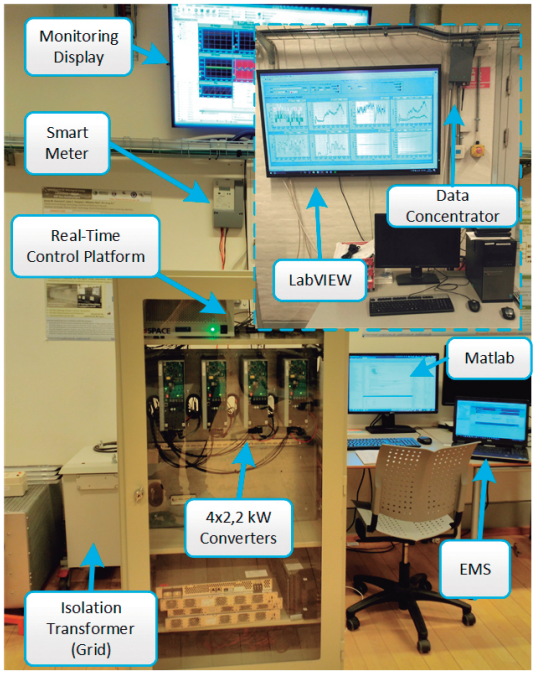

Figure 8.3: Hardware Setup for the tests.

The setup is composed of 4 converters with a total nominal power of 8 kW connected to the AC grid through an AC isolation transformer and to a common DC bus. In this system, the SMs are placed in the AC connection. These SMs are connected, as was mentioned in Section 8.2.2, to a data concentrator using a wireless mesh network. This data concentrator, shown in the block located at the top-right site of Figure 8.3, is connected to a central PC where the MDMS is running, which will be described in the following section.

Regarding the four converters, they are commanded from a real-time control platform which contains the necessary inner voltage, current and power control loops to ensure the stability of the system. Using an Ethernet communication, the real-time control platform is linked to a PC where the system is monitored. In addition, the power references for the power control are sent to the platform from a PC running MATLAB which uses the same Ethernet communication.

On the top of that, these power references are obtained from an EMS previously developed [13]. This EMS is running on a laptop connected to the local network of the laboratory through a wireless protocol (Wi-Fi). The system has as one of the input vectors the SMs readings corresponding to the households and global consumption, so it communicates with the MDMS for obtaining the readings, therefore, closing the loop.

As far as the PQ monitoring is concerned, no specific application has been developed, yet the THDI and THDU of each meter, as well as the voltage and PQ events, can be read from the MDMS using the provided web service, and visualized through a LabVIEW application whose functionalities will be described in the next subsection.

8.3.2 Application for smart metering monitoring

As explained in Section 8.2.2, the communication between the AMI and the MDMS is implemented by using a LabVIEW application. This application integrates most of the functionalities needed for the communication with the SMs installed in the above-described setup, and provides a GUI to manage the system. The GUI, shown in Figure 8.4, is composed of two main parts. On the top of the screen, the panels corresponding to different configuration options and notifications can be found. The rest of the screen is devoted to a tab structure with different capabilities.

Figure 8.4: Screenshot of the developed GUI.

In the first panel, (*Monitoring parameters*) the basic configuration to communicate with the head-end and subsequently the meters is made. The next panel named *Real-Time Monitoring* is used for the configuration of the on-demand reading module, as well as for checking the status of the performed queries, whereas the communication with the database is controlled in the panel named *Capture*. In addition, The LabVIEW interface is not only able to generate on-demand requests for the measurement of selected variables, but different configuration commands and loggers can also be read. Therefore, to check the status of this queries, the panel *On-Demand Commands* was developed. Finally, the last panel that can be found in the LabVIEW interface is devoted to the system alarms.

Regarding the tab structure, the first panel in Figure 8.4 and named as *Monitoring*, shows the real-time measures of the on-demand readings, which are from left to right and from top to bottom, 3-phase voltages, 3-phase currents, frequency, powers, THDU, THDI, global power factor, and energy. The second tab allows configuring and querying the voltage quality logger of the SMs for voltage events, whose possibilities are shown in the last subsection 8.3.4. The third tab with the name *Load Profile* is employed for the visualization and configuration of the load profile logger. This logger automatically records the energy measurements of the SMs for a given time interval that can be configured by the user. The tab four named as *Analysis Logger* is used for setting up and visualizing the analysis logger of the SMs, similar to the Profile Logger, but configurable by the user. In this test, it recorded information regarding current and voltage THDs and power factor for the PQ monitoring. Finally, the last tab is used for querying the power quality logger, where different PQ events are registered according to the EN 50160.

8.3.3 Profiles Monitoring for EMS

In the first scenario, the profile of a single household was generated by a 3-phase inverter, whilst measuring the output with a 3-phase OMNIA direct meter. This will emulate the measurements that will be recorded by one of the N SMs installed in each apartment of the building, denoted as the blue circles B in Figure 8.1.

The profile was generated using a stochastic high temporal resolution model where each appliance in the household is simulated individually and then aggregated. In this way, not only the active power references can be given to the inverter, but also the reactive power [14].

The resolution of the model is 1 minute, so the generated active and reactive power daily profile was composed of 1440 points. Thus, in order to downsize the length of the experiment each minute of the real profile was transform in 5 seconds of the simulation, so instead of needing a day for the experiment only 2 hours were employed. The on-demand readings feature was used, although, in a real implementation where the time is not downsized, the analysis logger will be employed with a maximum resolution of 5 minutes.

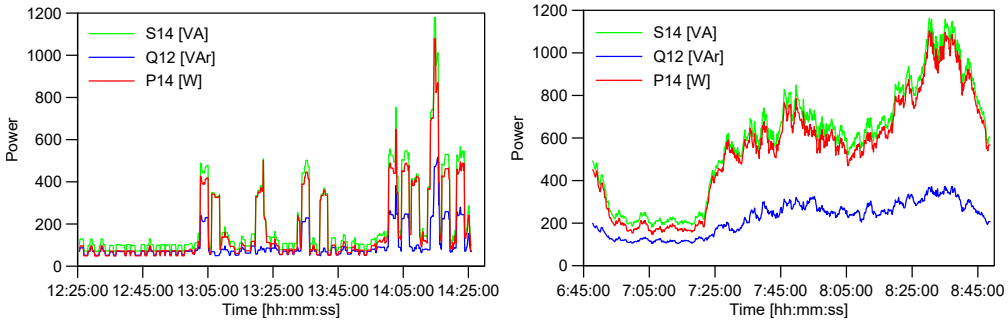

(a) Single Household Profile

(b) Aggregated Households Profile

Figure 8.5: Consumption profiles measured using the laboratory AMI and the test bench installation.

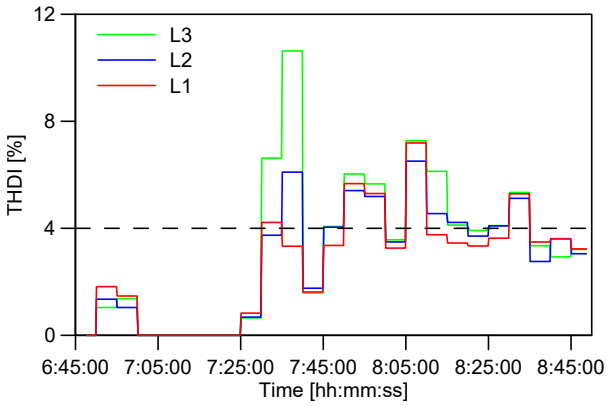

Figure 8.6: Current THD in the AC Building Bus.

In this case, The number of data point obtained from the SM was 716 readings of 26 registers queried simultaneously. If the length was 2 hours or 7200 seconds, a new data point was obtained with approximately an average period of 10 seconds, that in the real implementation without downsizing the time will be a measure every 2 minutes, therefore, the resolution will be slightly lower. Nevertheless, the results for the active, reactive and apparent power are shown in Figure 8.5 (a), and as it can be observed the resolution is more than enough to detect the fast power changes related to the switch on and off events in the household.

In the same way, a second scenario was tested, but using the daily profile of an aggregate of households, emulating the profile that can be read by an SM installed in the AC bus of the building (purple circle D). Using the above-mentioned stochastic model, in this case an aggregate profile of 16 households was simulated with 1-minute resolution, downsize in this case both the time, as in the previous scenario, as also the power, since the maximum peak obtained from the model was 18 kW and the maximum power of the converters is 2.2 kW. The obtained results for the power are shown in Figure 8.5 (b). This scenario also corresponds with the graphs represented in the GUI shown in Figure 8.4.

8.3.4 Continuous PQ monitoring

As well as monitoring the basic powers, voltages, currents or frequency, the SMs can monitor the THDI and the THDU. Therefore, in the above-presented scenario where the aggregated profile was simulated, additional harmonic distortion was added, and some PQ indices were also recorded.

The results are illustrated in Figure 8.6 were the THDI in the 3-phase is represented. The figure depicts that the THDI value is updated in the system every 5 minutes. Thus, as it was expected the information that can be obtained from the SMs cannot be compared with the PQ information recorded with a network analyzed. However, taking into account that PQ monitoring is not their main goal, they provide features that can be used for a rough estimation, and also compatible with the international standard that defines THD values for 10 minutes intervals.

8.3.5 PQ Events Detection

Finally, another PQ feature that most of the SMs implement is the detection of voltage deviations and PQ events. In these SMs, three types of voltage quality events can be detected.

- Long-term deviations: The system detects as long-term deviations, voltage changes that take longer than 10 s.

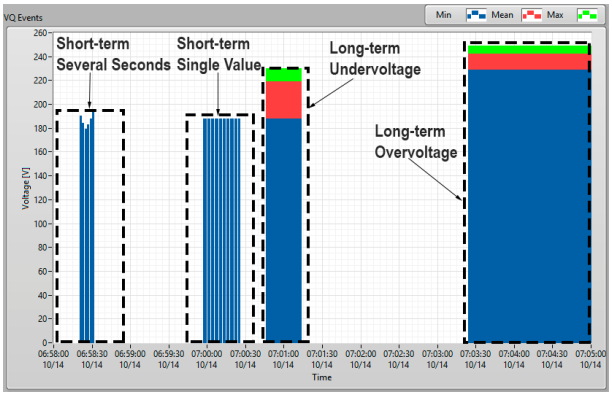

Figure 8.7: Detail of the VQ Logger tab of the LabVIEW application.

- Short-term deviations: The short-term deviations are those between 1 and 10 seconds.
- Voltage Outage: The voltage outage detects the periods when a very low voltage is applied to the SM.

In order to test this feature, the SMs was connected to a Grid Simulator (Chroma 61800) where short and long-term deviations were generated to test the detection features.

The detected events are shown in Figure 8.7. When a long-term voltage deviation is detected 3 values are recorded: the maximum (green), minimum (blue) and the mean (red) voltage for the period. Two cases of long-term deviations are shown, one for an undervoltage and the other for an overvoltage.

In the case of the short-term deviations, if the value is out of range for several seconds, the start and end points are recorded together with the maximum/minimum value as can be seen in the first events. However, if the event is shorter than two seconds, only the extreme value is accounted.

8.4 Conclusion

This work has addressed the additional functionalities that the new AMI adds to the paradigm of Smart Grids providing bi-directional communication and advanced measurements that can be included in other algorithmic layers. The application has been described from a hardware point of view and subsequently related to the communication architecture of a self-developed system based on a commercial AMI.

The system implementation has been shown from both the physical deployment in a test bench and from the software application built to collect the measurements. The results for different placement of the SM in the proposed architecture were shown for daily profiles generated with the inverters installed on the test bench and using all the AMI installed in the laboratory. The implementation proved that these profiles can be directly used in the EMS, therefore, enhancing the management capabilities of each individual consumer.

Finally, the PQ monitoring features of the SMs were shown. The results illustrated how the global current THD of the building can be assessed in a basic way without the usage of advanced devices, but only with the SMs. In addition, PQ quality events can also be detected being an essential tool not only for the users but also for the network operator.

Thus, this solution establishes evidence of the main role of the SMs in the Smart Grid infrastructure and the implementation of novel management strategies.

Acknowledgment

This work has been supported by the Danish Energy Technology Development and Demonstration Program (EUDP) through the Sino-Danish Project "Microgrid Technology Research and Demonstration" (meter.et.aau.dk) and also by the International Science & Technology Cooperation Program of China, project Number: 2014DFG62610.

References

[1] S. Zhou, M. A. Brown, Smart Meter Deployment in Europe: A Comparative Case Study on the Impacts of National Policy Schemes, Journal of Cleaner Production 144 (2016) 22–32. doi:10.1016/j.jclepro.2016.12.031.

[2] E. J. Palacios-García, Y. Guan, M. Savaghebi, J. C. Vásquez, J. M. Guerrero, A. Moreno-Munoz, B. S. Ipsen, Smart metering system for microgrids, in: IECON 2015 - 41st Annual Conference of the IEEE Industrial Electronics Society, IEEE, 2015, pp. 3289–3294. doi:10.1109/IECON.2015.7392607.

[3] A. Moreno-Munoz, J. J. Gonzalez De La Rosa, Integrating power quality to automated meter reading, IEEE Industrial Electronics Magazine 2 (2) (2008) 10–18. doi:10.1109/MIE.2008.923520.

[4] Y. Kabalci, A survey on smart metering and smart grid communication, Renewable and Sustainable Energy Reviews 57 (2016) 302–318. doi:10.1016/j.rser.2015.12.114.

[5] E. Rodriguez-Diaz, E. J. Palacios-Garcia, M. Savaghebi, J. C. Vasquez, J. M. Guerrero, Development and integration of a HEMS with an advanced smart metering infrastructure, in: 2016 IEEE International Conference on Consumer Electronics (ICCE), IEEE, 2016, pp. 544–545. doi:10.1109/ICCE.2016.7430724.

[6] L. I. Minchala-Avila, J. Armijos, D. Pesántez, Y. Zhang, Design and Implementation of a Smart Meter with Demand Response Capabilities, Energy Procedia 103 (2016) 195–200. doi:10.1016/j.egypro.2016.11.272.

[7] Y. Bai, H. Zhong, Q. Xia, Real-time demand response potential evaluation: A smart meter driven method, in: 2016 IEEE Power and Energy Society General Meeting (PESGM), IEEE, 2016, pp. 1–5. doi:10.1109/PESGM.2016.7742002.

[8] W. Kong, Z. Y. Dong, J. Ma, D. Hill, J. Zhao, F. Luo, An Extensible Approach for Non-Intrusive Load Disaggregation with Smart Meter Data, IEEE Transactions on Smart Grid 3053 (c) (2016) 1–1. doi:10.1109/TSG.2016.2631238.

[9] M. M. Albu, M. Sănduleac, C. Stănescu, Syncretic Use of Smart Meters for Power Quality Monitoring in Emerging Networks, IEEE Transactions on Smart Grid 8 (1) (2017) 485–492. doi:10.1109/TSG.2016.2598547.

[10] T. Demirci, A. Kalaycıoğlu, D. Küçük, Ö. Salor, M. Güder, S. Pakhuylu, T. Atalık, T. Inan, I. Çadırcı, Y. Akkaya, S. Bilgen, M. Ermiş, Nationwide real-time monitoring system for electrical quantities and power quality of the electricity transmission system, IET Generation, Transmission & Distribution 5 (5) (2011) 540. doi:10.1049/iet-gtd.2010.0483.

[11] E. Rodriguez-Diaz, F. Chen, J. C. Vasquez, J. M. Guerrero, R. Burgos, D. Boroyevich, Voltage-Level Selection of Future Two-Level LVdc Distribution Grids: A Compromise between Grid Compatibiliy, Safety, and Efficiency, IEEE Electrification Magazine 4 (2) (2016) 20–28. doi:10.1109/MELE.2016.2543979.

[12] L. Meng, A. Luna, E. R. Díaz, B. Sun, T. Dragicevic, M. Savaghebi, J. C. Vasquez, J. M. Guerrero, M. Graells, F. Andrade, Flexible system integration and advanced hierarchical control architectures in the microgrid research laboratory of aalborg university, IEEE Transactions on Industry Applications 52 (2) (2016) 1736–1749. doi:10.1109/TIA.2015.2504472.

[13] A. Anvari-Moghaddam, J. C. Vasquez, J. M. Guerrero, Load shifting control and management of domestic microgeneration systems for improved energy efficiency and comfort, in: IECON 2015 - 41st Annual Conference of the IEEE Industrial Electronics Society, IEEE, 2015, pp. 96–101. doi:10.1109/IECON.2015.7392082.

[14] E. J. Palacios-Garcia, A. Moreno-Munoz, I. Santiago, I. M. Moreno-Garcia, M. I. Milanes-Montero, Smart community load matching using stochastic demand modeling and historical production data, in: EEEIC 2016 - International Conference on Environment and Electrical Engineering, IEEE, 2016, pp. 1–6. doi:10.1109/EEEIC.2016.7555885.

9

Concluding remarks

9.1 Summary

The thesis has presented the modelling of energy consumption in the residential sector and its use for the evaluation and prediction of integration strategies and energy policies in the Smart Grid. This development has shown to be of particular interest in the current energy context with the integration of DER sources that require an energy management system which is able to cover the needs of end users at all times.

A stochastic modelling methodology has been used in all developments, which has allowed us to simulate the heterogeneous and unpredictable behaviour of users. In particular, a bottom-up methodology and engineering-based models with distribution techniques were employed. In this way, the total consumption of each house was obtained as the sum of the individual consumptions of each device.

The proposed technique allowed a separation of the study according to common influence factors. This led to the development of three independent sub-models for the simulation of the consumption due to lighting systems, heating and cooling elements and general appliances. However, by means of the sum of these subsystems and using different levels of aggregation more complex scenarios could be analysed.

This methodology also provided the model with great flexibility that allowed it to be used for the study of energy DR strategies and and the assessment of energy policies, all of them in a low level. In the same way, its high temporal resolution was a key point to consider in the integration of DER sources where the non-coincidence of production and consumption is a crucial factor.

Some conclusion for the domestic consumers and DER integration were drawn from this analysis. Some of them are the impact of new lighting technologies on the average power quality and the payback time of the initial investment, the influence in the network overcharge that air conditioning system might have, the essential role that consumer acceptance plays in DR strategies and the possibilities of combining individual with collective resources management to benefit both the end users and the whole Smart Grid.

It should also be pointed out that, in terms of functionality, its implementation as a web service based on JAVA EE technologies provided a seamless integration of third-party tools such as GAMS for the development of optimisation rules for demand response strategies or the application of validation techniques, analysis and advanced calculations in other tools such as MATLAB.

What is more, this philosophy facilitated the integration of the system with an energy management platform where Smart Meters data were combined with different meteorological and economic factors, as well as optimisation algorithms to the control an intelligent building. In this way, the development is not only a passive system for evaluation and analysis but also an active tool for the Smart Grid management whose future perspectives are promising.

9.2 Contribution

The main contributions made by the thesis are the following, which are presented in relation to the published articles included in the chapters of this document:

- Definition of a subdivision of consumptions in the residential sector based on the main influence factors. This division allowed them to be separated for both their study and the assessment of their improvement capabilities. (Chapter 2)

- Definition of the main DR strategies and key energy policies for the residential sector. (Chapter 2)

- Development of a consumption model for lighting consumption in the domestic sector that considered each point of lighting at a low level taking into account its technology, power and time of use. This also made it possible to study energy savings policies and the impact on the quality of the supply that the introduction of LED and CFL technologies in households might have. (Chapter 3)

- Development of a consumption model for heating and cooling consumption in the residential sector. In the same way as the previous one, the loads were modelled at a low level taking into account their type, the existence of thermostatic controls and the intervention of users with their behaviour. Likewise, the study was carried out in the region of Spain where climatic characteristics and the increasing acquisition power of users has led to the use of more air conditioning systems demonstrating its strong impact on the network. (Chapter 4)

- Development of a consumption model for residential appliances. A modelling of the low-level devices was proposed considering different operating schemes of fixed, variable or cyclical power. Their behaviour was also associated with the activities that the residents carry out in the dwelling. (Chapter 5)

- Integration of DR strategies in the modelling system at the individual device level. In addition, factors such as the users acceptance rates were incorporated to observe the impact at an aggregate level. (Chapter 5)

- Establishment of a simulation framework that integrates the model developed for consumption in the residential sector with historical production records and individually modelled storage systems. This scenario made it possible to evaluate and develop savings measures applied in a DER integration environment for a Smart Community. (Chapter 6)

- Development of a 2-level charging scheme for batteries that allows for the improvement of the hosting capacity of low-voltage networks in the presence of PV production. This scheme made it possible to use a percentage of the batteries for individual energy management operations in each household, whereas allocating another percentage for the DSO, who can charge and discharge them to avoid overcharging the grid during peak hours of massive production injection. (Chapter 6)

- Exploitation of the capabilities offered by smart metering systems for smart grids and especially in the context of distributed resources. (Chapter 7)

- Integration of smart metering systems and the developed models into a decision system for energy management in the scenario of an intelligent building. In this way, a better prediction and distribution of resources can be made. In addition, the intercommunication between information systems in the Smart Grid, web services and the Internet as the de facto support for all of them were highlighted. (Chapter 8)

9.3 Future works

The modelling system developed in the thesis, the energy management techniques studied and the final integration with smart metering systems and a context of distributed resources show the potential future lines that can be investigated.

- **To carry out an online implementation of the modelling system**: Until now, the consumption model for the residential sector operates offline, generating daily, monthly or annual profiles of 1 to N dwellings based on historical input data. A possible improvement would be the implementation of a system that could make predictions in real time using input monitored data as influence factors and previously knowing the necessary characteristics of the dwelling(s) to be simulated.

- **To feedback the model with real historical data**: Throughout the work, a modelling technique has been presented that is based on statistics and distributions corresponding to a region. Despite being validated, it can present limitations to make precise predictions in very specific and limited contexts. Since the model can be easily integrated with smart metering systems as presented, it would be reasonable to address the possibility of using such data for self-calibration and model correction to ensure even more accurate results.

- **To include more complex simulations of the appliances**: The simulated loads in the system take into account variable power cycles, thermostatic controls and even estimate the reactive energy consumed by means of an average power factor. However, with a focus on improving the power quality of the supply and the study of the interaction between loads, the simulation could be completed with the inclusion of basic harmonic emissions from these devices in order to have a theoretical framework for analysing these phenomena.

- **To incorporate new loads into the model**: Although the current development considers a wide variety of devices usually found in the residential sector, there are some disruptive technologies such as EVs that have still not been integrated. A key step in assessing the impact of this technology could be the development of a model based on the same principles where residents' activity and mobility will be related to the use of this type of vehicles and their connection to the network for charging. The possibility of this vehicles being used as an active element of the grid may even be considered.

- **To implement complex simulation of the low-voltage networks**: During the work, an effort has been made to model the network specially to study the interaction of renewable energy sources and the possibility of improving the hosting capacity, but it was limited to global parameters. Nevertheless, the high temporal resolution and level of disaggregation of the data can allow us to take this a step further with the simulation of a real community with heterogeneous consumption and considering the detailed electrical parameters of the system being therefore able to analyse variables such as voltage variations or harmonic distortion in several points.

- **To incorporate the simulation tool as a web service available for other systems**: Given that the entire system was developed following a decentralised philosophy where the model is presented as a RESTful web service, one of the most interesting points is its integration with other systems such as energy management tools, optimisation algorithms or direct load control, providing another additional data source in the context of the internet of things (IoT) for households, toward the massive acquisition of domestic parameters and the digitisation of energy.

Curriculum Vitae

Emilio José Palacios García

Emilio José Palacios-García was born in 1991 in Córdoba, Spain. He holds a BSc in Industrial Electronics and an MSc in Distributed Renewable Energies obtained from University of Córdoba, Spain. Since 2013 he has been participating in various research projects at the same institution with a national scope. He is currently pursuing the degree of PhD in this University, holding a National Research Grand funded by the Ministry of Education, Culture and Sport. The main research lines of this work are stochastic energy modelling of residential demand and the integration of distributed renewable resources. Likewise, since 2015 he collaborates with Aalborg University (Denmark) in different project related to Smart Metering, Demand Response and Home Energy Management Systems (HEMS). His interests are Smart Grids, Smart Metering, Stochastic Energy Modelling and Wireless Sensor Networks for EMS systems.